Studies on sustained Supersonic Combustion with Ramps and Cavities

A Thesis submitted in the partial fulfilment of the requirements for the award of the degree of

DOCTOR OF PHILOSOPHY

By

J.V.SATYANARAYANA MOORTHY

(ROLL NO:701212)

Under the Supervision of

Dr. G. Amba Prasad Rao
Professor
National Institute of Technology
Warangal

Dr. B.V.N. Charyulu
Scientist 'G'
Defence Research & Development
Laboratory, Hyderabad

DEPARTMENT OF MECHANICAL ENGINEERING
NATIONAL INSTITUTE OF TECHNOLOGY
WARANGAL (T.S.) INDIA 506 004

September 2018

NATIONAL INSTITUTE OF TECHNOLOGY
WARANGAL (T.S) INDIA 506 004

CERTIFICATE

This is to certify that the thesis entitled "**Studies on sustained Supersonic Combustion with Ramps and Cavities"** that is being submitted by Sri. **J.V. Satyanarayana Moorthy** in partial fulfilment for the award of Doctor of Philosophy (**Ph.D**) in the Department of Mechanical Engineering, National Institute of Technology, Warangal is a record of bonafide work carried out by him under our guidance and supervision. The results embodied in this thesis have not been submitted to any other Universities or Institutes for the award of any degree or diploma.

Dr. B.V.N. Charyulu
Scientist 'G'
Defence Research & Development Laboratory
Hyderabad

Dr. G. Amba Prasad Rao
Professor
Department of Mechanical Engineering
NIT- Warangal

Dedicated

to

My beloved

Parents, Teachers and Family

NATIONAL INSTITUTE OF TECHNOLOGY
WARANGAL (T.S) INDIA 506 004

DECLARATION

This is to certify that the work presented in the thesis entitled "**Studies on sustained Supersonic Combustion with Ramps and Cavities",** is a bonafide work done by me under the supervision of Prof. G. Amba Prasad Rao and Dr. B.V.N. Charyulu, was not submitted elsewhere for the award of any degree.

I declare that the written submission represents my idea in my own words and where other's ideas or words have not been included. I have adequately cited and referenced the original sources. I also declare that I have adhered to all principles of academic honesty and integrity and have not misinterpreted or fabricated or falsified any idea / data / fact / source in my submission. I understand that any violation of the above will be a cause for disciplinary action by the institute and can also evoke penal action from the sources which have thus not been properly cited or from whom proper permission has not taken when needed.

Date: (**J.V.SATYANARAYANA MOORTHY**)

Place: Warangal Research Scholar

Roll No. 701212

Acknowledgements

I take the opportunity to express my heartfelt adulation and gratitude to my supervisors, Dr. G. AMBA PRASAD RAO, Professor, Mechanical Engineering Department, National Institute of Technology, Warangal and Dr. B.V.N. CHARYULU, Scientist, Defence Research and Development Laboratory, Hyderabad for their unreserved guidance, constructive suggestions, thought provoking discussions and unabashed inspiration in nurturing this research work. Dr. Amba Prasad Rao has always been a source of strength and constant support. Spending many opportune moments under the guidance of the perfectionists at the pinnacle of professionalism has always been a blessing for me. The present work is a testimony to the alacrity and ardent personal interest exuded by them during this thesis work.

I sincerely thank, Prof. P.BANGARU BABU, Head Mechanical Engineering Department, National Institute of Technology, Warangal for his continuous support towards carrying out this research work.

Special thanks are also due to Prof. C.S.P. RAO and Prof. L. KRISHNANAND, Prof. S. SRINIVASA RAO former Heads of Mechanical Engineering Department, National Institute of Technology, Warangal for their timely suggestions and support in providing necessary department facilities and services towards successful completion of this research work.

I wish to express my sincere and whole hearted thanks and gratitude to my DSC members Dr. Madhu Murthy, Professor, Mechanical Engineering Department and Dr. Venu Vinod, Professor, Chemical Engineering Department for their kind help, encouragement and valuable suggestions in completing this research and course works successfully.

I am also indebted to the Director, my colleagues and friends in Defence Research and Development Laboratory, Hyderabad who supported me in conducting the necessary experiments which formed the backbone of my research work and for the resources to carry out computational studies. I also like to express my sincere thanks to all my friends and colleagues, especially to Dr. T. Karthikeya Sharma, Dr. A.R. Babu, Dr.A. Keche,

Dr. G. Nilesh, Dr. Sindhu Ravichettu, Mr. M.Vinod Babu of N.I.T., Warangal and Mr. B.Rajinikant, Mr. Dilip Kumar Yadav, Mr. Pradhap of DRDL, Hyderabad.

Words are inadequate to express my thanks to my parents, my family and my brother for exhibiting patience and unyielding support during this long and arduous journey. I want to express my sincere thanks to all those who directly or indirectly helped me at various stages of this work.

(J.V.SATYANARAYANA MOORTHY)

ABSTRACT

There has been a wide spread activity among combustion community with renewed interest in high-speed propulsion and realization of supersonic combustion ramjet engine for hypersonic flight applications. Therefore, supersonic combustion ramjet (SCRAMJET) is expected to be suitable for serving as an economical and effective propulsive system for hypersonic flight and gaining access to the space. A main source of energy release in scramjet is the combustor and for a given combustor configuration, its performance is determined primarily by fuel injection distribution and flame holding. Many theoretical, numerical and experimental research efforts have been made to investigate various aspects of the fuel injection inclusive of fuel mixing, reliable ignition, combustion stability and propulsion performance. Achievement of ignition and sustained combustion in high speed flows is a perennial challenge in supersonic combustion, and should be done within a short length of the combustor. The successful achievement of sustained supersonic combustion lies with good fuel injection scheme and flame holding.

Concepts for fuel injection in supersonic combustors that have been widely researched and adopted are wall injectors and strut injectors. Cavity based flame-holders have been tried out in scramjet combustors. Cavities provide re-circulation zones in the combustor which create conditions for increased residence time of air in the combustor and thus act as flame holders.

Thus, research necessitates study of coupling mechanism between the mixing of supersonic air/fuel streams and flame holding. Very few researchers have tried out ramps for imparting fuel injection. Generally, ramps are used to add axial velocity to the flow near the fuel injection with fuel injectors on the trailing edge of the ramp injecting fuel parallel to the flow. The flow over ramps creates counter-rotating vortices that increase mixing. Due to the supersonic flow in the scramjet, the ramps also create shocks and expansion waves which cause pressure gradients and enhance mixing. The main objective of the present study is to examine the coupling between the ramp assisted fuel injection and cavity flame holding as well as the potential for improving combustion in a scramjet combustor.

To understand the flow physics of supersonic combustion and other pertinent parameters, detailed computational studies, adopting the widely used commercial software ANSYS Fluent v15.0, have been conducted with hydrogen, aviation kerosene and ethylene as fuels. Flow field, along the length of combustor, is studied in terms of Mach number, static pressure, static temperature and mass fraction of species. A parameter, turbulence intensity has been chosen to observe the completeness of mixing. To overcome the issues with liquid fuels, gaseous ethylene is tried out as a candidate fuel for mixing and supersonic combustion.

Extensive numerical studies have been done for understanding parametric variation on a full-scale combustor, with and without cavities, with and without ramps and with ramp-cavity with ethylene as fuel. Fuel equivalence ratios of 0.3, 0.4, 0.6 and 0.8 are studied. Better flow-field effects are observed with fuel equivalence ratio of 0.8. However, it is noticed from mass fraction contours of species that considerable amount of fuel goes without combustion out of combustor. As a trade-off, fuel equivalence ratio of 0.6 is considered for studies on the full-scale, ramp-cavity configuration. In numerical studies, combustor entry Mach number is varied from 2, 2.5 and 3. Better performance is observed for the full-scale, ramp-cavity combustor with entry Mach number of 3. Detailed analysis has been carried out on the full-scale, ramp-cavity configuration with combustor entry Mach number of 3 and fuel equivalence ratio of 0.6.

Fuel is injected from four sets of ramps located in the combustor. Fuel injection pattern is studied by injecting the same amount of fuel with injection of fuel from three sets of ramps each time. In the first stage, fuel is not injected from the first set of 4 ramps, 2 each on top and bottom walls of the combustor. In the second stage, fuel is not injected from 2^{nd} set of 4 ramps. In the third stage, fuel is not injected from 3^{rd} set of 4 ramps. In the final stage, fuel is not injected from the 4^{th} set of two ramps, one each on top and bottom wall. In each case, the length of the combustor for mixing and subsequent combustion is different. The calculated values of thrust for 2^{nd} stage and 3^{rd} are observed to be 61.3 kgf and 58.71 kgf respectively. It may be inferred that the fuel injected from 1^{st} set of ramps would mix with supersonic air-stream in the 2^{nd} stage and combustion takes place

resulting in higher thrust. The pattern in third stage may also have been similar to the 2nd stage of injection of fuel in the combustor.

A full-fledged test facility has been designed and developed simulating the high altitude conditions in terms of total pressure and temperature. The instrumentation has been calibrated at regular intervals. Initially, a sub-scale combustor has been designed and studied experimentally, with physical ramps followed by cavities across the combustor on both top and bottom walls. The combustor performance is experimentally evaluated in terms of wall static pressures and temperatures, along the combustor. Hydrogen as a pilot fuel is employed for effective utilization of aviation kerosene. With the experience of sub-scale combustor studies, a full-scale combustor has been designed with cantilevered ramps along the combustor in four stages. In each of the first three stages, two ramps on the top wall and two ramps on the bottom wall are located. In the final stage, one ramp each on top and bottom walls are provided. Two cavities are configured on the top wall of the combustor. The top wall of combustor is designed with staged divergence to avoid thermal choking in the combustor. Tests have been conducted with aviation kerosene as fuel. In the full-scale combustor, the wall pressures are 1 to 1.2 bar. Temperatures are about 1500- 1800 K in the experiments. Variety of fuels such as hydrogen, aviation kerosene and ethylene fuels are employed in the studies.

It is noticed that fuel injection and flame holder together would be vital components for effective working of supersonic combustor. The advantage of providing ramps is that blockage to the flow is significantly less compared to other mixing devices. Numerical studies has established that ANSYS FLUENT has well-predicted the flow field characteristics. The studies on both sub-scale and full-scale combustors has established an achievement of sustained supersonic combustion with combined arrangement of ramps and cavities. It is observed the computed values of static pressure match closely with the experimental results.

CONTENTS

CHAPTER NO.	SECTION	SUB-SECTION	DESCRIPTION	PAGE NO.
			ACKNOWLEDGEMENTS	I
			ABSTRACT	III
			CONTENTS	VI
			LIST OF FIGURES	IX
			NOMENCLATURE	XV
			INTRODUCTION	1
	1.1		Background	5
1.0		1.1.1	Ramps	5
		1.1.2	Cavity Based Injection	6
	1.2		Organisation of thesis	8
			LITERATURE REVIEW	9
	2.1		Overview of scramjet development	9
	2.2		Studies on supersonic combustion	10
		2.2.1	Summary	17
2.0	2.3		Studies on effect of ramps and cavities	17
		2.3.1	Summary	23
	2.4		Observations from the Literature review	24
	2.5		Motivation	24
	2.6		Objectives of present studies and scope for present work	25
			METHODOLOGY	26
	3.1		Computational Studies	26
		3.1.1	Brief Introduction about package used	27
		3.1.2	Governing equations for computational studies	28
		3.1.3	Grid Independence Study	36
		3.1.4	Validation with experimental work	40
3.0		3.1.5	Studies on effect of type of fuels, Mach number, Equivalence ratios and fuel injection pattern	40
	3.2		Experimental programme	42
		3.2.1	Development of Sub-scale test facility	42
		3.2.2	Description of Sub-scale combustor	44

		3.2.3	Full scale Test facility	48
		3.2.4	Full scale combustor	49
		3.2.5	Instrumentation	50
			RESULTS AND DISCUSSION	52
	4.1		Computational Studies	52
		4.1.1	Variation of parameters on combustor configuration	52
		4.1.1.1	Studies on Combustor at Mach number 3 without Ramps and cavities	53
		4.1.1.2	Combustor with ramps only	56
		4.1.1.3	Combustor with cavities only	59
		4.1.1.4	Comparison of the combustors with and without ramps and cavities	63
		4.1.1.5	Vorticity and recirculation of ramps and cavities	67
		4.1.2	Studies on full-scale combustor with aviation kerosene as a fuel	69
		4.1.2.1	Studies on Full-scale ramp-cavity combustor at entry Mach 2 with aviation kerosene as a fuel	69
4.0		4.1.2.2	Studies on full scale combustor with entry Mach 3 with Aviation kerosene as a fuel	74
	4.2		Effect of Fuels	78
		4.2.1	Studies on Full-scale combustor with Ethylene as fuel at combustor entry Mach 3condition	80
		4.2.2	Comparison studies on ramp-cavity full-scale combustor for different entry Mach numbers with ethylene as a fuel	91
	4.3		Comparison studies on ramp-cavity full-scale combustor for different fuel equivalence ratios at Mach Number 3 with ethylene as a fuel	96
	4.4		Effect of fuel injection pattern	99
	4.5		Validation with experimental work	113
	4.6		Experimental Studies on full-scale combustor with aviation kerosene as fuel at combustor entry Mach 2	114
	4.7		Plates	119
5.0			Summary and Conclusions	122
6.0			Recommendations for Future Work	128
			Papers Published Based on Present Work	129
			References	130
			Appendix - I	
	A1		Experimental Studies on a sub-scale combustor with aviation kerosene as fuel	137
		A.1.1	Variation of wall static pressure on top wall of sub-scale combustor	137

	A.1.2	Variation of Temperature along subscale combustor	140
		Appendix – II	
A2		Experimental studies on full-scale combustor with aviation kerosene as a fuel	143
	A.2.1	Variation of static pressure along full-scale combustor	143
	A.2.2	Variation of Temperature along the full scale combustor	145
		Appendix – III	
A3		Computational studies on sub-scale combustor	148
	A.3.1	Computational studies on sub-scale combustor with hydrogen as pilot and kerosene as main fuel at entry Mach number 2	148
	A.3.2	Studies on a sub-scale combustor with Aviation kerosene as fuel at entry Mach number 2.5	153
		Appendix – IV	
A4		Full scale combustor with Wall Injection and without ramps and cavities	158
	A.4.1	Combustor with cavities and Wall Injection for combustor entry Mach 3	158
	A.4.2	Studies with full scale combustor at entry Mach 3 with Aviation kerosene	163
		Appendix – V	
		Note on Development work on scramjet Combustor in various countries	166
		Appendix – VI	
		Theoretical Rocket Performance Assuming Frozen Composition During Expansion	167
		NASA CEC-71 Computation	168

LIST OF FIGURES

Sl. No.	DESCRIPTION	Page No.
	Chapter 1	
1	Fig.1.1 Ramp injection	6
2	Fig.1.2 Ramp injector geometry in sub-scale combustor	6
3	Fig.1.3 Cavity injector geometry	7
	Chapter 3	
4	Fig.3.1 Flow path of the combustor	36
5	Fig. 3.1 (a) Grid Generation for Ramp Cavity Combustor	37
6	Fig. 3.1 (b) Grid for Ramp	38
7	Fig. 3.1 (c) Grid for Cavity	39
8	Fig. 3.1 (d) Flow characteristics along the combustor	39
9	Fig. 3.1 (e) Static Pressure variation along the combustor	39
10	Fig.3.2 Sub-scale combustor test facility	43
11	Fig.3.3 Sub scale Ramp-cavity combustor	45
12	Fig.3.4 (a) Injection scheme: Sub-scale Ramp-Cavity combustor	46
13	Fig.3.4 (b) Injection locations of Sub-scale Ramp-Cavity combustor	47
14	Fig.3.4 (c) Injection scheme: Full-scale Ramp-Cavity combustor	48
15	Fig.3.4 (d) Arrangement of Ramps & Cavities in the full scale combustor	48
16	Fig. 3.5 Full scale combustor test facility	49
17	Fig. 3.6 Full-scale Ramp-cavity combustor	50
	Chapter 4	
18	Fig.4.1 Full-scale combustor with ramps and cavities	53
19	Fig.4.2 (a) Variation of Mach number along the simple combustor	54
20	Fig.4.2 (b) Variation of Static pressure (Pa) along the simple combustor	55
21	Fig.4.2 (c) Variation of static temperature (K) along combustor	55

22	Fig.4.3 (a) Mach number contour along the combustor with ramps only	57
23	Fig.4.3 (b) Variation of static pressure (Pa) along the combustor with ramps only	57
24	Fig4.3 (c) Variation of static temperature (K) along the combustor with ramps only	58
25	Fig.4.4 (a) Mach number contour along the combustor with cavities only	60
26	Fig.4.4 (b) Static Pressure (Pa) contour along the combustor with cavities only	60
27	Fig.4.4 (c) Static temperature (K) contour along the combustor with cavities only	61
28	Fig.4.4 (d) Velocity vectors depicting Recirculation at Cavities	61
29	Fig.4.5 (a) Variation of Mach number with length	64
30	Fig.4.5 (b) variation of static pressure along combustor	64
31	Fig.4.5 (c) Variation of static temperature along combustor	64
32	Fig. 4.6 (a) Turbulence Intensity contours for various types of configurations	65
33	Fig.4.6 (b) Effect of Ramp cavities on turbulence intensity to enhance mixing	66
34	Fig.4.6 (c) Mass fraction contours for Mach 3 flow in combustor	66
35	Fig.4.7 (a) Velocity vectors for vortices near the ramps	67
36	Fig.4.7 (b) velocity vectors depicting recirculation at the cavity	68
37	Fig.4.8 Ramp-cavity combustor (Full-scale)	69
38	Fig.4.9 (a) Mach number distribution along the combustor	70
39	Fig.4.9 (b) Static pressure (Pa) contour along the combustor	71
40	Fig.4.9 (c) Static temperature (K) contours along the combustor.	72
41	Fig.4.9 (d) Mass fractions of species with aviation kerosene at Mach 2	73
42	Fig.4.9 (e) Flow parameters along the combustor with aviation kerosene as fuel at Mach 2	74
43	Fig.4.10 (a) Flow field parameters along the combustor with aviation kerosene as fuel for two entry Mach numbers.	75
44	Fig.4.10 (b) Mass fraction of species along the combustor with aviation kerosene as fuel	76
45	Fig.4.10 (c) Averaged Mass fractions of species across the combustor section	76

46	Fig.4. 11 (a) Mach number variation along the full-scale combustor	79
47	Fig.4.11 (b) Static pressure variation along the full-combustor scale	79
48	Fig.4.11 (c) Static temperature variation along the full-scale combustor	79
49	Fig.4.12 Mach number variation along the combustor	82
50	Fig.4.13 Comparison of variation of Mach number for Mach 3.0 condition	83
51	Fig.4.14 Static Pressure (Pa) along the combustor for Mach 3.0 condition	84
52	Fig.4.15 Static Temperature(K) contours along the combustor for Mach 3.0 condition	86
53	Fig.4.16 Ethylene Mass fraction contours at combustor entry Mach 3	88
54	Fig.4.17 Oxygen mass fraction contours along the combustor	89
55	Fig.4.18 Mass fraction of H_2O along the combustor	90
56	Fig.4.19 Mass fraction of CO_2 along the combustor	90
57	Fig. 4.20 (a) Variation of Mach number along the combustor.	92
58	Fig.4.20 (b) Variation of Static Pressure along the combustor	93
59	Fig.4.20(c) Static Temperature variation along the combustor	94
60	Fig.4.20 (d) Mass fractions of species along the combustor	95
61	Fig.4.21(a) Mach numbers along the combustor	97
62	Fig.4.21 (b) Static pressure along the combustor	97
63	Fig.4.21 (c) Comparison of Static temperature along the combustor	97
64	Fig.4.21 (d) Comparison of Mass fractions of species along the combustor	98
65	Fig.4.22 Arrangement of Ramps in the Combustor	100
66	Fig.4.22 (a) Mach number contours along the combustor for the 1st stage of fuel injection	100
67	Fig.4.22 (b) Static pressure (Pa) contours for the 1st stage of injection	101
68	Fig.4.22 (c) Static temperature (K) contours for the 1st stage of injection	102
69	Fig.4.22 (d) Mass fraction contours along the combustor for	102

	the 1st stage of injection	
70	Fig.4.23 (a) Mach number contours for the second stage of fuel injection	104
71	Fig.4.23 (b) Static pressure (Pa) contours for second stage of fuel injection	104
72	Fig.4.23(c) Static temperature (K) contours for second stage of fuel injection	105
73	Fig.4.23 (d) Mass fraction of species for second stage of fuel injection	105
74	Fig.4.24 (a) Mach number contours for third stage of fuel injection	106
75	Fig.4.24 (b) Static pressure (Pa) contours for third stage of fuel injection	107
76	Fig.4.24 (c) Static temperature (K) contours for third stage of fuel injection	107
77	Fig.4.24 (d) Mass fractions of species for third stage of fuel injection	108
78	Fig.4.25 (a) Mach number contours along combustor for 4th stage of fuel injection	109
79	Fig.4.25 (b) Static pressure (Pa) contours for fourth stage of fuel injection	109
80	Fig.4.25 (c) Static temperature (K) contours for 4thstage of fuel injection	110
81	Fig.4.25 (d) Mass fractions of species along combustor for fourth stage of fuel injection	111
82	Fig.4.26 (a) Comparison of flow field for staged fuel injection pattern	111
83	Fig.4.26(b) Comparison of flow field for staged fuel injection pattern (Mass fractions)	112
84	Fig. 4.27 Comparison of top wall pressures in full scale combustor	113
85	Fig. 4.27(a) Schematic diagram of the full-scale combustor	114
86	Fig. 4.27 (b) Variation of static pressure along the top wall of the full-scale combustor	116
87	Fig. 4.27(c) Variation of static pressure during the test	116
88	Fig. 4.27 (d) Variation of Temperature along the full- scale combustor	117
89	Fig. 4.27 (e) Variation of Temperature during the test	118
	PLATES	
90	I. Sub-scale Combustor	119
91	II. Full-scale Combustor	120

APPENDIX-1		
92	Fig A.1 (a) Top wall static pressure along the sub-scale combustor	137
93	Fig A.1 (b) Top wall static pressure along the sub-scale combustor	139
94	Fig A.1 (c) Top wall static pressure along the sub-scale combustor	140
95	Fig. A.1.2 (a) Variation of temperature with Time	141
96	Fig. A.1.2 (b) Variation of temperature with Time	141
97	Fig. A.1.2 (c) Variation of temperature with Time	142
APPENDIX - 2		
98	Fig.A.2. Schematic diagram of Full-scale combustor	143
99	Fig:A.2 (a) Variation of static pressure during 2nd test	143
100	Fig.A.2 (b) Variation of static pressure during 3rd test	144
101	Fig.A.2.(c) Variation of Temperature along the full- scale combustor	145
102	Fig.A.2.(d) Variation of Temperature along the full- scale combustor	146
APPENDIX-3		
103	Fig.A.3.1 Subscale Ramp Cavity Combustor	148
104	Fig.A.3.1 (a) Mach number contour along the combustor for non-reacting flow	149
105	Fig.A.3.1 (b) Mach number contour along the combustor for reacting flow	149
106	Fig.A.3.1(c) Static pressure contour along the combustor for non-reacting flow	150
107	Fig.A.3.1 (d) Static pressure contour along the combustor for reacting flow	150
108	Fig.A.3.1. (e) Comparison of numerical studies with experimental work for a sub-scale combustor.	151
109	Fig.A.3.1(f) Static temperature contour along the combustor for non-reacting flow	152
110	Fig.A.3.1 (g) Static temperature contour along the combustor for reacting flow	152
111	Fig.A.3.2 (a) Mach number contour along the combustor with fuel addition	154
112	Fig.A.3.2 (b) Mach number contour along the combustor with combustion	154

113	Fig.A.3.2 (c) Static pressure (Pa) contour for non-reacting flow	155
114	Fig.A.3.2 (d) Static pressure (Pa) contour along the combustor for reacting flow	155
115	Fig.A.3.2 (e)Static temperature (K) contour along the combustor for non-reacting flow	155
116	Fig.A.3.(f) Static temperature (K) contour along the combustor for reacting flow	156
117	Fig.A.3.2(g) Flow parameters along the combustor for non-reacting flow	157
118	Fig.A.3.2 (h) Flow parameters along the combustor for reacting flow at entry Mach 2.5	157
APPENDIX-4		
119	Fig.A.4.1 Comparison of flow field for wall injection with and without combustion.	158
120	Fig.A.4.1(a) Comparison of wall injection and fuel combustion with and without cavities	159
121	Fig.A.4.2 (a) Mach number distribution along combustor with combustor entry Mach 3	160
122	Fig.A.4.2 (b) Static pressure (Pa) distribution with combustor entry Mach 3	160
123	Fig.A.4.2 (c) Static temperature (K) distribution along the combustor with entry Mach 3	161
124	Fig.A.4.2 (d) Mass fractions of species along combustor with combustor entry Mach3	161
125	Fig.A.4.2 (e) Mass fractions of species across the combustor section	162
126	Fig.A.4.3 (a) Mach number contour along the combustor with combustor entry Mach 3	163
127	Fig.A.4.3 (b) Static pressure (Pa) distribution with combustor entry Mach 3	163
128	Fig.A.4.3 (c) Static temperature (K) distribution along the combustor with entry Mach 3	164
129	Fig.A.4.3 (d) Mass fractions of species along the combustor with combustor entry Mach 3	165

NOMENCLATURE

p	Static pressure
T	Total temperature
M	Mach number
Pa	Pascal
K	Kelvin
ρ	Density
μ	molecular Viscosity
Sc_t	turbulent Schmidt number
D_t	turbulent diffusivity
$\bar{\bar{\tau}}$	Stress tensor
R_i	the net rate of production of species i by chemical reaction
S_i	The rate of creation by addition from the dispersed phase plus any user-defined sources.
τ	the unit tensor
$M_{w,i}$	molecular weight of species i
$R_{i,r}$	Arrhenius molar rate of creation/destruction of species i in reaction r

INTRODUCTION

High speed propulsion could be a reality with the effective development of hypersonic flights. The ramjet and scram jet engines are credited with the working under such application. The limit imposed by deceleration of hypersonic free stream air to subsonic speeds in the combustion chamber results in dissociation of the combustion products, increase in the heat energy of the airstream such that further heat addition in the combustor becomes difficult. The ramjet engine works efficiently with subsonic air speed at the combustion chamber and heat addition becomes difficult at higher free stream flight Mach number and the engine will not contribute to the useful thrust. With further increase in speed, the terminal shock associated with subsonic combustion leads to both significant pressure losses and thereby resulting in considerable energy loss. Efficiency of combustion will be very low. It becomes more efficient to maintain the flow at supersonic speed throughout the engine and to add heat through combustion at supersonic speed. As the speed of the air increases beyond Mach 5, to overcome the problems of combustion with higher free stream Mach numbers, research efforts were initiated to work on supersonic combustion ramjets, called SCRAMJETS. Supersonic combustion Ramjet (SCRAMJET) is a tool to conquer the longer distances in shorter time scales. Realization of high speed transport within short time is possible with the development of scramjets. In supersonic combustion, hypersonic air stream of Mach 6 and above is allowed through the inlet where it is diffused to supersonic airstream through a series of oblique shock waves and enters the combustor. In the combustor, fuel is injected and mixed with the supersonic airstream and combustion takes place. Supersonic combustion continues to be a subject of research for combustion scientists working in the area of high speed propulsion.

In supersonic combustion ramjets, inlet, combustor and nozzle are important components from the design and performance perspective. Mixing and flame holding poses constraints due to the short span of length of the combustor and exotic materials are needed to withstand higher thermal loads within the combustor. Due to low residence time of the order of 1 ms in the combustor, it is very difficult to achieve sustained supersonic combustion and positive thrust. The flow field within the combustor of

Scramjet engine is very complex and poses challenge in design and development of supersonic combustor. Sufficient and rapid fuel-air mixing to achieve the desired chemical reaction and heat release within the short residence time, minimization of Stagnation pressure loss resulting in high Combustion efficiency are the requirements in the design of Supersonic combustor. Ignition and sustained combustion are required to be achieved within the short length of the combustor.

In supersonic combustor, effective mixing of the fuel and air is imperative for the scramjet combustor performance. Mixing of two high speed streams of air and fuel to achieve ignition, flame holding and sustained combustion are the major issues in supersonic combustion.

Hydrogen and hydrocarbon fuels have been studied for the applications of both space and military. Initial studies on scramjet combustor development have been conducted with hydrogen as the fuel. Hydrogen as a fuel has advantages of rapid mixing, combustion and high heat release due to its high energy content. The diffusive coefficient of hydrogen is very high. Hydrogen is reference fuel for supersonic combustion studies. Hydrogen is the candidate fuel in space applications. The chemistry of Hydrogen is simple. However, Hydrogen is used mostly for space applications. Due to its high specific volume, it is difficult to use Hydrogen for defence applications. Also, due to safety and storage space limitations, hydrocarbons are preferred as fuels in missiles. Of late, hydrocarbon fuels such as aviation kerosene, JP 7 have been used.

There are various methods of fuel injection attempted to achieve thorough mixing, ignition and sustained combustion in the Supersonic Combustor. The fuel injector distribution in the engine shall be such that it yields uniform combustion products before entering the nozzle for efficient expansion. At flight Mach numbers up to Mach 10, fuel injection may have a normal component into the flow from the inlet, but at higher Mach numbers, the injection must be axial to provide fuel momentum which provides significant engine thrust. Early scramjet research focused on both parallel as well as normal fuel injection to the main flow to explore the benefits associated with them.

In parallel injection, fuel flows parallel to the air in the engine but separated by a splitter plate. Shear layer is created at the end of the splitter plate which is formed due to different velocities of fuel and air. Shear layer is the primary source of mixing the fuel

with the air for proper combustion. Normal fuel injection consists of an injection port on the wall of a scramjet. The port injects the fuel normal to the flow of air. Normal fuel injection creates a detached normal shock upstream of the injector which causes separation zones upstream and downstream of the injector. The separation zones provided due to shock structure cause increased pressure losses that affect the efficiency of the engine. The downstream separation regions can be used as a flame holder. Due to poor mixing, combustion efficiency is low in this injection method.

Over the years, research has led to devise strategies for efficient fuel injection into high speed air such as wall injection, strut injection, Ramp injection, Cavity injection, use of pylons etc. However, each method has got its advantages and limitations. While wall injection ensures thorough mixing of fuel and air, the penetration is less and the stagnation pressure losses are very high. Parallel injection requires intrusive devices in the combustor such as ramps, struts and pylons. American and Japanese researchers worked on strut injectors to achieve the supersonic combustion [23, 24]. Russian and Chinese researchers studied the use of cavities for fuel injection and flame holding. Struts are useful for mixing the fuel with air but the blockage area is high. Cavities provide the re-circulation zones in the combustor which create conditions for increased residence time of air in the combustor and also act as flame holders. However, the stagnation pressure losses are high with the cavities. Cavities are classified as open or closed cavities based on the length-to-depth ratio and shear layer reattachment. Open cavities ($L/d<10$) are preferred in supersonic flow due to low pressure losses experienced by open cavities.

Very few researchers have tried out ramps for the fuel injection. Ramps are used to add axial velocity to the flow near the fuel injection with fuel injectors on the trailing edge of the ramp injecting fuel parallel to the flow. The flow over the ramps creates counter-rotating vortices that increase the mixing. Due to the supersonic flow in the scramjet, the ramps also create shocks and expansion fans which cause pressure gradients that also increase mixing. Compression ramps are elevated above the floor and expansion fans create troughs in the floor.

As discussed above, earlier research work has been carried out with fuel injection through wall and through fuel injection struts, ramps, cavities to achieve sustained supersonic

combustion but the issues still remain with limitations of mixing and sustained combustion. Also, the studies have been conducted with small, lab-scale combustors. While ramps are known to aid better mixing by creating vortices and pressure gradients in the flow, limited work has been reported on ramps.

It is observed from literature, that studies have been conducted mostly with Hydrogen as fuel and cavities are used as flame holding devices only. Ramps have been used in a limited way for fuel mixing with the supersonic airstream. The combined effect of ramps and cavities is not published widely in the literature.

In the present work, the use of ramps and cavities for mixing and flame holding in the supersonic combustor has been explored and studied. Hydro-carbon fuel, viz. aviation kerosene is used in experimental work. Supersonic test facility has been established. Hot vitiated air simulating the combustor entry conditions of pressure and temperature for Mach 2 to Mach 3 flow corresponding to free stream Mach numbers of 6-8 is used to conduct the tests. Supersonic nozzles have been realized. Combustor hardware including ramps and cavities, both constant area combustor and divergent combustor in sub-scale and full scale have been designed and developed. Tests on three sub-scale and three scaled combustors have been conducted. Ramps are made and integrated with the combustor in constant area section. Pilot Hydrogen has been used to provide temperatures in the combustor for self ignition of aviation kerosene injected in liquid form. Wall pressures are measured along the centreline of the top wall of the combustor. Gas temperatures in the combustor have also been measured.

Experimental studies involve cost intensive facilities for arriving at optimal design with the consideration of parameters affecting supersonic combustion. Simulation studies permit to arrive at optimization of systems and processes. Numerical studies have been conducted by researchers mainly with Hydrogen as fuel investigating the flow field for estimating the performance. In the present work, numerical studies have been conducted with Hydrogen as a fuel for mixing studies and combustion studies are carried out using aviation kerosene and gaseous ethylene fuels injecting into Mach 2, 2.5 and Mach 3 airstreams. Commercial software, Fluent version 15.0 is used for CFD studies. Unstructured grid has been used. Grid independence study has been carried out. Flow field has been evaluated. Performance of Ramp-Cavities has been studied in terms of

pressures, temperatures and thrust values. Variation in Mach number, injection flow pattern and fuel mass flow rate (fuel equivalence ratio) has been studied and analysed. For the combustor configurations that are used in investigation, the optimum fuel injection pattern and fuel mass flow rates have been generated.

1.1 Background:

Ramps are useful for injection and mixing of fuel with supersonic stream of air. Cavities provide re-circulation zones of high temperature fuel-air mixtures aiding for self-ignition and flame holding. Cavities are useful for flame stabilization in supersonic combustors. Details of ramps and cavities are briefly given in the following.

1.1.1 Ramps:

One of the strategies to overcome the mixing issue is generation of axial vortices. Axial vortices possess a better far field mixing characteristics. They propagate to a considerable distance, even with the suppressing tendency of the supersonic core flow. Ramp injectors generate axial vortices. Figure 1.1 and 1.2 depict the characteristics of Ramp injectors' flow field.

The following are the features of the ramp injectors.

1) The spillage vortices (contra rotating vortices) are generated by Ramp compression.
2) Pre-compression is carried out by the Ramp face produces favourable region for fuel injection.
3) Stagnation region is observed near the leading edge of the Ramp injector
4) Baroclinic torque is generated by the interaction of reflected shockwave with the base injection.
5) Generation of Recirculation zone at the Ramp base helps in flame holding and stabilization
6) Lift-Off of the contra rotating vortices from the wall is observed which is due to Magnus effect.

The strength of the spillage vortices increases with increase of core flow Mach number, thus retaining the performance at higher operating conditions.

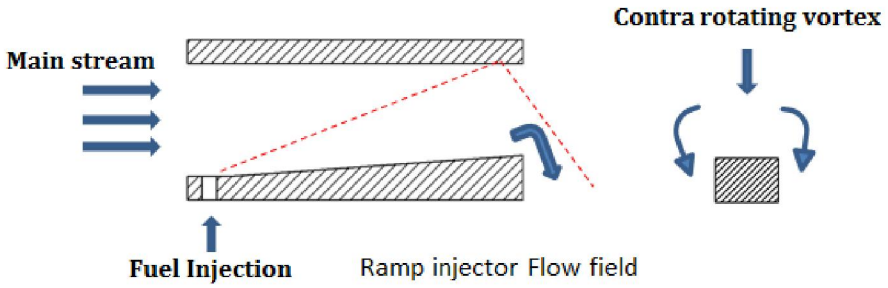

Fig.1.1 Ramp injection

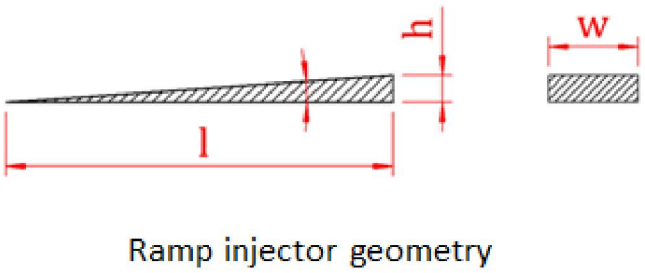

Fig.1.2 Ramp injector geometry in sub-scale combustor

1.1.2 Cavity based injection:

Generation of acoustic oscillations is also considered to be a better candidate to achieve mixing. Unsteady shear layers generate acoustic oscillations. Wall mounted cavities generates these oscillations to aid the mixing enhancement. Fig 1.3 shows Cavity that is characterized by L/D ratio. Cavities are classified by the shear layer separation and its reattachment. For cavities of L/D less than 5, the shear layer reattaches way past the trailing edge of the cavity and generates acoustic oscillations. These cavities are called as 'Open Cavities'. This type of oscillations aids in penetration of fuel. For L/D more than 7, the separated shear layer attaches to the bottom wall of the cavity, which aid in flame holding characteristics. These cavities are 'Closed cavities'. When L/D is one or close to one, they are square and transition cavities. They exhibit a very low level of oscillations.

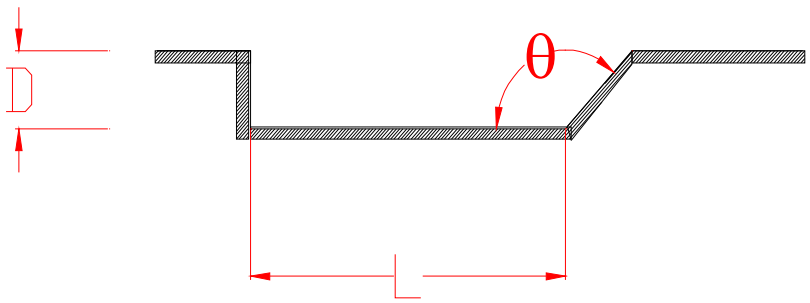

Fig: 1.3 Cavity injector geometry

The following are the main features of the cavity injectors.

1) Cavities increase the residence time of the fuel.
2) Weak shock waves are generated at the leading edge of the cavity caused by the separated shear layer that is followed by an expansion.
3) There will be a strong shock at the trailing edge, caused by the shear layer reattachment.
4) If the trailing edge is at an angle, then the strength of the trailing edge shock is reduced and acoustic oscillations will be suppressed proportionally.
5) Fuel distribution is carried out because of the compression shock generated at the leading edge & expansion waves at the ramp base and thus increasing the lateral spread of the fuel.
6) Vortices shed from the cavities help better mixing and scooping out of fuel trapped in the cavities.
7) Micro mixing is done by acoustic mode oscillations
8) Re-circulation zone at the cavities is useful for flame holding and stabilization
9) Cavity avoids Thermal choking by increasing the flow area.

1.2 Organization of the thesis:

This report includes a review of literature on the experimental and computational work carried out on supersonic combustors, fuel injection devices, mixing and flame holding under Chapter-2. Methodology for carrying out computational studies and experimental programme in the present study is described in Chapter-3. A discussion on the results obtained from the experimental program is presented in Chapter-4. Summary and conclusions drawn from the present investigation are listed out in Chapter-5. Recommendations for the future work and a list of references are presented at the end. Appendices include the experimental and computational studies on sub-scale and full-scale combustors.

LITERATURE REVIEW

Aero thermodynamic ducts (Athodyds) are the devices that are commonly employed in air-breathing propulsion. The essential feature of these devices is that there are no rotating parts that distinguish from other aero engines. Ramjets and scramjets are the widely employed athodyds for high speed propulsion. Rene Lorin of France is credited with the invention of the ramjet engine, in 1913. Athodyds can operate with a higher maximum cycle operating temperature as the limit imposed by turbine presence on the maximum cycle operating temperature can be increased. The ramjets do not take-off by themselves and are not efficient at low subsonic speeds as the air dynamic pressure is not sufficient to raise the cycle pressure to efficient operational values. Ramjets are useful to meet the requirements of increased thermal efficiency in the free stream Mach number range of 1-5. If the free stream Mach number increases beyond 5, Ramjets are not efficient because of the inability to add further heat to already high enthalpy airstream, molecular dissociation and terminal shock generation with the subsonic combustion. To overcome the issues with subsonic combustion at higher Mach numbers, supersonic combustion is a potential alternative. Supersonic combustion is a challenging area of interest to the combustion community. In supersonic regime, the air residence time is of the order of milliseconds between the air capture at the inlet and exit from the nozzle. Mixing and combustion of fuel in the supersonic airstream are two key issues in the development of supersonic combustor. To arrive at the present scope of research, a detailed literature review along with the efforts made by different researchers in achieving supersonic combustion is presented.

2.1 Overview of SCRAMJET Development:

Research efforts in the area of scramjet combustion are initiated about sixty years ago. Curran (2001) reviewed the Scramjet research efforts worldwide. He brought out the research work conducted in fundamental areas as well as application in the realization of the scramjet engine.

Initial work was done by Ferri (1964) and Billig (1972) on the basic, fundamental processes and issues related to shock structures and heat release due to combustion. Work

included building fixed geometry engines over a wide range of Mach numbers and maximising the performance of engines.

2.2 Studies on Supersonic combustion:

Ferri (1964) worked on the supersonic diffusive combustion system. He worked on chemistry of Hydrogen air system, analyzed the problems related to turbulent mixing. He worked on the shock structures that avoid the issues related to heat release that result due to combustion. After working on the fundamental issues, he worked on scramjet engines that are built on fixed geometry. His efforts were to maximize the performance of these engines over a wide range. He concluded that a three dimensional engine could address the issues, if thermal compression effects are considered in the design.

Billig (1972) carried out an analysis of the thermodynamic processes related to supersonic combustion and concluded that performance gains can be theoretically achieved at lower Mach numbers. He worked on matching the fuel injection processes to produce the required regions of thermal compression.

Billig *et al.* (1972) conducted basic work on supersonic combustion ramjet missile (SCRAM) programme to develop ship launched missile for U.S. Navy. It is envisaged to use hydrocarbon fuel. In his tests, he used various methods of injection. He evaluated combustors with different geometries. Reactive fuels such as HiCal-3-D and hydrocarbon-pentaborane blends were used. His work resulted in developing combustor-inlet isolators to prevent adverse flow reactions.

Meshcheryakov and Sabelnikov (1988) studied divergent ducts for supersonic combustion and estimated the combustion efficiency. They also studied complex structure of pseudo shocks. With these studies, large amount of data base was generated. Russian research concentrated on mixing and combustion processes in two and three dimensional ducts with various fuels, ignition systems and flame stabilization devices for both scramjet and dual mode engines.

Vinogradov *et al.* (1990) documented the results of fixed geometry two-dimensional model with three shock inlet. The tests were conducted at a design Mach

number of 6 and were carried out at CIAM. Axi-symmetric class of engines was also tested extensively. In both models, multiple cavities were used for flame stabilization.

Rothstein (1992) studied the effect of Hydrogen injection into a heated supersonic flow using Planar Induced Fluorescence (PLIF) method. In his studies, Hydrogen jet was injected at sonic velocity into supersonic, Argon-oxygen stream at Mach 1.5 condition. PLIF was used to capture the flow field with hydroxide radical tracking. Jet penetration depth was measured during the experiments. Jet to free stream dynamic pressures was compared in the higher range. Empirical relations were formed for jet penetration depth. Temperatures in the reacting flow were calculated.

Billig and Sullins (1993) developed classic modelling approach for SCRAM work. This approach was based on Crocco power law relationship. This was used in the modelling of Scramjet combustion processes including wall shear and heat transfer. These studies were aimed at overall optimization of the scramjet engines. This was successfully used in Dual mode combustion ramjets.

Sabelnikov *et al.* (1993) reported on the German-Russian scramjet technology research and development effort. The experimental programme was carried out with connected-pipe testing of a rectangular subscale combustor and free jet testing of subscale scramjet engines. Combustor configuration was evolved with isolator, rectangular divergent section with a step configuration and a diffuser section. Tube injectors, wall-mounted ramp injectors and wedge shaped, partial span swept strut injectors were used with single and stage injection. Tests were conducted at Mach 6 conditions to obtain valuable data.

Chase and Tang (1995) explained the formation of National Aerospace Plane (NASP) project aimed at developing Single stage to orbit vehicle, X-30. It is planned to use Hydrogen fuel with this vehicle over a range of Mach 4-15. Under NASP programme, a rectangular airframe integrated scramjet development was planned, component technology base was developed and modular engines were tested in Mach 4-7 with three-strut configuration and step strut design.

Walther *et al.* (1995) described the subscale rectangular combustor tests at Mach 5 and 6 conditions under German-Russian joint research. The engine was constructed with a three ramp inlet, an isolator, a divergent combustor and a divergent exhaust

nozzle. These tests showed that there is a strong coupling between combustor and inlet at Mach 6 condition which reduced at Mach 5.

Sancho *et al.* (1996) discussed the PREPHA programme of France. This programme concentrated on hydrogen fuelled scramjet technology. Studies included Computational Fluid Dynamics, materials, vehicle systems and test facilities. Rectangular combustion chambers with fuel injection struts were tested at simulated Mach numbers of 6. One strut is configured with normal, angled and base injection. The other strut consisted of expansion and compression ramp injectors.

Bouchez *et al.* (1996) worked on the fuel injection pattern through three injection struts at a nominal flight Mach number of 6. CFD models were used to obtain quantitative and qualitative flow models. These models were compared with experimental measurements. CFD approach was used to resolve issues of ignition, flame stabilization, mixing and combustion efficiencies, the studies also included total pressure losses in the combustor and unsteady flow conditions. In this study, point of origin of the pre-combustion shock in the combustor was determined.

Bouchez *et al.* (1996) described Wide Range Ramjet (WRR) approach which uses variable geometry combustor with moving panels that are actuated by computer control for maximizing the performance. WRR operates with kerosene fuel in subsonic combustion mode and with hydrogen fuel in supersonic combustion mode. Further higher speeds are achievable with the use of oblique detonation wave. Physical variable throat can be used in WRR configuration.

Mitani *et al.* (1997) reported an extensive testing on a two dimensional subscale engine at simulated flight Mach numbers of 4, 6 and 8 using hydrogen as fuel. The fuel injection was through top wall and / or side wall for pilot and main fuel injectors which provided both perpendicular and parallel injection. Strut was used as a compression device. They found that inlet-combustor interactions were attenuated with shock generating ramps in the flow path.

Tani *et al.* (1997) described the effects of varying the engine internal geometry on internal aerodynamic performance. It was found that central full span strut ensures fuel distribution across the height of the duct but splits the flow into two smaller channels. It generates a bow shock that can cause boundary layer separation at the wall, adding

further blockage to the already reduced flow area. The reflected shock interaction with fuel injection- ignition processes was also studied.

Paull and Stalker (1998) described testing of scramjet combustors in T4 tunnel at the University of Queensland. Mixing and combustion studies were conducted with hydrogen as fuel. Effect of shocks on mixing and burning, skin friction measurements and numerous gas dynamic investigations were carried out. Data was collected to correlate the ground and proposed flight test, Hyshot, programme data.

Raush *et al.* (1999) described the NASA initiative on airframe-integrated dual mode scramjet powered X vehicles, called Hyper-X. X-43 A, a small hypersonic aircraft was to be air launched with a booster stage from B-52 aircraft. McClinton *et al.* (1999) explained the flight launch plan of X-43A vehicles at Mach 7 and Mach 10 demonstrating the 5s of combustor burning time. This project is initiated by NASA.

Faulkner *et al.* (1999) described the development of a two dimensional, dual-mode, and hydrocarbon scramjet engine for missile propulsion in Mach 4-8 regime. This programme by U.S. Airforce was named HyTech. The engine design used a mixed compression inlet and a fuel cooled structure for the internal flow passage.

Kanda *et al.* (2000) studied the scramjet engine through experiments at Mach 8 condition using Hydrogen as fuel. Strut was used in the combustor along with the ramp block downstream of the strut. They observed good burning when fuel was injected normally. Startability of the inlet was good due to high pressure in the inlet caused due to ramp compression surface. It was recommended that parallel fuel injection and normal fuel injection should be carried out together. Thrust increases with the improved geometry of the ramp compression block.

Gruber *et al.* (2000) evaluated the combustor performance with fuel injection from two aero-dynamic ramps. Wall cavity is located downstream injectors for flame holding. Experimental studied simulated flight Mach number of 4-5 and compared with baseline configuration which consisted of a cavity of L/d = 4.8 with upstream hydrogen fuel injection from wall flushed injection at 15^0 low angle. Aerodynamic ramp was configured with 9 injectors arranged in an array of 3 rows, arranged at an angle. They observed that the baseline injection is better in terms of mixing, fuel-air distribution, combustor pressure ratios, thrust levels and range of operating equivalence ratios.

Abdel Salam *et al.* (2000) studied numerically mixing process in scramjet combustor with raised and relieved ramps at 0^0 and 5^0 side sweep angles. Fuel injection was parallel to the airstream. They observed that the unswept relieved ramps provide better mixing than unswept raised ramps. However, swept ramps were found to be better in mixing both in non-reacting and reacting flows.

Eklund *et al.* (2001) investigated numerically the effect of aerodynamic ramps in a dual mode scramjet combustor. Ethylene was used as fuel. Cavity was used as flame holder. Three step models were used for modelling Ethylene kinetics. Equivalence ratio was 0.70. They found that the mixing and combustion were not good with the aerodynamic ramps. Ignition, pressure rise and heat release were not seen in the dual mode combustor.

Aristides *et al.* (2003) studied the aero ramp configuration with plasma torch for ignition and flame-holding in scramjet combustor experiments. They have studied the combustion with hydrogen and hydrocarbon (ethylene) as fuels. They found that hydrogen combustion was comparable with unswept physical ramp injection experimental results. For ethylene combustion, air was used as feed stock for plasma torch and aerodynamic ramp continued to be flame holder for longer time during the experiment after the plasma torch was extinguished. Wall pressure rise was continuous along the combustor length.

Shrinivasan *et al.* (2004) conducted experiments with strut based cavities and strut based ramps to study the mixing pattern in supersonic flow with transverse injection. They varied the injection location in their experiments. Mole fraction contours of all cases were compared. Wall pressure measurements were taken. They observed that mixing and mixing length are better with cavities for good mixing. In cavities, injection upstream of the cavity is better. They have also studied and found that in case of ramps, injection just upstream of the ramp is better location.

Aristides *et al.* (2005) conducted experiments in a Mach 2 supersonic air flow to evaluate aerodynamic ramp injector. Hydrogen and ethylene were used as fuels. Wide range of equivalence ratios was tested. Wall pressures and wall temperatures were measured. Ethylene was operated within the limits of $0.14 < \varphi < 0.48$. With hydrogen fuel, combustion was good and comparable with physical ramp combustor with lower tunnel temperatures. Combustion efficiencies varied from 75% for a low equivalence

ratio to 45% at the highest equivalence ratio. Both subsonic and supersonic combustion could be observed.

Aristides *et al.* (2006) studied scramjet combustor with methane and ethylene as fuels. Aero ramp was used for injecting fuel and plasma torch ignited the fuel. Mach 4 condition was tested. Equivalence ratios were varied to find out the operability ranges of the combustor. Wall pressures and temperatures were measured to indicate the combustion. Subsonic and supersonic modes of combustion were observed with good combustion in case of ethylene fuel. Methane fuel did not give better results as with ethylene in the studies. There was good comparison with CFD simulations.

Pandey and Singh (2010) reviewed both experimental and computational studies on flow field of supersonic combustor with different fuels for better mixing and flame holding.

HOU Lingyuna *et al.* (2011) conducted numerical studies on three dimensional reacting flows in a staged supersonic combustor. They used a swept ramp injector as the second stage wall injection to obtain the optimum stream-wise vortices. Central strut injection was used in the first stage. They found that residual oxygen was used in the second stage fuel injection near the wall and caused more heat release. Further, the strong shock waves in the isolator were avoided and wall pressure rise could be found with more fuel burning and without thermal choking. Parallel injection from the swept ramp injector resulted in low total pressure loss and higher combustion efficiency.

Chapuis *et al.* (2012) carried out a comprehensive numerical study of the HyShot II Scramjet combustor. Reynolds Average Navier Stokes (RANS) based models and Large Eddy Simulation (LES) based models with semi-detailed reaction kinetics were used. The mixing – combustion physics on the flow in the High Enthalpy Shock Tunnel Go'ttingen (HEG) were focussed. Computational data from RANS and LES computations were combined with data from the HEG experiments and compared with the Hyshot II flight tests at two different flight altitudes(28 and 33 km). It was observed that LES model captured the experimental wall pressure and heat flux data well for both 33 km and 28 km. RANS model predicted wall pressure and heat flux data for 28 km case only. Flow is found to be unsteady at both the altitudes and equivalence ratio is important, riches mixtures being prone to transitional flow features.

Manna *et al.* (2013) conducted numerical work on optimization of flight worthy scramjet combustor with struts as fuel injection and mixing device with hydrocarbon fuel. They found unburnt kerosene in the base line configuration. With modified fuel injection and modified strut locations, they observed improvement in thrust (18.3%) and combustion efficiency (18.6%). compared to the baseline configuration.

YeTian *et al*. (2015) investigated the effect of equivalence ratio and fuel distribution on combustion performance at Mach 2.0 condition. Numerical simulations and experiments were conducted. With equivalence ratio of 0.6, there were differences in combustion performance of different fuel distribution cases and when the total equivalence ratio was 0.8, the combustion performance was same for all cases of fuel distribution. It was observed that the flow structure of dual mode scramjet was stable when the subsonic combustion happened. With the increase of total equivalence ratio, there was thrust increase.

Tahsini and Mousavi (2015) investigated the effect of impinging oblique shock on combustion efficiency when hydrogen was injected into the supersonic cross flow. The 2D simulation showed that the shock impinging upstream of the injection slot, tilting the fuel jet to the upstream, increasing the oblique shock strength, and using hydrogen peroxide in fuel stream increase the combustion efficiency.

Wei Huang *et al.* (2015) studied numerically the mixing process between the injectant and air in supersonic flow. They investigated the interaction of oblique shock wave with the hydrogen jet and the angle of the wedge. They observed that the incident shock wave influences the mixing and the wedge angle of 20^0 in the range considered for study and at the wedge angle hydrogen is in the separation zone upstream of the jet orifice.

Zong *et al.* (2015) have conducted experiments with ethylene fuel in a model combustor with cavities and struts upstream of the cavities. Fuel was injected from the strut leading edges and duct wall located upstream of the cavity location. They observed that as more fuel is injected from strut, combustion will shift to divergent combustor and flow becomes supersonic due to availability of rich fuel in that zone.

2.2.1 ***Summary***: *It is observed from the literature that both experimental and computational investigations have been carried out to understand flow field characteristics in supersonic combustion. Initial investigations were concentrated on establishing the basic features, aero-thermodynamic relations and addressing the fundamental issues related to supersonic combustion. In an attempt to attain supersonic combustion, mixing and flame stabilization are observed to be the challenges. Researchers attempted to improve mixing of fuel-high velocity air stream for better combustion. Mixing studies were conducted by employing various mixing devices such as struts, cavities, pylons and ramps. It is observed that predominantly, hydrogen was used as fuel while hydrocarbon fuels were also tried out. Investigations were also carried out for flight testing of SCRAMJET engine. Studies with very high Mach numbers (M 4-15) are also tried out.*

2.3 Studies on effect of Ramps and Cavities:

Supersonic combustion with cavities has been studied experimentally and numerically by researchers. There is extensive published literature on cavities in supersonic combustion. In case of application of ramps, the work was carried out mainly with aero-ramps and to some extent with physical ramps. The work carried out with physical ramps for mixing and cavities as flame holders in a combustor is not much published in literature. Ramps are mostly referred in the inlets, ahead of fuel mixing and as cavity aft walls.

Stouffer *et al.* (1993) used four wall ramps in a supersonic combustor and injected Hydrogen fuel from the base of compression and expansion ramps in their experimental work. They observed auto-ignition occurred instantly for compression ramps and pilot hydrogen or saline was used for ignition of fuel from expansion ramps. Wall pressures and heat flux measurements were made. It was found that heat flux varied across the length and width of the combustor. Effect of fuel equivalence ratio on Mach number, wall pressures and combustion efficiency was studied.

Miller *et al.* (1996) studied experimentally the application of swept ramp injectors for fuel injection in supersonic flow. One set of compression ramps and one set of expansion ramps were used for comparison. UV emission imaging and Planar Laser Induced Fluorescence (PLIF) imaging are used to study the near field mixing. IR water

emission diagnostic was used for studying the far field mixing. Compression ramp injector ignited within short length compared to expansion ramp injector. They observed similar amounts of penetration for both compression and expansion ramp injectors. The combustion efficiency was found to be less than 50%.

Wilson *et al.* (1997) conducted experimental studies on the role of ramps in improving the penetration and mixing of fuel (Mach 1.9) with supersonic air stream at Mach 2.9. Fuel was injected at an angle of 25^0 parallel to the compression ramp. They have studies seven cases of compression ramps. They identified mechanisms like baroclinic torque, vorticity, magnus force for increasing the mixing. Shadowgraph and Mie scattering techniques were used to analyze the flow field. They observed that the penetration increased by 22%, plume expansion, a measure of mixing efficiency by 39% and concentration decay rate 27%. There was a total pressure loss of 17% with the use of ramps in the low angled injection.

Baurle *et al.* (1998) studied supersonic missile combustor both numerically before test and experimentally. Wall mounted fuel injection with cavity flame holders was employed in a pilot combustor configuration. Both reacting and cold flow conditions were simulated. They observed good mixing. Total pressure losses were minimum. With the reacting flow simulation studies, it was possible to make corrections to the combustor and avoid thermal choking. Simulations were comparable with experiments.

Gruber *et al. (*1999) carried out fundamental studies to evaluate the concepts of cavities as flame holder in supersonic flows. Experimental studies were conducted with open type cavities for two L/d ratios. He studied different aft angles of cavity and offset ratios in a non-reacting flow field. Effect of the cavity geometry on the shear layer, pressure, residence time has been identified and computational analysis of the flow field has been carried out.

Tarun Mathur *et al.* (2001) conducted supersonic combustion experiments with wall mounted cavities. Gaseous ethylene fuel was injected upstream of the cavity into supersonic air stream at Mach 1.8 and Mach 2.2 conditions. They observed combustion with equivalence ratios in the range of 0.25 to 0.75. In these experiments, spark plug was used as ignition source. They found intense combustion which was captured with the

video recording. They carried out one dimensional analysis and estimated a combustion efficiency of around 80% with skin friction coefficient of 0.0028.

Yu *et al.* (2004) investigated kerosene combustion in a Mach 2.5 flow using a model supersonic combustor with a cross section area of 51mm x 70 mm. Cavity modules were integrated as fuel injectors and flame holders. Experiments were conducted with pure liquid and with effervescent atomization. They characterized the flow conditions and compared. Direct photography, schileren imaging and planar laser induced fluorescence (PLIF) imaging of OH radical were used to examine the cavity characteristics and spray structure. They found effectiveness of gas barbotage in atomization and secondary atomization when kerosene sprays interact with a supersonic cross flow. Through OH PLIF images, it was confirmed that a local high temperature radical pool exists within the combustor. Measured static pressure distributions showed that effervescent atomization leads to better combustion performance. It was also observed through the experiments that those cavity characteristics are different in non-reacting and reacting supersonic flows.

Kyung Moo Kim *et al.* (2004) carried out numerical study on supersonic combustion with cavity based hydrogen fuel injection. Slot nozzles were used. Reactive flow field was studied with various inclined cavities with different wall aft angles, offset ratios and combustor lengths. They found that cavities enhance mixing and combustion while increasing the total pressure loss compared with no cavities - case. They have concluded that there exists an appropriate length of the cavity with respect to combustion efficiency.

Tianwen FANG *et al.* (2008) investigated the characteristics of supersonic cold flows over cavities both experimentally and numerically. The effects of cavities of different sizes on supersonic flow field were analyzed. They found that cavities with length to depth ratio of 5-9 are useful. The cavity rear wall angle between 30º to 60º will not affect the cavity flow but affects the shear layer and vortices in cavities.

Ming-Bo Sun *et al.* (2008) studied experimentally the flame characteristics in a supersonic combustor with cavities when hydrogen fuel was injected upstream of the cavity. OH – planar laser induced fluorescence was used to track OH radical in the flow field. Cavity L/d of 7 was used. They observed that cavity shear layer anchors a steady

flame, jet-induced vortices help in transport of combustion products into jet. Flame spreaded with the counter rotating vortex until the ignition completed. Products of combustion flow into the cavity due to cavity shear layer move to cavity front wall due to recirculation, heating the cavity and thereby pre-heating the fuel in the cavity.

Kumaran and Babu (2009) studied numerically supersonic combustion in three model combustor configurations with cavities and kerosene as fuel. Non- reacting and reacting flow conditions were explored. They have observed that the penetration and spreading of the fuel increased with the increased fuel injection pressure in the reacting flow condition. Combustion efficiency values are more realistic when spray model was used for modelling the injection of the fuel.

Rajasekaran *et al.* (2009) studied numerically the supersonic combustor with kerosene fuel in a Mach 2.5 flow. Cavities are located in the combustor. The flow field has been studied. They observed that the wall pressures have been compared with experiment except in cavity region where pressures are over-predicted due to combustion. Vikramaditya and Job Kurian (2009) studied the pressure oscillations in a supersonic cavity. Ramps of different angles have been used in the experiments. Unsteady pressure measurements have been carried out at the floor and walls of the cavities. Ramp angles of 15^0, 30^0, 45^0, 60^0, 75^0 and 90^0 have been studied. With cavity ramp angle of 45^0, decreases the amplitude of oscillations and acoustic wave was not observed. Higher velocity was found in ramp angle of 30^0 and no acoustic wave in 15^0 ramp angles.

Pandey *et al.* (2011) carried out CFD analysis of wall injector with cavity at Mach 2 condition. Hydrogen was used as fuel upstream of the cavity. They observed high thrust and low shock formation with a maximum temperature of 2100K.Wei Huang *et al.* (2012) have studied the effect of geometric parameters on the drag of the cavity flame holder based on variance analysis method. They have numerically studied the hydrogen fuelled scramjet combustor with a cavity flame holder. The effect of geometric parameters, i.e., upstream depth, ratio of length to upstream depth, ratio of downstream to the upstream depth and the swept angle on the drag force of the cavity flame holder for a heated flow were studied using variance analysis method. They found that the ratios of the upstream depth to the downstream depth and length to the upstream depth are

substance on the drag force of the cavity flame holder. The drag force of the cavity flame holder is the largest if the downstream depth is equal to the upstream depth.

Mishra and Sridhar (2012) carried out a numerical study on the effect of fuel injection angle on the performance of a 2-D supersonic cavity combustor. In this study, direct injection of hydrogen fuel into the cavity with various injection angles for no-reacting and reacting flow conditions was studied using Fluent software. They have observed low velocity recirculation zones. They found that 135^0 injection angle leads to maximum pressure losses in non-reacting conditions and 120^0 in reacting conditions. 120^0angle shows better mixing. Injection angle does not affect air entrainment. 120^0 injection angle shows highest combustion efficiency due to mixing in reacting conditions.

Hangbo Wang *et al.* (2013) investigated the characteristics of cavity assisted hydrogen jet combustion in a supersonic flow at a Mach number of 2.52, simulating flight Mach 6 conditions. With various cavity configurations, fuelling schemes and equivalence ratios, they found that combined cavity shear-layer/ recirculation stabilized combustion mode seemed to be the most robust one with a cavity flame holder.

Mohamed Arif and Sangeetha (2013) carried out computational analysis of a scramjet engine combustor with the multiple ramp-cavity injectors for both cold flow and reacting flows. They used different configurations of cavities, backward facing step and ramp configurations with different fuel injection angles in the model combustor. They observed that ramp-cavity injectors help to lift the fuel away from wall and enhance the mixing and flame holding and explained the extent of combustion in terms of temperature and pressure.

Zhen Huaping *et al.* (2013) conducted numerical investigation on interaction of jet with supersonic laminar flow with a compression ramp. They have defined relative increment of normal force and jet amplification factor as the criterion for evaluation of jet control performance. They found that 120^0 is relatively optimal angle. There is no influence of jet temperature on pressure distribution in cold gas simulations. They observed that when the pressure ratio of jet to free stream is fixed, the relative force increment varies little with increasing Mach number and the jet amplification factor increases. Wei Haung *et al.* (2013) investigated the performance of cantilevered ramp injector in supersonic flow with Mach 2condition. They observed that the cantilevered

ramp injector with higher swept and ramp angles has higher combustion efficiency and higher drag force.

Haiyan Wu *et al.* (2013) studied both numerically and experimentally the effect of cavities and heat transfer mode of the cavities with hydrogen fuel. Nero-particle Plane Laser Scatter and Plane Laser-induced Fluorescence methods were used to study shear layer of the cavity. Large Eddy Simulation (LES) was used to study the effect numerically. They analyzed the shear layer effect on supersonic flow, heat transfer in combustion and transpiration cooling in cavities. They observed that flame spreads to the upstream through the shear layer of the cavities, wall temperature at cavity aft edge is highest and wall materials are protected by transpiration cooling.

Nitin (2014) numerically studied double cavity combustor with liquid hydrogen fuel injection in the Mach 2 supersonic flow. He observed cavities help in flame stabilization with higher static temperature and more vortex zone in cavities. Jeyakumar et al (2014) investigated experimentally the characteristic of axi-symmetric aft ramp cavities in Mach 1.3 flow. Cavities with fillets at fore-walls and no fillets were compared. They found aft ramp cavities with fillet provide better mixing and fewer losses in total pressure.

Pratheek Srivatsava and Pandey (2014) numerically investigated hydrogen fuel injection into Mach 4 supersonic airstream just upstream the cavity. The cavity L/d ratio is considered 3. They have used species transport model for combustion. They observed increased mixing and combustion efficiency and increased pressure loss. They noted that there is a particular length of the cavity to match with the higher combustor efficiency and reduction in total pressure loss.

Zhang *et al.* (2014) have conducted experimental studies on model combustor at Mach 2.5 with cavities using vaporized kerosene as fuel. Injection of fuel was carried out in two stages with two dislocated cavities to study the combustor performance parameters. Injection pattern was studied to understand its effect on wall pressure, thrust increment, temperatures and unstart condition of the combustor. They observed that the total equivalence ratio of 0.5 equally injected from both injectors resulted in avoiding combustor unstart condition, higher wall pressures and higher thrust.

Ombrello *et al.* (2015) conducted experiments with two different ignition methods, spark discharge and pulse detonation (PD) techniques in a supersonic

combustor with ethylene fuelled cavity. They found PD produced high pressure and temperature exhaust allowing ignition at lower tunnel temperatures and pressures than the spark discharge. However, this also caused disruption to the cavity flow field leading to decreased cavity burning and extinction. Simulations showed decreased cavity burning, causing blockage of cavity fuel due to high pressure from detonation until PD exhausted. When cavity is filled sufficiently, the decrease in burning during PD ignition process could be avoided.

Barnes and Segal (2015) conducted experiments with cavities as flame holders. They observed that complex flow field due to interaction between the cavities and the core supersonic flow. Cavity oscillations, dynamics of cavity-free stream shear layer, dynamics of cavity recirculation zones, effect of cavity geometry on the local flow field, effect of fuel injection parameters on local mixing, fuel injection parameters and conditions on flame holding, blow-out were studied and cavity blow out limits are found to be sensitive for non-reacting and reacting conditions.

Amaranatha and Jack Edwards (2015) carried out LES /RANS simulation of ethylene combustion inside a cavity flame holder combustor. Combustor with cavity on the top wall and injection upstream and into the cavity were used. Analysis of the flame structure predicted by the LES/RANS method indicates that the flame propagates into a stoichiometric to fuel-rich mixture near the cavity. CO completely converted to CO_2 by the time the flow reached exit of the combustor.

Sivabalan Mani *et al.* (2015) have conducted numerical studies on the supersonic combustors with cavities.C_2H_6-CO_2-H_2O fuel is used with different cavities. They observed that cavities create a recirculation zone for flame stabilization. They identified that a cavity combustor with 45^0 forward ramp angle, injection at 1.6 times the hydraulic diameter from the inlet and injection at an angle of 45^0 opposing the main flow performs better with higher exit temperature.

***2.3.1: Summary**: It was observed that many researchers on combustion are focussing their interest on adopting, ramps and cavities, independently, for achieving mixing and flame stabilization respectively. Most of the work was carried out with hydrogen as fuel. Ramps of various kinds, viz., aero ramps, physical ramps, wall ramps, cantilevered ramps etc have been explored. Cavities with varying L/d ratios and different aft angles have been studied. Turbulence models such as RANS and LES have been*

largely used to understand the flow field characteristics. Advanced imaging techniques such as UV emission and PLIF have been explored for visualization of shocks and mixing pattern... Ramps could provide mixing due to contra rotating vortices that develop baroclinic torque. Cavities provide recirculation zones that increase temperature locally and act as flame holding devices. Studies also reported on fuel injection angle. Investigations were carried out in both non-reacting and reacting modes.

2.4 Observations from the Literature review:

a) SCRAMJET combustion is continued to be an area of research, predominantly in high altitude propulsion.

b) SCRAMJET combustor performance is evaluated in terms of static pressures and temperatures.

c) Hydrogen is the most commonly used fuel for combustion.

d) Efforts were made to improve mixing with devices such as struts, ramps and pylons. Aero-ramps have also been tried out.

e) Cavities were employed for flame holding.

f) Injection of fuel is done through wall, struts and cavities.

g) Studies were concentrated mainly on sub-scale models.

h) Flow visualization techniques were also employed.

i) Supersonic combustion phenomenon is combustor configuration specific.

j) Studies on combined effect of Ramps and Cavities are not reported, as seen from the available, published literature.

2.5 Motivation:

High speed propulsion is gaining lot of interest among combustion community. Studies all over the world are being focussed on achieving sustained supersonic combustion. Therefore, an attempt is made to investigate into the combined effect of ramps and cavities for the chosen combustor configuration.

2.6 Objectives of present studies and scope for present work:

In the present work, emphasis is given on achieving sustained supersonic combustion with the combined effect of ramps and cavities.

a) Experimental evaluation of Ramp-Cavity enabled combustor using aviation kerosene.
b) Experimental studies of the geometry effect on supersonic combustion with above configuration.
c) Conduct extensive numerical simulations for flow field analysis of the combustor with and without ramps, with and without cavities, with and without ramps and cavities.
d) Conduct computational studies and analyze the fuel injection strategies through Ramps.
e) Carry out computational studies and analyze the effect of variation in Combustor entry Mach number, fuel and equivalence ratio.

METHODOLOGY

The thesis work involves both computational studies and experimental efforts. Computational studies are carried out to establish the application of ramps and cavities in supersonic combustion. Effect of fuels, combustor entry Mach number, fuel equivalence ratio and fuel injection pattern have been explored with Ethylene as fuel on a full-scale combustor. Experimental facility has been designed and developed in Defence Research and Development Laboratory. Studies are carried out on sub-scale and full-scale combustors. The details are given in the two sections below.

3.1 Computational Studies:

Computational studies are carried out to study the effect of ramps and cavities for mixing and flame holding in supersonic combustion. Full scale combustor of cross section 275 mm x 86 mm and 1850 mm in length was considered for studies. This combustor is studied for development of Hypersonic Technology Demonstrator Vehicle. Fluent (version 15) software is used. The results of the studies are validated with experimental data. Simulations were conducted with Mach 3 entry condition and ethylene fuel. Studies are initially conducted (i) without ramps and cavities, (ii) with ramps, (iii) with cavities and (iv) with ramps & cavities to establish the role of ramps and cavities in mixing and flame stabilization. The performance of the combustor flow field is evaluated in terms of static pressure, static temperature and Mach number. The fuel is injected from staggered ramps configured in the combustor section on both top and bottom walls of the combustor. In the first three stages, two ramps are located each on top and bottom walls. In the fourth stage one ramp each on top and bottom wall is configured. Fuel is injected equally on the sides and edge of each ramp. Numerical studies are carried out to evaluate the mixing and flame holding for sustained combustion. Hydrogen, aviation kerosene and ethylene are the fuels studied. Parametric studies are carried out to study the effect of fuel equivalence ratio, fuel injection strategies and combustor entry Mach number. Fuel equivalence ratios are varied from 0.3 to 0.8 and the effect on Mach number, static pressure and static temperature including mass fractions of reactants and products are

studied. The variation in combustor entry Mach number and fuel injection configuration has been studied. Experimental conditions are simulated with aviation kerosene as fuel for Mach 2 condition.

3.1.1 Brief Introduction about package used:

The simulations are carried out using the ANSYS Fluent software. The software has been validated for hypersonic flows. Aviation kerosene, Hydrogen and gaseous Ethylene are used as fuels. For the present study, fuel injection has been considered in such a way that heat addition should not cause any upstream interaction leading to combustor non-start condition.

Simulations are carried out with combustor entry Mach number of 2, 2.5 and 3. ANSYS Fluent v15.0 software is used. The software has been validated for flows involving supersonic combustion. In the present work, the density based solver is used to transport the multi-species system. The transport equations are solved using the explicit discretization scheme. The realizable k-ε model with standard wall function is used to transport the multi-species system which is better compared to k-ω model. Single step chemistry model is considered. The laminar finite-rate model is used for solving the species volumetric reaction. This model computes the chemical source terms using Arrhenius expressions, and ignores the effects of turbulent fluctuations. Parallel processing is achieved through Message Passing Interface (MPI) technique.

BOUNDARY CONDITIONS

The stagnation pressure at the inlet to the combustor is 5 bar corresponding to the high altitude conditions. The inlet of the combustor model is defined as Pressure Far Field with different Mach Numbers. In each simulation, constant Mach number is considered at the inlet and hence Far field pressure condition is employed. The Outlet of the model is defined as Pressure Outlet. The inlet of the ramp holes is defined as the Mass Flow Inlet with total mass flow rate of 133 gm/s for equivalence ratio 0.6. Only half of the combustor is considered for simulation purpose, the wall along the length and at mid-point of the width is considered as symmetry plane. The combustor walls are considered adiabatic wall condition.

Parameter	Air	Ethylene
Po, bar	5	12
To, K	1000	253
M	3	-
Fuel mass flow rate	-	133 gm/s

- **Solver:** Density based solver with explicit scheme
- **Discretization**: Second order
- **Turbulence model:** ***k-ε*** Realizable model with enhanced wall functions
- **Species**: C_2H_4, O_2, CO_2, and H_2O for the case of Ethylene studies
- **Reaction model:** Laminar volumetric model
- **Fuel mass flow rate** : 133 gm/s (ethylene)
- **Fuel Temperature** : 253 K
- **Fuel Pressure** : 1200000 Pa (for ethylene)

3.1.2 Governing equations for computational studies:

The following governing equations are used for simulation in Fluent code

The Mass conservation equation:

The equation for conversation of mass, or continuity equation, can be written as follows:

$$\frac{\partial \rho}{\partial t} + \nabla.(\rho \bar{v}) = S_m \quad \ldots \quad (1)$$

The Source S_m is the mass added to the continuous phase from the dispersed second phase

Momentum Conservation Equations:

Conservation of momentum in an inertial reference frame is given as:

$$\frac{\partial}{\partial t}(\rho \bar{v}) + \nabla.(\rho \bar{v}\bar{v}) = -\nabla p + \nabla.(\bar{\tau}) + \bar{F} \quad \ldots \quad (2)$$

Where ρ is the static pressure, $\bar{\tau}$ is the stress tensor and $\bar{F}$ is and external body force respectively.

The Stress tensor is given by $\bar{\tau} = \mu\left[(\nabla \bar{v} + \nabla \bar{v}^T) - \frac{2}{3}\nabla.\bar{v}I\right]$

Where μ *is* the molecular viscosity, I is the unit tensor and the second term on the right hand side is the effect of volume dilation.

Energy Equation:

$$\frac{\partial}{\partial t}(\rho E) + \nabla.\left(\bar{v}(\rho E + P)\right) = -\nabla\left(\sum_j h_j J_j\right) + S_h \quad \ldots \quad (3)$$

Equations of State:

The transport equations described above must be augmented with constitutive equations of state for density and for enthalpy in order to form a closed system. In the most general case, these state equations have the form

$$\rho = \rho\,(p,T)$$

$$dh = \frac{\partial h}{\partial T} l_p\, dT + \frac{\partial h}{\partial p} l_T\, dp \quad \ldots \quad (4)$$

$$= c_p\, dT + \frac{\partial h}{\partial p} l_T\, dp$$

$$= c_p = c_p\,(p,T) \quad \ldots \quad (5)$$

Various special cases for particular material types are described below.

Incompressible Equation of State

This is the simplest case: density is constant and c_p can be (at most) a function of temperature

$$\rho = \rho_{spec}$$

$$dh = c_p\, dT + \frac{dp}{\rho}$$

$$c_p = c_p\,(T)$$

Ideal Gas Equation of state

For an ideal gas, density is calculated from the ideal gas law and c_p can be (at most) a function of temperature

$$\rho = \frac{wP_{abs}}{R_o T} \quad \ldots \quad (6)$$

$$dh = c_p\, dT$$

$$c_p = c_p\,(T)$$

Where w is the molecular weight, P_{abs} is the absolute pressure and R_0 is the universal gas constant

Mass Diffusion in Turbulent Flows

In turbulent flows, ANSYS FLUENT computes the mass diffusion in the following form

$$\bar{J}_i = -(\rho D_{i,m} + \frac{\mu_t}{Sc_t})\nabla Y_i - D_{T,i}\frac{\nabla T}{T} \quad \ldots \quad (7)$$

Where Sc_t is the turbulent Schmidt number, by default Sc_t is 0.7.

The Laminar Finite – Rate Model

The laminar finite–rate model computes the chemical source terms using Arrhenius expressions,

$$R_i = M_{w,i}\sum_{r=1}^{N_R}\hat{R}_{i,r} \quad \ldots \quad (8)$$

Where $M_{w,i}$ is the molecular weight of species i and $\hat{R}_{i,r}$ is the Arrhenius molar rate of species i

r, the reaction is written as

$$\sum_{i=1}^{N}\hat{V}_{i,r}M_i \leftrightharpoons \frac{k_{f,r}}{k_{b,r}}\sum_{i=1}^{N}\hat{V}_{i,r}M_i$$

Where

N = number of chemical species

$\hat{V}_{i,r}$= stoichiometric coefficient

$\hat{V}_{i,r}$= stoichiometric coefficient

M_i= denotes species i

$k_{f,r}$ = forward rate constant

$k_{b,r}$ = backward rate constant

For a non-reversible reaction,

$$\overline{R_{i,r}} = \Gamma\left(v''_{t,r} - v'_{t,r}\right)\left(k_{f,r}\prod_{f-1}^{N}[C_{j,r}]\ (n'_{j,r} + n''_{j,r})\right),$$

Where

$C_{j,r}$ = molar concentration of species j in reaction r (kmol/m^3)

$n'_{j,r}$= rate exponent for reactant species j in reaction r

$n''_{j,r}$= rate exponent for product species j in reaction r

For a reversible reaction,

$$\dot{R}_{i,r} = \Gamma\left(v''_{t,r} - v'_{t,r}\right)\left(k_{f,r}\prod_{f-1}^{N}[C_{j,r}]\left(n_{j,r} - k_{b,r}\right)\prod_{f-1}^{N}[C_{j,r}]\,v''_{j,r}\right) \quad \ldots (9)$$

$\Gamma$is the net effect of third bodies

$$\Gamma = \sum_{J}^{N} \gamma_{j,r} C_j$$

Where $\gamma_{j,r}$ is third body efficiency of jth species in the rth reaction.

The forward rate constant,$k_{j,r}$ is computed using the Arrhenius expression.

$$k_{f,r} = A_r T^{\beta_r} e^{-E_r/RT} \quad \ldots \quad (10)$$

Where

A_r = pre -exponential factor

β_r = temperature exponent

E_r = activation energy (J/ kmol)

R = universal gas constant (J/kmol-K)

$$k_{b,r} = \frac{k_{f,r}}{K_r}$$

$$k_r = \exp\left(\frac{\Delta S_r}{R} - \frac{\Delta H_r}{RT}\right)\left(\frac{P_{atm.}}{RT}\right)\sum_{i=1}^{N}\left(v''_{i,r} - v'_{i,r}\right) \quad \ldots \quad (11)$$

Where P_{atm}= 101325 Pa.

The term within exponential function is the change in Gibbs free energy

$$\frac{\Delta S_r}{R} = \sum_{i=1}^{N}\left(v''_{i,r} - v'_{i,r}\right)\frac{S_i}{R} \quad \ldots \quad (12)$$

$$\frac{\Delta H_r}{RT} = \sum_{i=1}^{N}\left(v''_{i,r} - v'_{i,r}\right)\frac{h_i}{RT} \quad \ldots \quad (13)$$

Where $S_i$and h_i are the entropy and enthalpy of the ith species at atmospheric temperature. T

$$k_{b,r} = A_{b,r} T^{\beta_{b,r}} e^{-E_{b,r}/RT} \quad \ldots \quad (14)$$

Where,

$A_{b,r}$=backward reaction pre-exponential factor

$\beta_{b,r}$ = backward reaction temperature exponent

$E_{b,r}$= backward reaction activation energy (J/kmol)

Transport Equations for the Realizable k-ε Model

$$\frac{\partial}{\partial t}(\rho k)\frac{\partial}{\partial x_j} + ((\rho k u_j) = \frac{\partial}{\partial x_j}\left[\left(\mu + \frac{\mu_t}{\sigma_k}\right)\frac{\partial_k}{\partial x_j}\right] + G_k + G_b - \rho\epsilon - Y_M + S_k \quad \ldots \quad (15)$$

and

$$\frac{\partial}{\partial t}(\rho \varepsilon)\frac{\partial}{\partial x_j} + ((\rho \varepsilon u_j) = \frac{\partial}{\partial x_j}\left[\left(\mu + \frac{\mu_t}{\sigma_\varepsilon}\right)\frac{\partial_\varepsilon}{\partial x_j}\right] + \rho C_1 S\varepsilon + \rho C_2 \frac{\varepsilon^2}{k+\sqrt{V\varepsilon}} + C_{1\varepsilon}\frac{\varepsilon}{k}C_{3\varepsilon}G_b + S_\varepsilon$$

$$\ldots \quad (16)$$

Where

$C_1 = \max\left[0.43, \frac{\eta}{\eta+5}\right], \eta = S\frac{k}{\varepsilon}, S = \sqrt{2SS}$ $\quad \ldots \quad (17)$

$$\mu_t = \rho C_\mu \frac{k^2}{\varepsilon}$$

$$C_\mu = \frac{1}{A_0 + A_s \frac{kU^*}{\varepsilon}}$$

$$U^* = \sqrt{S_{ij}S_{ij} + Q_{ij}\tilde{Q}_{ij}}$$

$$A_0 = 4.04, A_s = \sqrt{6}\cos\emptyset$$

$$\emptyset = \frac{1}{3}cos^{-1}(\sqrt{6}W), \text{ W} = \frac{S_{ij}S_{jk}S_{ki}}{\tilde{S}^3}, \tilde{S} = \sqrt{S_{ij}S_{ij}}, S_{ij} = \frac{1}{2}\left(\frac{\partial u_j}{\partial x_i} + \frac{\partial u_i}{\partial x_j}\right) \quad \ldots \quad (18)$$

$$\frac{\partial}{\partial \tau}(\rho Y_i) + \nabla.(\rho \bar{v} Y_i) = \nabla \bar{J}_i + R_i + S_i \quad \ldots \quad (19)$$

$$\bar{J}_i = -\rho D_{i,m} \nabla Y_i - D_{T,i} \frac{\nabla T}{T} \quad \ldots \quad (20)$$

$$\bar{J}_i = -(\rho D_{i,m} + \frac{\mu_t}{Sc_t}) \nabla Y_i - D_{T,i} \frac{\nabla T}{T} \quad \ldots \quad (21)$$

$$\bar{J}_i = -\rho D_{i,m} \nabla Y_i - D_{T,i} \frac{\nabla T}{T}$$

$$\bar{J}_i = -(\rho D_{i,m} + \frac{\mu_t}{Sc_t}) \nabla Y_i - D_{T,i} \frac{\nabla T}{T} \quad \ldots \quad (22)$$

$$Le_i = \frac{k}{\rho c_\rho D_{i,m}} \quad \ldots \quad (23)$$

$$\frac{\partial}{\partial t}(\rho k) + \frac{\partial}{\partial x_i}(\rho k u_i) = \frac{\partial}{\partial x_j}\left(\tau_k \frac{\partial k}{\partial x_j}\right) + G_k - Y_k + S_k \quad \ldots \quad (24)$$

$$\frac{\partial}{\partial t}(\rho \omega) + \frac{\partial}{\partial x_i}(\rho \omega u_i) = \frac{\partial}{\partial x_j}\left(\tau_\omega \frac{\partial \omega}{\partial x_j}\right) + G_\omega - Y_\omega + D_\omega + S_\omega \quad \ldots \quad (25)$$

$$\frac{\partial}{\partial \tau}(\rho \bar{v}) + \nabla(\rho v v) = -\nabla \rho + \nabla(\bar{\tau}) + \rho g + \bar{F}$$

$$\bar{\tau} = [(\nabla \bar{v} + \nabla \bar{v}^{\,T}) - \frac{2}{3} \nabla . \bar{v} I] \quad \ldots \quad (26)$$

$$\frac{\partial}{\partial \tau}(\rho Y_1) + \nabla(\rho \bar{V} Y_1) = -\nabla J_1 + R_1 + S_1 \quad \ldots \quad (27)$$

$$J_1 = -\rho D_{1,m} \nabla Y_1 - D_{r,1} \frac{\nabla \gamma}{\gamma}$$

$$J_1 = -(\rho D_{1,m} + \frac{\mu_1}{sc_1}) \nabla Y_1 - D_{r,1} \frac{\nabla \gamma}{\gamma} \quad \ldots \quad (28)$$

$$\frac{\partial}{\partial \tau}(\rho\omega) + \frac{\partial}{\partial_{x1}}(\rho\omega u_1) = \frac{\partial}{\partial_{x1}}\left(r_\omega \frac{\partial \omega}{\partial x_1}\right) + G_\omega - Y_\omega + D_\omega + S_\omega \quad \ldots \quad (29)$$

$$\emptyset_2 = max\left[2\frac{\sqrt{x}}{0.09\omega y}, \frac{500\mu}{\rho y^2 \omega}\right] \quad \ldots \quad (30)$$

$$G_k = \min(G_k, 10\rho\beta * k\omega) \quad \ldots \quad (31)$$

$$G_W = \frac{\propto}{v_1} G_k \quad \ldots \quad (32)$$

$$\alpha_\infty = F_{1\alpha_{\infty,1}} + (1 - F_1)\alpha_{\alpha_{\infty,2}}$$

$$\alpha_{\infty,1} = \frac{\beta_{11}}{\beta_\omega} - \frac{x^2}{\sigma_{w,1}\sqrt{\beta^*_\infty}}$$

$$\alpha_{\infty,2} = \frac{\beta_{12}}{\beta_\omega} - \frac{x^2}{\sigma_{w,2}\sqrt{\beta^*_\infty}}$$

$$\tau_k = \mu + \frac{\mu_1}{\sigma_k}$$

$$\tau_\omega = \mu + \frac{\mu_1}{\sigma_\omega}$$

$$\mu_\tau = \frac{\rho k}{\omega} \frac{1}{\max\left[\frac{1}{\alpha^*}, \frac{SF_2}{a1\omega}\right]}$$

$$\sigma_k = \frac{1}{F_1/\sigma_{k,1} + (1 - F_1)/\sigma_{k,2}}$$

$$\sigma_\omega = \frac{1}{F_1/\sigma_{\omega,1} + (1 - F_1)/\sigma_{\omega,2}}$$

$$F_1 = \tanh(\emptyset_1^4)$$

$$\emptyset_1 = \min\left[\max\left(\frac{\sqrt{k}}{0.09\omega y}, \frac{500_\mu}{\rho y^2 \omega}\right), \frac{4\rho k}{\sigma_{\omega,2} D_\omega^+ y^2}\right] \quad \ldots \quad (33)$$

$$D_\omega^+ = max\left[2\rho \frac{1}{\sigma_{\omega,2}} \frac{1}{\omega} \frac{\partial k}{\partial x_j} \frac{\partial \omega}{\partial x_j}, 10^{-10}\right]$$

$$F_2 = \tanh(\emptyset_2^2)$$

$$\emptyset_2 = max\left[2\frac{\sqrt{k}}{0.09\omega y}, \frac{500_\mu}{\rho y^2 \omega}\right] \quad \ldots \quad (34)$$

$$Y_k = \rho\beta^* k\omega$$

$$Y_k = \rho\beta\omega^2$$

$$\beta_i = F_1\beta_{i,1} + (1 - F_1)\beta_{i,2}$$

$$D_\omega = 2(1 - F_1)\rho \frac{1}{\sigma_{\omega,2}} \frac{\partial k}{\partial x_j} \frac{\partial \omega}{\partial x_j} \quad \ldots \quad (35)$$

$\sigma_{k,1} = 1.176, \sigma_{\omega,1} = 2.0$, $\sigma_{k,2} = 1.0$, $\sigma_{\omega,2} = 1.168$

$\alpha_1 = 0.31, \beta_{i,1} = 0.075$, $\beta_{i,2} = 0.0828$

$$k_{b,r} = \frac{k_{f,r}}{k_{eq}}$$

$$K_r = \exp\left(\frac{\Delta S_r}{R} - \frac{\Delta H_r}{RT}\right)\left(\frac{P_{atm}}{RT}\right)^{\sum_{i=1}^{N}(v''_{i,r} - v'_{i,r})} \quad \ldots \quad (36)$$

$$R_{i,r} = r\,(v''_{i,r} - v'_{i,r})\left(k_{f,r}\prod_{j=1}^{N}[C_{j,r}]\right)(n'_{j,r} - v''_{j,r})) \quad \ldots \quad (37)$$

$$R_{i,r} = r\,(v''_{i,r} - v'_{i,r})\left(k_{f,r}\prod_{j=1}^{N}[C_{j,r}]\right)\left(n'_{j,r} - k_{b,r}\prod_{j=1}^{N}[C_{j,r}\,]\,v''_{j,r}\right) \quad \ldots \quad (38)$$

3.1.3 Grid Independence Study:

The flow path of the full-scale combustor is shown below. The computations with different flow conditions have been evaluated.

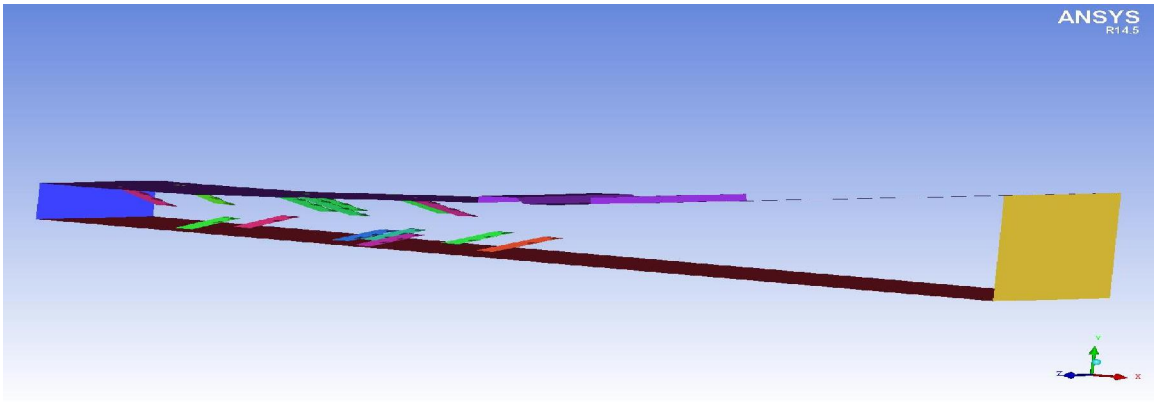

Fig.3.1 Flow path of the combustor

Fluent software is used to carry out the computational studies on a ramp-cavity based scramjet combustor for non-reacting and reacting flow conditions. Before carrying out all the simulations, it is ensured that solution is grid independent. Grid independency study has been performed by considering 2 million, 4 million and 8 million grids.

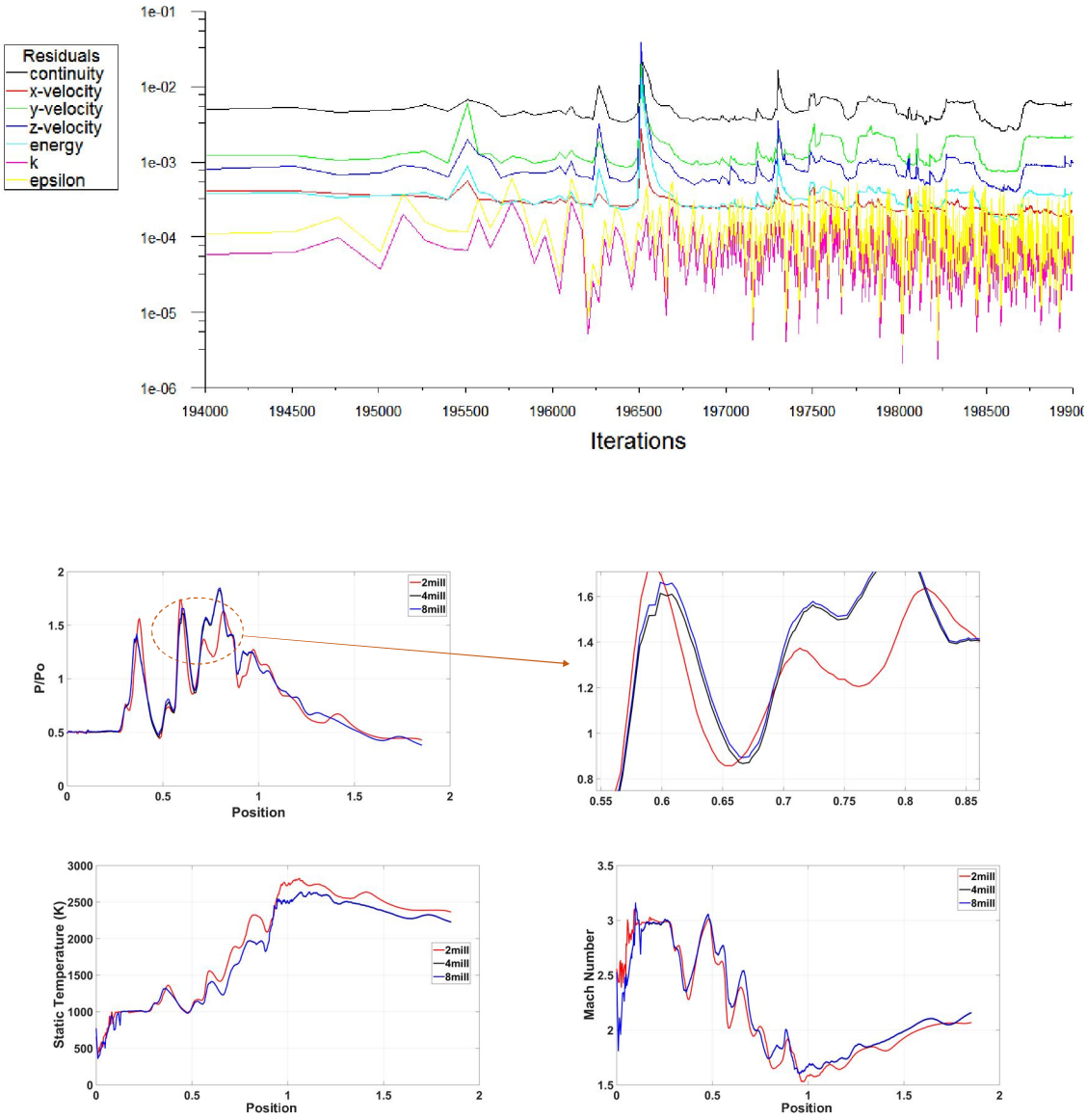

Fig. 3.1 (a) Flow characteristics along the combustor

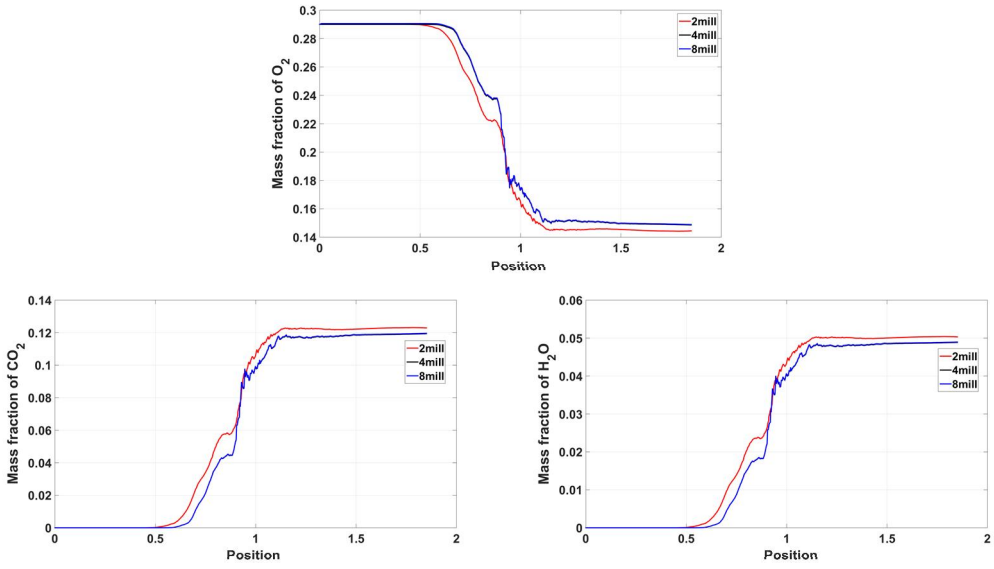

Fig. 3.1 (b) Static Pressure variation along the combustor

Ethylene fuel combustion with supersonic airstream at combustor entry Mach number 2 and 3 has been analysed for the studies. For the latter case, results are shown in the Fig. 3.1(a) and (b). Mach number, static pressure, static temperature and mass fractions of species have been plotted along the combustor length and compared for three different grids, sizing 2 million, 4 million and 8 million respectively in Fig. 3.1. Most of the grid cells are populated in combustor region and surroundings in all three directions, where flow gradients are more pronounced. It is seen from these figures that there is no significant difference in the solutions of 4 million and 8 million grids. The results are looking identical. The difference is very small, less than 1%, whereas, the change is noticeable in the solutions of 2 million and 4 million grids. Hence, it can be concluded that simulation results are independent of grid size, 4 million onward. Four millions-grid case captured the flow properly. Further increase in grid size will not add anything further in the simulation results. Therefore, for all the subsequent numerical simulations, 4 million-grid has been used confidently.

3.1.3(a) Grid generation :

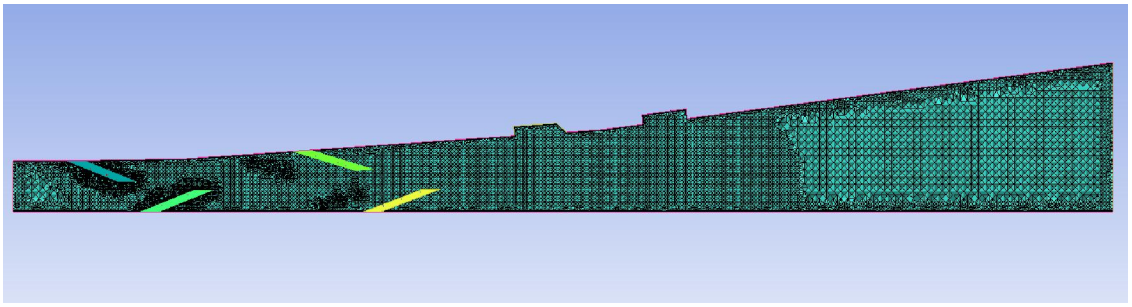

Fig. 3.1 (c) Grid generation for Ramp Cavity Combustor

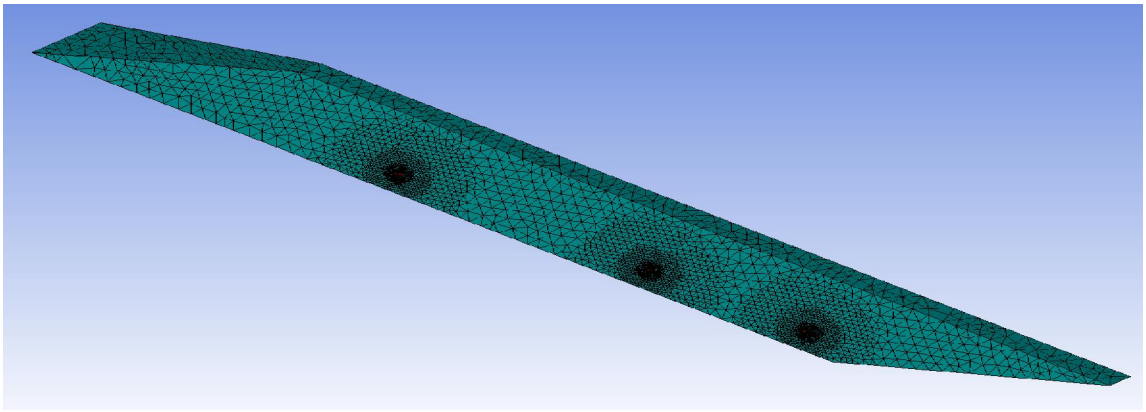

Fig. 3.1 (d) Grid for Ramp

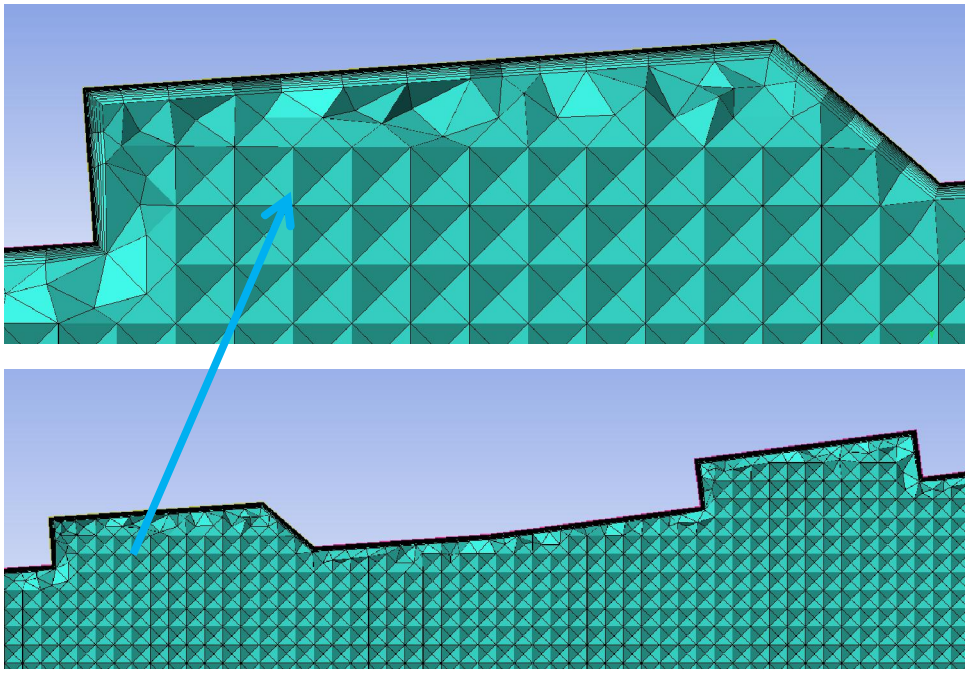

Fig. 3.1 (e) Grid at cavity

Grid generation has been depicted in Fig.3.1 (c), (d) and (e) above. Four million-grid is used for evaluation of the flow field. The grid is unstructured. As shown in fig 3.1 (d) and (e), fine grids are used near ramps and cavities to capture the flow phenomenon, mixing and recirculation at these regions.

3.1.4 Validation with experimental work:

Fluent has been proven for analysis of supersonic combustor. Many simulations have been carried out and published in literature. Fluent commercial software has been used to carry out the simulation studies with a set of parametric studies on subscale and scaled scramjet combustors. Validation of the software and grid size employed in the studies has been carried out against experimental studies with both sub-scale and scaled combustors. The validation of computational studies with full scale combustor is presented in the Chapter entitled "Results and discussion".

3.1.5 Studies on effect of type of fuels, Mach number, equivalence ratios and fuel Injection pattern:

Aviation kerosene is used as fuel in the experimental studies to evaluate its performance in supersonic combustion. As aviation kerosene is liquid fuel, break-up of liquid droplets, evaporation of kerosene and mixing with supersonic airstream are difficult and also involve ignition delay which contribute to incomplete combustion of fuel with supersonic stream of air.

To overcome the issues of mixing with supersonic airstream, gaseous ethylene is a prospective candidate as fuel for mixing with air. Ethylene chemistry is simple compared to aviation kerosene. Due to ignition delay and issues with mixing and flame stabilization compared to aviation kerosene, gaseous ethylene is a better choice.

Mach numbers:

Combustor entry Mach number corresponds to the free stream Mach number at higher altitude. The studies are conducted with combustor entry Mach numbers of 2 and 2.5 for Hydrogen & aviation kerosene in respect of sub-scale combustor; 2 and 3 for

aviation kerosene; 2, 2.5 and 3 for ethylene in the case of full scale combustor. The combustor entry Mach number is typically one third of the free stream Mach number. The flow field in the combustor for different combustor entry Mach numbers is studied in terms of Mach number, static pressure, static temperature and concentration of species.

Equivalence ratio:

For the fuels studied, equivalence ratio of 0.6 is used in the computational studies. In addition, equivalence ratio is varied in the computational studies. Equivalence ratio of 0.2, 0.3, 0.4, 0.6 and 0.8 has been used for analysis of the flow field in the full scale combustor with combustor entry Mach number of 3. Parametric studies are conducted with ethylene as fuel.

Fuel injection pattern:

In the full scale combustor, ramps are located in a staggered way along the combustor. Ramps are located two each on the top and bottom walls of the combustor in the first three stages and one each on the top and bottom wall in the fourth stage. In each ramp, there are fuel injection holes on both edges of the ramps and at the tip. Fuel is injected transversely and at an angle into the core of the combustor section. Fuel is injected at an equivalence ratio of 0.6 into the combustor through all the injectors equally in the ramps. In the parametric studies, variation of fuel injection pattern is studied. Fuel is not injected from one set of the ramps in each of the study and the fuel is injected equally in the remaining ramp injectors. For instance, in the first stage, fuel is not injected through the first four ramps located on the top and bottom walls from the combustor inlet and fuel is injected from the remaining ramps in the combustor. The incoming supersonic stream of air passes through the first set of ramps without injection of fuel, decelerated due to positioning of the ramps and fuel injection, mixing and combustion are carried out from the second set of ramps in the combustor. Similarly, the fuel injection pattern is studied for the other cases by switching off the fuel injection from one set of ramps each time. The fuel injection pattern in the combustor is an interesting parametric study of mixing and combustion of fuel with supersonic stream of air in the full scale ramp-cavity combustor.

3.2 Experimental programme:

Experimental programme is conducted with the development of test facility in the laboratory. Initially, a sub-scale vitiated air test facility is developed. Facility is developed to provide air mass flow rate of 1 kg/s for 15s. Initial tests are conducted using the test facility. While progressing with the testing, a full-scale test facility is designed and developed that provides vitiated air at 15 kg/s. The full- scale test facility is made operational to conduct full-scale combustor test for duration of about 20 s.

3.2.1 Development of Sub-scale test facility:

Fig. 3.2 depicts the sub-scale scramjet combustor test facility. Facility consists of vitiated air heater, supersonic contoured nozzle, air, hydrogen and oxygen feed lines, spark ignition system and transition duct. Wall pressure and temperature measurements are carried out to measure the stagnation pressure and temperature respectively. Hydrogen burner consists of H_2, O_2 and air injectors and ignition system. Hydrogen, Oxygen and air are injected into the burner through the injectors. The feed systems consist of pressurized tanks and are connected to the burner by means of high-pressure piping. The rate of flow of these gases is controlled by the inlet pressures and electro-pneumatic valves. Flow meters are installed to measure the flow rates of air, oxygen and hydrogen entering into the vitiated air heater. All the test devices and equipment are calibrated thoroughly before conducting each test.

In the presence of spark caused by the high-energy ignition system, hydrogen and air are injected into the heater (burner) to take part in the combustion process and as a result temperature and pressure of the test gas increases. The oxygen injected into the (heater) burner replenishes the oxygen consumed during the burning of air with Hydrogen. The air, Hydrogen and Oxygen mass flow rates are maintained to be steady throughout the test duration. Sub-scale combustor test facility is established to provide the air mass flow rate of about 1kg/s of air in the test section.

The vitiated air is allowed to expand through an axi-symmetric supersonic nozzle with the desired exit Mach number. Contoured nozzles are designed and realized for each of

the exit Mach number to simulate the flow conditions. The accelerated vitiated air flows through a transition duct, to provide a uniform flow at the entry of the constant area combustor, with minimum losses. The transition duct is designed and introduced to convert from axi- symmetric to rectangular cross section with smooth transition. Vitiated air heater wall stagnation pressure and temperature are measured to match the simulated high altitude conditions in the vitiated air heater. The heater (burner) stagnation temperatures were measured with Tungsten-Rhenium thermocouples.

The test facility and the combustor components have been checked for the accuracy by conducting cold flow tests. Flow measurements are made with calibrated flow meters. Pressure transducers and temperature sensors are calibrated with standard, master gauges. The values have been monitored for consistency. The variation in measurements is within 2% and is acceptable.

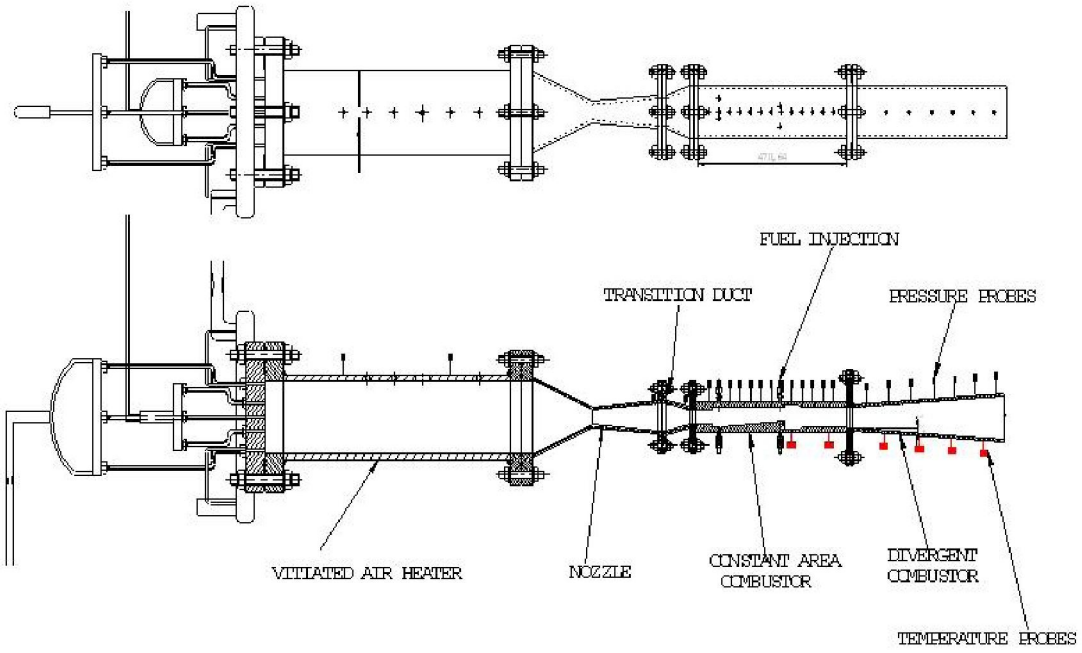

Fig.3.2 Sub-scale combustor test facility

3.2.2 Description of Sub-scale combustor:

The supersonic combustor has two parts; one constant area section with backward facing step in which the ramps and cavities are located and the second one is diverging area combustor as shown in Fig.3.3. Constant area section of the combustor consists of the fuel injection system, physical ramps, and three ramps on the bottom wall of the combustor and two on the top wall of the combustor as shown in the Fig.3.3. The ramps are spaced alternately in the combustor to reduce the blockage area and to provide the required condition for compression and mixing of fuel with the supersonic airstream. Cavities are located across the section of the combustor immediately after the ramps which are intended to be used for flame stabilization. Open cavities are used in the system which are useful for supersonic flow conditions. Diverging section of the combustor is designed along with the constant area section to avoid thermal choking of the flow.

Aviation Kerosene fuel is injected transversely upstream the ramps through five orifices of 0.4 mm diameter through the top and the bottom walls of the combustor. Kerosene is also injected through five 0.4 mm orifices parallel to the flow through the ramp base. Pilot Hydrogen is injected to ensure the ignition and sustained combustion of kerosene fuel. Wall pressures along the axial length of the Hydrogen burner, convergent - divergent nozzle, transition duct and supersonic combustor are measured with strain gauge type pressure transducers. The burner stagnation temperature and the wall temperatures are measured with Tungsten-Rhenium thermocouples. Skin temperatures are also recorded during the test.

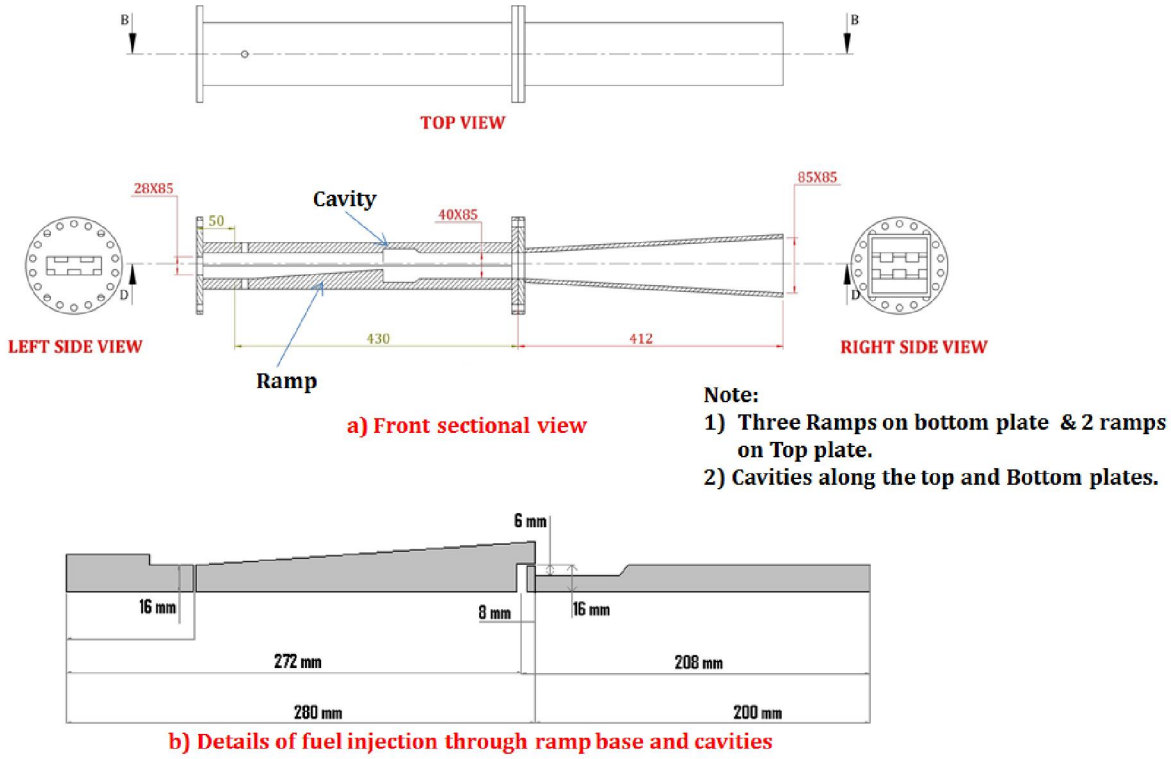

Fig. 3.3 Sub-scale Ramp-cavity combustor

Combination of Ramp and Cavity injectors:

The overall performance of Ramp and Cavity injectors can be improved by combining them properly. The combination of cavities and ramps generate a three dimensional flow field and turbulence for better mixing and combustion. Ramps will enhance the fuel penetration in to the core and cavities will enhance the flame holding characteristics. The ramp generated axial vortices can be utilized to scoop out the hot gases generated at cavities thus improving the combustion efficiency. Thus Ramp and cavity combination shows promising characteristics for better scramjet combustor performance. Table 3.1 shows the design considerations for selection of various parameters.

Table 3.1

S. No	Parameter	Requirement / effect
	Ramp Injector	
1	Length (l)	Evaporation length of droplets
2	Wedge angle (θ_1)	Compression and shock strength
3	Ramp base width (w)	Area blockage by ramp
4	Ramp Spacing (w_1)	Minimum blockage area-distribution
	Cavity Injector	
1	Length (L)	Ramp base height
2	Cavity depth (D)	L/D ratio needed
3	Trailing edge angle (θ)	Shock strength at the Trailing Edge

Injection Schemes:

(i) Sub-scale combustor: Fig.3.4 (a):

a. Leading edge normal injection upstream of the ramp

- to enhance the fuel spread caused by the spillage and the spillage vortex.
- to provide film cooling for ramp from the core flow.

b. Parallel injection through the ramp base

- to inject the fuel into the periphery of the contra rotating vortices that stretches the fuel air interface.

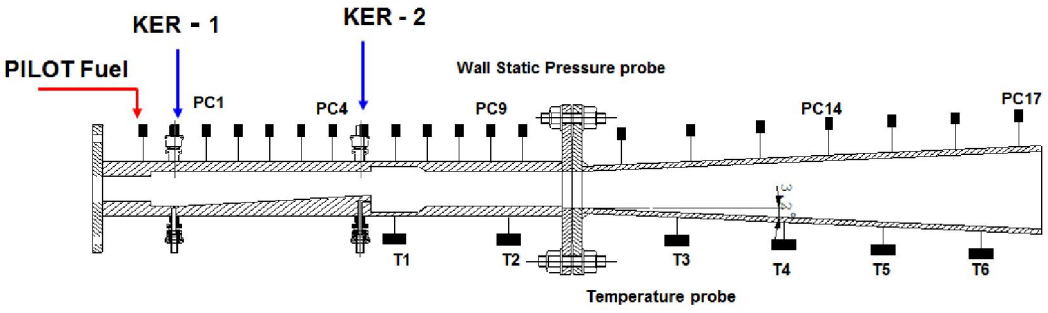

Fig. 3.4 (a) Injection scheme: Sub-scale Ramp-cavity combustor

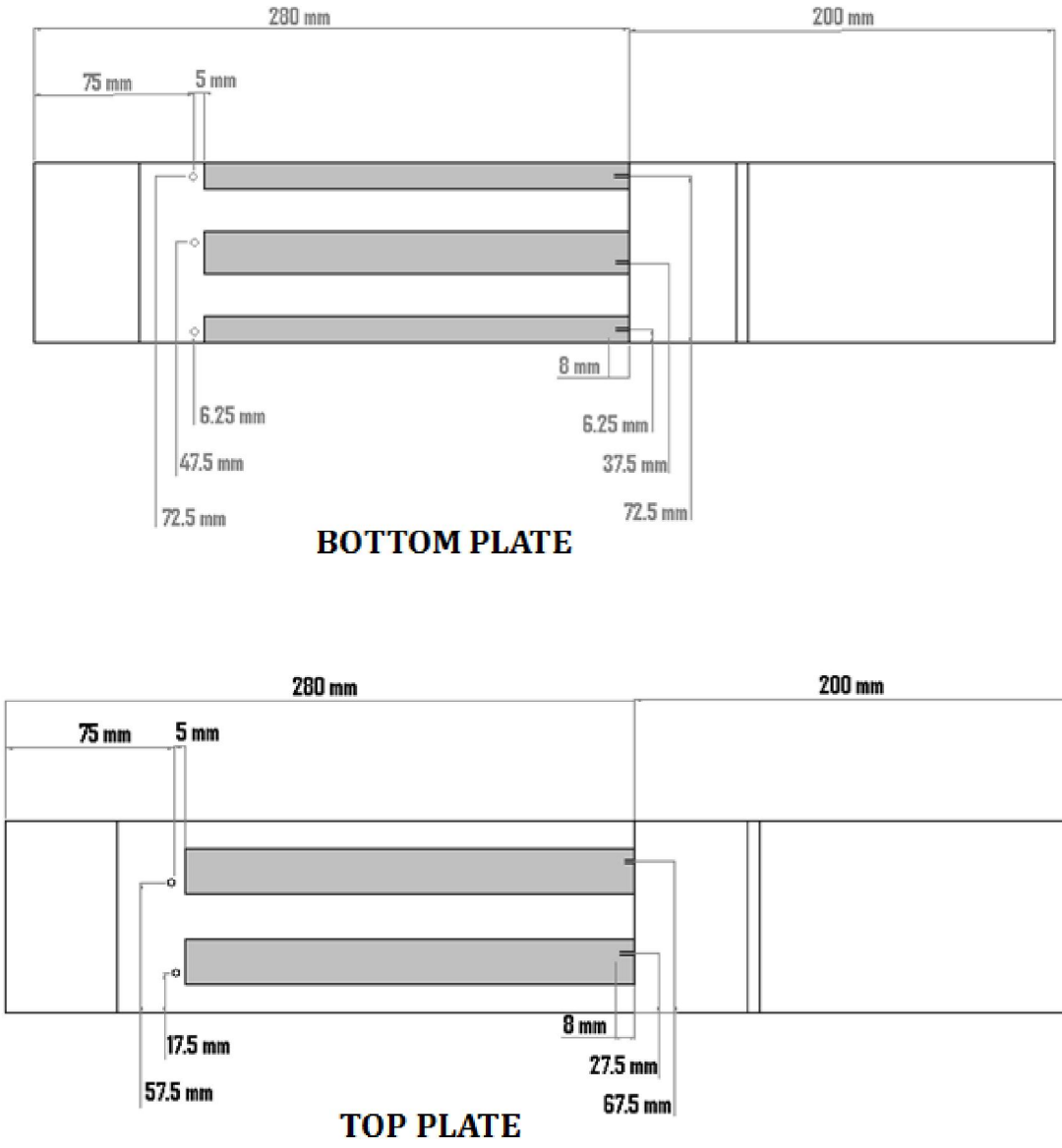

Fig. 3.4(b) Injection Locations of Sub Scale Combustor

(ii) Full-scale combustor:

Injection of fuel is carried out through the ramps in the full-scale combustor as shown in Fig.3.4 (c). Two ramps on each top and bottom wall of the combustor in the first three stages and one ramp each on top and bottom wall of the combustor in the fourth stage of injection is configured in the combustor as shown in Fig. 3.4 (d). Seven holes are provided in each ramp, 3 on each side and one at the tip to inject the fuel into the combustor.

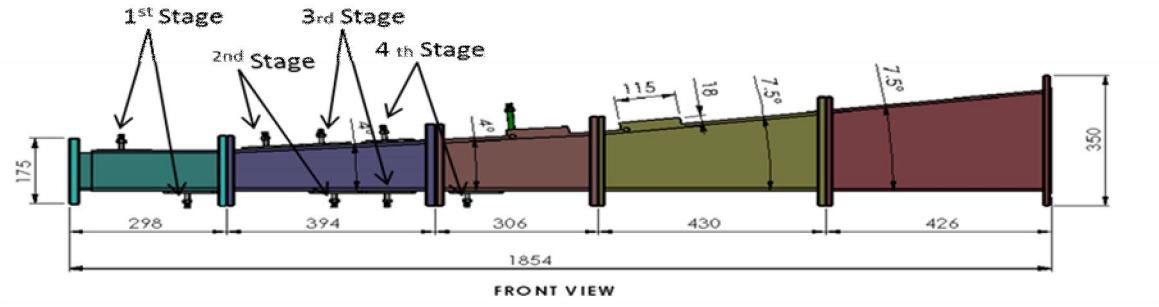

Fig. 3.4 (c) Injection scheme: full-scale Ramp-cavity combustor

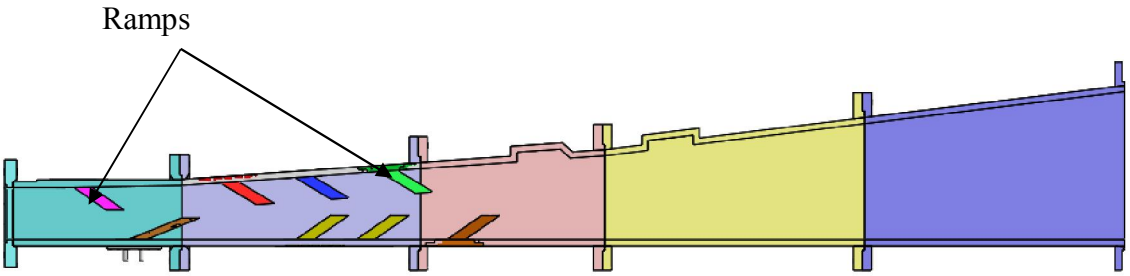

Fig. 3.4 (d) Arrangement of Ramps and cavities in the full scale combustor

3.2.3 Full scale Test facility:

Full scale test facility (Fig.3.5) is developed to meet the mass flow rate requirements of the sized combustor. The facility is designed to develop vitiated air mass flow rate of 15 kg/s at 1500 K, simulating the high altitude condition. Air and Hydrogen burn to generate the high temperature gas simulating the stagnation conditions corresponding to high altitude. Oxygen is used to replenish the oxygen content in the air. The air heater consists of a circular section followed by the divergent sections which increase the stagnation temperature of the hot air. Circular to rectangular transition duct is used prior to the supersonic nozzle for the flow to pass through the two dimensional nozzle and the combustor. The combustor is supported by a frame to position the smaller sections that are joined to make the combustor. The air facility is water cooled to protect the metallic surfaces during combustion of air with hydrogen to generate the stagnation

pressure and total temperature. Supersonic nozzle is designed for the nozzle exit Mach number. Nozzle is of contoured design to reduce the losses.

Wall pressures are measured through pressure probes mounted on the top wall of the air heater section. Temperatures are measured to ensure the conditions required for supersonic stream of air at the combustor entry condition.

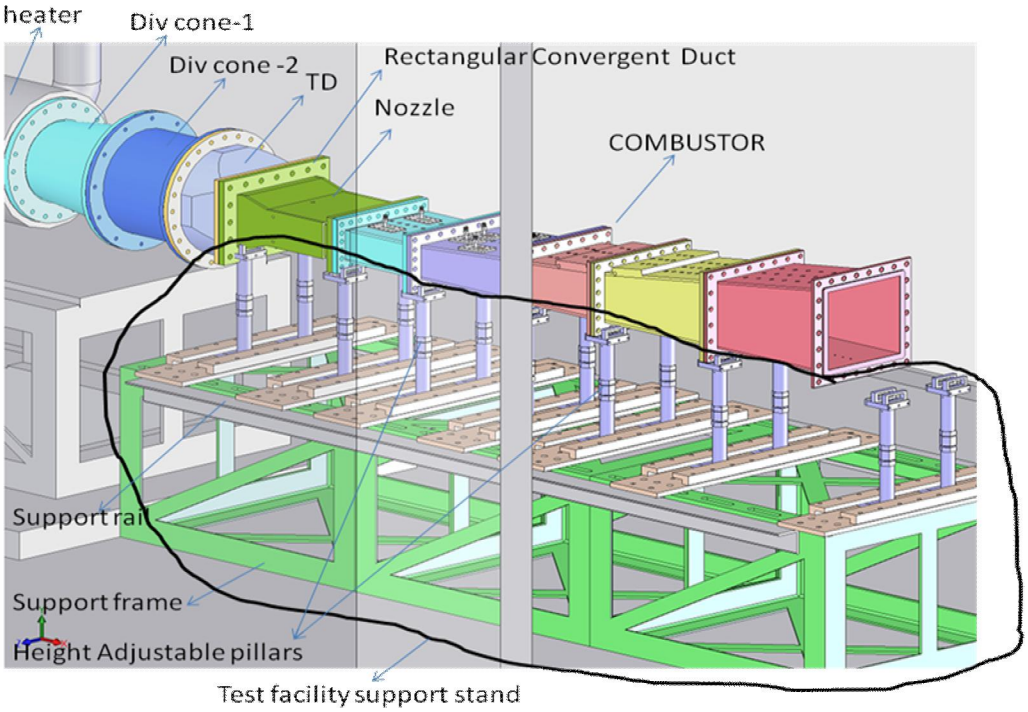

Fig.3.5 Full scale combustor test facility

3.2.4 Full scale combustor:

Full scale combustor (Fig.3.6) consists of continuously varying diverging sections of the combustor. The combustor size varies from 275 mm x 86 mm at the start of the combustor to 275 x 251 at the exit of the combustor. The length of the combustor is about 1.8 m. Top wall of the combustor varies with 4 degree divergence angle in two sections followed by 7.5 degree divergence angle in the next two sections . Cantilevered ramps are located along the top and bottom walls of the combustor and are staggered along the combustor sections. There are two ramps each on top and bottom walls of combustor in three stages followed by one ramp each on top and bottom wall. The ramps are located to provide minimum blockage area and improve the mixing in the combustor as fuel is mixed

with supersonic airstream. Two cavities are located on the top wall of the combustor to provide the flame holding for sustained supersonic combustion. Open cavities of length about 100 mm and 18 mm depth are used. Ramps are provided for mixing of the fuel with supersonic airstream and cavities are used to provide the flame holding during combustion. Divergence is provided in the combustor to avoid thermal choking of the flow.

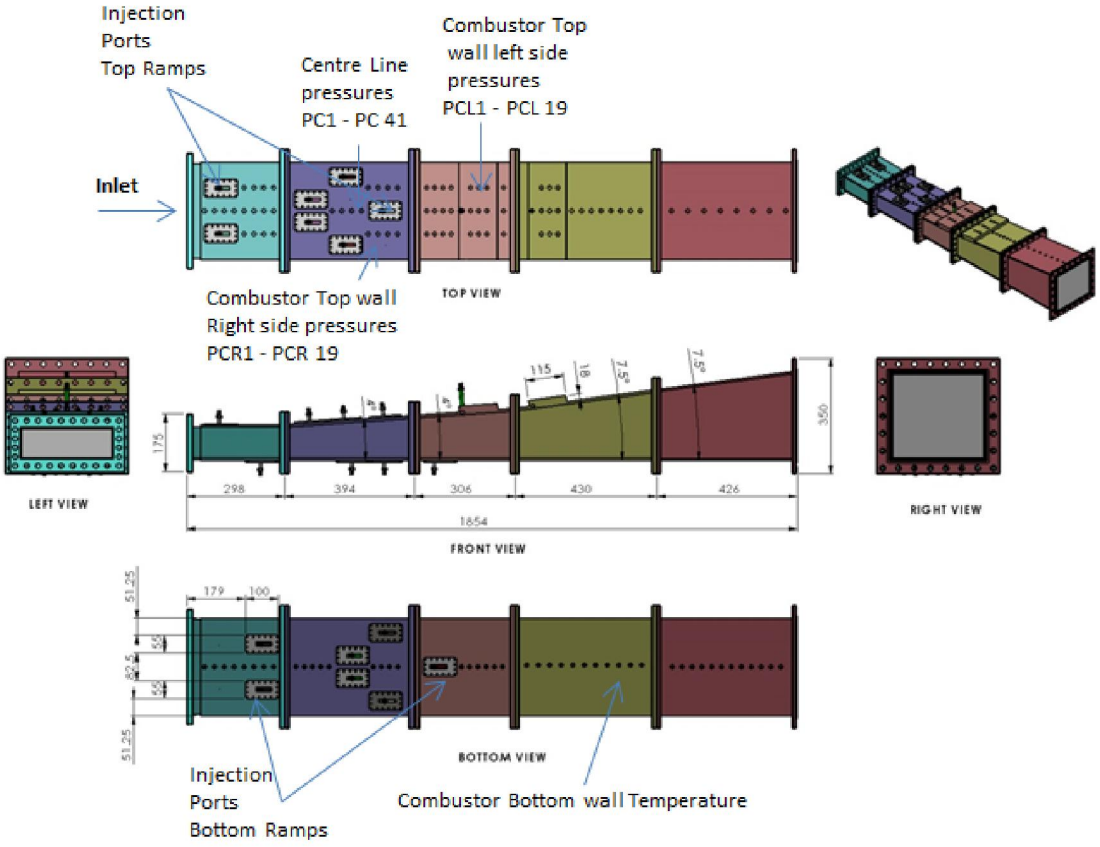

Fig: 3.6 Full-scale Ramp-cavity combustor

3.2.5 Instrumentation:

Sub-scale and full-scale tests have been carried out with ramps and cavities suitably located in the combustor. In the case of sub-scale combustor, physical ramps along the top and bottom walls of the combustor have been configured. Staged injection of fuel is carried out both at the beginning of the ramps and at the ramp base prior to cavities. To simulate the conditions at high altitude in terms of stagnation pressure and total temperature, air, hydrogen and oxygen for replenishment of oxygen content in the

air, are used. For this, air, hydrogen and oxygen are introduced into the burner in the calculated quantities. Calibrated flow meters are used for metering the flow of the gases into the burner.

In the tests that are carried out, combustor pressure is measured on the top wall of the combustor. Absolute pressure transducers of 0-5 bar range are employed for the measurements.

All pressure transducers used in the combustor are working with metallic strain gauges

- Honeywell make, Model z,

0-5 ksc range,

Sensitivity: 30 mv/V

Accuracy: $\pm$ 0.25 % of full scale value.

- Temperature is measured with R type, K type and B type thermo couples.

R type:

Range: 0-1650^0 C

Accuracy: $\pm$ 0.1%

Sensitivity: 8 mv/^{0}C

K type:

Range: 0-1200^0 C

Accuracy: $\pm$ 0.1%

Make: Omega

Sensitivity: 0.4 mv/^{0}C

B type:

Range: 0-1800^0 C

Accuracy: $\pm$ 0.1%

Aviation kerosene is used as fuel with pilot Hydrogen in the sub-scale combustor experiments and Aviation kerosene, Hydrogen are fuels used in simulation studies.

Aviation kerosene is used as fuel in experimental studies with full scale combustor. Aviation kerosene, Hydrogen and Ethylene are the fuels used in full scale combustor simulation studies.

RESULTS AND DISCUSSION

The design and fabrication methodologies adopted for the conduct of experimental and numerical studies on supersonic combustion with different configurations are elucidated in the previous sections/chapters. In the present chapter, the results obtained in experimental and numerical works with ramp-cavity arrangement in the combustor are discussed.

4.1 Computational Studies:

In order to arrive at an optimal geometry of combustor configuration and operating parameters, extensive numerical studies have been carried out and the combustor performance is evaluated under the following conditions:

i. Combustor without ramps and cavities
ii. Combustor with ramps alone
iii. Combustor with cavities alone
iv. Combustor with wall injection
v. Combustor with cavities and wall injection
vi. Combustor with ramps and cavities.

In addition, the computational studies are done to study the effect of fuel, equivalence ratio, entry Mach number and fuel injection pattern.

4.1.1 Variation of parameters on combustor configuration:

Development of Combustor is very important for the experimental of supersonic combustion studies. Mixing and sustained combustion are the important parameters in the effective working of supersonic combustor. Various geometric configurations and fuel injection schemes of full scale combustor have been studied numerically to establish the mixing and flame stabilization of fuel with supersonic airstream in the combustor.

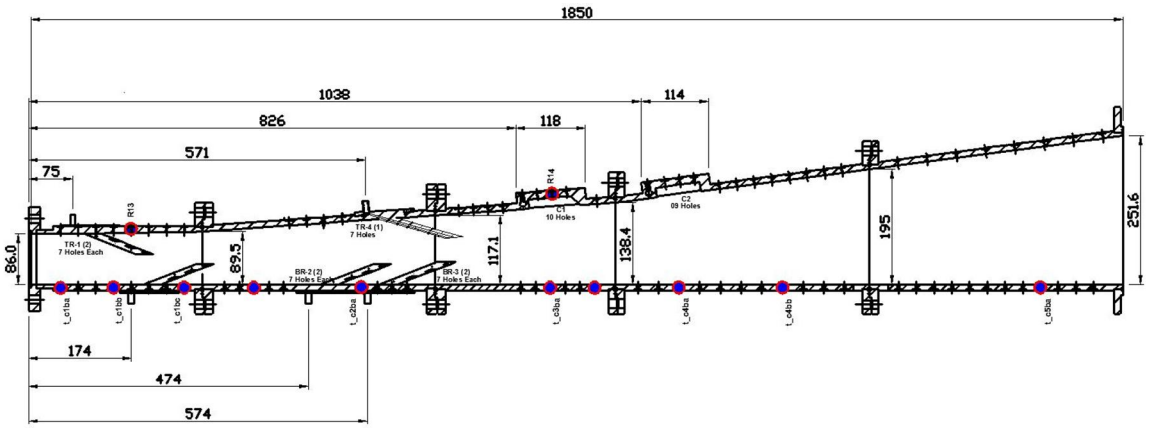

Fig.4.1 Full-scale combustor with ramps and cavities

Fig.4.1 shows a full-scale combustor with ramps and cavities, used in the simulation.

Computational studies are carried out on various combustor configurations as described above prior to finalize the ramp-cavity configuration.

4.1.1.1 Studies on Combustor at Mach number 3 without Ramps and cavities:

A full-scale combustor without ramps and cavities is considered for computational study to evaluate the performance. The combustor of cross section 86 mm X 275 mm with a length of 1850 mm is considered as illustrated in Fig. 4.1. The combustor is configured with one constant area section and other diverging sections with top wall divergence. Diverging portions of the combustor are provided to avoid thermal chocking. High speed air is allowed to flow through the combustor simulating the high altitude conditions. The stagnation pressure at the inlet to the combustor is 5 bar with stagnation temperature of 1000 K at the entry of the combustor corresponding to the high altitude conditions. The inlet of the combustor model is defined as Pressure Far Field. In each simulation, constant Mach number of 3 is considered at the inlet and hence Far field pressure condition is employed. The Outlet of the model is defined as Pressure Outlet.

Only half of the combustor is considered for simulation purpose, the wall along the length at mid-point of width is considered as a symmetry plane. The combustor walls are considered adiabatic wall condition. Density based solver with explicit scheme is used with second order discretization. Flow field is studied in terms of the Mach number, static pressure and static temperature along the combustor.

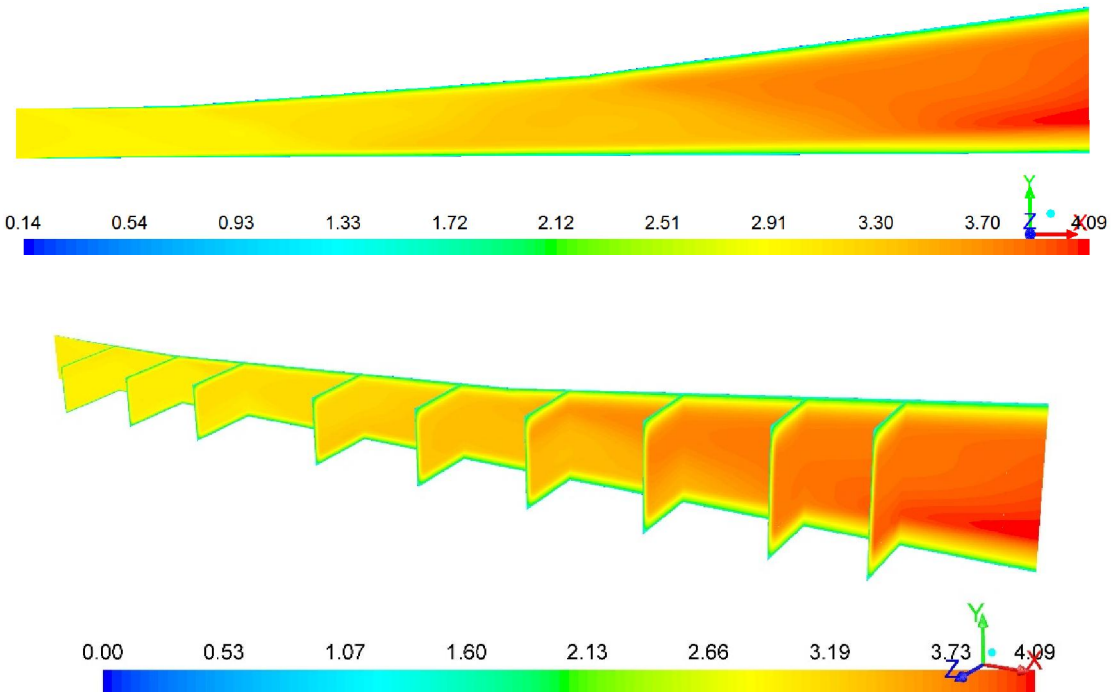

Fig.4.2 (a) Variation of Mach number along the simple combustor

Fig.4.2 shows contours of Mach number, static pressure and static temperature in the combustor (without any components inside). The contour plots at various sections are also shown. A supersonic airstream alone is considered to enter the combustor with entry Mach number 3. It can be seen from Fig.4.2 (a) that the Mach number is in the range of 2.5 to 2.9 in the constant area combustor. It is predicted that the airstream passes through the diverging combustor and the velocity increases. Mach number is observed to be increasing in the diverging portion to about Mach 3.5 due to area increase. The Mach number at the exit of the combustor is even higher, about 3.7, relative to entry Mach number. Core area of the diverging section of the combustor is observed to be of high Mach number.

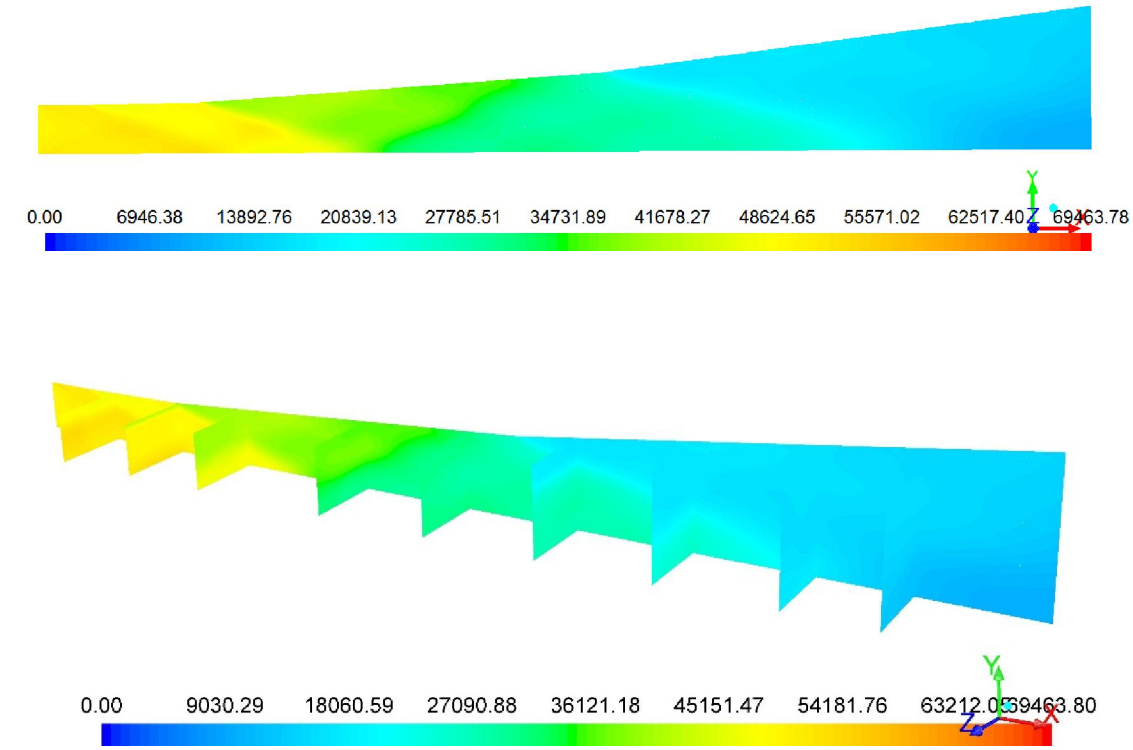

Fig.4.2 (b) Variation of Static pressure (Pa) along the simple combustor

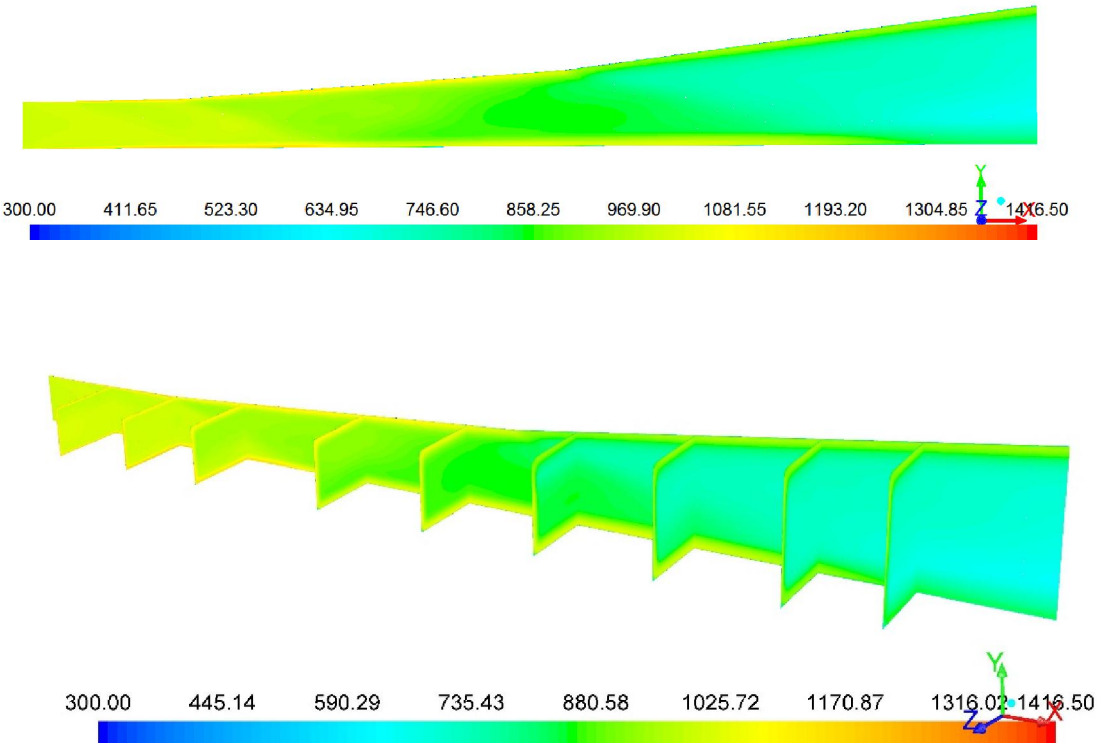

Fig.4.2 (c) Variation of static temperature (K) along combustor

The computations revealed sharp increase in static pressure values along a simple combustor, as can be seen in Fig.4.2 (b). The air stream gets accelerated as it enters the diverging part of combustor and thus static pressure is observed to be 0.5 bar at the exit of the combustor. Fig.4.2(c) depicts the static temperature along the combustor. This shows a similar trend with temperature decreasing from the entry of the combustor till the diverging portion of the combustor. It is seen that the boundary layer near the walls of the combustor shows higher temperature. There is no rise in the static pressure and temperature in the combustor except the changes due to geometric variation.

4.1.1.2 Combustor with ramps only

In this simulation, a full-scale combustor is configured with ramps inside the combustor for mixing studies and to evaluate the performance. Cavities are not considered. The combustor of cross section 86 mm X 275 mm with a length of 1850 mm is considered as illustrated in Fig. 4.1. The combustor consists of one constant area section and other diverging sections with top wall divergence. Diverging portions of the combustor are provided to avoid thermal chocking.

It is observed from literature that ramps are used for mixing of the fuel in the supersonic flow. A set of ramps, 7 in the top wall and 7 in the bottom wall are designed for this combustor configuration. These ramps are used for both fuel injection and mixing with airstream. Ramps are staggered along the length of the combustor. Two ramps each on top and bottom wall are located in the first three stages. One ramp is provided in the fourth stage. The model combustor with ramps is studied to explore the effect of ramps. High speed air is allowed to flow through the combustor simulating the high altitude conditions. The stagnation pressure at the inlet to the combustor is 5 bar and stagnation temperature of 1000 K at the entry of the combustor corresponding to the high altitude conditions. The inlet of the combustor model is defined as Pressure Far Field. In each simulation, constant Mach number of 3 is considered at the inlet and hence Far field pressure condition is employed. The Outlet of the model is defined as Pressure Outlet. Only half of the combustor is considered for simulation purpose, the wall along the

length and mid-point of width is considered as symmetry plane. The combustor walls are considered adiabatic wall condition. Density based solver with explicit scheme is used with second order discretization. Flow field is studied in terms of the Mach number, static pressure and static temperature along the combustor.

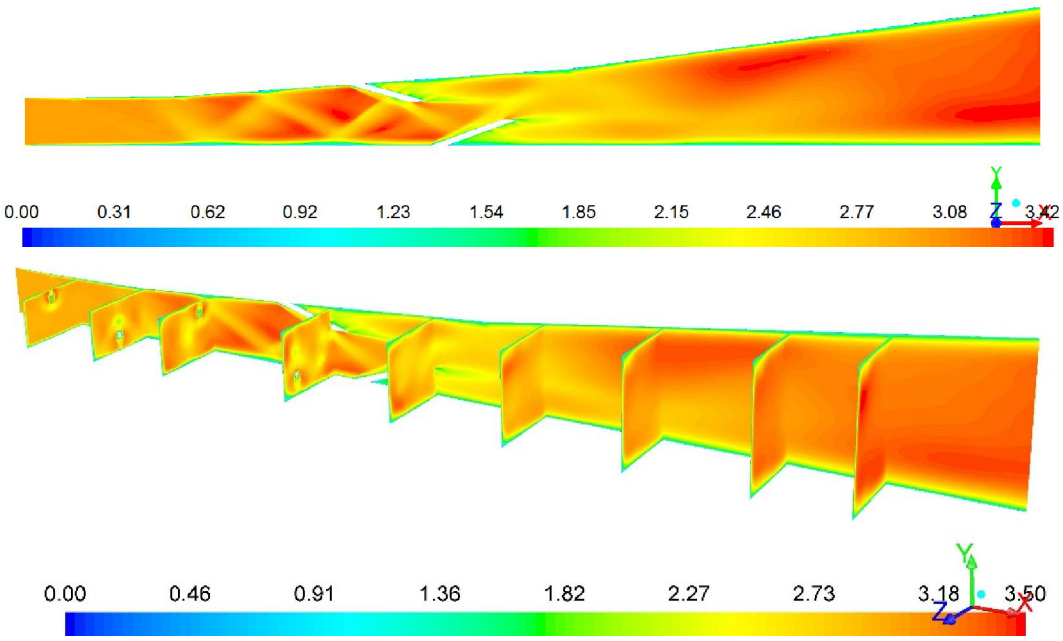

Fig.4.3 (a) Mach number contour along the combustor with ramps only

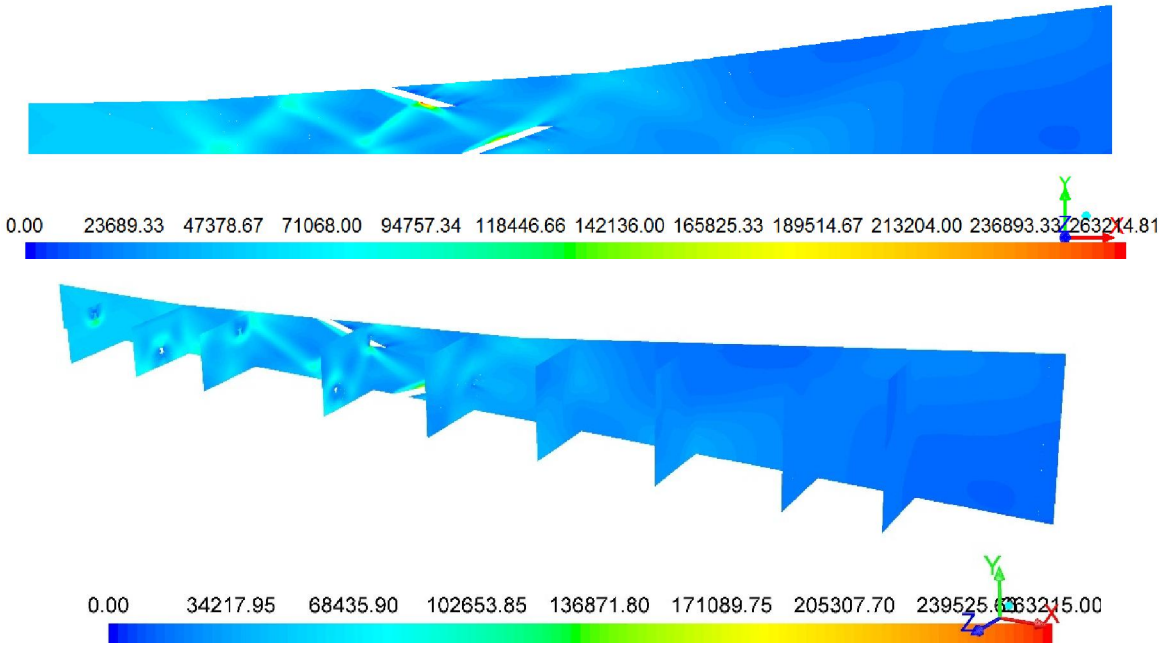

Fig.4.3 (b) Variation of static pressure (Pa) along the combustor with ramps only

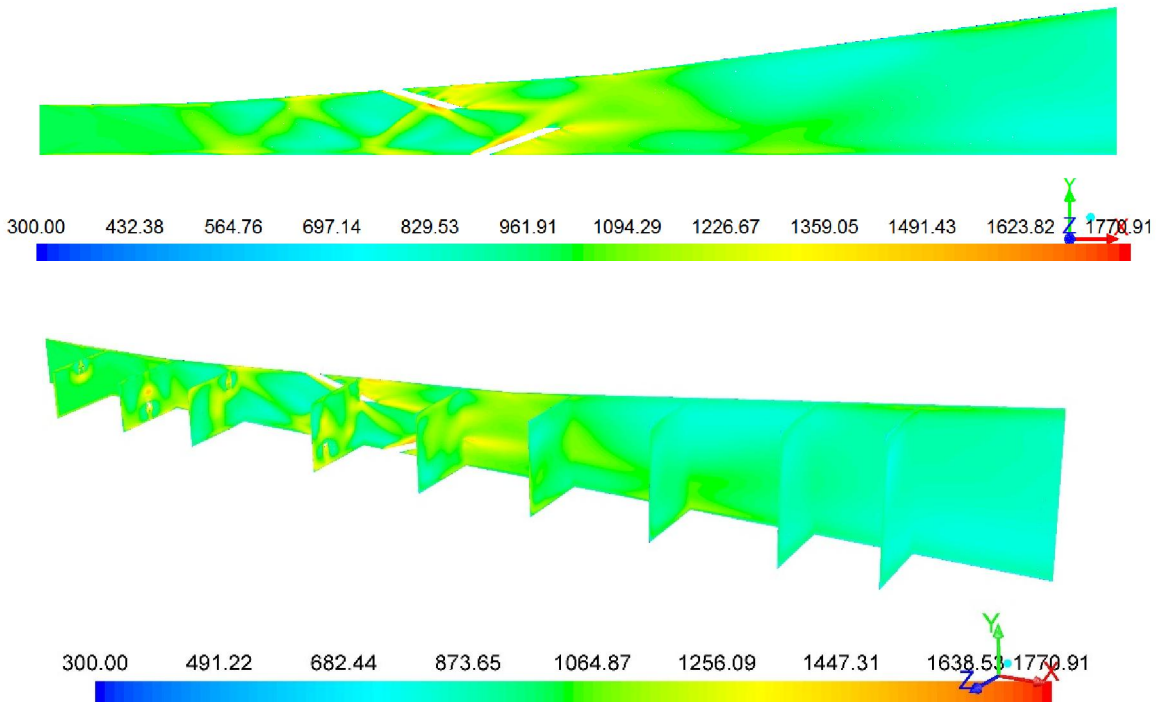

Fig4.3 (c) Variation of static temperature (K) along the combustor with ramps only

Fig.4.3 shows the contours of Mach number, static pressure and static temperature along the combustor with ramps only. Fig.4.3 (a) depicts the Mach number contours along the combustor. It can be observed that three dimensional multiple shocks are generated in the vicinity of ramps due to vortices that promote thorough mixing. The ramps reduce Mach number near to it due to compression in the ramps and the flow expands downstream in the combustor. Mach number at the ramps locally becomes 1.6 and again increases in the diverging combustor. It is observed that Mach number decreases to 1.6 along a thin layer due to existence of boundary layer at the top and bottom walls of the diverging combustor.

The static pressure contour along the combustor in Fig. 4.3 (b) shows the three dimensional shocks in the ramps zone in the combustor and corresponding pressure variation. Static pressure decreases after ramps and again increases where ramps are not located in the combustor. The static pressure decreases in the diverging combustor, with a consequent increase in Mach number. The static temperature contours along the combustor in Fig.4.3 (c) show rise in the temperature along with the static pressure in the ramps zone of the combustor. Rise in static temperature along the ramps are predicted.

Static temperature increases after the ramps. Therefore, rise in static temperature and pressures are observed in the diverging combustor that continued towards the exit of the combustor. The results are in line with the experiments conducted and studied by Wilson *et al.* (1997) on the role of ramps in improving the penetration and mixing of fuel with supersonic air stream due to mechanisms like baroclinic torque, vorticity, magnus force.

4.1.1.3 Combustor with cavities only

It is established in the literature that flame holding could be possible with Cavities as the cavities generate recirculation zones in the combustor.

In this simulation, a full-scale combustor with two cavities configured on the top wall of the combustor without ramps is considered to evaluate the performance. The combustor is of cross section 86 mm X 275 mm with a length of 1850 mm as illustrated in Fig. 4.1. The combustor has one constant area section and other diverging sections with top wall divergence. Diverging portions of the combustor are provided to avoid thermal chocking. High speed air is allowed to flow through the combustor simulating the high altitude conditions. The stagnation pressure at the inlet to the combustor is 5 bar and stagnation temperature of 1000 K at the entry of the combustor corresponding to the high altitude conditions. The inlet of the combustor model is defined as Pressure Far Field. In this simulation, constant Mach number of 3 is considered at the inlet and hence Far field pressure condition is employed. The Outlet of the model is defined as Pressure Outlet. Only half of the combustor is considered for simulation purpose, the wall along the length and at mid-point of the width is considered as symmetry plane. The combustor walls are considered adiabatic wall condition. Density based solver with explicit scheme is used with second order discretization. Flow field is studied in terms of the Mach number, static pressure and static temperature along the combustor.

The temperature is observed to increase in the cavities which may be due to recirculation zone present in the cavities. Therefore, cavities may be used in the supersonic combustion for flame holding for achieving sustained combustion.

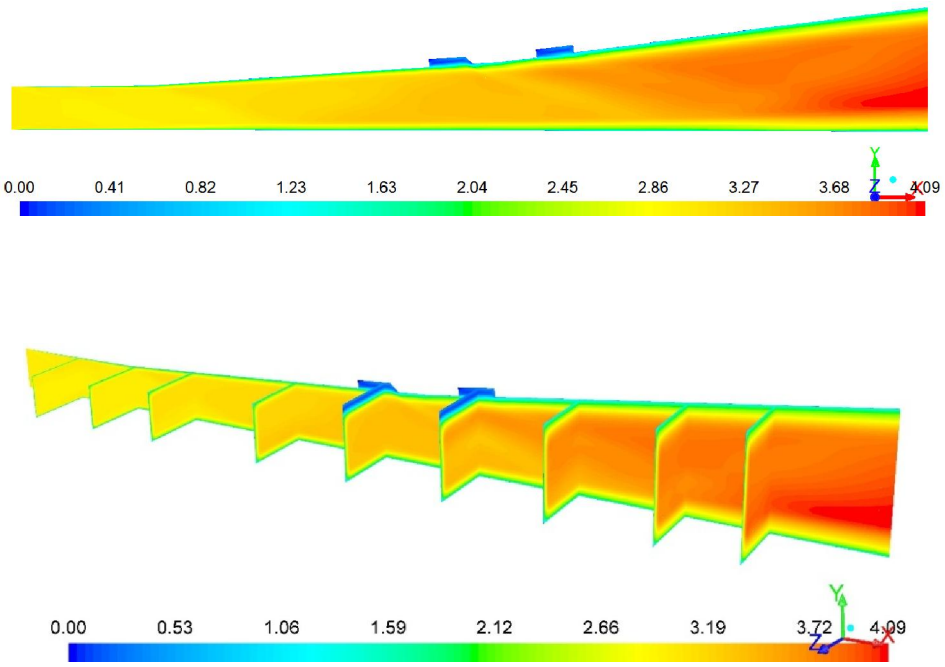

Fig.4.4 (a) Mach number contour along the combustor with cavities only

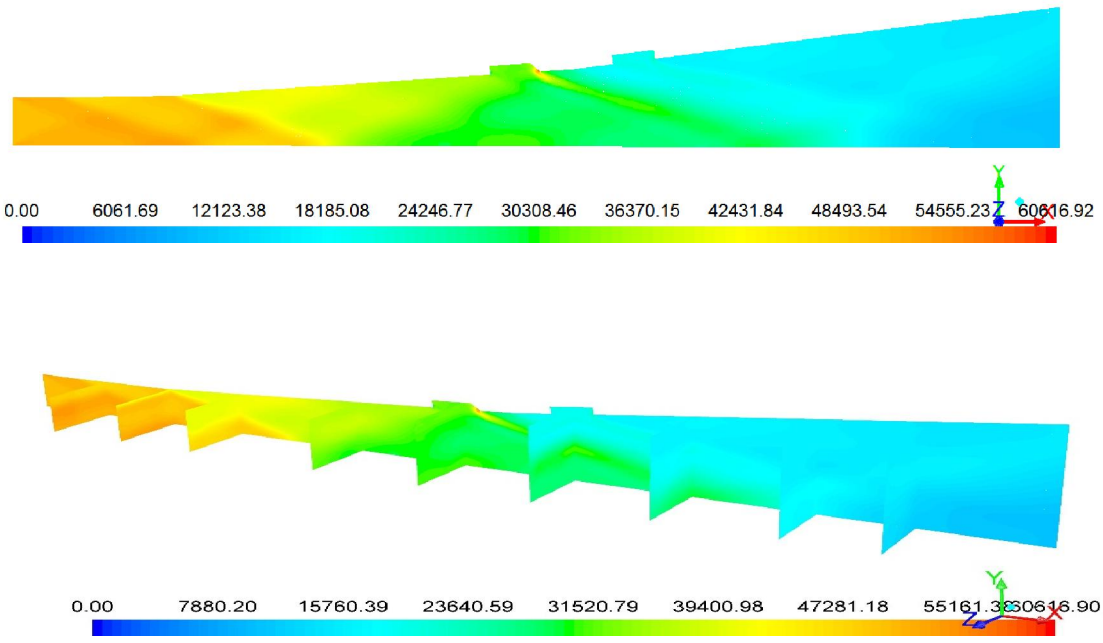

Fig.4.4 (b) Static Pressure (Pa) contour along the combustor with cavities only

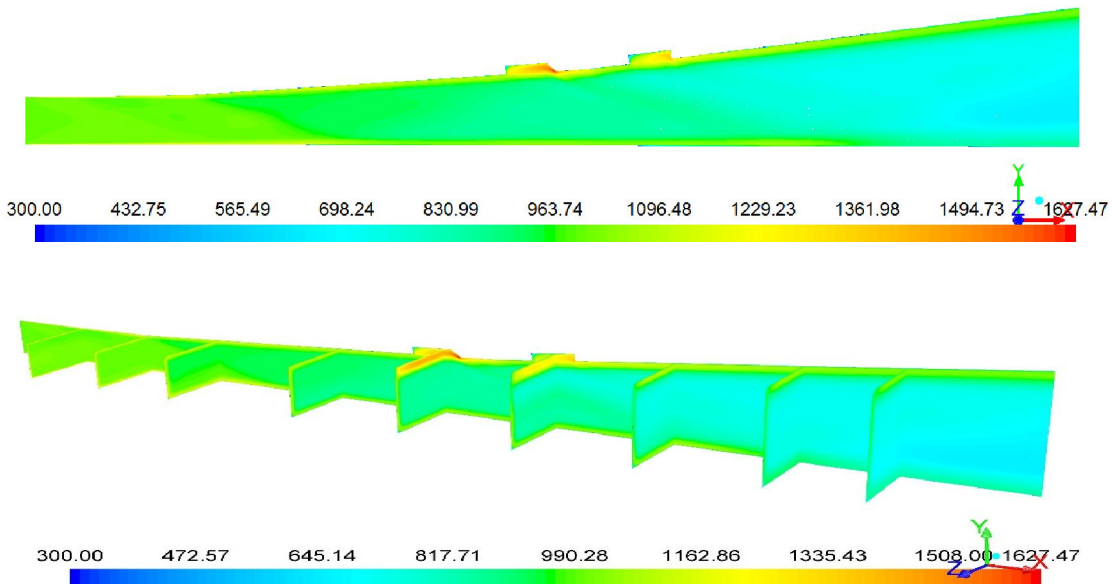

Fig.4.4 (c) Static temperature (K) contour along the combustor with cavities only

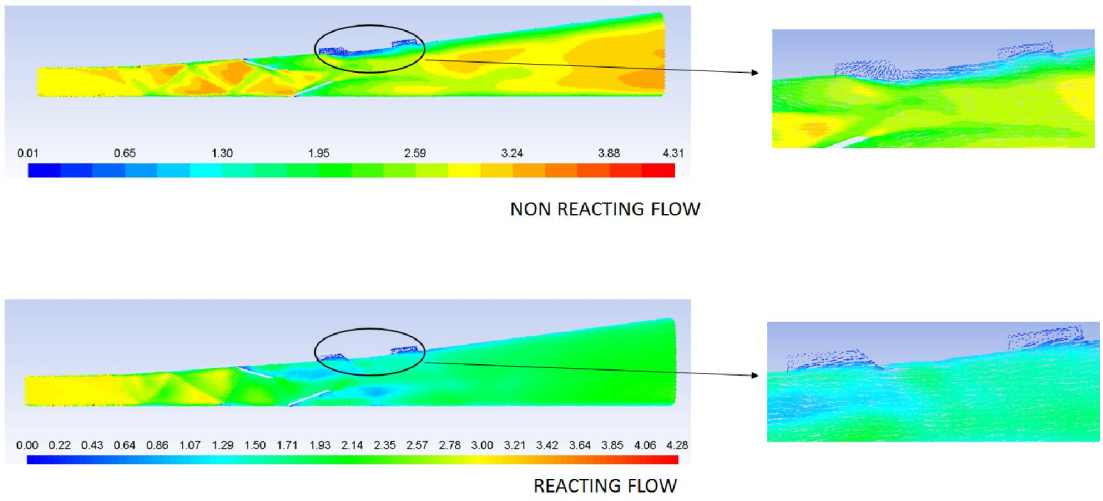

Fig.4.4 (d) Velocity vectors depicting Recirculation at cavities

Flow field parameters are shown in Fig.4.4 for a combustor with cavities along its length. The predicted Mach number contours along the combustor are shown Fig.4.4 (a).The cavities are provided at 826 mm and 1038 mm from combustor entry along the top wall of the combustor. When the supersonic airstream enters the combustor, flow becomes locally subsonic in the cavities as the flow gets decelerated with recirculation zones. Flow accelerates as it further passes through the diverging portion of the

combustor. The Mach number at the exit of the combustor is about 3.6. Fig.4.4 (b) shows the static pressure contour in the combustor. It can be observed that the static pressure in the combustor is higher in aft wall of the first cavity and a shock originating from the cavity may be observed. The pressure is locally higher in the combustor and there is a reduction in static pressure in the diverging portion of the combustor. The static temperature in the combustor in Fig.4.4(c) also depicts similar trend. The static temperature in the cavities is high establishing the fact that the cavities act as flame holders due to recirculation zones present in it. Static temperature in the cavities rises to about 1500 K. Static temperature is seen to be decreasing in the diverging portion of the combustor. However, it can be observed that there is a thick layer with higher temperature of about 1000 K at the boundary near the walls of the combustor. This can be seen especially along the top wall of the combustor. This is similar to the studies by Baurle *et al.* (1998) on the role of cavities in supersonic combustion in which good mixing with minimum total pressure losses was observed.

The combustor without ramps and cavities shows the pattern which is influenced by the geometry. In case of the combustor with ramps, there are shocks due to impingement of fuel with the oncoming supersonic air stream. There is a shock-shock interaction and shock boundary layer interaction as seen from the static pressure contours. In addition, velocity vectors (Fig. 4.7(a&b)) show generation of contra rotating vortices that contribute to better mixing. The combustor with cavities provides recirculation zones in the cavities due to which temperature rises locally and cavities act as flame holders. Locally, high temperatures are found in the cavities that will increase the flame stability. In the above simulations, it is observed that the ramps assist in fuel injection and mixing while cavities are useful for flame stabilization.

A study has been carried out on the full scale combustor with ramps and cavities with combustor entry Mach number 3 with the same boundary conditions. The results obtained are compared with combustor without ramps and without cavities. The combustor flow field is evaluated in terms of Mach number, static pressure and static temperature and compared with the plots of the following section. A parameter, turbulent intensity has been used to compare and discuss the application of ramps and cavities in the combustor. Velocity vectors are also presented.

In the above sections, detailed numerical experiments are performed to observe the effect of ramps and cavities independently.

4.1.1.4 Comparison of the combustors with and without ramps and cavities:

A model, full-scale combustor with ramps and cavities is considered for studies. Ramps and cavities as considered in the earlier cases are located in the combustor. The combustor of cross section 86 mm X 275 mm with a length of 1850 mm is considered as illustrated in Fig. 4.1. The combustor consists of one constant area section and other diverging sections with top wall divergence. Diverging portions of the combustor are provided to avoid thermal chocking. Seven ramps on the top wall and seven ramps on the bottom wall with fuel injection holes are arranged in a staggering configuration. Two cavities are positioned on the top wall. A computational study has been carried out to evaluate the performance. High speed air is allowed to flow through the combustor simulating the high altitude conditions. The stagnation pressure at the inlet to the combustor is 5 bar and stagnation temperature of 1000 K at the entry of the combustor corresponding to the high altitude conditions. The inlet of the combustor model is defined as Pressure Far Field. The Outlet of the model is defined as Pressure Outlet. Only half of the combustor is considered for simulation purpose, the wall along the length and at mid-point of the width is considered as a symmetry plane. The combustor walls are considered adiabatic wall condition. Density based solver with explicit scheme is used with second order discretization. Flow field is studied in terms of the Mach number, static pressure and static temperature along the combustor.

A comparison is done for all the above cases. Fig.4.5 illustrates the comparison of static pressure, static temperature and Mach number contours along the combustor with ramps and cavities, with ramps, with cavities and without ramps and cavities. The comparison is done when ethylene is used as fuel, while maintaining a combustor entry Mach number 3.

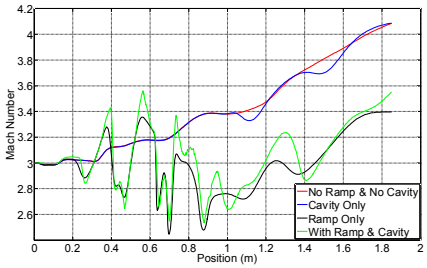

Fig.4.5 (a) Variation of Mach number with length

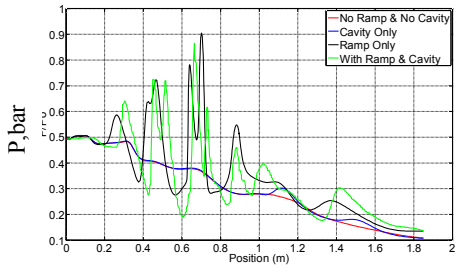

Fig.4.5 (b) variation of static pressure along combustor

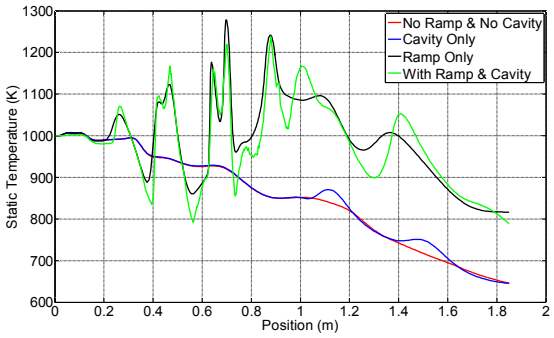

Fig.4.5 (c) Variation of static temperature along combustor

Higher static pressure can be observed in the combustor with ramps only. Mach number is lower in case of combustor with ramps compared to the combustor with cavities and without ramps and cavities. However, the Mach number is still in supersonic regime. It can be observed that there is a rise in static temperature in the combustor with ramps compared to the combustor configurations without ramps and cavities and with cavities. In the case of combustor configuration with ramps and cavities, Mach number is higher in the ramps zone and higher than the Mach number in the combustor with ramps only. Static pressure rise in the combustor with ramps and cavities is higher than the combustor with ramps, cavities and without ramps and cavities. Static temperature shows a higher value of about 1200 K in the supersonic combustor with ramps and cavities compared to the other cases studied for comparison. Static temperature rise is observed in the diverging portion of the combustor indicating sustained heat release and supersonic combustion.

Turbulent intensity is a measure of mixing due to turbulence. Turbulence intensity parameter contours are shown in the Fig. 4.6 (a). Turbulence intensity contours are generated for all the configurations viz. combustor without ramps & cavities, with only cavities, with ramps, and with injection from ramps & cavities. In the case of combustor without ramps and cavities, the turbulence is low indicating low mixing. In the case of cavities, the core of the combustor will have low turbulence while the boundary near the walls shows better mixing. Wall injection with cavity shows more turbulence compared to wall injection without cavity. Combustor with ramps located in the combustor show good turbulence with high intensity of mixing. Contours of combustor with ramps and cavities show high degree of turbulence in the core extending upto the cavities and turbulent intensity throughout the combustor configuration including the diverging portion of the combustor. Turbulence intensity plots of combustors showing the effect of ramps and cavities in the combustor are shown in Fig. 4.6 (b). It can be observed that the percentage of turbulence intensity for the combustor with ramps and ramps & cavities is higher than that for other combustors. It may be stated that the ramps provide better mixing in the combustor as indicated in the turbulence intensity plots.

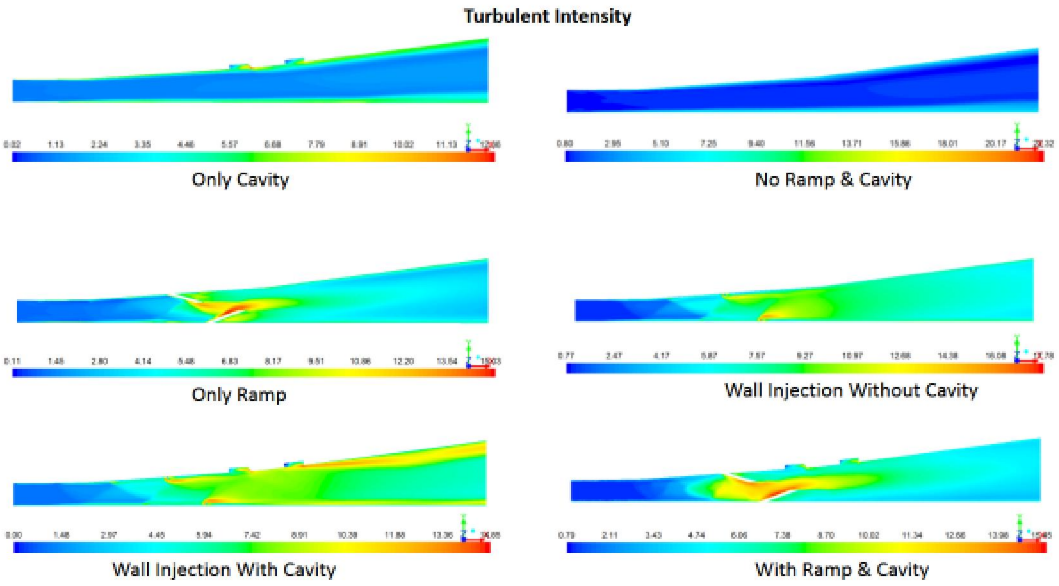

Fig. 4.6 (a) Turbulence Intensity contours for various types of configurations

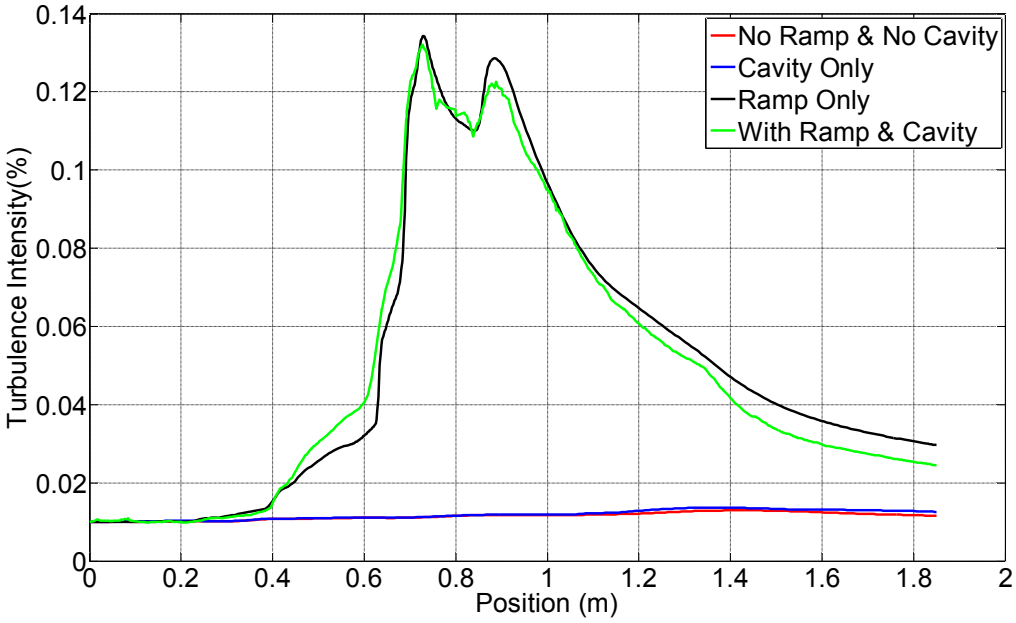

Fig.4.6 (b) Effect of Ramp cavities in turbulence intensity to enhance mixing

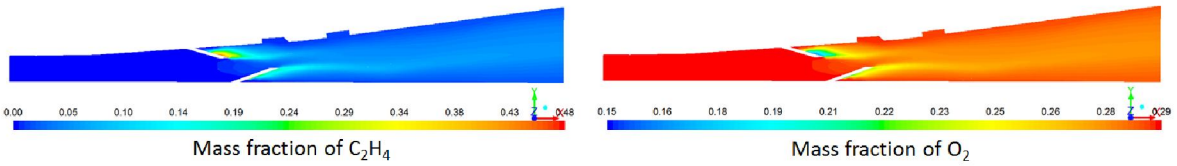

Non reacting flow

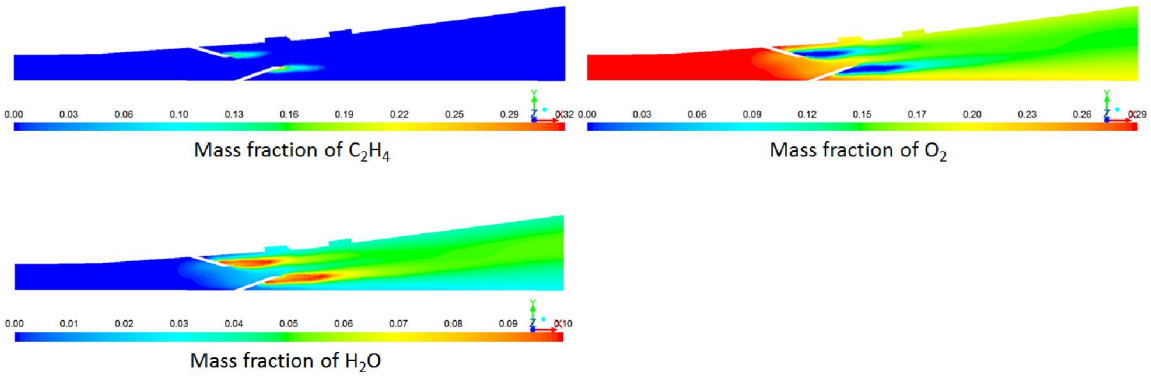

Reacting flow

Fig.4.6 (c) Mass fraction contours for Mach 3 flow in combustor

4.1.1.5 Vorticity and recirculation of ramps and cavities:

Fig.4.7 (a) and (b) show vorticity and recirculation near the ramp and cavity respectively. Velocity vectors near the ramp indicate contra rotating vortices. These vortices help in better mixing of fuel with the supersonic airstream. Recirculation is observed in the cavities as represented by the velocity vectors. This enhances the temperature locally and the flame stabilization.

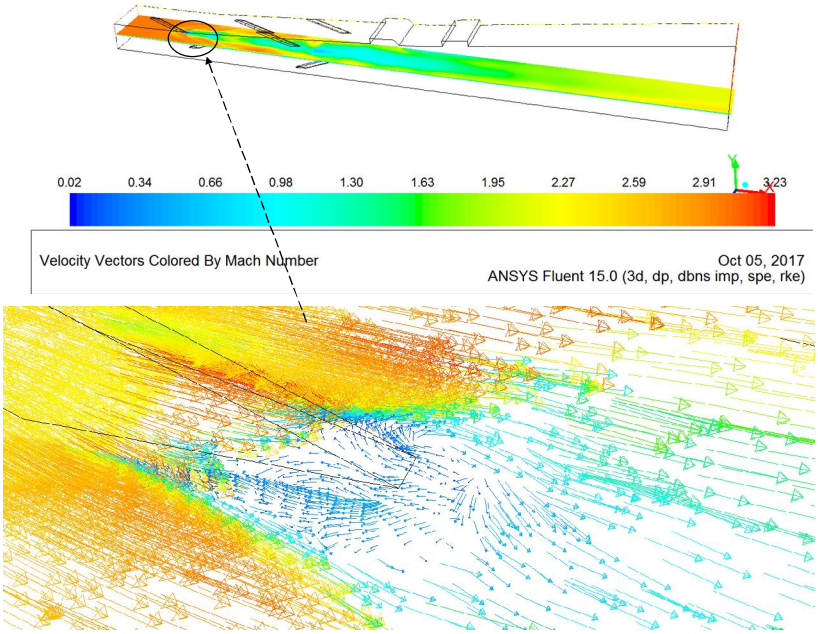

Fig.4.7 (a) Velocity vectors for vortices near the ramps

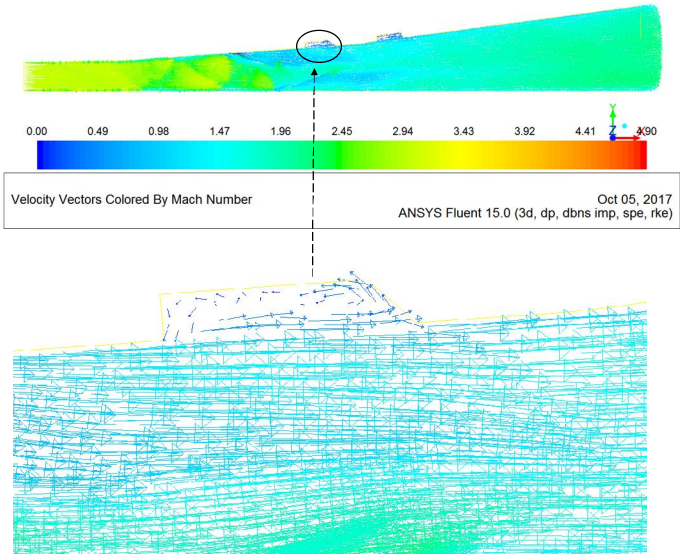

Fig.4.7 (b) Velocity vectors depicting recirculation at the cavity

From the study of the various combustor configurations studied viz., without ramps and cavities, with ramps, with cavities, with the ramps and cavities, it can be observed that the combustor configuration with ramps and cavities is a more suitable candidate for providing mixing of fuel and air and flame holding together.

Therefore, further studies are carried out with ramps and cavities together on a full-scale combustor. The schematic diagram of the combustor with ramps and cavities is shown in Fig.4.1 and is reproduced in Fig.4.8.

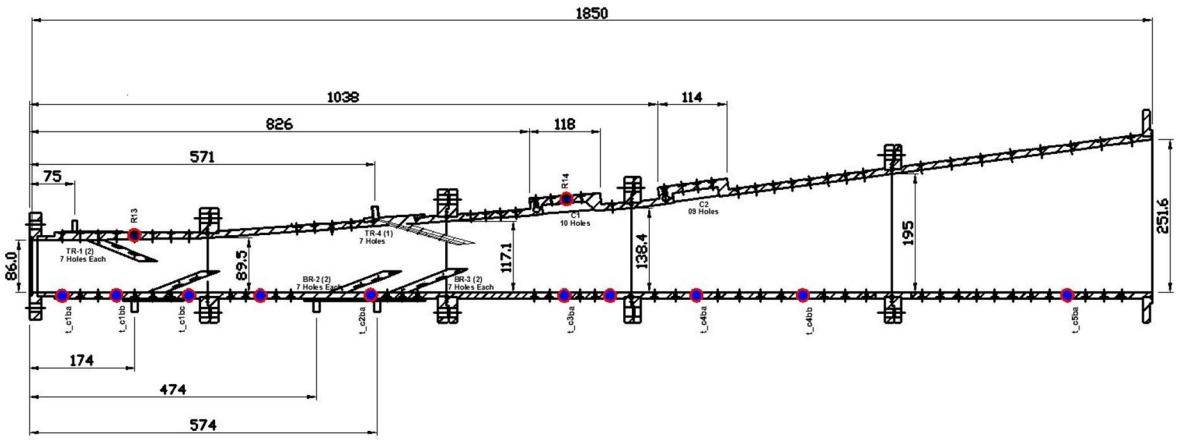

Fig.4.8 Ramp-cavity combustor (Full-scale)

Considering the full-scale combustor with ramps and cavities, effect of fuel, entry Mach number and injection pattern are studied and described in the following sections.

4.1.2 Studies on full-scale combustor with aviation kerosene as a fuel:

Computational studies are conducted on full - scale, ramp-cavity combustor with aviation kerosene as fuel and fuel equivalence ratio of 0.6 for two conditions of combustor entry Mach number 2 and 3. Fuel is injected from the ramps located in the combustor. The performance of combustor is studied in terms of Mach number, static pressure, static temperature contours along the combustor. For droplet model, spherical drag law, droplet vaporisation (law 1 &2), droplet boiling (law 3) are used in the simulations carried out in ANSYS Fluent.

4.1.2.1 Studies with Full-scale ramp-cavity combustor at entry Mach 2 with aviation kerosene as a fuel:

Computational studies are conducted to simulate the flow field and predict Mach number, static pressure, static temperature and mass fractions of species along the combustor.

A model, full-scale combustor with ramps and cavities is considered for studies. Ramps and cavities as considered in the earlier cases are located in the combustor. The combustor of cross section 86 mm X 275 mm with a length of 1850 mm is considered for simulation and illustrated in Fig. 4.8. The combustor consists of one constant area section and other diverging sections with top wall divergence. Diverging portions of the combustor are provided to avoid thermal chocking. Seven ramps on the top wall and seven ramps on the bottom wall with fuel injection holes are arranged in a staggering configuration. Two cavities are positioned on the top wall. . High speed air is allowed to flow through the combustor simulating the high altitude conditions. The stagnation pressure at the inlet to the combustor is 5 bar with stagnation temperature of 1000 K at the entry of the combustor corresponding to the high altitude conditions. Aviation kerosene is used as fuel and simulations are carried out with combustor entry Mach numbers 2 and 3 respectively. The inlet of the combustor model is defined as Pressure Far Field. The Outlet of the model is defined as Pressure Outlet. Only half of the combustor is considered for simulation purpose, the wall along the length and at mid-point of the width is considered as a symmetry plane. The combustor walls are considered adiabatic wall condition. Density based solver with explicit scheme is used with second order discretization. Flow field is studied in terms of the Mach number, static pressure and static temperature along the combustor. In this section, simulation studies are carried out with combustor entry Mach number 2 and results are presented.

The parameters thus obtained through simulations are shown in Fig.4.9. (a), (b) & (c)

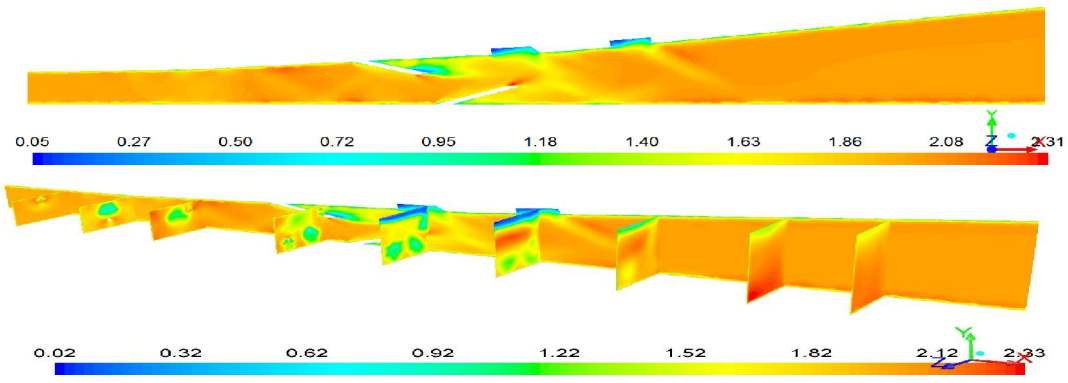

Fig.4.9 (a) Mach number distribution along the combustor

The Mach number distribution is depicted in Fig.4.9 (a). The spread across the planes is also shown. It can be seen that the supersonic airstream enters the combustor at Mach 2. It takes a while for vaporization of fuel before it gets mixed homogeneously with airstream. It can be observed that the Mach number decreases when fuel is injected from the ramps due to fuel addition and mixing. The flow compresses due to ramps and increases in the position where ramps are not located. The Mach number is locally subsonic (about 0.4 to 0.7) in the cavities due to formation of recirculation zones. It can be seen that flow is almost stagnant in some parts of cavities. However, higher value of Mach number can be observed at the tip of the ramp and next to the cavities. After the cavities, the Mach number increases, in the diverging portion of the combustor. The Mach number increases to about 2.1 at the centre-line of the combustor.

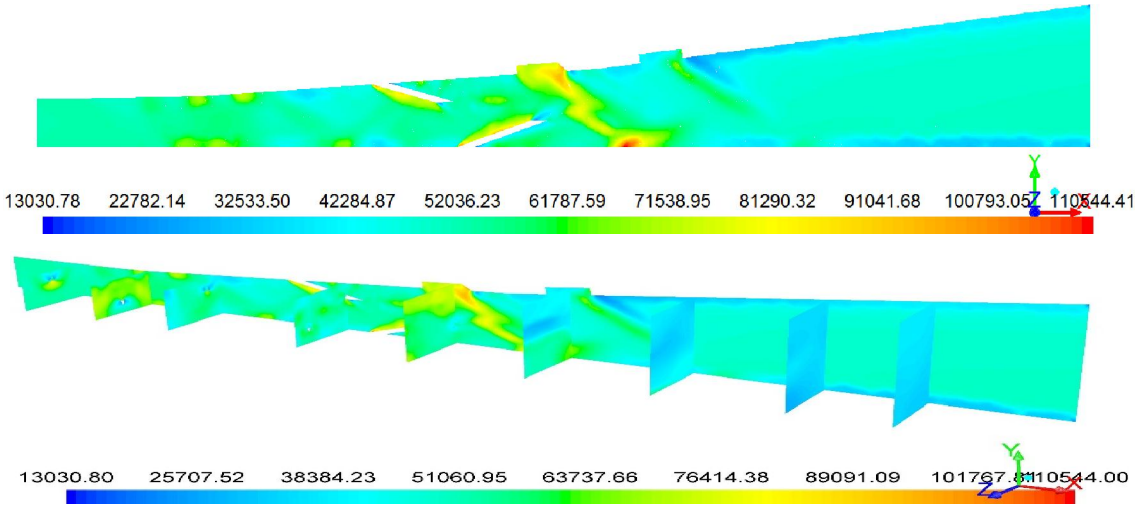

Fig.4.9 (b) Static pressure (Pa) contour along the combustor

Static pressure contours are shown in Fig.4.9 (b). The predictions indicated that the static pressure rises in the ramps as the fuel is injected from the ramps and mixes with the supersonic airstream. However, the reduction in static pressure is observed in the area where ramps are not located as expansion takes place. As the supersonic airstream enters cavity floor which spreads along the cross section of the combustor, it can be observed that there is a higher pressure. The pressure rise is predominantly seen in the first cavity compared to second cavity. The static pressure reduces to the ambient pressure at the exit of the diverging portion of the combustor.

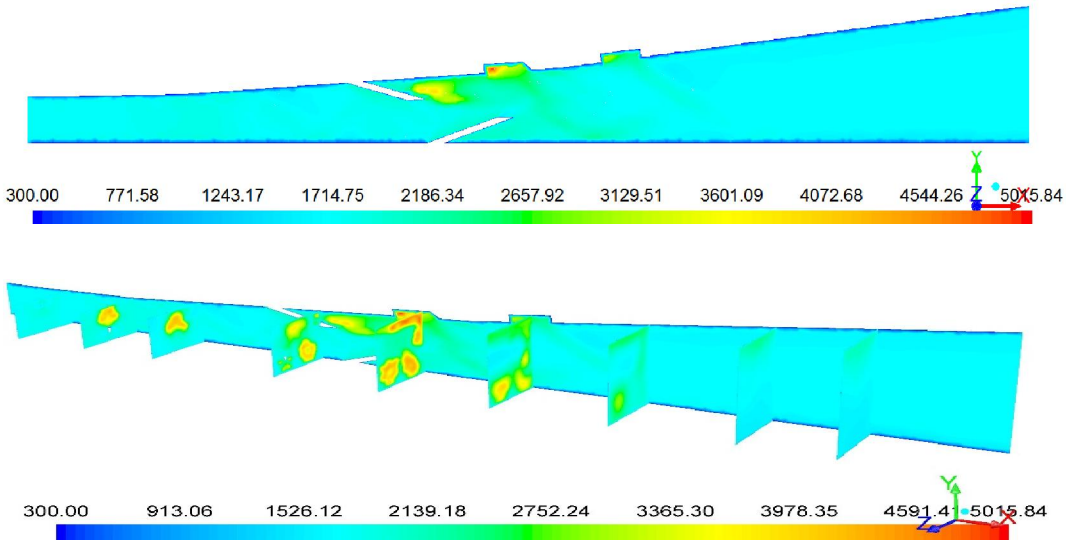

Fig.4.9 (c) Static temperature (K) contours along the combustor.

Static temperature contour along the combustor is depicted in the Fig.4.9(c). It can be seen that there is rise in static temperature upto the ramps zone in the combustor. Static temperature increases at the ramps, similar to that in the case of static pressure, at fuel injecting ramps. At some pockets near the ramps, the static temperature reaches a value of about 3000 K. Locally high temperatures are seen in the cavity zones that act as flame holders and due to the presence of recirculation zone in the cavities. The rise in static temperature is observed to have spread completely in the first cavity compared to the second cavity. The static temperature continues to be high, about 1500-1800 K, in the diverging portion of the combustor.

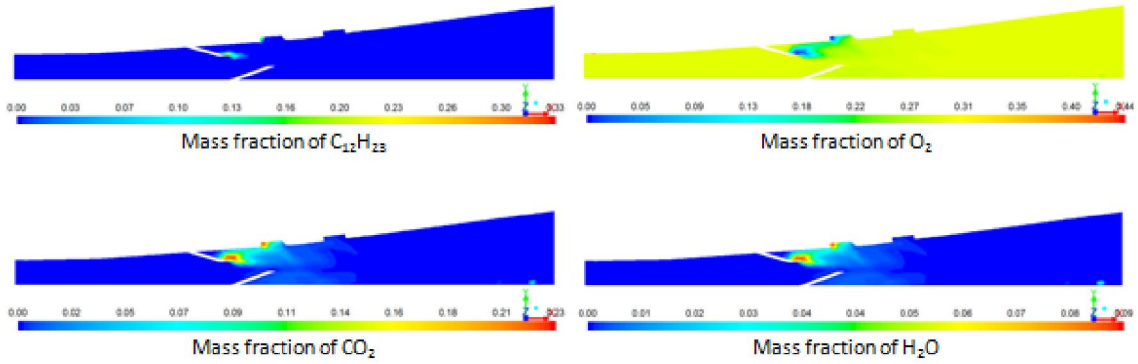

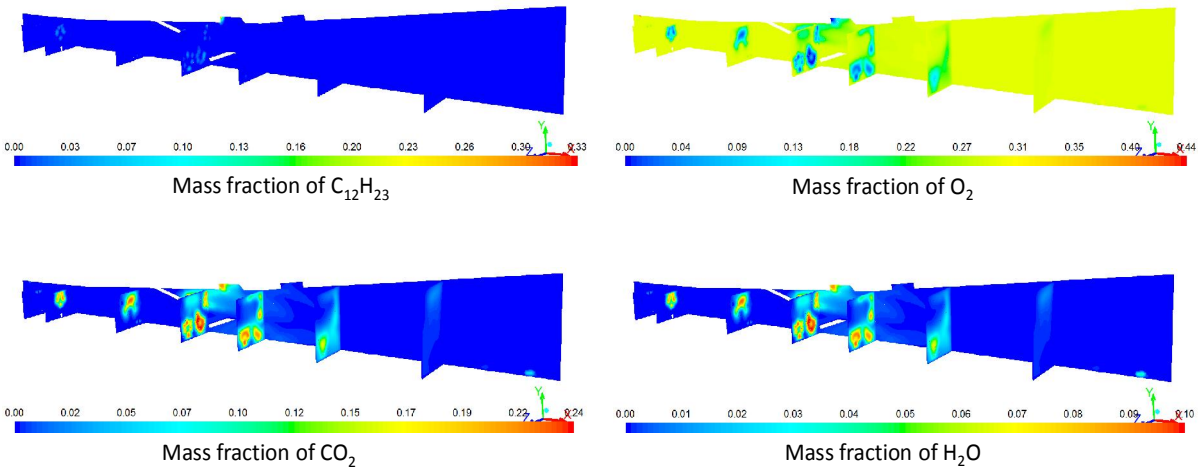

Fig.4.9 (d) Mass fractions of species with aviation kerosene at Mach 2

Mass fractions of species are shown in Fig.4.9 (d). It can be observed that aviation kerosene mixes with supersonic stream of air as it is injected through the ramps. The mass fractions of species are shown in the planes along the combustor length to capture the spread of the species across the cross section at the plane.

In the figure showing the cross section of the combustor at various planes along the combustor, the mass fraction of aviation kerosene is observed in the ramps and upto the cavity zone in the combustor. This may be due to the time delay in aviation kerosene breaking into liquid droplets and then vaporizing before mixing with supersonic stream of air. Oxygen mass fraction in Fig.4.9 (d) shows that mixing of oxygen with aviation kerosene takes place in the ramps, cavities and in the diverging portion of combustor. However, considerable oxygen mass fraction is available for mixing with additional fuel. Fig. 4.9 (d) also depicts the mass fraction of CO_2 along the combustor, in the ramps zone and cavities. Mass fraction is high towards the end of ramps indicating combustion taking place with time delay. CO_2 mass fraction is seen in the diverging portion of the combustor.

Formation of H_2O mass fraction can be observed at the ramps and cavities zone and in the diverging portion of the combustor. The concentration is more towards the end of the ramps and mass fraction of H_2O can be seen in the diverging portion of the

combustor. Formation of H_2O can be seen in the cavities indicating the high temperature, recirculation zones in the cavities that support the sustained combustion. This may be observed in the cross sectional planes shown along the combustor near the ramps and cavities along the combustor.

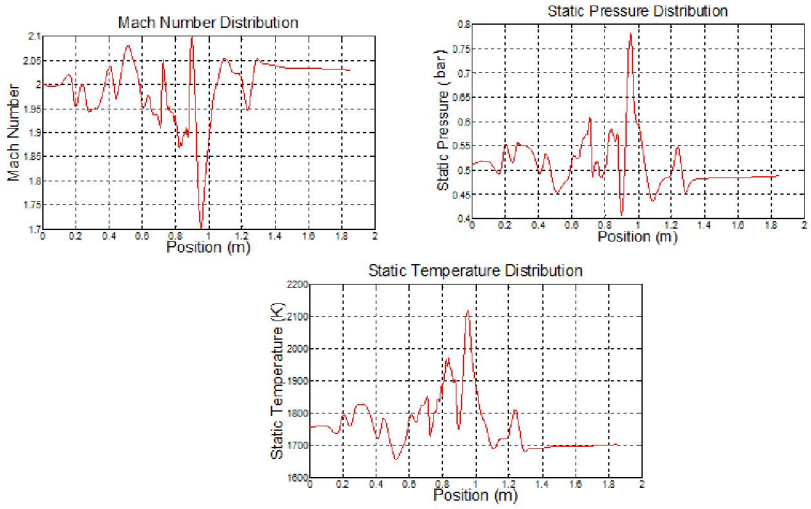

Fig.4.9 (e) Flow parameters along combustor with aviation kerosene as fuel at Mach 2

Fig.4.9 (e) shows the flow parameters along the combustor with aviation kerosene as fuel when supersonic airstream enters combustor at Mach 2. It can be seen that Mach number reaches to a value of 1.7 near cavities. Static pressure rises near the ramps indicating mixing of fuel. Static temperature rises after the ramps and in cavities.

4.1.2.2 Studies on full scale combustor with entry Mach 3 with Aviation kerosene as fuel:

Computational studies are carried out on a ramp-cavity, full-scale combustor with aviation kerosene as fuel at an equivalence ratio of 0.6. Fuel is injected through ramps. Combustor entry Mach number is varied to 3 and similar set of simulations are done, the traces of flow field parameters are obtained and are compared in Fig.4.10 (a). It can be observed that the trends are similar for the case of Mach 2.

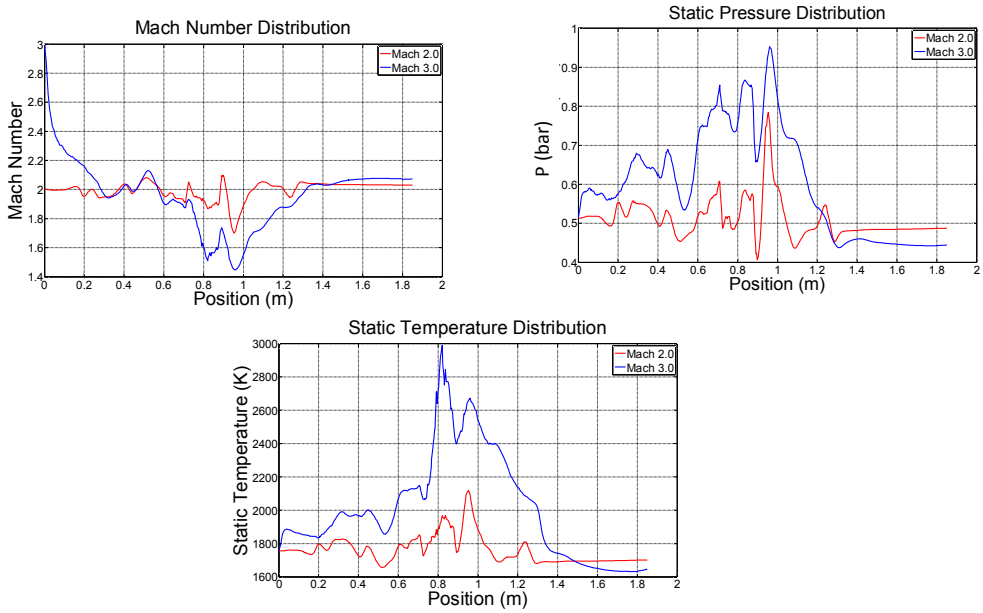

Fig.4.10 (a) Flow field parameters along the combustor with aviation kerosene as Fuel for two entry Mach numbers.

It can be seen that the Mach number is supersonic throughout the combustor. There observed to sharp fall in Mach number at the end of ramps (x<850mm). With higher Mach number 3, it can be seen that there is a reduction in Mach number to 1.2 at the end of the ramps. This could be due to presence of multiple oblique shocks decelerating the high velocity airstream. Static pressure along the combustor is high for combustor entry Mach 3. Compared to combustor entry Mach 2, with aviation kerosene as fuel, static pressure is observed to be consistently higher for the supersonic airstream with combustor entry Mach 3 due to fuel mixing in the ramps and subsequent combustion. Static pressure in the diverging portion of the combustor is less and in line with the supersonic combustion trend. The static temperature for combustor entry Mach 3 condition is also high from the beginning of the combustor, in the diverging portion and is less after 1.5 m from the start of the combustor. This is in line with variation of static pressure. The difference in static temperature plots show that the heat addition is high which indicates sustained supersonic combustion.

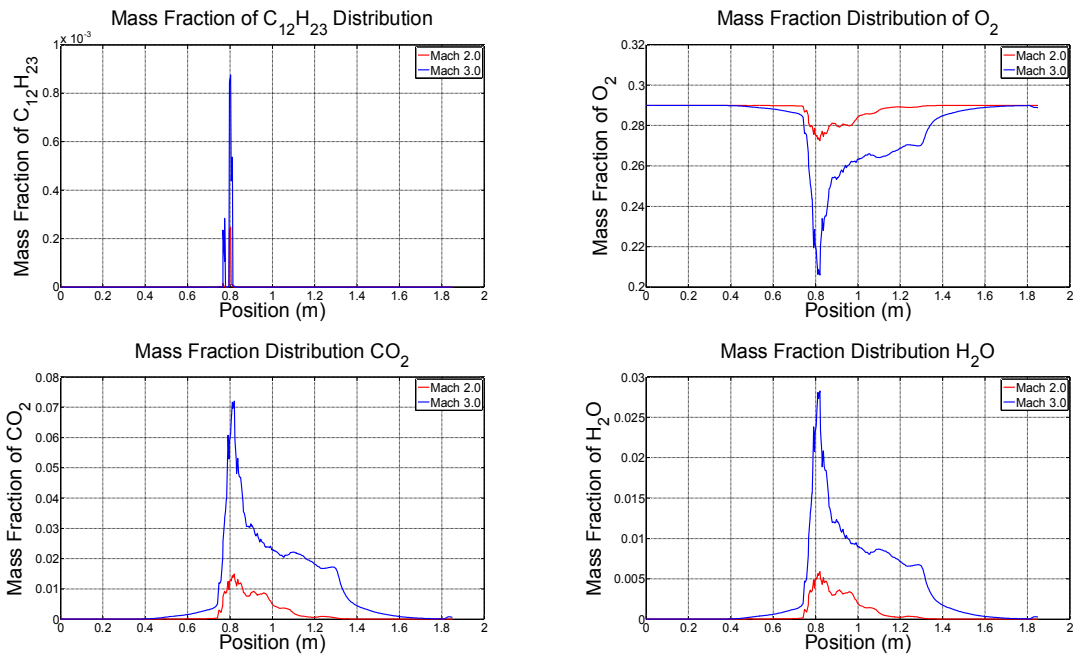

Fig.4.10 (b) Mass fraction of species along the combustor with aviation kerosene as fuel

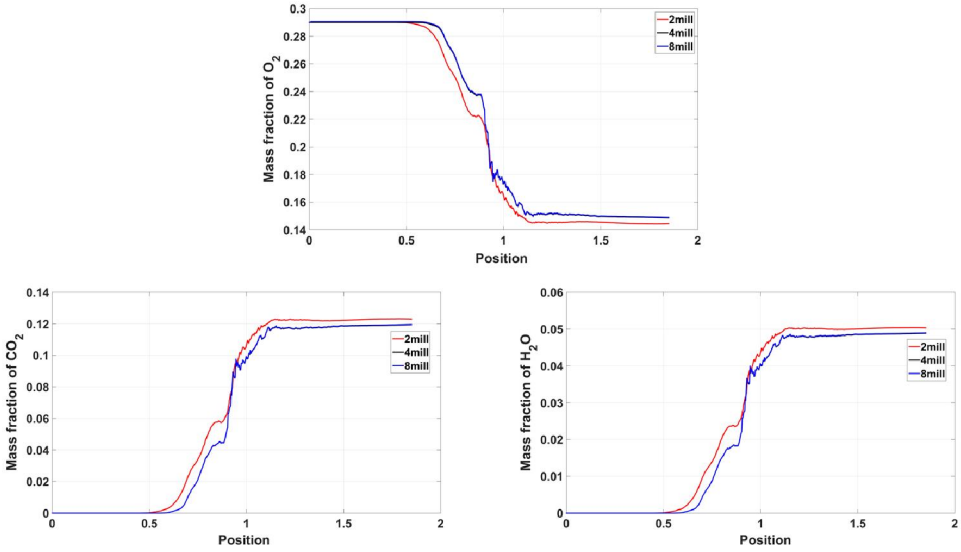

Fig.4.10 (c) Averaged Mass fraction of species across the combustor section

The mass fractions of species along the combustor for both combustor entry Mach 2 and Mach 3 supersonic airstreams are shown along the centre-line of the combustor in Fig.4.10 (b) with combustion of aviation kerosene as fuel. Mass fraction of aviation kerosene depicts that its maximum concentration is observed at 800 mm from the

combustor entry and depletion thereafter. Oxygen mass fraction also indicates that by 800 mm from the combustor entry, the concentration decreases maximum for Mach 3 condition compared to Mach 2. Similar trend is observed with the mass fractions of CO_2 and H_2O.The formation of product species is high for Mach 3 condition. Flow conditions are considered same for both the simulations except the entry Mach numbers. The mass fractions of fuel, oxygen, products of combustion are plotted along the centre line of the combustor. The variation in the plot along the combustor is due to the variations in the volume cell considered to plot the oxygen and H_2O content. However, the averaged mass fractions of the species along the combustor cross section as shown in Fig.4.10(c), depict the constant quantity of oxygen and H_2O indicating same quantity in the combustor. Similar plots are drawn along the centre-line of the combustor for the simulations studies carried out.

From the computational study of combustion of aviation kerosene in the full-scale, ramp-cavity combustor, it is observed that variation of Mach number with combustor entry Mach 3 is significant compared to Mach 2 condition. There is marginal rise in static pressure but static temperature is higher throughout the combustor except towards the exit of the combustor. Due to liquid form of aviation kerosene involving the various functions; break up of liquid particles, vaporizing and mixing with supersonic airstream for supersonic combustion, it may be effective with combustor entry Mach 2 for the case of aviation kerosene.

As mentioned earlier, the simulation studies show better performance with aviation kerosene as fuel for combustor entry Mach number 2 and 3. However, experimental studies conducted with aviation kerosene as fuel demonstrate the requirement of higher self-ignition conditions for the combustion of aviation kerosene. Liquid fuels are to break-up and vaporize before mixing with the supersonic airstream. Due to ignition delay, complete combustion of fuel with air is difficult. To overcome the issues with liquid hydrocarbon fuels, gaseous fuel such as ethylene is the candidate fuel for supersonic combustion studies.

4.2 Effect of Fuels:

Fuel used in the combustion process plays an important role in achieving sustained supersonic combustion. In this study, three different fuels are used. Hydrogen is known to be high energy carrier and has been extensively used as a propellant and as a fuel in space applications. However due to handling difficulties, the focus is shifted by the researchers on aviation kerosene as a fuel. Over the years, experimental work has been done both in India and abroad. In recent times, due to the availability of high speed computing facilities, researchers started working on fuels alternative to aviation kerosene. Thus, Ethylene as a gaseous fuel does not pose difficulties and due to its simple carbon chemistry, has emerged as a candidate fuel. It is now being explored by many researchers. Aviation kerosene and ethylene are well preferred hydrocarbon fuels. Experimental studies have been conducted with aviation kerosene to evaluate the performance of the combustor and compare with simulation studies. However, liquid fuel is required to undergo the breakup of particles, vaporization process prior to mixing with the supersonic airstream. Pilot Hydrogen fuel is required for providing self-ignition condition for aviation kerosene. As the residence time of supersonic airstream in the combustor is less, of the order of 1 ms, the reaction of fuel with air is mixing dominated, gaseous ethylene is explored as candidate for fuel in the supersonic combustion studies. Ethylene being a gaseous hydro carbon fuel, it is relatively easy to achieve mixing and combustion in a supersonic combustor.

A comparison is made with aviation kerosene and ethylene as fuel on a full-scale supersonic combustor with ramp and cavity configuration. Combustor entry Mach number was considered to be Mach 3. Fig.4.11 (a) shows variation of Mach number along the combustor. Mach number contour with ethylene fuel along the combustor shows that there is a rise in the ramps zone and in the cavities. Mach number increases in the diverging portion of the combustor. In the case of aviation kerosene, it can be seen that there is reduction in Mach number immediately in the combustor to about 2 and reduces to about 1.3 in the cavity zone. Mach number increases in the diverging portion of the combustor.

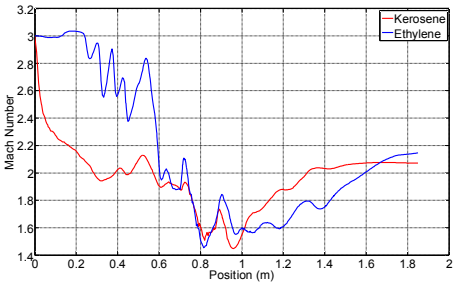

Fig.4. 11 (a) Mach number variation along the full-scale combustor

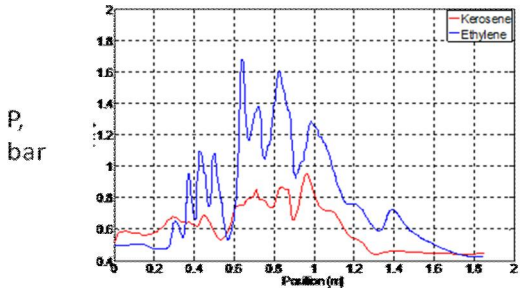

Fig.4.11 (b) Static pressure variation along the full-scale combustor

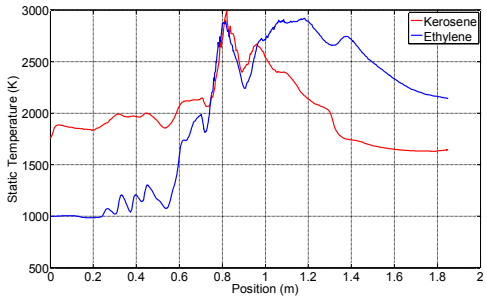

Fig.4.11 (c) Static temperature variation along the full-scale combustor

Variation of static pressure along the combustor for aviation kerosene and ethylene as fuels for the full-scale combustor is shown in Fig.4.11 (b). The static pressure rise in the ramps is very high in the ramps for ethylene and increases to about 1.6 bar. With aviation kerosene as fuel, the pressure rise is seen to be very less compared to static pressure contour with ethylene as fuel. Variation of static temperature contours along the combustor for aviation kerosene and ethylene as fuels is shown in the Fig.4.11 (c). Static temperature increases gradually in the ramps zone and rises to a high value in the cavities and continues to be high in the diverging portion of the combustor. Static temperature increase can be seen in the beginning of the combustor, in the ramps zone and cavities with aviation kerosene as fuel. It can be observed that Static temperature decreases in the diverging portion of the combustor compared to that with ethylene fuel. The heat release with ethylene as fuel is observed to be high compared to the aviation kerosene as fuel in the ramp-cavity combustor.

It is observed that ethylene as fuel is easy to mix with supersonic stream of air flowing in the supersonic combustor. This is more important in high speed air flows where combustion is predominantly based on the mixing due to short residence time of air in the combustor. Based on these studies, further work is carried out with ethylene as fuel in the supersonic combustor.

Computational studies have been carried out on a full-scale combustor for checking the suitability of ethylene as fuel. Detailed results have been herewith presented for a case of combustor entry Mach number 3.Computational studies are carried out on full-scale combustor with ethylene as fuel. Combustor entry conditions of 2, 2.5 and 3 have been simulated for ethylene fuel to evaluate the effect of combustor entry Mach number on the flow field. The performance of the ramp-cavity combustor has been studied in terms of variation of Mach number, static pressure, static temperature and mass fractions of species along the combustor.

4.2.1 Studies on Full-scale combustor with Ethylene as fuel at combustor entry Mach 3 condition:

A model, full-scale combustor with ramps and cavities is considered for studies. Ramps and cavities are considered as in the earlier cases and are located in the combustor. The combustor of cross section 86 mm X 275 mm with a length of 1850 mm is considered as illustrated in Fig. 4.12. The combustor consists of one constant area section and other diverging sections with top wall divergence. Diverging portions of the combustor are provided to avoid thermal chocking. In this case, ethylene fuel (133gm/s) is injected. Seven ramps on the top wall and seven ramps on the bottom wall with fuel injection holes are arranged in a staggering configuration. Two cavities are positioned on the top wall. High speed air is allowed to flow through the combustor simulating the high altitude conditions. The stagnation pressure at the inlet to the combustor is 5 bar with stagnation temperature of 1000 K at the entry of the combustor corresponding to the high altitude conditions. Ethylene is used as fuel with equivalence ratio of 0.6 and simulations are carried out with combustor entry Mach number 3. The inlet of the combustor model is defined as Pressure Far Field. The Outlet of the model is defined as Pressure Outlet. Only half of the combustor is considered for simulation purpose, the wall along the length and

at mid-point of the width is considered as a symmetry plane. The combustor walls are considered adiabatic wall condition. Density based solver with explicit scheme is used with second order discretization. Flow field is studied in terms of the Mach number, static pressure and static temperature along the combustor.

The studies are carried out for both mixing and combustion cases. It is considered that ethylene (133 gm/s) is injected into the combustor through the fuel injection ramps located in the combustor while maintaining an equivalence ratio of 0.6. For this condition, the computational studies are carried out to observe the variation in Mach number, static pressure, static temperature and species concentration for the cases of non-reacting (cold flow with fuel addition) and reacting (combustion) flows.

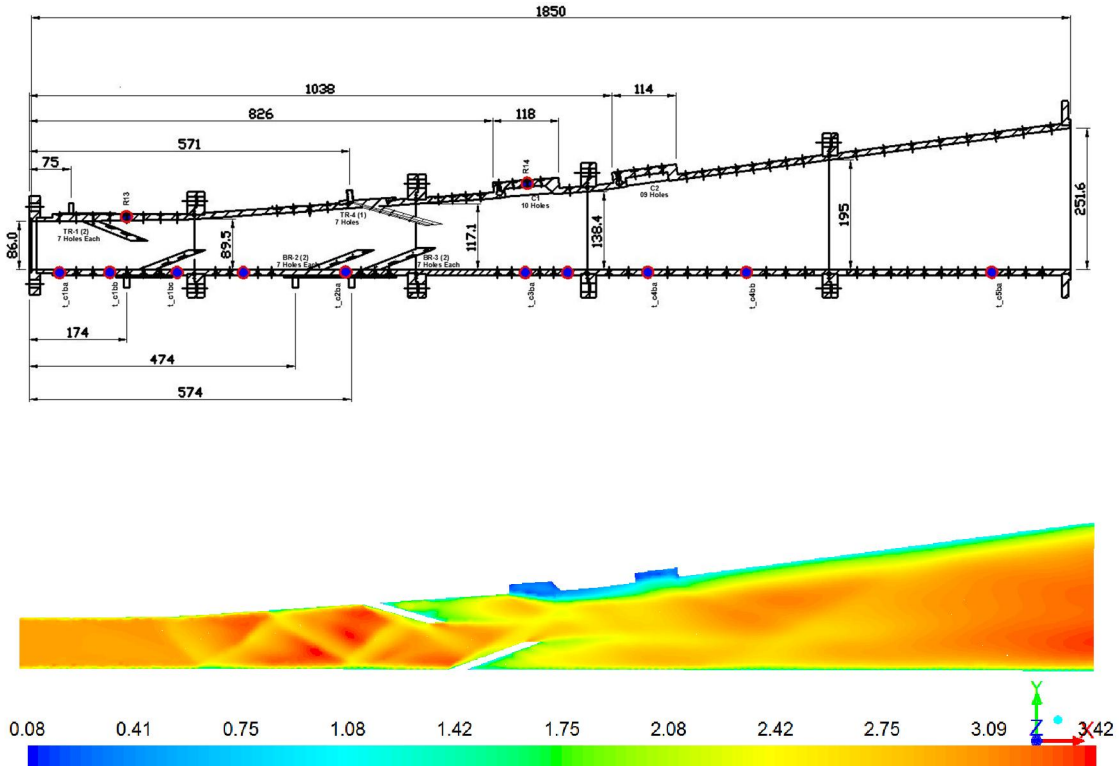

(a) Non reacting flow with ethylene at combustor entry M 3.0

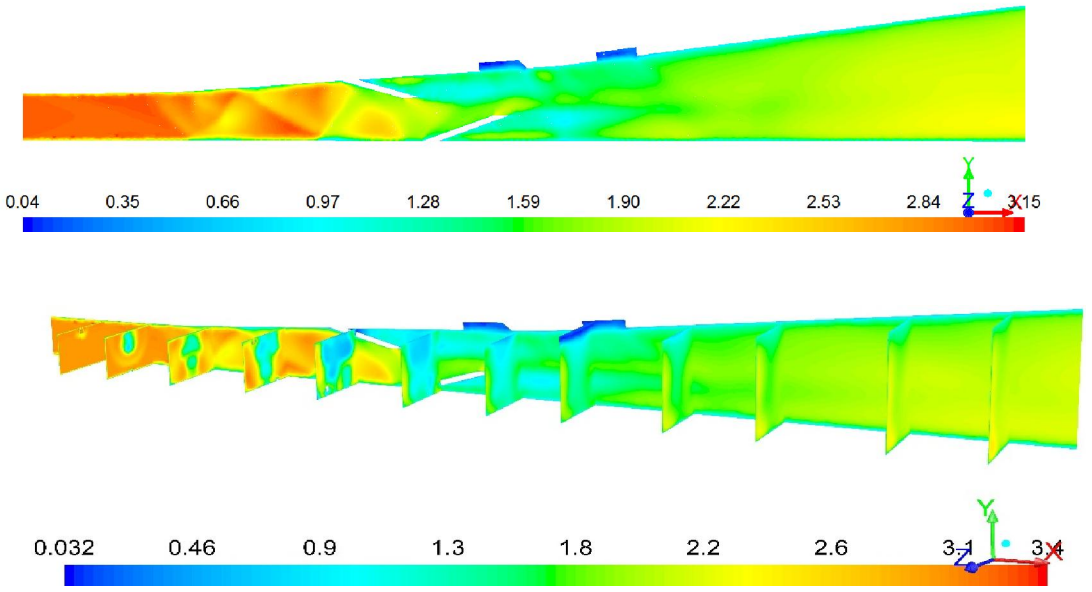

(b) Reacting flow with ethylene at combustor entry M3.0

Fig.4.12 Mach number variation along the combustor

The variation of Mach number along the length of the combustor is depicted in Fig.4.12 (a) for cold flow with fuel injection (with no combustion). It can be seen that there is a drop in Mach number along the length. The Mach number is 3.0 at the entry and decreased after certain length where the ramps are provided. At the vicinity of ramps, a significant drop is observed in Mach number due to thorough mixing. Also, the predictions revealed the formation of three dimensional oblique shocks in the ramp zone. The shocks have resulted enhanced mixing of the fuel with the supersonic airstream. Also, inclusion of ramps develop contra rotating vortices in the supersonic air stream and induce baro-clinic torque which results in proper mixing of fuel with incoming supersonic air. However, local increase in Mach number is observed within the span of ramps (x<800mm). At the downstream of ramps, the flow has reached a Mach number of about 1.5. However, at the zone adjacent to end of ramps and cavities, the flow decelerated due to entrainment of airstream in the cavities. It can be clearly observed that within the cavities, the flow is subsonic due to the presence of recirculation zones. Also, it can be further noted that along the wall extending from the cavities, the flow further decelerated with the local variations in the value within the major portion of the combustor. The shear layer is decreasing along the combustor while the Mach number is

increasing. It is interesting to see further acceleration towards the end of combustor. This is due to the diverging portion of the combustor. This has established the improvement of flow with combined effect of ramps and cavities.

The behaviour of Mach number has slightly got deviated in case of combustor with combustion as represented in Fig.4.12 (b). In case of reacting flow (combustion), the flow is still supersonic in the close regions of ramps but got decelerated at the entry regions of cavities. It can be clearly observed that the flow is supersonic at the end of the combustor but with slight decrease when compared to non-reacting flow. This can be substantiated that the combustion of fuel has resulted in marginal drop in Mach number but with significant increase in static pressure. The combustion of fuel has driven the flow with more energy that would lead to higher thrust. At the exit of the combustor, the drop in Mach number is observed to be about 30%. It can further be seen that the fluctuations in Mach number as well as static pressure are more significant in the zone of cavities than in the regions of ramps. This is demonstrating the fact of the mandatory provisions such as cavities in achieving flame stabilization.

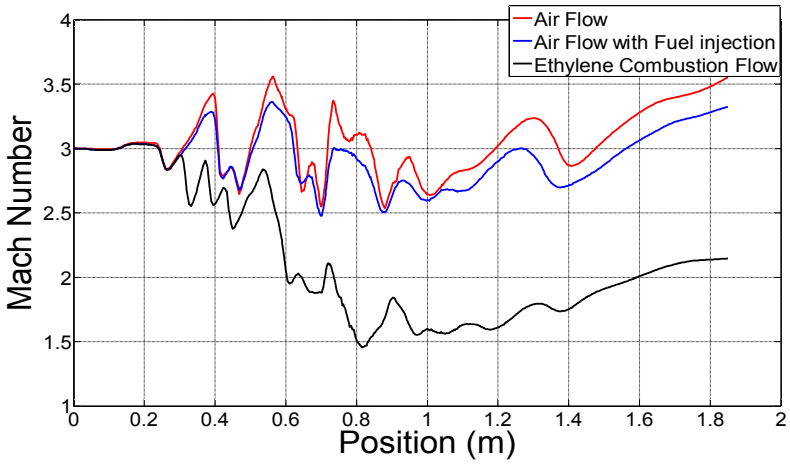

Fig.4.13 Comparison of variation of Mach number for Mach 3.0 condition

Fig.4.13 depicts the plot comparing Mach number along the combustor for various events along the combustor. As seen from the plots, the Mach number decreased with combustion along the combustor. This is due to fuel injection, deceleration due to shocks emanating from the impingement of fuel with air, shock structure and mixing. However, the Mach number continues to be supersonic throughout the combustor.

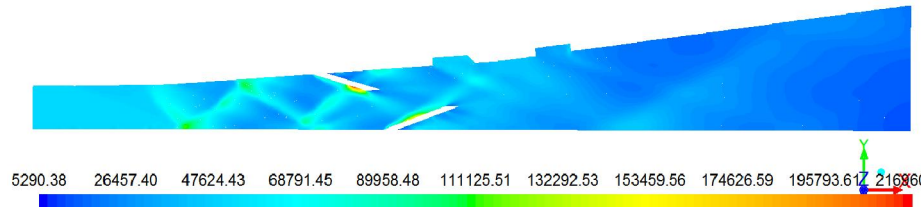

(a) Non reacting flow with ethylene at combustor entry M 3.0

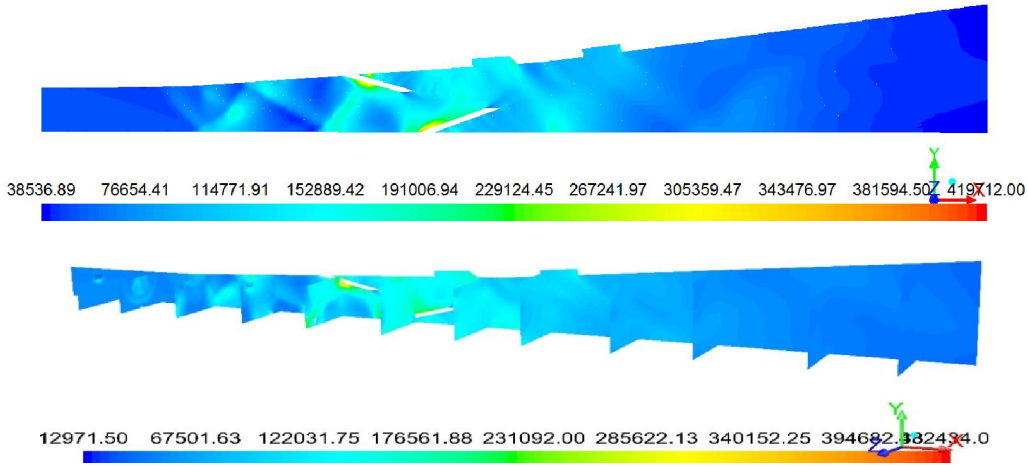

(b) Reacting flow with ethylene at combustor entry M3.0

Fig.4.14 Static Pressure (Pa) along the combustor

The static pressure along the combustor is shown in Fig.4.14 (a) for cold flow with fuel injection. It is observed that the pressure increases in the ramp zone and there is a slight decrease in the pressure due to the arrangement of the ramps. Ramps are arranged alternately in the combustor section and there is an angle of divergence on the top wall of the combustor. Due to these variations in the geometry of the combustor, there is a corresponding variation in static pressure in the combustor with ramps. At the ramps, due to better mixing of fuel with air, there is an increase in pressure and due to expansion fan, the pressure reduces after ramps. Fuel mixing is also enhanced due to multiple three dimensional shocks and results in the pressure rise. After the ramps, the pressure decreases in the position of the cavities because of expansion and increases due to recirculation zone in the cavity. There is a pressure rise in the cavity zone due to recirculation and further the pressure reduces in the diverging combustor. The pressure variation along the combustor follows supersonic flow pattern.

In the reacting flow (combustion), shown in Fig. 4.14 (b), the pressure remains low near to the ramp zone and the variation is dominant in the ramps zone due to multiple shocks. The pressure rise is high locally near the fuel injecting ramps indicating thorough mixing and combustion. There is continued pressure rise in the cavity zone which is caused due to recirculation zone in the cavities and higher pressure is clearly seen in the combustor. The pressure reduces and reaches the ambient pressure towards the end of the diverging combustor. Variation of static pressure along the combustor is shown in Fig.4.14 (c). It can be observed that the pressure rise is marginal with fuel mass addition prior to combustion in the supersonic airstream. The static pressure rise is high and more dominant in the cavities zone with heat addition compared to ramps zone. This may be due to mixing occurring in the ramps and heat addition that takes place downstream indicating high pressure rise. The static pressure rise is about 1 bar between cold flow with fuel addition and combustion. Also, there is a static pressure rise of about 0.5 bar between ramp zone and downstream ramps, near cavities. It can be seen that the pressure variation clearly indicates supersonic combustion in the combustor.

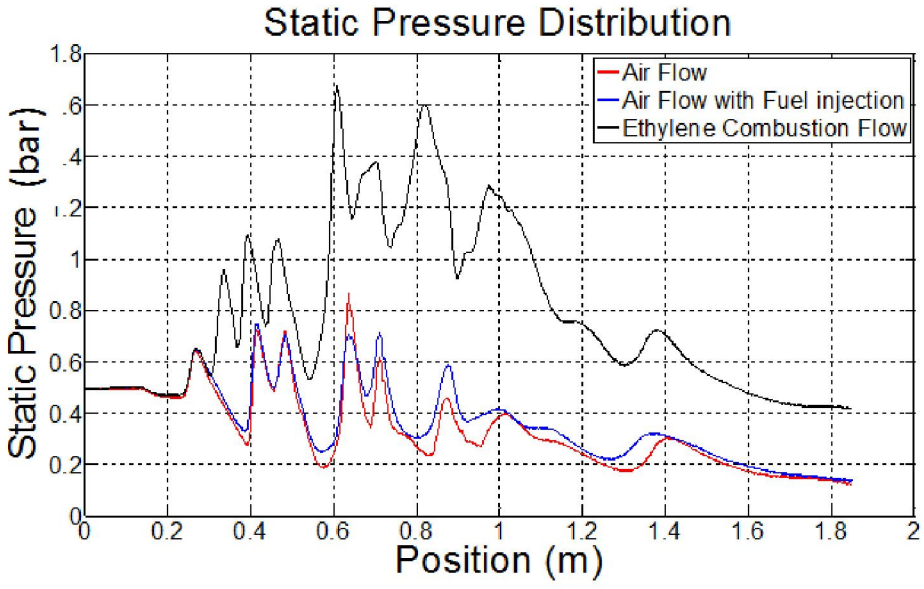

Fig.4.14(c) Comparison of variation of Static pressure (Pa) for Mach 3.0 condition

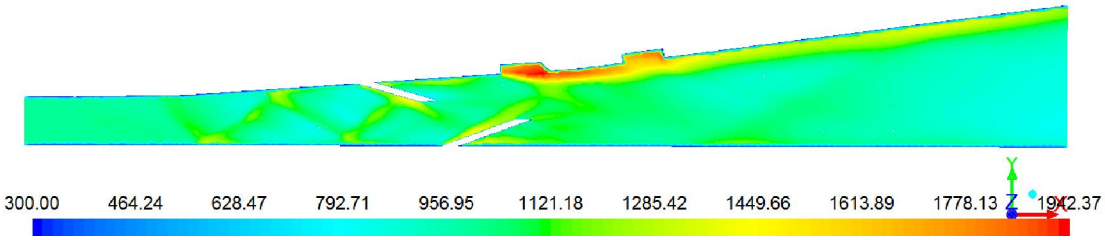

(a) Non reacting flow with ethylene at combustor entry M 3.0

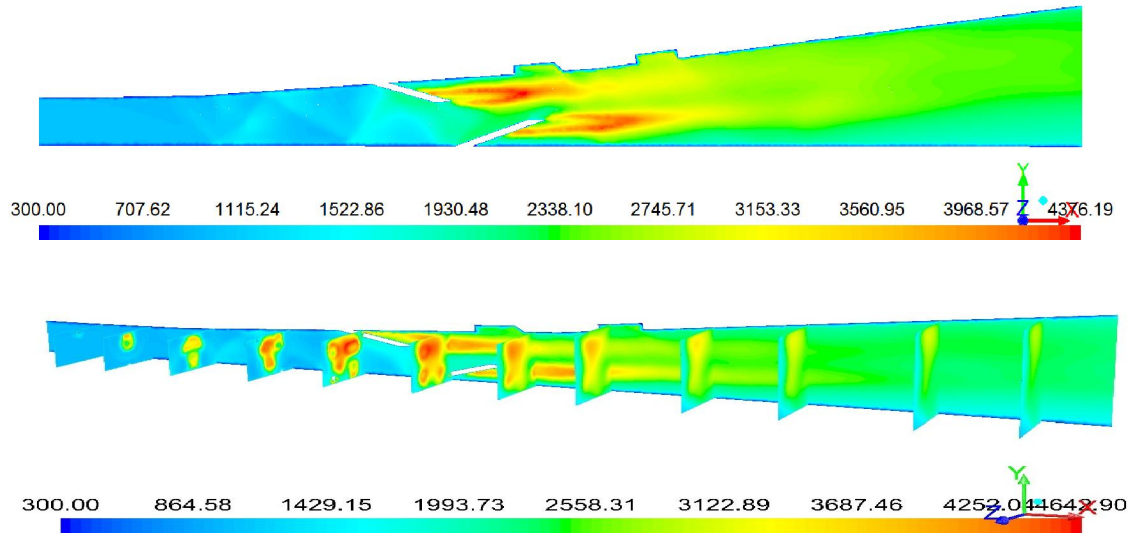

(b) Reacting flow with ethylene at combustor entry M 3.0

Fig.4.15 Static Temperature (K) contours along the combustor

The variation of static temperature along the combustor is depicted in Fig.4.43 (a) for cold flow with mass addition (non-reacting flow). The three dimensional shock structure and rise in temperature are clearly observed in the ramp zone. From the point of fuel injection from the ramps and upto cavities in the combustor, the increase in temperature is noted. However, there is a marked difference in temperature rise at the cavities. The temperature in the cavities is locally, about 1800 K. This may be due to low velocity flow reaching near stagnation temperature in the cavities. Hence, cavities support flame stabilization. The shear layer along the top wall of the combustor is observed to carry high temperature, about 1200 K. Static temperature of air fuel mixture in the diverging combustor is also locally high.

In Fig. 4.15 (b), the static temperature contour in the case of combustion (reacting flow) is shown. In the case of combustion, the temperature is observed to be high from the beginning of the ramps in the combustor at the point of fuel injection in the ramps

zone. This clearly shows the occurrence of combustion of ethylene with oxygen in the supersonic air stream. The higher temperature continues in the zone upto cavities. As with the static pressure pattern, the temperature in the cavities is high providing conditions for flame stabilization and sustained combustion. The static temperature continues to be high in the diverging combustor and is locally, about 2000 K at the exit of the combustor. This indicates higher heat release in the combustor due to thorough mixing and combustion.

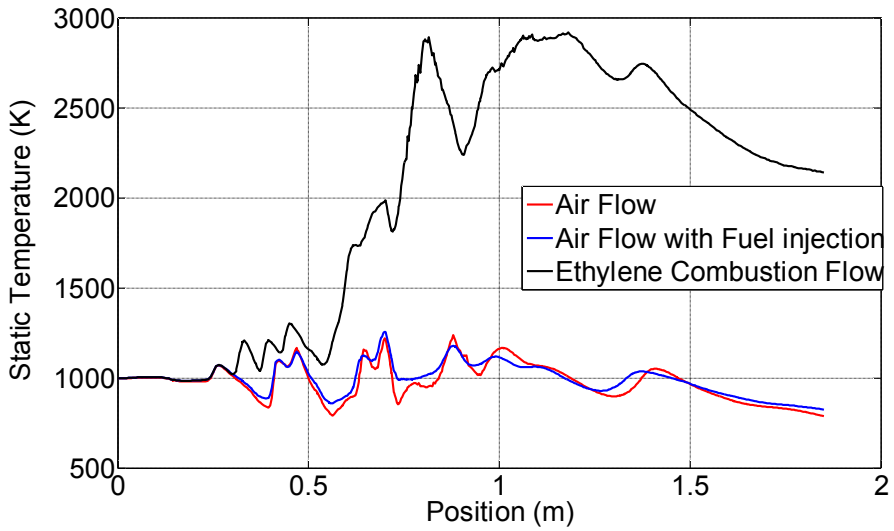

Fig.4.15 (c) Comparison of variation of Static Temperature for Mach 3.0 condition

Fig.4.15 (c) shows the static temperature plots along the combustor for supersonic airflow, mixing and combustion conditions. The difference in static temperature between cold air flow and air with fuel addition is not significant. However, the difference in temperature between combustion phase and mixing phase is very high. The static temperature follows the pattern with fluctuations in the ramps, higher temperature in the cavities due to recirculation zone, and decreasing in the diverging combustor.

The concentrations of species along the length of the combustor are also captured and presented herewith.

i) Ethylene mass fraction:

Ethylene is injected through ramps into the supersonic stream of air. Variation in mass fraction of Ethylene along the centre-line of the combustor is shown in Fig.4.16 (a) with fuel addition for cold flow (non-reacting flow). Mixing of ethylene continues

downstream the ramps upto the cavity zone and the ethylene mass fraction decreases thereafter leaving certain cross section of combustor. The spread of ethylene across the cross section of the combustor at various planes is also depicted in the figure. This shows the ethylene content in the airstream and mixing along the combustor. Ethylene mass fraction becomes negligible in the diverging combustor.

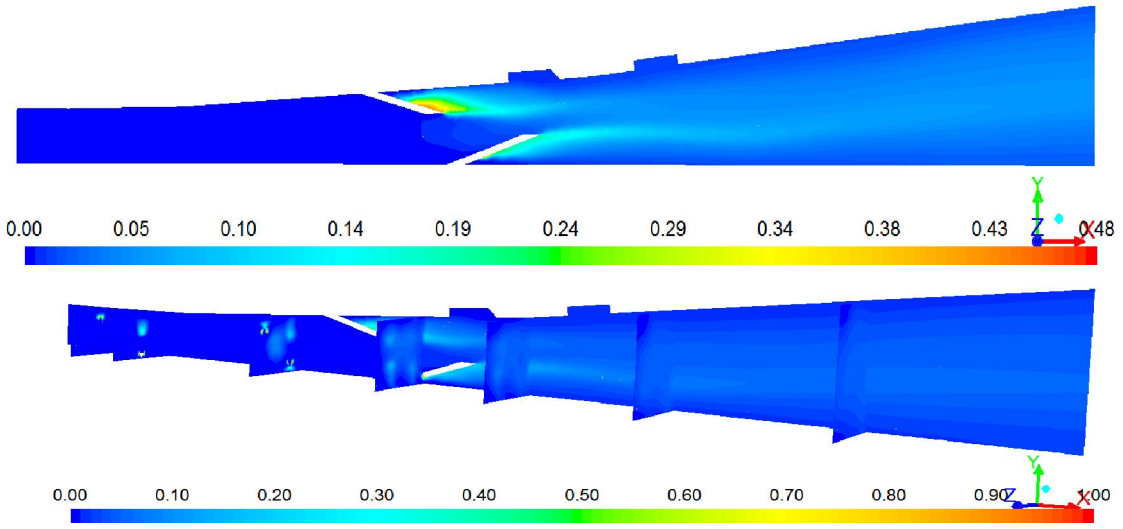

(a) Ethylene mass fraction contours in non-reacting flow

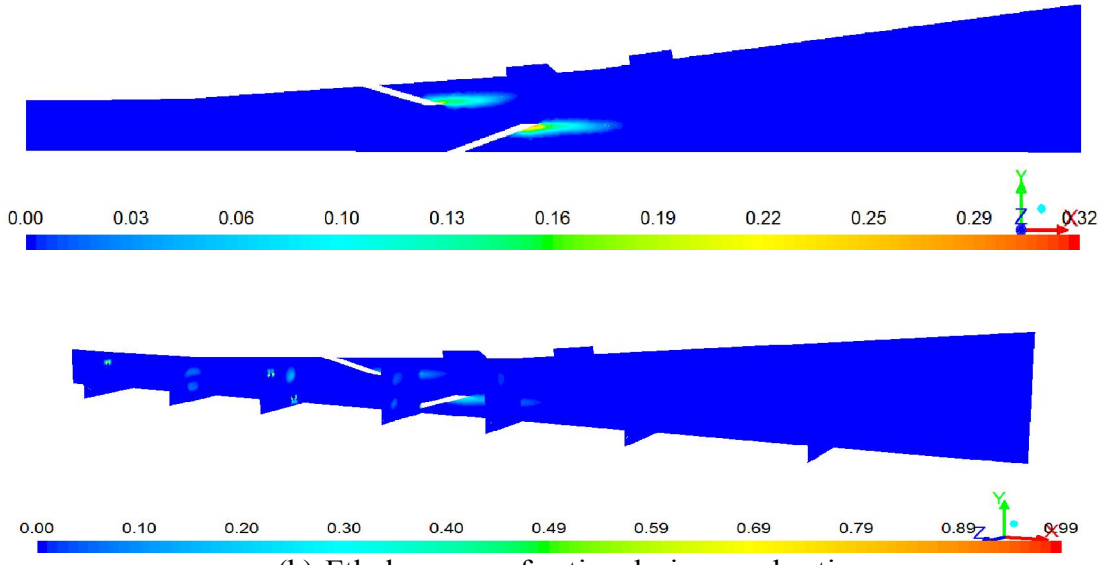

(b) Ethylene mass fraction during combustion

Fig.4.16 Ethylene Mass fraction contours at combustor entry Mach 3

In the case of reacting flow shown in Fig.4.16 (b), the ethylene fuel mixes with supersonic air stream at the ramps and combustion takes place. As the flow moves towards the cavities, the ethylene mass fraction reduces and becomes negligible towards the cavity zone upstream of the second cavity. This indicates complete mixing and combustion of ethylene with air in the reacting flow.

ii) Oxygen mass fraction:

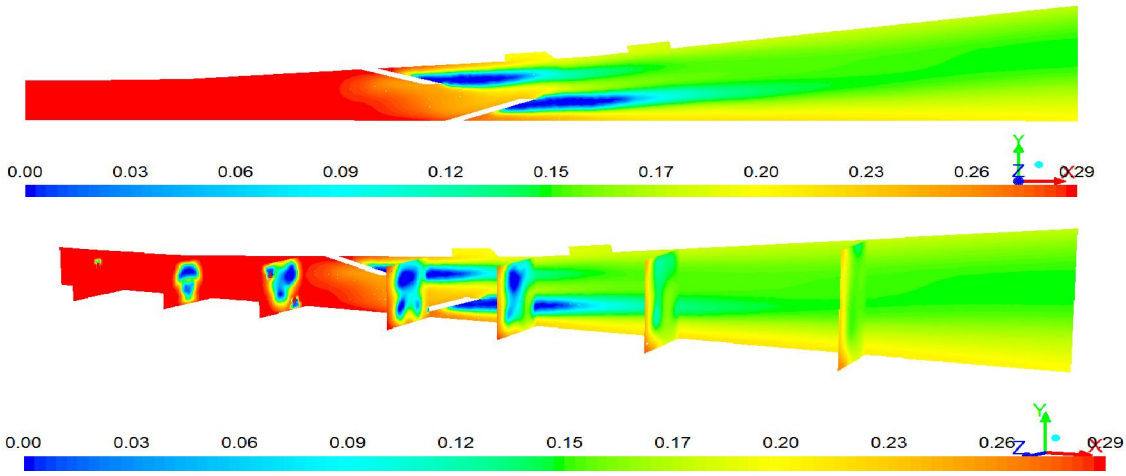

Reacting flow

Fig.4.17 Oxygen mass fraction contours along the combustor

In the case of reacting flow, the oxygen content in the air takes part in combustion effectively from the second set of ramps as seen in the Fig.4.17, shown in the above figure at various planes. The combustion continues downstream the ramps in the cavity zone. In the reacting flow, the cavities also provided recirculation zones and oxygen in the air reacted with fuel.

iii) Mass fraction of H_2O:

In Fig.4.18, mass fraction contour of H_2O (a product of combustion) during combustion of Ethylene with supersonic airstream, is shown. The water vapour content forms at a distance from the entry of the combustor, from the second set of ramps and continues through the ramps, at the plane of injection. The water vapour content is observed to be more downstream of the ramps and near the cavity zone of the combustor. Similar trend is seen in the diverging portion of combustor.

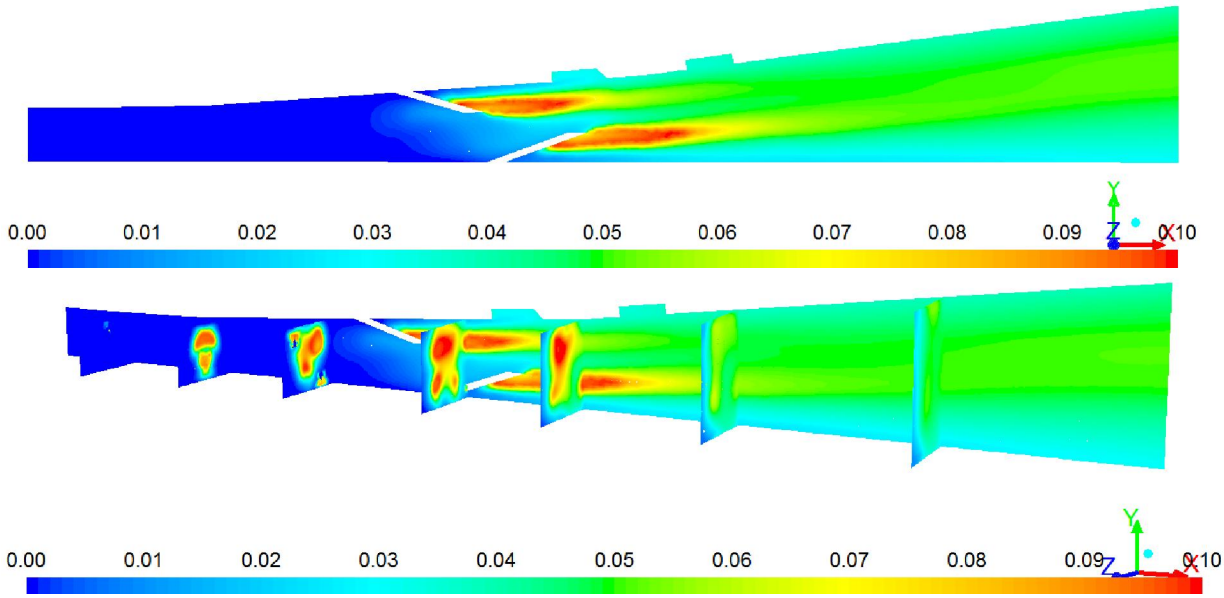

Fig.4.18 Mass fraction of H_2O along the combustor

iv) Mass fraction contours of CO_2:

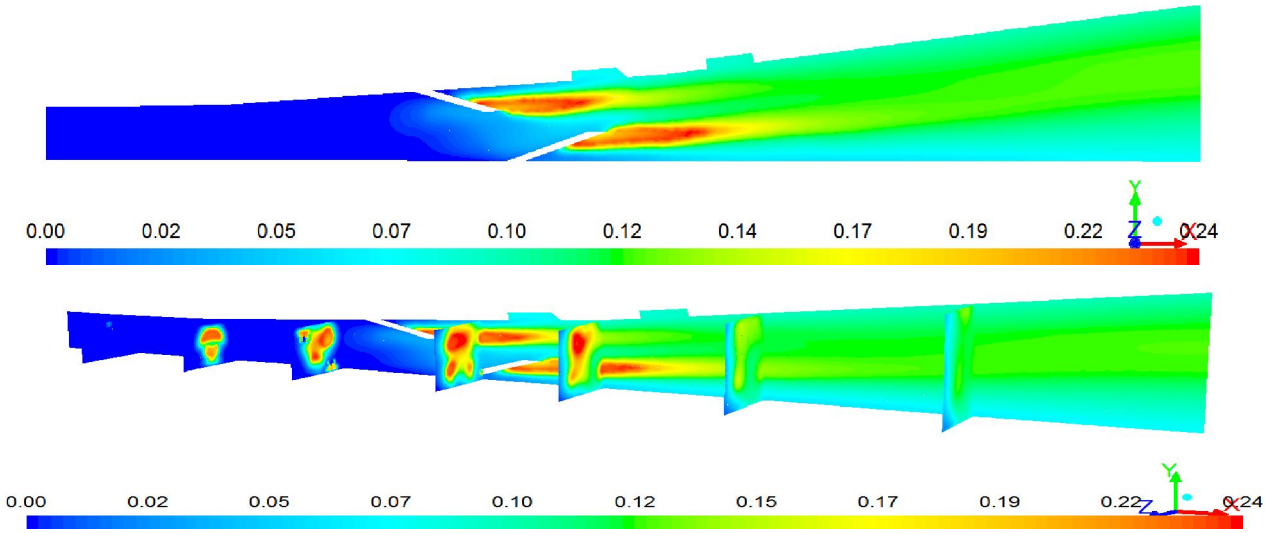

Fig.4.19 Mass fraction of CO_2 along the combustor

Fig.4.19 shows mass fraction contours of CO_2 as a product during combustion. It can be observed that CO_2 is formed at the fuel injection ramps which continues downstream of the ramps in the cavity zone also. It is observed that the combustion is more from the second set of ramps whereas the initial set of ramps contributed for better mixing of air with the fuel. The combustion continued in the diverging portion of the

combustor also to some extent. As shown in the figure, the combustion of fuel with air has been carried out across the cross section of the combustor. It may be inferred that the distance required for mixing is the length between the fuel injecting ramps.

4.2.2 Comparison studies on ramp-cavity full-scale combustor for different entry Mach numbers with ethylene as a fuel:

Computational studies of Ramp-Cavity combustor have been carried out with ethylene as fuel. Combustor entry Mach number has been varied from Mach 2, Mach 2.5 and Mach 3. The combustor of cross section 86 mm X 275 mm with a length of 1850 mm is considered as illustrated in Fig. 4.12. In this case, ethylene fuel (133gm/s) is injected. Seven ramps on the top wall and seven ramps on the bottom wall with fuel injection holes are arranged in a staggered configuration. Two cavities are positioned on the top wall. High speed air is allowed to flow through the combustor simulating the high altitude conditions. The stagnation pressure at the inlet to the combustor is 5 bar with stagnation temperature of 1000 K at the entry of the combustor corresponding to the high altitude conditions. Ethylene is used as fuel with equivalence ratio of 0.6 and simulations are carried out. The inlet of the combustor is considered pressure far field condition to maintain a constant inlet Mach number 2, 2.5 and 3 in each simulation. Fuel is introduced into the combustor through fuel injecting holes from the ramps. The flow field analysis has been done for all the cases. The contours of Mach number, static pressure and static temperature have been generated and comparison is made in terms of the static pressure, static temperature and Mach number.

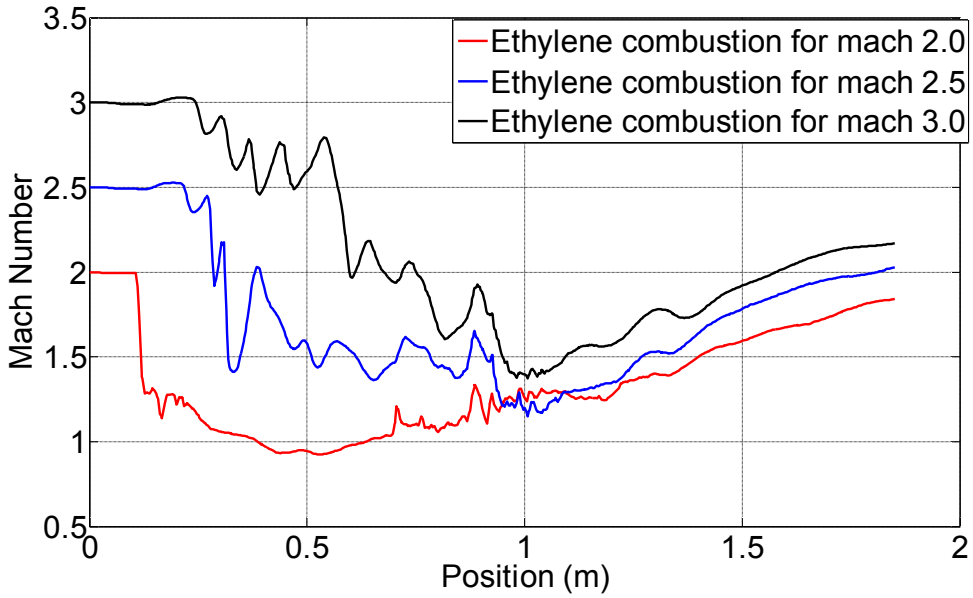

Fig. 4.20 (a) Variation of Mach number along the combustor.

Fig.4.20 (a) shows the Mach number distribution along the combustor. The trends are similar irrespective of Mach number along the length of combustor. There are variations in Mach number due to mixing in the zone of ramps. It is observed that Mach number decreases in cavities and rises in the diverging part of combustor. However, it is seen that Mach number suddenly drops to about 1.3 from 2 at a distance of about 120 mm from the entry of the combustor due to strong oblique shocks in the case of combustor with entry Mach number 2. With Mach 2.5 and Mach 3combustor cases, multiple oblique shock structures and mixing due to ramps cause variations in the Mach number as seen in the plots. It is observed that locally, there will be subsonic pockets with Mach number below 1.0 in the case of combustor entry Mach 2. In other cases, the Mach number remains supersonic throughout the combustor. It can also be observed that there is a decrease in the Mach number in the zone where cavities are positioned and the Mach number increases in the diverging part of combustor. From these plots, it can be observed that with the combustor entry Mach number of 3, the Mach number in the combustor follows the trend that remains supersonic throughout the combustor. Thus, it can be concluded at this stage that with higher entry Mach number, sustained supersonic

combustion can be obtained with ramp-cavity combustor. The Mach number, static pressure and static temperature are taken at the centreline of the symmetry plane.

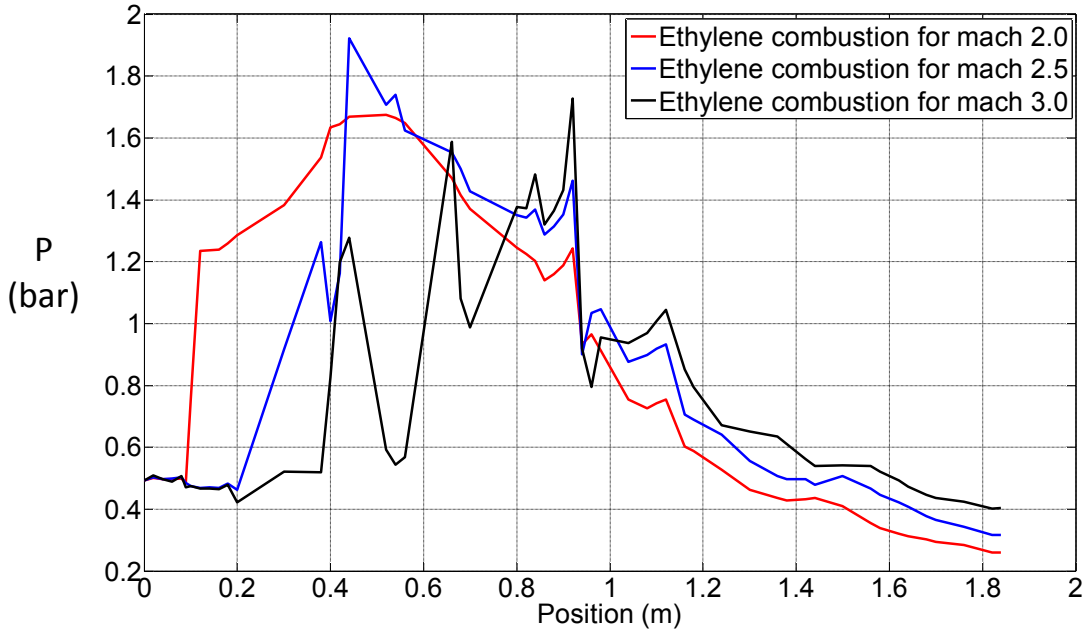

Fig.4.20 (b) Variation of Static Pressure along the combustor

Fig.4.20 (b) depicts the variation of static pressure along the combustor for entry Mach numbers 2, 2.5 and 3. It can be seen that in all the cases, the static pressure at the entry to the combustor is the test facility nozzle exit pressure. In the case of combustor entry Mach number of 2, there is a sudden rise in the static pressure at about 120 mm from the entry of the combustor corresponding to the reduction in Mach number. This may be due to the strong oblique shocks in the combustor. Static pressure rises and falls in the ramp zone due to mixing as a result of vortices. It is seen that the static pressure reduces at the zone of cavities and increases in the following section of the combustor. This may be due to reflecting shocks emanating from the cavities. The pressure reduces further in the diverging combustor. In the case of entry Mach number 2.5, similar pattern is observed as with Mach 2. However, the pressure has risen to above 2.5 bar and then varies in the ramp zone alternately in line with the Mach number contour. The pressure decreases in the cavities due to sudden expansion and increases in the recirculation zones. In the plot showing static pressure for combustor entry Mach number 3, the pressure rises in the ramp zone due to mixing of fuel and air and is following the trend. The static

pressure increased to 1.7 bar in the combustor. After the ramps, the pressure decreased due to diverging portion of the combustor. The pressure fall in the zone of cavities is due to expansion which rises again because of reflecting shocks from the cavity wall. The pressure decreases in the diverging portion of the combustor in line with the supersonic combustion. Thus, the pressure at the exit of combustor is just above ambient pressure corresponding to the altitude simulated indicating accelerated flow condition prevailing in the combustor.

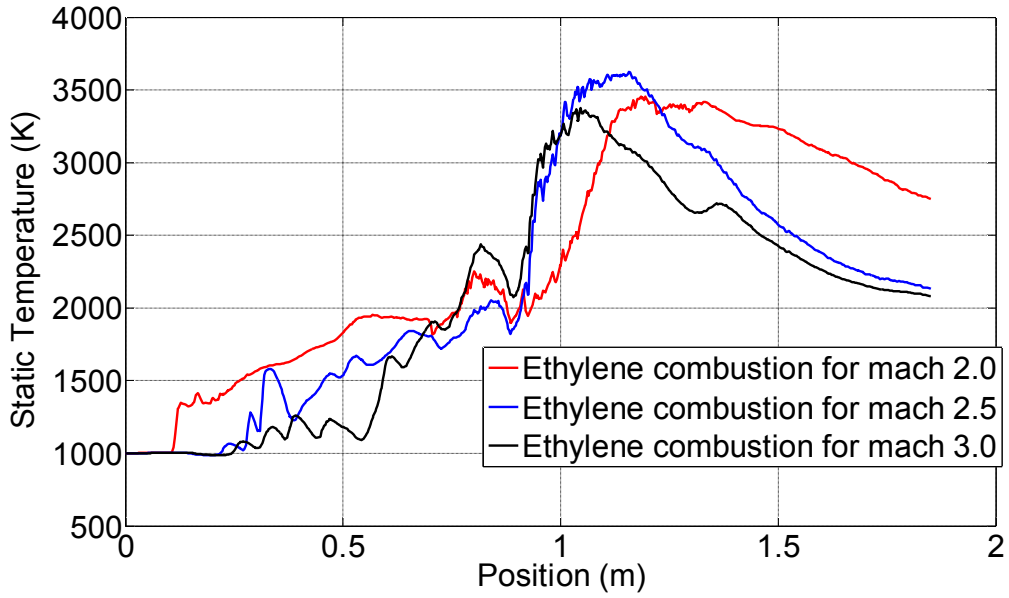

Fig.4.20(c) Static Temperature variation along the combustor

The static temperature variation along the combustor for the different combustor entry Mach numbers is depicted in Fig.4.20 (c). The static temperature plot is also similar in trend with Mach number and static pressure plots. Starting with 1000 K, the static temperature value increased to a maximum of about 3400 K, locally. The high value of temperature may also be due to the complete combustion assumed for the simulation studies. In the case of combustor entry Mach number 2, the static temperature rise started at 120 mm, increased further in ramps and in the position of the cavities. In the case of combustor entry Mach number of Mach 2.5, the static temperature fluctuated in the ramps zone due to mixing, compression in the ramps and expansion where ramps are not located. The static temperature rise can be seen in the cavity zone. Static

temperature reduces in the diverging combustor. In the case of combustor entry Mach number 3, the static temperature variation in the ramps indicate better mixing as the temperature rise can be observed after 550 mm from the beginning of the combustor which increased continuously except in the position of the cavities because of expansion in the area. The static temperature further increases indicating the recirculation zone in the cavity due to which the flame stabilization and supersonic combustion is sustained in the combustor. The static temperature reduces further in the diverging combustor.

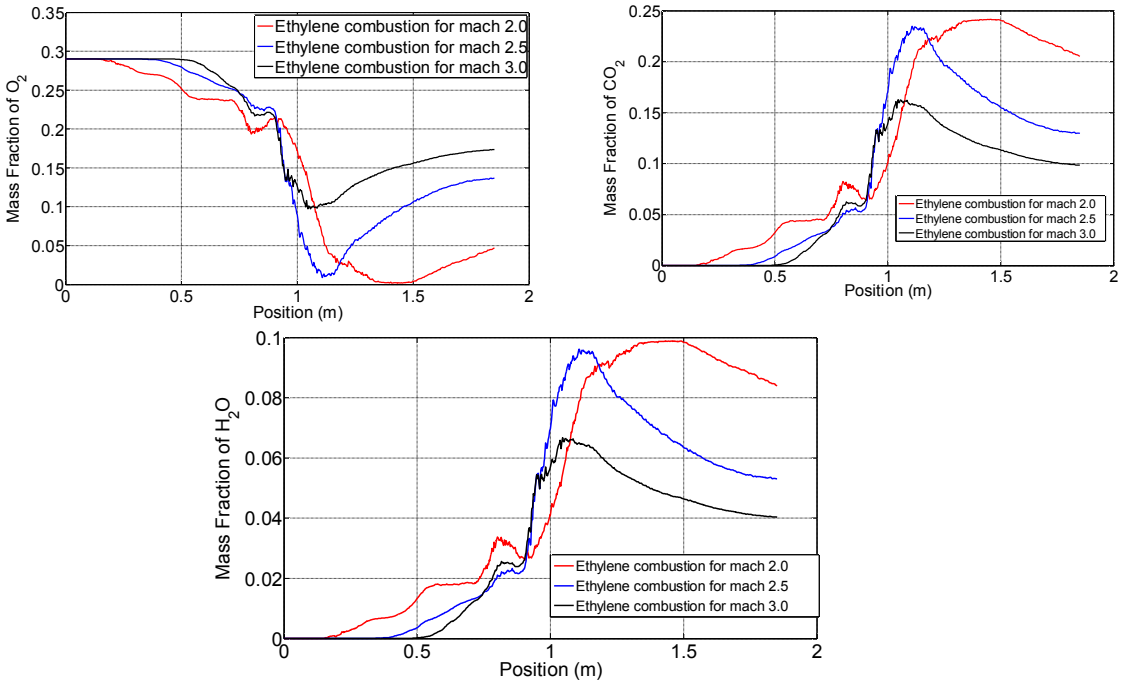

Fig.4.20 (d) Mass fractions of species along the combustor

The mass fractions of species are plotted along the centre line of the combustor in Fig.4.20 (d) for different combustor entry Mach numbers. In the case of oxygen, mass fraction decreases gradually in the ramps zone and after 1 m length there is a maximum reduction in the content. The oxygen mass fraction plot in the case of Mach 2.5 also shows similar pattern. In the case of combustor entry Mach number of 3, the oxygen content decreases after 400 mm from the start of the combustor where mixing and combustion happens. This continues upto 1.2 m of the combustor. The increase in mass fraction of Oxygen in the diverging combustor may be due to the completion of most of the combustion of ethylene.

The mass fraction contour of CO_2 shows that for combustor entry Mach number 2, the mass fraction increases from about 200 mm and continuously increases upto 0.8 m of combustor length, slightly reduces and then increases upto 1.4 m of the combustor length. This indicates combustion to continue in the diverging portion of the combustor also. In the case of combustor entry Mach numbers 2.5 and 3, the increase in CO_2 mass fraction starts after 400 mm from the start of the combustor and continues upto 1.1 m of combustor length. This may be due to complete mixing and combustion between 400 mm to 1100 mm length of the combustor.

The mass fraction of H_2O for combustor entry Mach number 2.0 shows a similar trend as that of CO_2mass fraction in the combustor. The increase in the case of combustor entry Mach number 3 is at about 550 mm from the start and continued upto 1000 mm length of the combustor. This indicates the combustion could be completed in a relatively short length of the combustor. The drop in the mass fractions of $CO_2$and H_2O may be due to the dispersion and quantities are negligible.

It can be observed that when the combustion entry Mach number is 3, the Mach number in the combustor is supersonic throughout, the pressure rise is as per the expected trend and the temperature rise is substantial indicating supersonic combustion, compared to the combustor entry Mach numbers 2 and 2.5. It may be concluded that for the combustor configuration with ramps and cavities as located in this combustor, combustor entry Mach number 3.0 is more suitable for sustained supersonic combustion.

4.3 Comparison studies on ramp-cavity full-scale combustor for different fuel equivalence ratios at Mach number 3 with ethylene as a fuel:

The combustor of cross section 86 mm X 275 mm with a length of 1850 mm is considered as illustrated in Fig. 4.12. In this case, ethylene fuel is injected. Seven ramps on the top wall and seven ramps on the bottom wall with fuel injection holes are arranged in a staggered configuration. Two cavities are positioned on the top wall. High speed air is allowed to flow through the combustor simulating the high altitude conditions. The stagnation pressure at the inlet to the combustor is 5 bar with stagnation temperature of 1000 K at the entry of the combustor corresponding to the high altitude conditions.

Ethylene is used as fuel (133gm/s) with equivalence ratio of 0.6 and simulations are carried out. The inlet of the combustor is considered pressure far field condition to maintain a constant inlet Mach number 3 in each simulation. Fuel is introduced into the combustor through fuel injecting holes from the ramps. The flow field analysis has been carried out for all the cases. The contours of Mach number, static pressure and static temperature have been generated and comparison is made in terms of the static pressure, static temperature and Mach number. The fuel equivalence ratio is varied to study the effect of fuel mass injected into the combustor with the combustor entry Mach number 3.

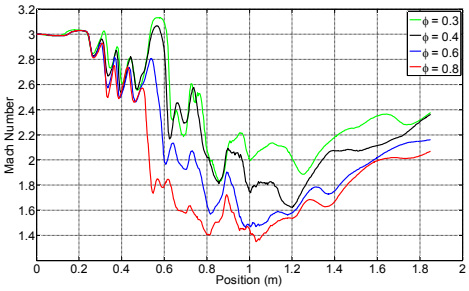

Fig.4.21(a) Mach numbers along the combustor

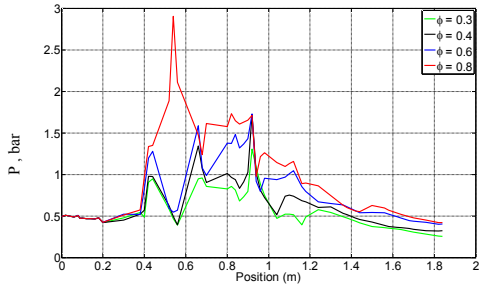

Fig.4.21 (b) Static pressure along the combustor

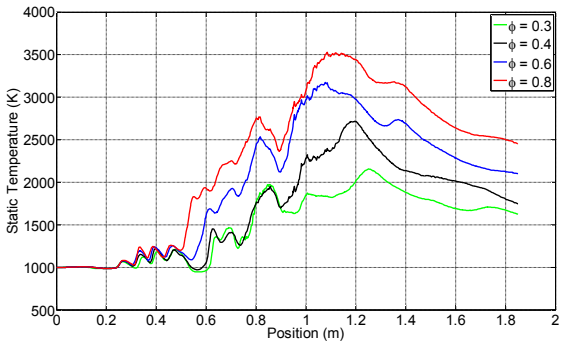

Fig.4.21 (c) Comparison of Static temperature along the combustor

Comparison of the flow field parameters along the combustor for various equivalence ratios is shown in Fig.4.21 (a), (b), (c) and (d). Mach number distribution along the combustor shows that for equivalence ratio of 0.8, the Mach number locally reduces below 1.5. Mach number variation is in line with the shocks in the ramps and expansion in the cavities. It can be said here that slightly lean mixture performs better in

achieving supersonic combustion. The static pressure variation shows that the static pressure rise is low for equivalence ratios of 0.3 and 0.4. The static pressure rise is about 1 bar for equivalence ratios of 0.6 and 0.8. Static temperature variation shows that the rise in static temperature is high with fuel equivalence ratios of 0.6 and 0.8 and marked in the diverging combustor also, ensuring heat release during supersonic combustion.

Comparison of mass fractions of species also shows that for the fuel equivalence ratios of 0.6 and 0.8, the oxygen mass fraction reduces to a 0.1 and 0.05 respectively compared to other two cases. The mass fraction of products also indicates higher values indicating complete combustion. The products of combustion viz; CO_2 and H_2O are high with rich mixtures. The overall analysis with variation of equivalence ratio, it may be observed that 0.6 equivalence ratio may be more suitable for the combustor configuration.

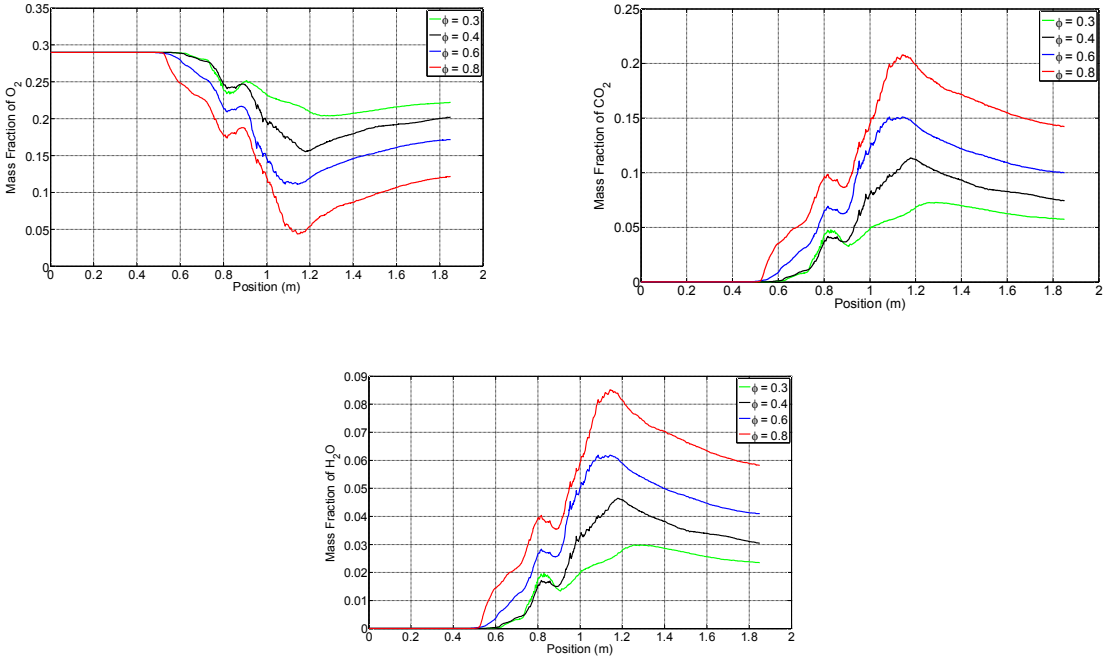

Fig.4.21 (d) Comparison of Mass fractions of species along the combustor

From the simulations, it is observed that the higher the entry Mach number the better is supersonic flow throughout the combustor and therefore further study is done with Mach 3 and for equivalence ratio of 0.6.

4.4 Effect of fuel injection pattern:

The combustor of cross section 86 mm X 275 mm with a length of 1850 mm is considered as illustrated in Fig. 4.12. In this case, ethylene fuel is injected. Seven ramps on the top wall and seven ramps on the bottom wall with fuel injection holes are arranged in a staggered configuration. Two cavities are positioned on the top wall. High speed air is allowed to flow through the combustor simulating the high altitude conditions. The stagnation pressure at the inlet to the combustor is 5 bar with stagnation temperature of 1000 K at the entry of the combustor corresponding to the high altitude conditions. Ethylene is used as fuel (133gm/s) with equivalence ratio of 0.6 and simulations are carried out. The inlet of the combustor is considered pressure far-field condition to maintain a constant inlet Mach number 3 in each simulation. Fuel is introduced into the combustor through fuel injecting holes from the ramps. The flow field analysis has been carried out for all the cases. The contours of Mach number, static pressure and static temperature have been generated and comparison is made in terms of the static pressure, static temperature and Mach number.

Injection of fuel into the combustor is achieved through the ramps located in the first two sections of the combustor ahead of the cavities. The fuel is equally distributed at all the stages through ramps. Numerical study is conducted to study the effect of fuel injection pattern by varying the injection of the fuel into the combustor. In the first case, fuel is not injected in the first set of four ramps in the top and bottom walls. The fuel is distributed equally among the remaining ramps located in the combustor. The supersonic stream of air entering the combustor passes through the first set of ramps and velocity reduces marginally. Injected fuel from the remaining ramps gets mixed with the incoming air stream. Mixing and combustion of fuel with the air takes place.

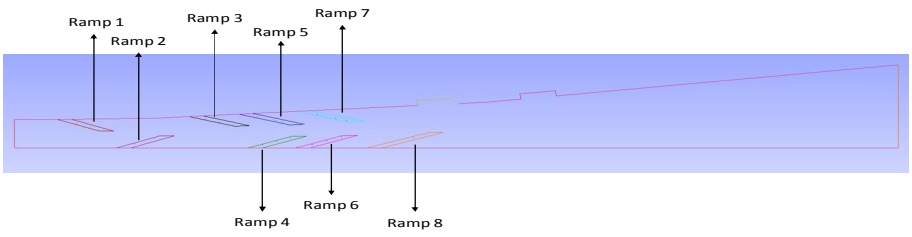

Fig.4.22 Arrangement of ramps in the combustor

Fig.4.22 above shows the arrangement of ramps in the combustor. Ramps 1 and 2 constitute 1st stage with two ramps each on top and bottom walls. Ramps 3 and 4 constitute 2nd stage; ramps 5 and 6 constitute 3rd stage with two ramps each on top and bottom walls. Ramps 7 and 8 are considered with one ramp each on top and bottom walls.

Table: 4.1 Fuel injection pattern

Stage	Description	Thrust, kg
All 4 stages	When fuel is injected through all Ramps	37
Stage-1	Fuel not injected through 1st set of Ramp Injectors	47.12
Stage-2	Fuel not injected through 2nd set of Ramp Injectors	61.3
Stage-3	Fuel not injected through 3rd set of Ramp Injectors	58.71
Stage-4	Fuel not injected through 4th set of Ramp Injectors	43.46

Case i) Fuel is injected from the ramps except the first set of two ramps on the top wall and two ramps on the bottom wall of the combustor:

Fig.4.22 (a), (b), (c) show the Mach number, static pressure and static temperature along the combustor when the fuel is not injected from the first set of two ramps each on the top and bottom walls of the combustor. The fuel (133gm/s) is equally distributed from the remaining ramps of the combustor.

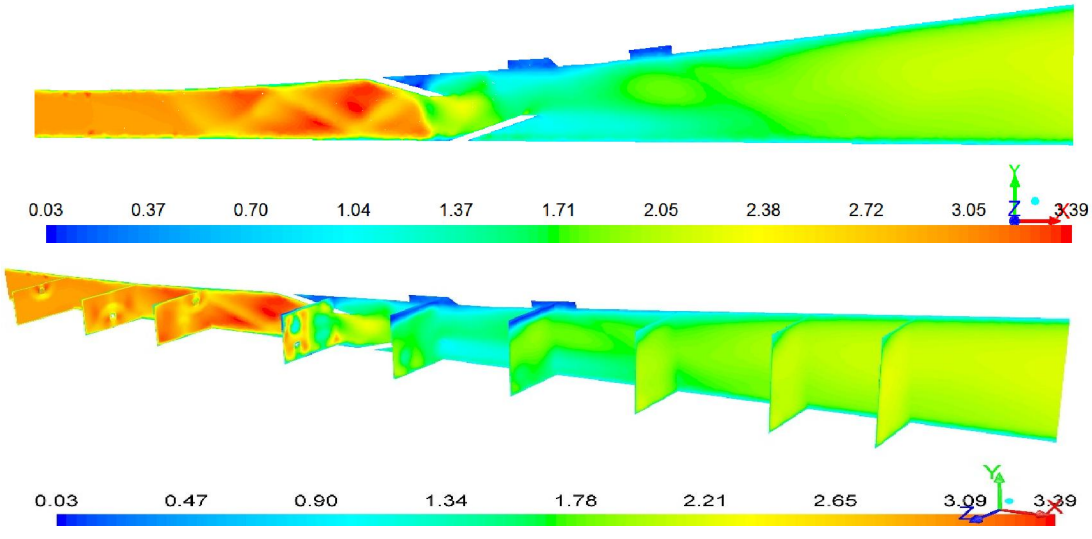

Fig.4.22 (a) Mach number contours without fuel injection from 1st set of ramps

Fig.4.22 (a) shows the Mach number contour along the combustor. With the combustor entry Mach number of 3, the flow is compressed in the first set of ramps, decelerates and mixes with fuel from the ramp injectors located subsequently in the combustor. At the location of ramps, three dimensional oblique shocks are observed. The flow velocity increases locally with the increase of Mach number, decelerates to about Mach 1.3 after the ramps. It can be observed that the Mach number at the boundary layer is about 1.7 on both sides of the wall and becomes locally subsonic after the ramps. This may be due to injection of fuel. After the ramps, the flow decelerates corresponding to the rise in the pressure indicating heat addition due to combustion. In this zone, the flow Mach number in the core is about 1.7-2.0. The flow in the position of cavities is subsonic where recirculation zone is formed and the flow recovers to supersonic in the diverging portion of combustor. At the boundary layer, the Mach number is about 1.3 extending till the exit of the combustor.

It can be observed from Fig. 4.22 (b) that the static pressure in the combustor shows a marked increase in the ramp zone due to local compression and decreases due to expansion where ramps are not positioned. At the end of the ramps, it can be seen that there is a pressure rise indicating mixing and combustion of airstream. The flow continues to be at a higher pressure till the end of the cavities.

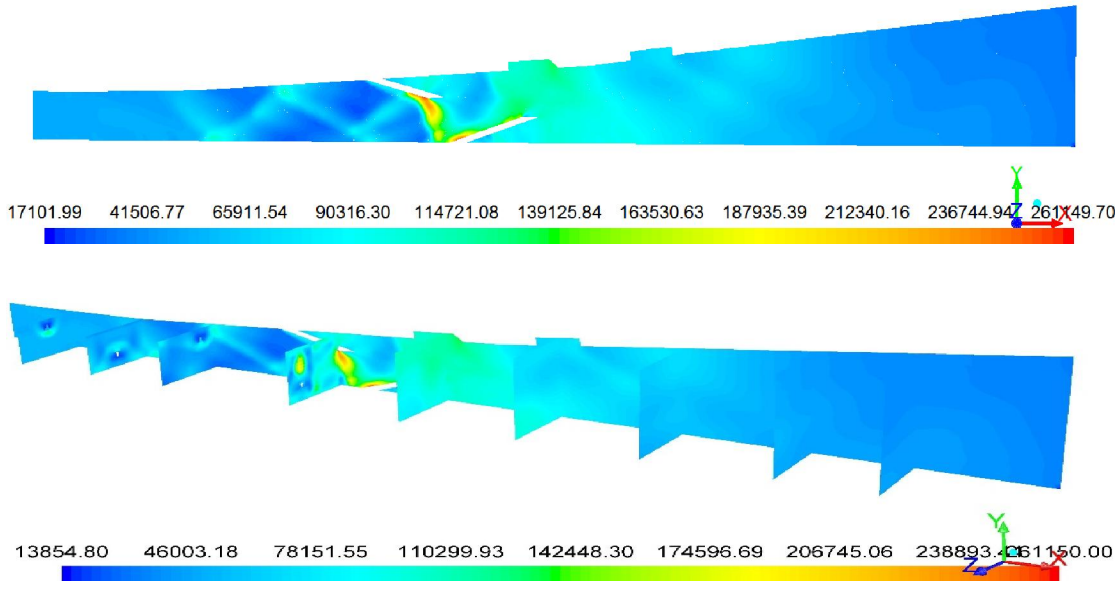

Fig.4.22 (b) Static pressure (Pa) contours without fuel injection from 1st set of ramps

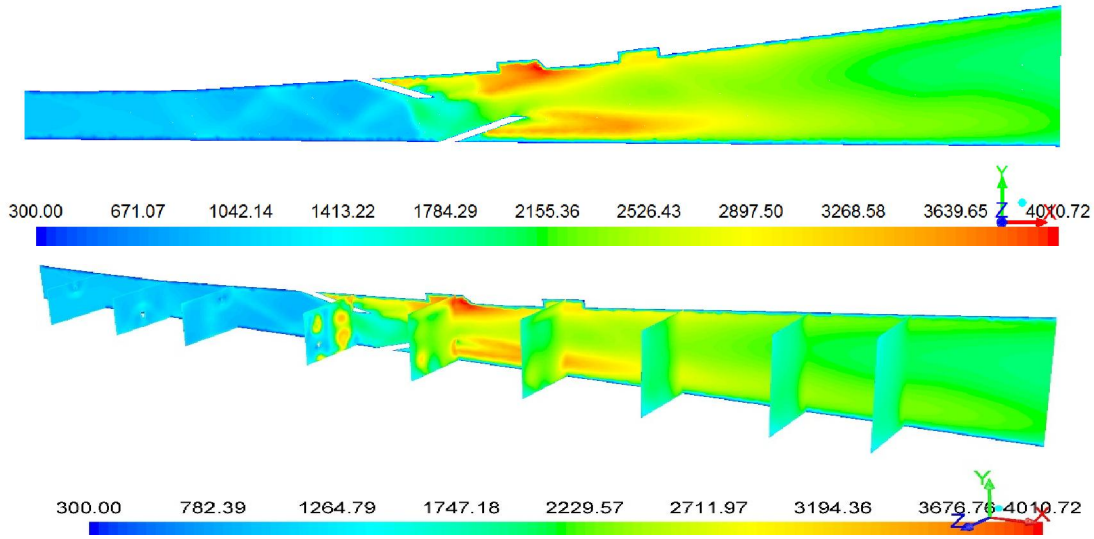

Fig.4.22 (c) Static temperature (K) contours without fuel injection from 1st set of ramps

The static temperature contours are depicted in the Fig.4.22 (c). It can be observed that the static temperature increases in the ramp zone although there is a layer of reduced static temperature along the top and bottom walls of the combustor. The rise in static temperature is dominant in the zone after the final ramps and in the cavities due to the presence of recirculation zone aiding the combustion. The static temperature rise is high in the first cavity compared to the second one. The static temperature continues to be high in the diverging combustor till the exit. Higher static temperature is observed in the top and bottom walls of the combustor while the core of the combustor is at a slightly lower temperature. The static temperature contour shows a sustained supersonic combustion.

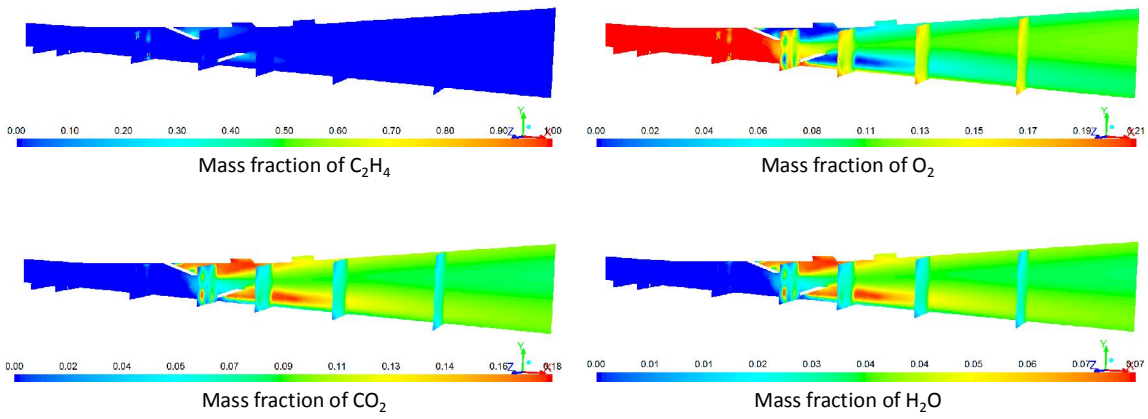

Fig.4.22 (d) Mass fraction contours without fuel injection from 1st set of ramps

Fig.4.22 (d) shows the mass fractions of species along the combustor. Ethylene mass fraction shows that the ethylene fuel is mixed well with the ramps as found along the combustor at various planes. Ethylene mixing with supersonic airstream continues till the cavities. Oxygen mass fraction reduces at the ramps zone where the fuel mixes with air. Oxygen mass fraction shows a marked decrease in the in the cavities because of local recirculation zone in the cavities aiding the combustion. Mass fractions of CO_2 and H_2O show that the species are formed in the ramp zone and becomes higher in the cavities which indicate combustion. The mass fractions of these two species continue to be high in the diverging combustor. It can be observed that the mass fractions confirm the mixing and supersonic combustion in the combustor.

Case ii) Fuel is injected from the ramps except the second set of two ramps on the top wall and two ramps on the bottom wall of the combustor:

Fig.4.23 depicts the fuel injection pattern in which the fuel (133gm/s) is injected from the first, third and fourth sets of ramps except the second set of ramps in the combustor. In this the fuel is equally injected from the ramps. The fuel injected from the first set of ramps mixes with supersonic air stream as it travels through the second set of ramps and combustion may be more effective. Fig.4.23 (a) shows the variation of Mach number contour along the combustor. It can be observed that the Mach number is high in the beginning of the combustor when fuel injection is carried out through first set of

ramps leaving the second set of ramps. It can be seen that the Mach number reduces due to combustion in the zone following the ramps and cavities and then increases to about 2.3 towards the exit of the diverging combustor. The Mach number is less at the walls of the combustor due to boundary layer.

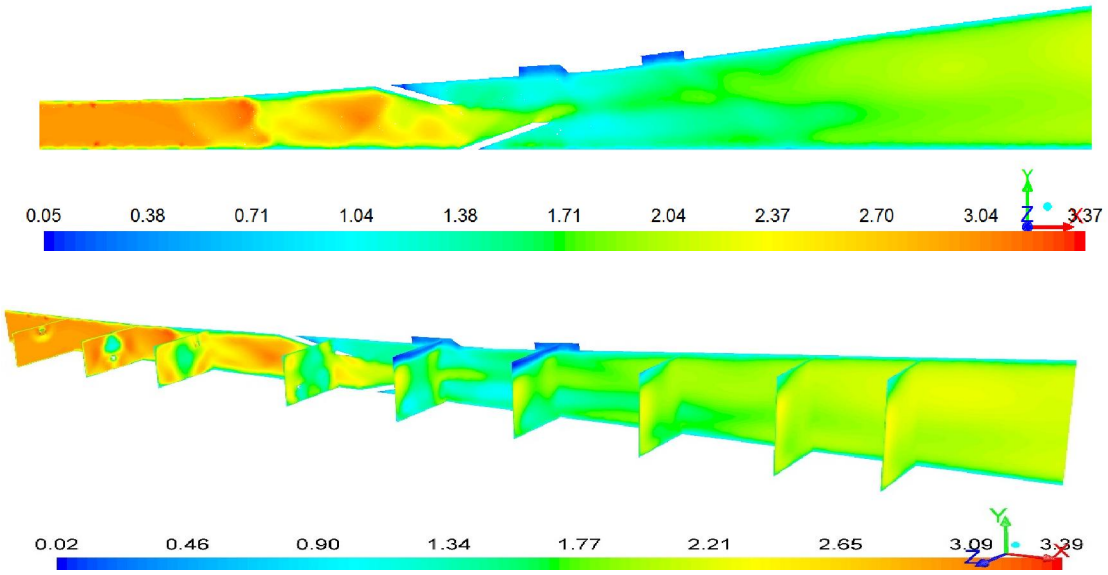

Fig.4.23 (a) Mach number contours without fuel injection from 2nd set of ramps

The static pressure contour is shown in Fig.4.23 (b). It is observed that there is a reduction in static pressure in the ramps where the expansion fans are located. The static pressure rise of about 1.6 bar is observed in the ramps due to combustion which increases to about 2.0 bar locally. Higher static pressure is also observed in the aft wall of the first cavity. Static pressure reduces to ambient by the exit of the diverging combustor.

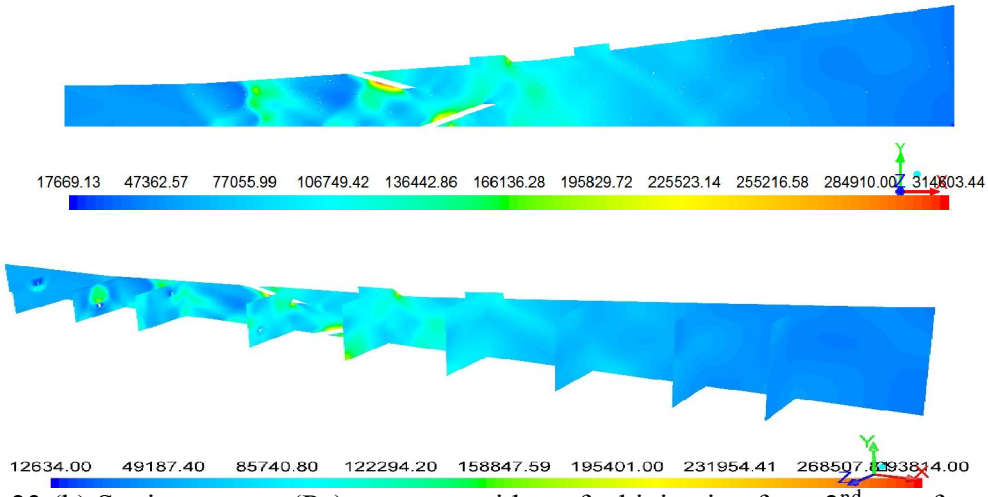

Fig.4.23 (b) Static pressure (Pa) contours without fuel injection from 2nd set of ramps

Static temperature contours are shown in Fig.4.23 (c). It can be seen that static temperature rises and continues to be high after the ramps, in the cavities and in the diverging combustor indicating recirculation at cavities and sustained combustion in the combustor. The static temperature rises to a maximum temperature of about 3600 K locally, near the aft end of the first ramp and in the core of the combustor towards the bottom wall. The static temperature is about 2000 K in the core of the diverging portion of the combustor.

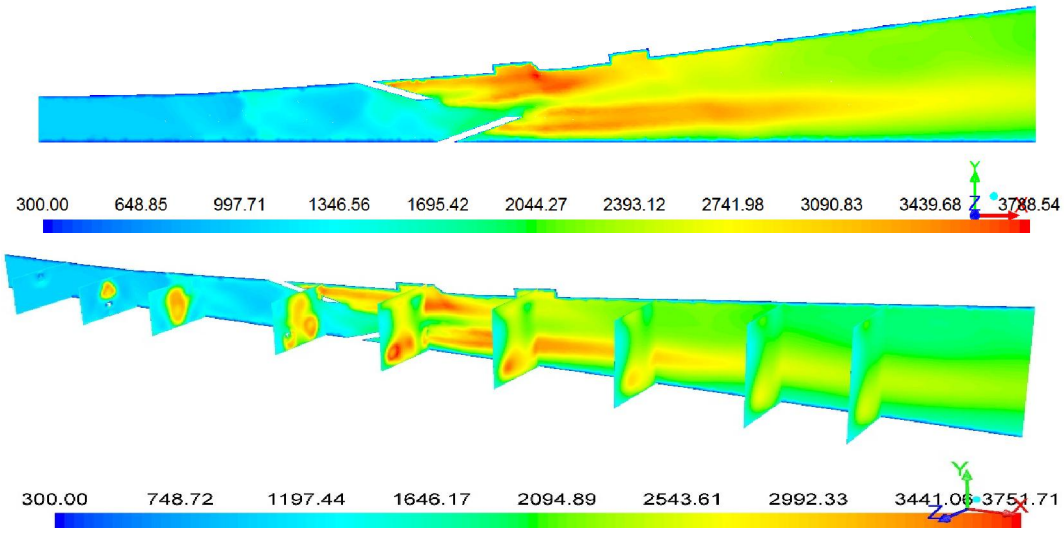

Fig.4.23(c) Static temperature (K) contours without fuel injection from 2nd set of ramps

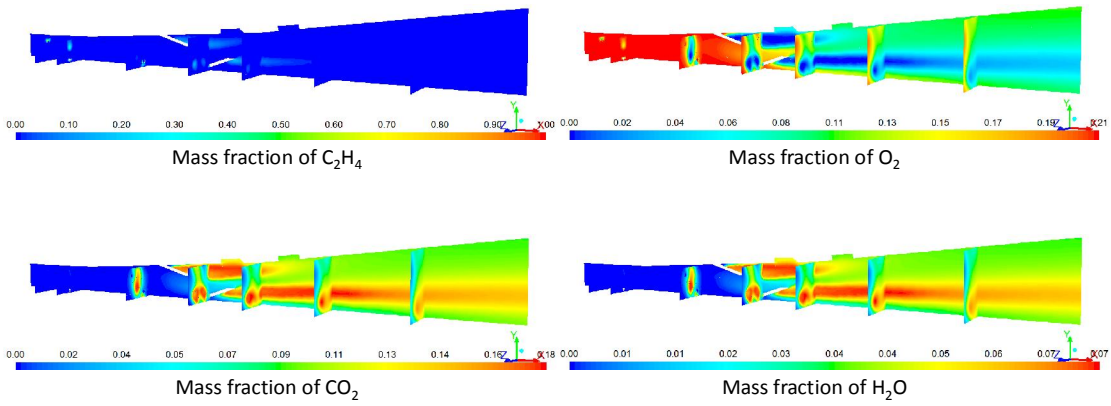

Fig.4.23 (d) Mass fraction of species without fuel injection from 2nd set of ramps

Fig.4.23 Fuel injection pattern except 2nd set of two ramps each on top & bottom walls

Fig.4.23 (d) shows the mass fraction contours of species. Ethylene mass fraction contour shows ethylene mixing with air at the injection from ramps and continues till the end of the cavities, indicating good mixing. Oxygen mass fraction contour also shows that the mass fraction reduces at the point of combustion with fuel. Similarly, the mass fractions of CO_2 and H_2O also show increase in the content indicating formation of combustion products in the ramp zone, in the cavities and in the diverging combustor.

Case iii) Fuel is injected from the ramps except the third set of two ramps on the top wall and two ramps on the bottom wall of the combustor:

Fig.4.24 depicts contours of the Mach number, static pressure, static temperature and mass fractions of species along the combustor when the fuel (133gm/s) is injected from the ramps except the third set of ramps in the combustor. The Mach number contour is depicted in Fig.4.24 (a). It can be seen that Mach number reduces near the top and bottom walls till the exit of the combustor. The Mach number decreases in the ramps and cavities of the combustor. The Mach number will be very low in the cavities indicating recirculation zone that helps in flame stabilization. The Mach number increases towards the diverging combustor.

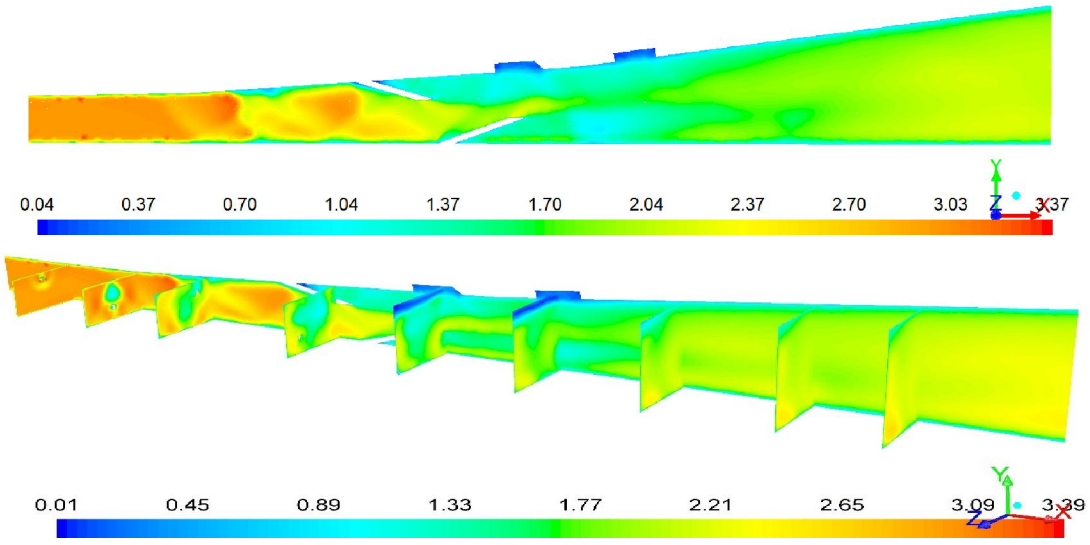

Fig.4.24 (a) Mach number contours without fuel injection from 3rd set of ramps

The static pressure rises in the ramps, as seen in Fig.4.24 (b), to a value of above 2 bar at the fuel injectors due to fuel injection and combustion. The static pressure continues to be high in the diverging combustor upto the cavities and reduces at the exit of the diverging combustor, indicating supersonic combustion.

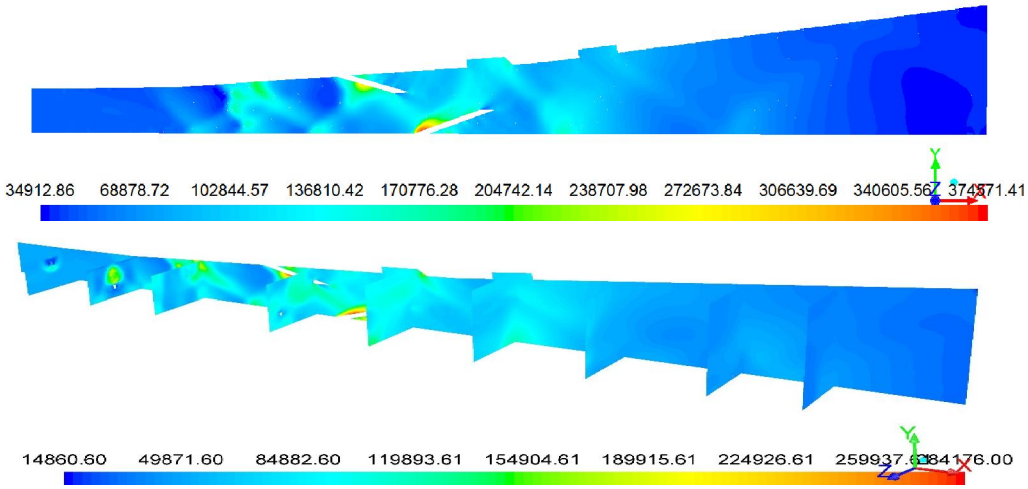

Fig.4.24 (b) Static pressure (Pa) contours without fuel injection from 3rd set of ramps

The static temperature as seen in Fig.4.24 (c) raises towards the end of the ramps and in the cavities upto the end of the diverging combustor indicating combustion. The static temperature is slightly lower near the walls of the combustor. The lower temperature along the bottom wall of the diverging portion of the combustor is about 1000 K. The temperature rise in the cavities can be observed to be about 3000 K which helps in sustained supersonic combustion.

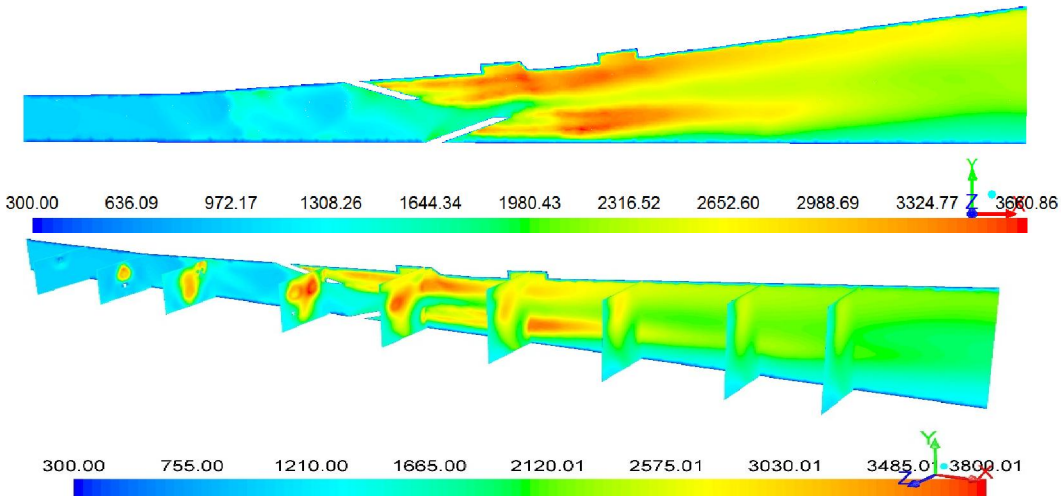

Fig.4.24 (c) Static temperature (K) contours without fuel injection from 3rd set of ramps

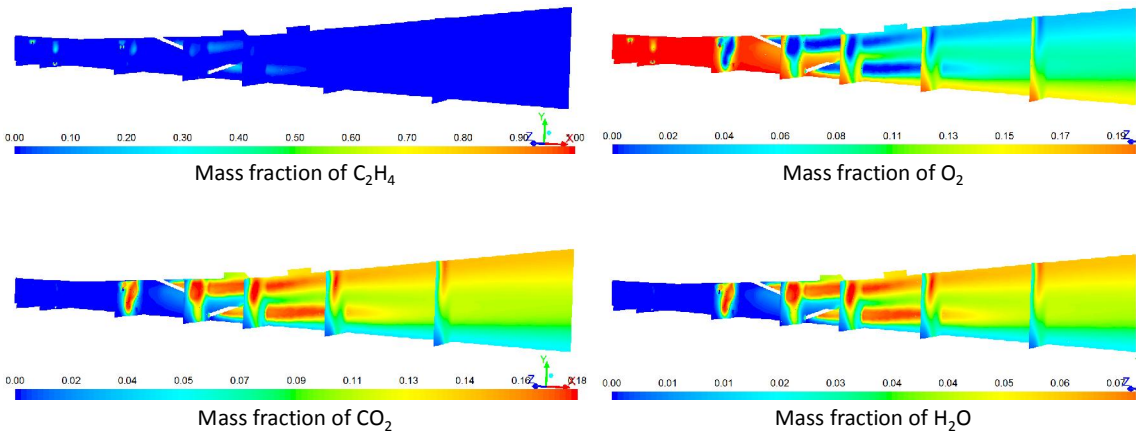

Fig.4.24 (d) Mass fractions of species without fuel injection from 3rd set of ramps

Fig.4.24 Fuel injection except 3rdset of two ramps each on top and bottom walls

The Mass fractions of the species are shown in Fig.4.24 (d). The mass fractions of species show that ethylene mixes with air and combustion takes place at the ramps. Mixing and combustion of ethylene with air continues till the end of the cavities. Oxygen content reduces in the ramps and cavities. Certain amount of oxygen is found to be present along the bottom wall of the diverging combustor. Mass fractions of CO_2 and H_2O indicate combustion at the ramps upto cavities and in the diverging combustor.

Case iv) Fuel is injected from the ramps except the fourth set of two ramps one each on the top wall and bottom wall of the combustor:

The flow field captured along the combustor in the case of fuel (133gm/s) injection from first three sets of ramps, leaving the final set of two ramps in the combustor is depicted in Fig.4.51. Figure shows the Mach number, static pressure, static temperature and mass fraction contours.

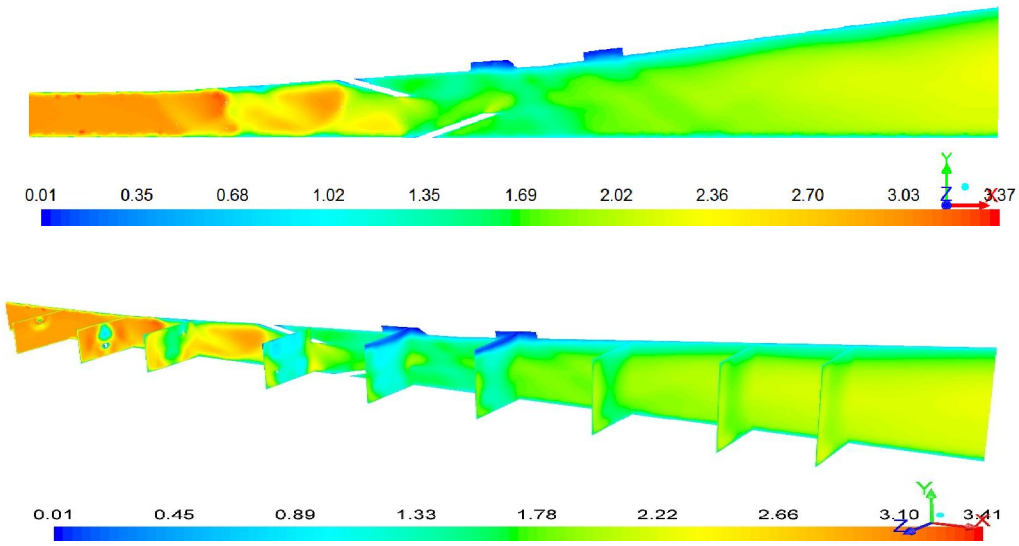

Fig.4.25 (a) Mach number contours without fuel injection from 4th set of ramps

Fig.4.25 (a) shows Mach number contour along the combustor. It can be observed that Mach number reduces due to combustion in the ramps and increases due to expansion where ramps are not located. Mach number decreases further in the combustor at the final set of ramps. This may be due to combustion of the fuel mixed with the supersonic airstream ahead of the final set of ramps. Mach number reduction can be observed in the cavities and along the boundary layer in the combustor. The reduction in Mach number can be seen in the top wall of the combustor compared to the bottom wall. Mach number increases in the diverging combustor towards exit.

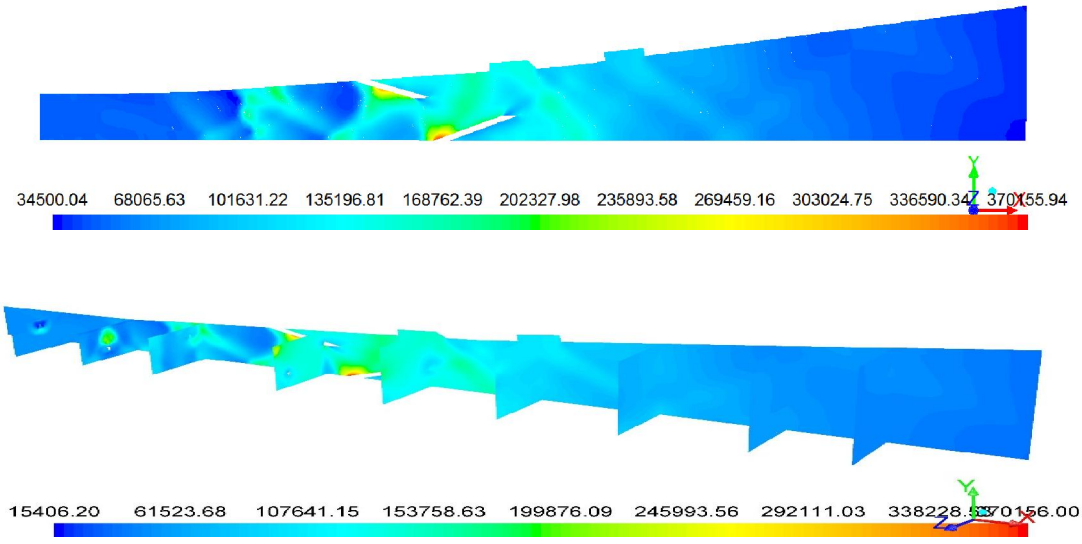

Fig.4.25 (b) Static pressure (Pa) contours without fuel injection from 4th set of ramps

Static pressure contours as shown in Fig.4.25 (b) rise to the highest value at the ramps. The static pressure in the ramps is observed to be about 1.7 bar in the combustor and locally at the ramps is about 3 bar. High pressure continues in the cavities and reduces towards the exit of the combustor. The pressure rise is clearly seen towards the end of the ramps and in the two cavities along the top wall of the combustor. Pressure shocks emanating from the cavities can be observed. The static pressure at the exit corresponds to the ambient condition.

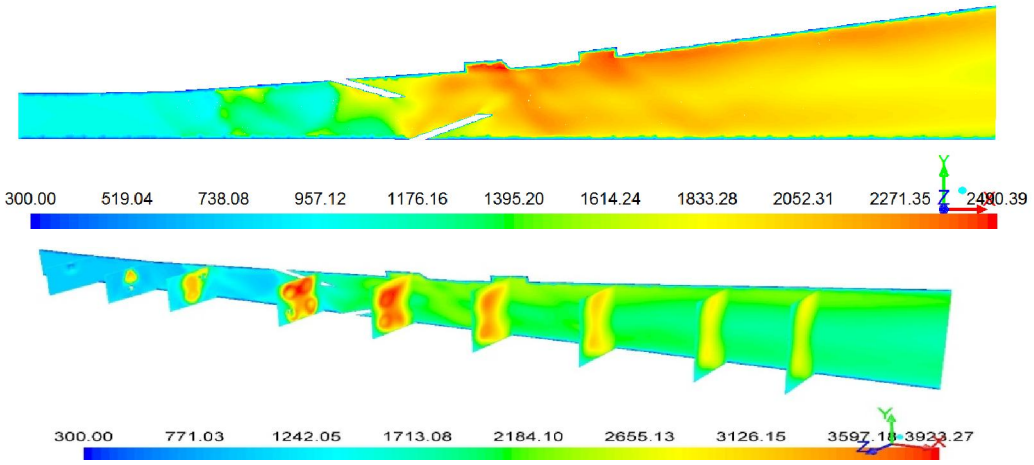

Fig.4.25 (c) Static temperature (K) contours without fuel injection from 4th set of ramps

Static temperature contours shown in Fig.4.25 (c) indicate higher temperature in the ramps. The static temperature in the cavities is observed to be locally, very high, about 2400 K. The temperature along the boundary of walls record a lower temperature compared to the core of the combustor. The rise in static temperature can be seen all along the boundary till the exit of the combustor.

Mass fraction contours in Fig.4.25 (d) show that ethylene fuel mixes with oxygen in the air. The mass fraction of ethylene shows good mixing with oxygen of the supersonic airstream. Reaction of ethylene with air is observed in the ramps zone. The rise in the temperature continues in cavities due to recirculation zone present in the combustor. Ethylene diffuses into the air and it is observed to continue upto the cavities. Oxygen mass fraction also shows similar pattern. The mass fractions of CO_2 and H_2O show the formation of the products in the ramps and cavities that continues in the diverging combustor. The flow field shows that the contribution of first cavity is more compared to the second cavity.

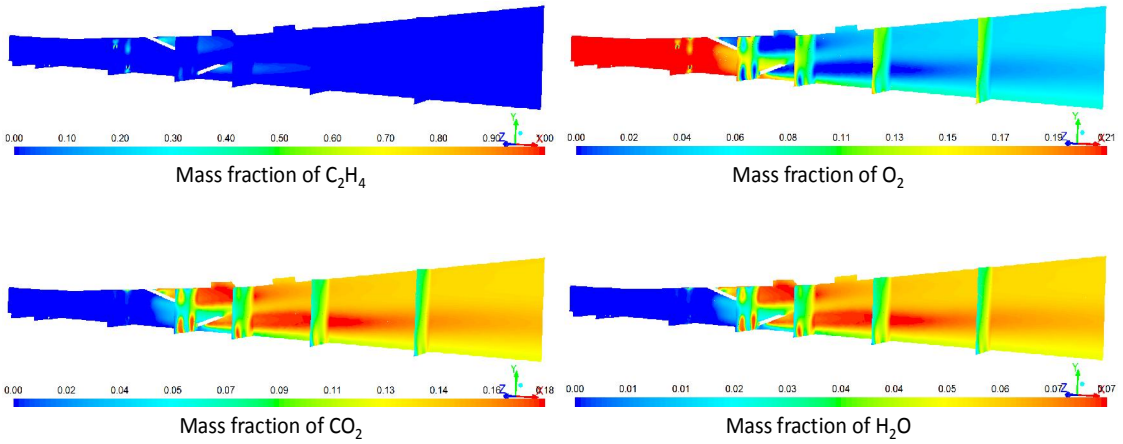

Fig.4.25 (d) Mass fractions of species without fuel injection from 4th set of ramps

Fig.4.25 Fuel injection pattern except fourth set of ramps on top and bottom walls

The comparison of Mach number, static pressure, static temperature and mass fractions of species is depicted in Fig.4.26 for all the above cases of staged fuel injection leaving one set of ramps in the combustor, in each case.

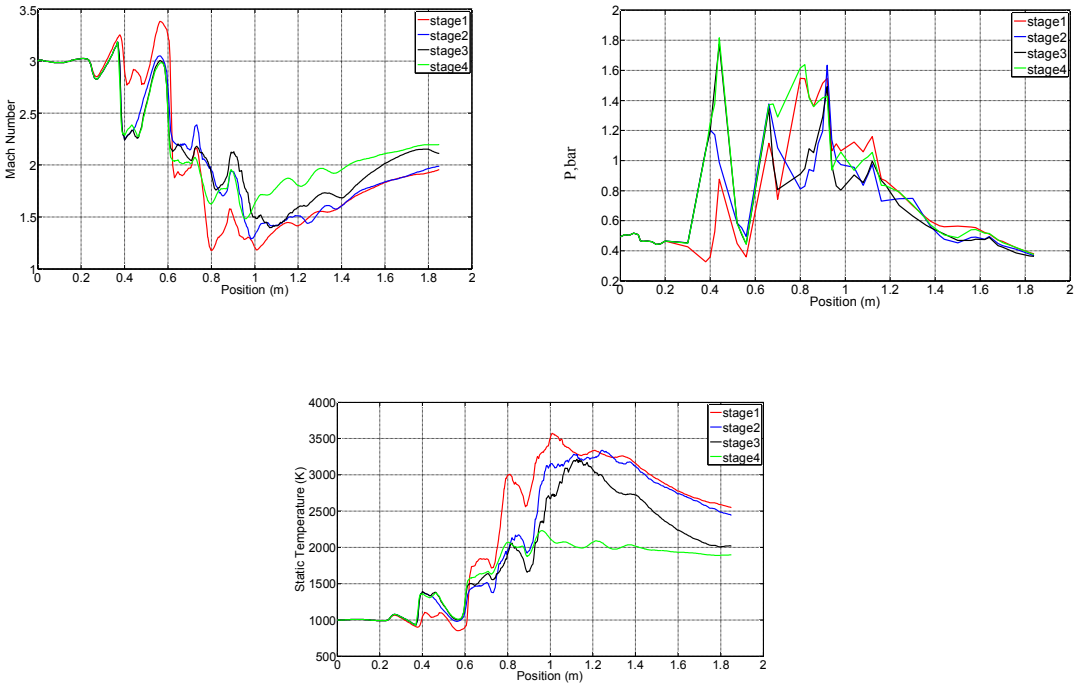

Fig.4.26(a) Comparison of flow field for staged fuel injection pattern

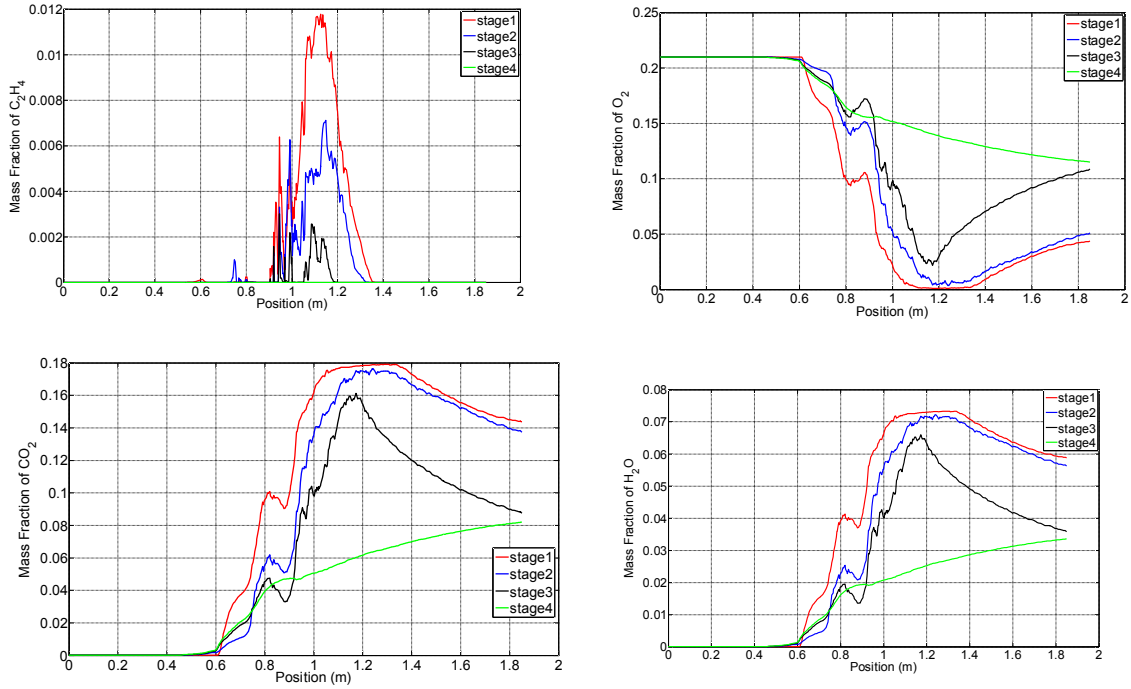

Fig.4.26 (b) Comparison of Mass fractions for staged fuel injection pattern

The Mach number distribution shows that injection from stage 2, 3 and 4 is better than injection from stage 1. However, the trend remains similar in all cases. In the case of stage 1 fuel injection scheme where fuel is not injected from the first set of two top and bottom ramps, the Mach number reduces close to 1.5 while the Mach number of the other injection schemes from ramps show sufficiently higher Mach number except near cavities. This may be due to the mixing of the fuel with air in the subsequent stages leaving the first set of ramps.

The static pressure profile shows that the static pressure of injection pattern without first stage of injection gives very low pressure in the ramp zone due to expansion where ramps are not there. The static pressure rises to about 2 bar maximum in the ramps. It can be observed that the static pressure reduces in the cavities and increases due to reflecting shocks from the wall. The pressure reduces in the diverging combustor. In the case of other injection patterns, the trend remains same with similar variation in the static pressure and the maximum pressure rise is about 1.5 bar. The static temperature rise is very high in the case of injection patterns as shown in the figure depicting the static

temperature comparison. In the injection schemes where the injection is not carried out from second and third set of ramps respectively, the fuel injected from first set of ramps will be mixing with fuel thoroughly and combustion takes place. Out of the two injection patterns, with the fuel injection from the ramps other than the second set of top and bottom ramps, the rise in static temperature shows significant combustion. The mass fractions of species also show that ethylene mass fraction and oxygen mass fraction mix near the ramps and decrease in the zone after ramps and cavities. It is also seen that corresponding rise in the mass fractions of CO_2 and H_2O indicate complete combustion. From the values of thrust, Mach number, static pressure and static temperature, it may be inferred that the injection pattern in which the fuel is not injected from second and third ramps are more suitable fuel injection schemes in that order compared to the other two fuel injection schemes.

4.5 Validation with experimental work:

Experiments have been conducted using full-scale combustor with aviation kerosene, injected at Mach 2 condition at the entry to the combustor. Supersonic air mixes with fuel in the ramps and flame stabilization is provided at the cavities. Experimental work is described in section 4.6. Computational studies have been carried out simulating the experimental conditions and wall static pressure values are shown in the Figure 4.27.

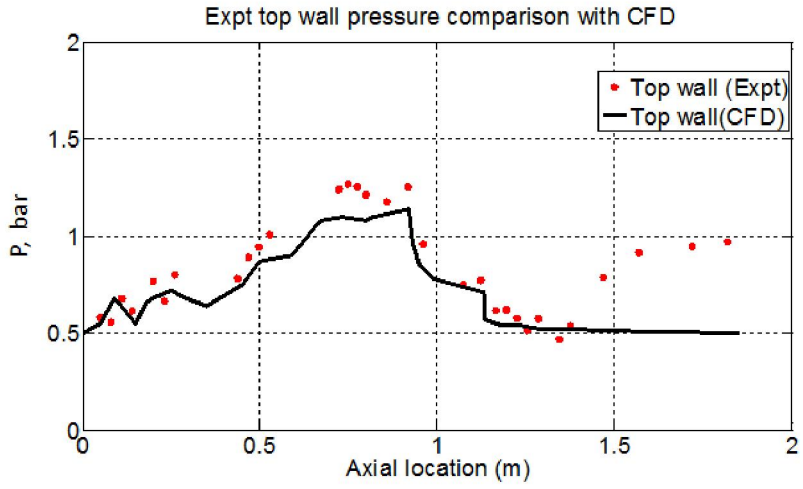

Fig.4.27 Comparison of combustor top wall pressures in full-scale combustor

Fig. 4.27 shows the static pressure distribution along the combustor with the experimental data for a full scale combustor. Computational studies have been conducted with aviation kerosene at combustor entry Mach number 2. Experimental conditions have been simulated. Static pressure along the combustor has been plotted. Measured values of pressure during experiment have been plotted along the combustor length. In this comparison, the numerical studies follow the trend and compare well with the experiment. In the ramps zone, the experiment shows higher pressure. Static pressure decreases in the diverging portion of the combustor. As the ambient pressure is 1 bar, the static pressure towards the end of the combustor will reach atmospheric pressure in the case of experiment due to flow separation in the diverging section of the combustor. In the computational work, the ambient pressure is considered to be the value corresponding to the high altitude condition. Except towards the end of combustor, the experimental values match with the computational work and validate the computational studies.

4.6 Experimental studies on full-scale combustor with aviation kerosene as fuel at combustor entry Mach 2:

After gaining experience with the sub-scale combustor initially, in achieving sustained supersonic combustion, further studies are explored on a full-scale combustor. Fig.4.2 (a) depicts the schematic diagram of the full-scale combustor, provided with four stages of ramps and cavities on the top wall of the combustor. Ramps are staggered along the top and bottom walls.

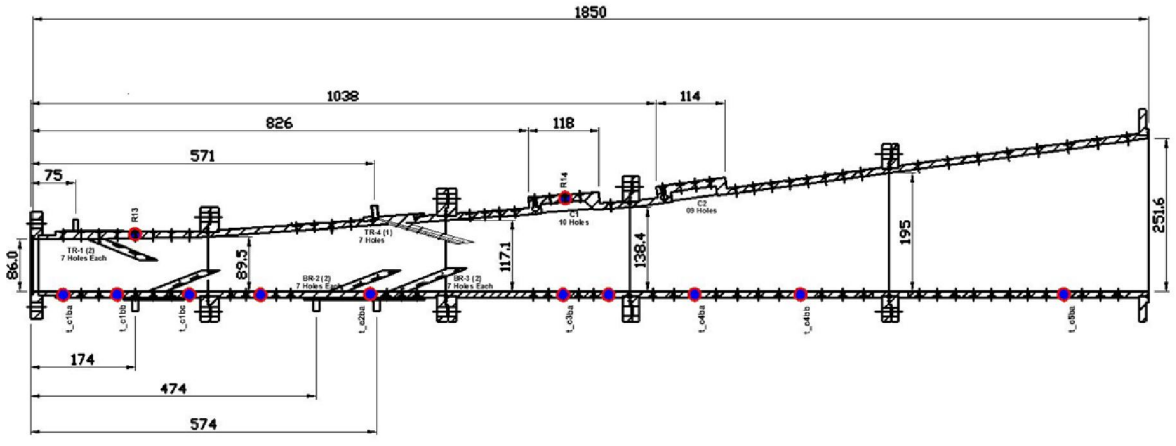

Fig. 4.27(a) Schematic diagram of the full-scale combustor

The variation of wall static pressure along the full-scale combustor for non-reacting flow (without combustion) and reacting flow (with combustion) cases are shown in Fig.4.27 (b). In this study also, aviation kerosene is used as a fuel (133gm/s) in the combustor with entry Mach number of 2, with an equivalence ratio of 1.13.

Wall pressures are observed to be higher in the case of reacting flow compared to non-reacting flows. It can be observed that there is rise in the wall static pressure to a value of about 1.2 bar at the ramps spreading to a distance x < 1000 mm. However, there is a sudden drop in the region of cavities. The rise in wall pressure in the ramps could be due to sudden shocks emanating from fuel impingement with enhanced mixing and combustion. On the downstream of ramps, due to formation of contra-rotating vortices, baroclinic torque is developed that leads to further rise in pressure. It can be observed that static pressure rises in the first cavity and shows marked decrease in the second cavity. This may be due to the location of the second cavity in the combustor. As with the non-reacting flow, the pressure in the diverging section of the combustor decreases and approaches atmospheric pressure at the exit of the combustor. The steep rise in static pressures in the local regions of the combustor is observed with respect to time and the same is illustrated in Fig.4.27(c). The selective pressure data of wall pressures measured at different locations along the combustor is shown as pc1, pc8, pc13, pc19, pc26 and pc30 along the combustor

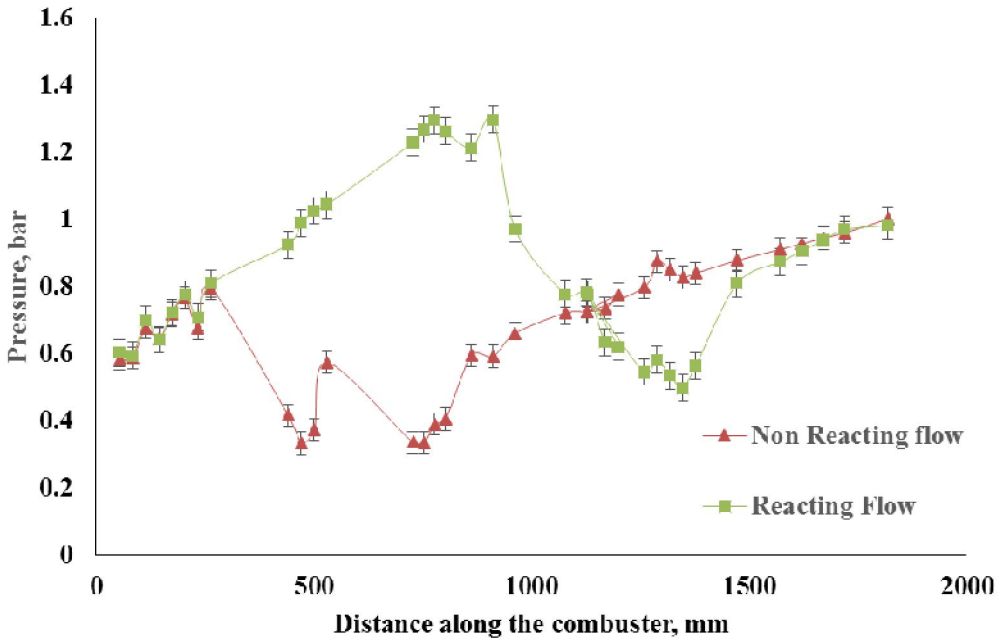

Fig. 4.27 (b) Variation of static pressure along the top wall of the full-scale combustor

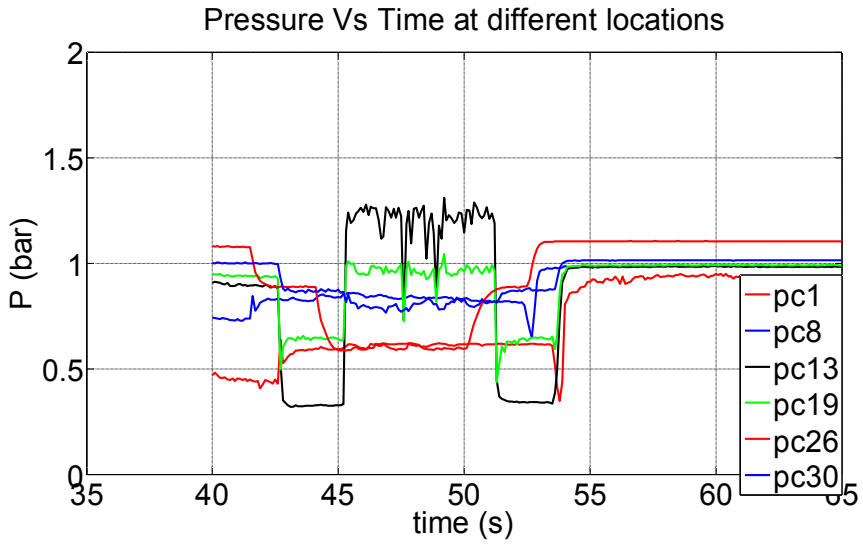

Fig. 4.27(c) Variation of static pressure during the test

It can be seen that the rise in pressure is different in first cavity compared to second cavity in all these experiments and the contribution of second cavity needs to be explored. Aviation kerosene being liquid fuel is required to break into fine droplets, vaporise and mix with the oxygen content in the air for combustion to take place. To

overcome the issues with liquid fuels, gaseous fuels may be used to achieve mixing and supersonic combustion within the short residence time of the combustor.

Fig.4.27 (d) shows variation of the temperature along the combustor for reacting condition. The plot indicates rise of temperature in the ramps and cavities which continues in the diverging portion of the combustor. There is a temperature rise of about 1000 K. This indicates sustained combustion. Wall temperature rise during the test is shown with change in time in Fig.4.27 (e) for different wall temperature locations. The plot shows a substantial rise in temperature including the diverging portion of the combustor. Temperatures are measured along the combustor at different locations, viz. near ramps, near cavities and divergent portion of the combustor and given in the Fig.4.27 (e) as R5, R7, R9, R11, R12, R13 and R14.Temperatures show rise near ramps, after cavity and downstream combustor indicating mixing of fuel with supersonic airstream and combustion.

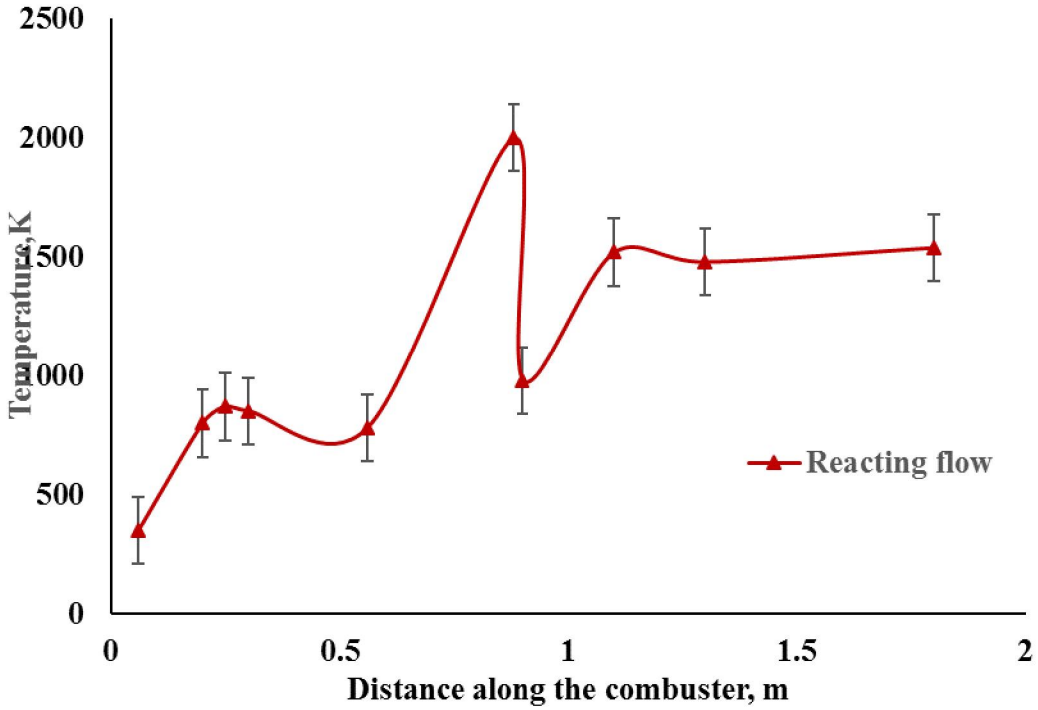

Fig. 4.27 (d) Variation of Temperature along the full- scale combustor

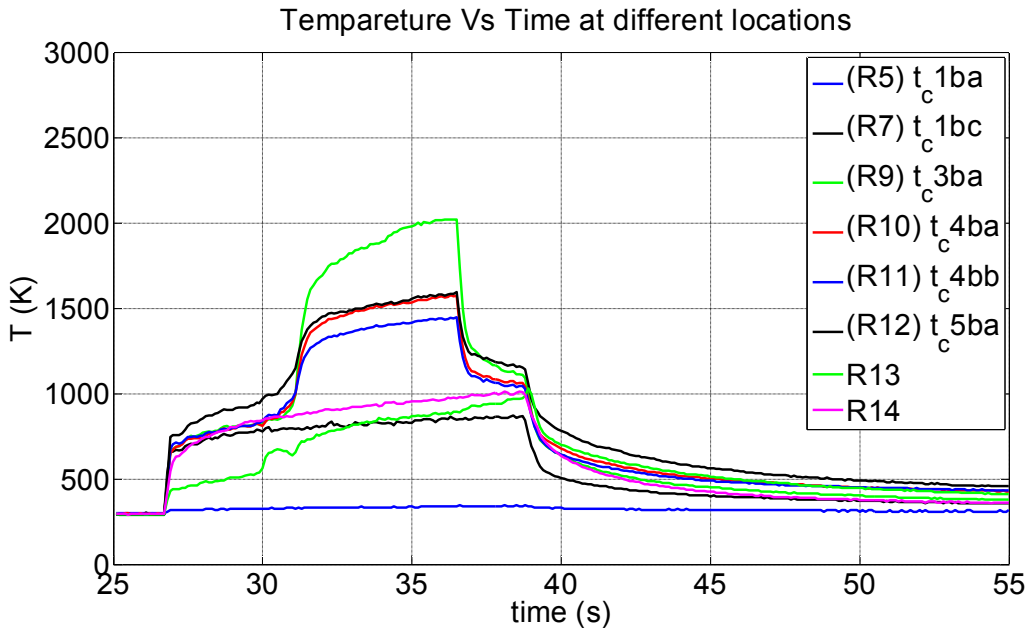

Fig. 4.27 (e) Variation of Temperature during the test

It can be seen from the tests conducted on sub-scale and full-scale combustors with aviation kerosene that the mixing and sustained combustion could be achieved in all the tests. However, in one test each of the sub-scale and full-scale combustors, the wall static pressures and temperatures are comparatively less than that in other tests. This could be because of issues with the vaporising and mixing of the liquid aviation kerosene fuel with the supersonic airstream. For these reasons, it is necessary to use a gaseous fuel which can easily be miscible with supersonic airstream. Gaseous ethylene is a candidate fuel for achieving supersonic combustion. Computational studies are carried out with ethylene as fuel to study the performance of the ramp-cavity supersonic combustor. As seen from the results of sub-scale and full-scale experiments, the wall static pressure is 3.5 bar in one experiment and 2.2 bar in the remaining two experiments in the case of subscale combustor, the wall static pressure in case of full scale combustor is 1.2 bar in full-scale combustor. The temperatures in sub-scale combustor are about 1400 K -2000 K in sub-scale combustor and 1200 K-1600 K in two tests of the full-scale combustor

4.7 PLATES

I. Sub-scale Combustor

(a)

(b)

II. Full-scale Combustor

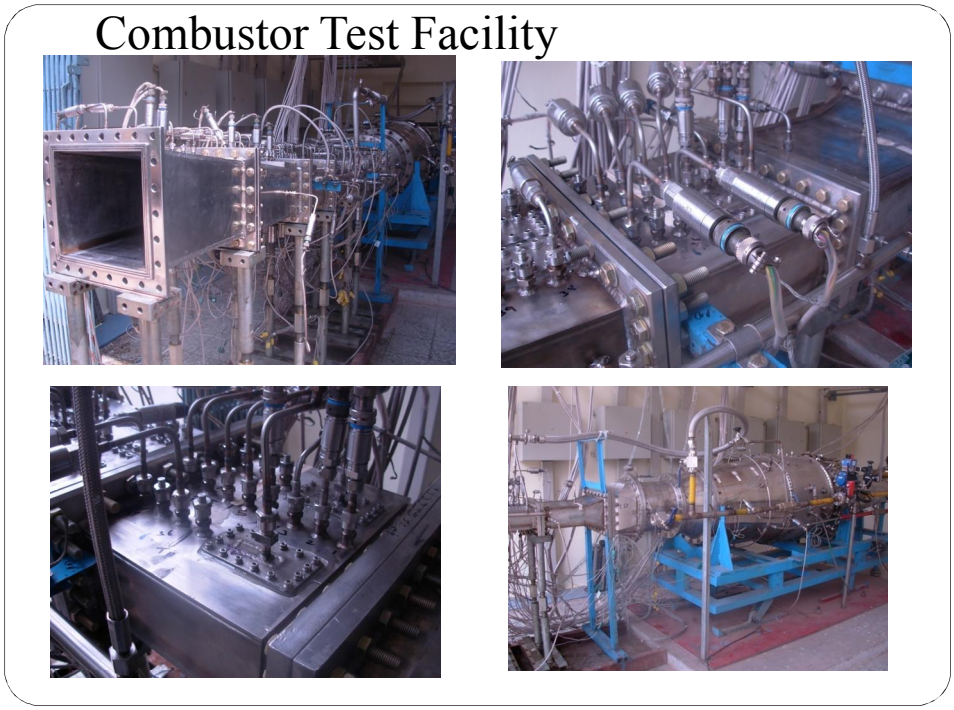

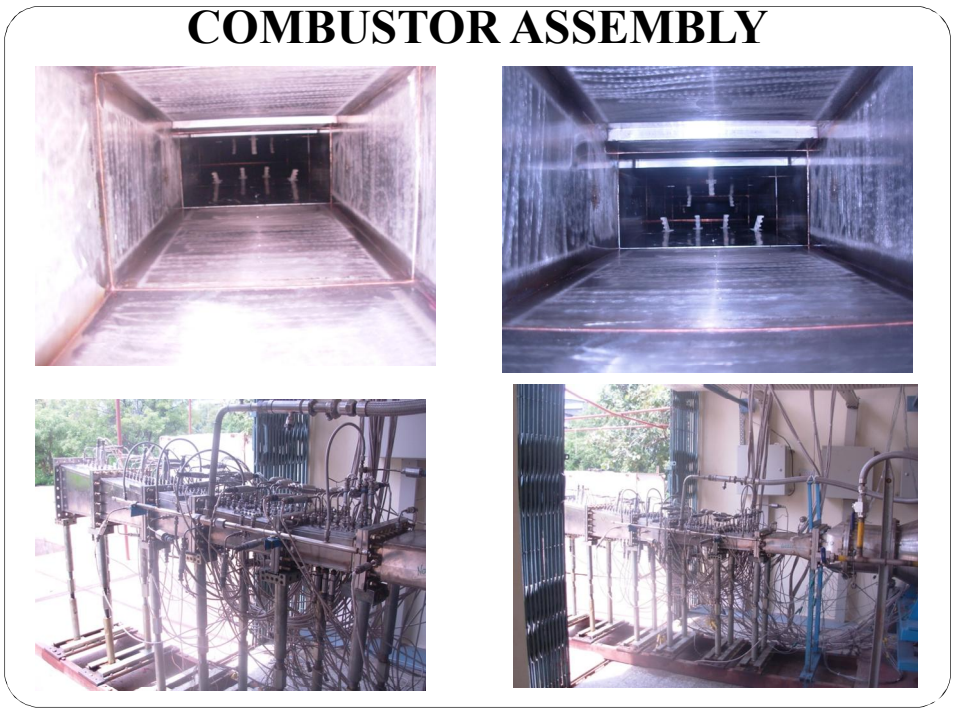

Supersonic Combustor Test

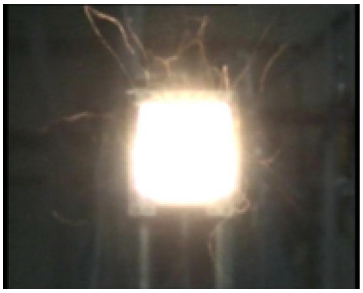

SUMMARY AND CONCLUSIONS

The present work has dealt with both experimental and numerical analysis of supersonic combustor for achieving sustained combustion. For this purpose, a full-fledged supersonic combustion experimental test facility is developed. Experimental Studies are conducted with Aviation Kerosene as a fuel on both sub-scale and full-scale combustors. For mixing of fuel-air and flame holding, ramps and cavities respectively have been incorporated and thus Ramp-Cavity combustor hardware has been realized. Combustor performance is evaluated in terms of wall pressures and wall temperatures. These are measured with calibrated pressure gauges and temperature sensors.

Parametric studies have been carried out by conducting extensive numerical experiments considering different fuels, equivalence ratio, entry Mach number and injection pattern. The studies are used to establish the need for ramp-cavity combustor. Flow field parameters such as Mach number, static pressure, temperature and species variation across the length of the combustor are predicted and discussed. The conclusions drawn from the present study are listed below.

1. Extensive numerical experiments were carried out to study the independent effect of (i) ramp alone, (ii) cavity alone and (iii) with and without ramp-cavity arrangement to evolve combustor configuration. It is revealed that ramp-cavity configuration is suitable for the chosen combustor configuration.

2. Parametric studies have been extensively carried out on ramp-cavity combustor with the help of Fluent v15.0 software to understand the effect of fuel, entry Mach number, equivalence ratio and fuel injection pattern of the combustor. The species variations upon combustion are predicted well with the CFD tool.

3. Good agreement between numerical studies and experimental results is observed.

4. Shock structures near ramps are captured with the numerical experiments. Contra-rotating vortices at the ramps and re-circulation zones within the cavities are traced in the numerical experiments.
5. Contours of combustor with ramps and cavities depict high degree of turbulence in the core extending upto the cavities and turbulence intensity

throughout the combustor. Thus present studies established the mandatory provision for cavities for the purpose of flame holding.

6. Among the chosen entry Mach numbers viz. 2, 2.5 and 3, sustained supersonic combustion was observed throughout the combustor with combustor entry Mach number 3.

7. It is predicted that adoption of rich mixtures would allow supersonic combustion with near complete combustion. However, the studies showed good mixing and combustion with fuel equivalence ratio of 0.6.

8. The computational studies established that ethylene could be explored as a promising fuel for supersonic combustion.

9. When the fuel is not injected from the first set of ramps, the flow Mach number in the core is observed to be in the range of 1.7-2 in the core of the combustor.

10. When the fuel is not injected from the third set of ramps, temperature rise in the cavities can be observed to be about 3000 K, locally which helps in sustained supersonic combustion.

11. The injection pattern in which the fuel is not injected from second and third ramps are more suitable injection schemes in that order compared to the other two fuel injection schemes.

12. Provision of ramps would reduce the blockage effect when compared to adoption of pylons, struts employed for mixing process.

13. Experimental studies on ramp-cavity established that in case of reacting flow, the wall pressure increases continuously, near the ramps, indicating mixing and combustion.

14. Also, it is observed that static pressure rises in the first cavity, relative to second cavity. Static pressures measured in the diverging portion of the full scale combustor also depict higher pressure initially indicating supersonic combustion followed by reduction in pressure in the diverging section.

15. It can be seen that in the experiments, the static pressure towards the exit of the combustor shows rise in pressure to equalise with the ambient conditions.

SUMMARY TABLE

COMPUTATIONAL STUDIES:

Sl. No.	*Combustor Configuration*	*Fuel*	*Entry Mach No.*	*Equivalence Ratio*	*Remarks*
1	Full Scale without ramps and cavities 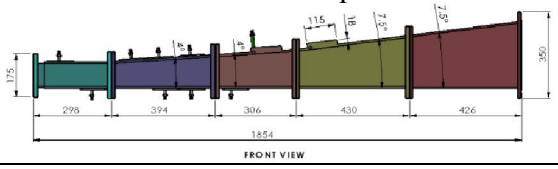	-	3	-	Base line combustor configuration
2	Full scale with ramps and without cavities 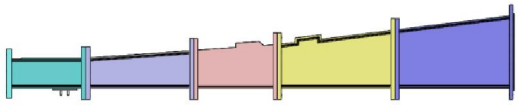	-	3	-	Effect of ramps is studied
3	Full scale with cavities and without ramps 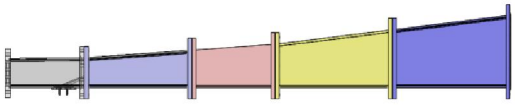	-	3	-	Effect of cavities is observed
4	Full scale with ramps and cavities 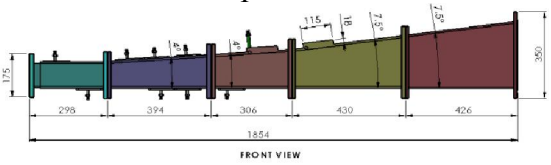	-	3	-	Combined effect of ramps and cavities is studied
5	Full scale with ramps and cavities 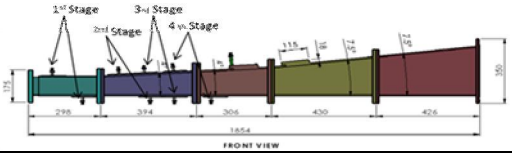	Aviation kerosene	2	-	Computational studies at combustor entry Mach 2
6	Full scale with ramps and cavities 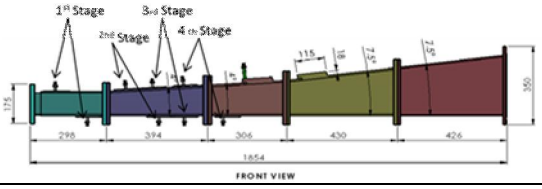	Aviation kerosene	3	-	Computational studies at combustor entry Mach 3
7	Full scale with ramps and cavities 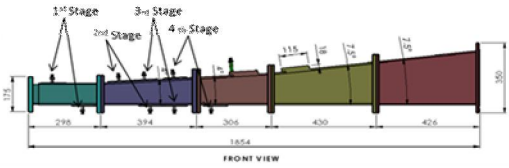	Ethylene	3	0.6	Computational studies at combustor entry Mach 3 with ethylene as fuel

8	Full scale with ramps and cavities 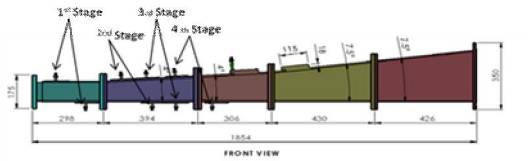	Ethylene	2.5	0.6	Computational studies at combustor entry Mach 2.5 with Ethylene as fuel
9	Full scale with ramps and cavities 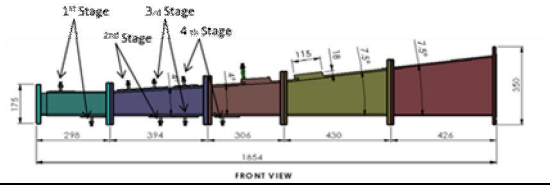	Ethylene	2	0.6	Computational studies at combustor entry Mach 2 with Ethylene as fuel
10	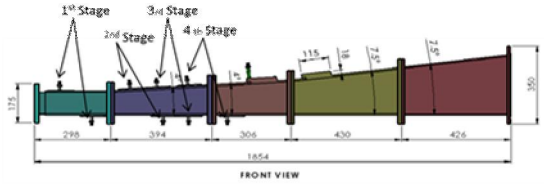	Ethylene	3	0.6	Studies with injection at Ø = 0.2, 0.4, 0.6, 08
11	Full scale with ramps and cavities 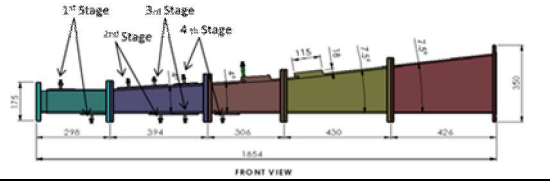	Ethylene	3	0.6	No injection from first set of 2 ramps each on top and bottom walls
12	Full scale with ramps and cavities 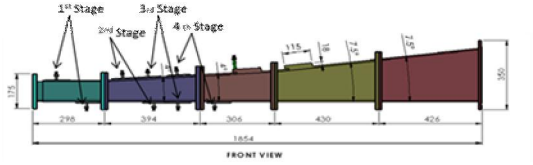	Ethylene	3	0.6	No injection from second set of 2 ramps each on top and bottom walls
13	Full scale with ramps and cavities 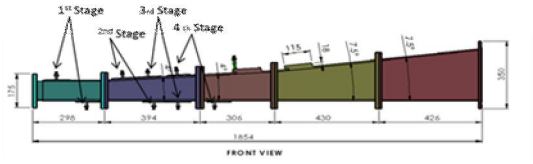	Ethylene	3	0.6	No injection from third set of 2 ramps each on top and bottom walls

14	Full scale with ramps and cavities 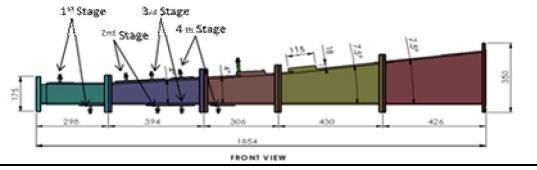	Ethylene	3	0.6	No injection from fourth set of one ramp each on top and bottom walls
15	Sub-scale combustor with ramps and cavities 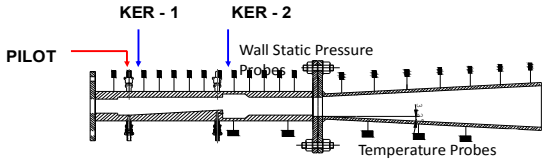	Aviation kerosene	2		Computational studies with sub-scale combustor with aviation kerosene as fuel
16	Sub-scale kerosene with ramps and cavities17 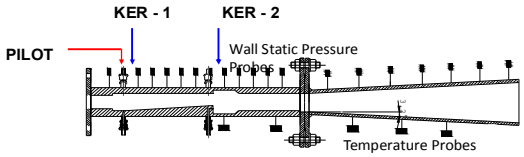	Aviation kerosene	2.5		Computational studies with sub-scale combustor with aviation kerosene as fuel
17	**Combustor with cavities and Wall Injection for combustor entry Mach 3** 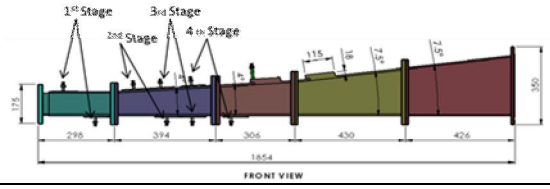	Ethylene	3		Computational studies with full-scale combustor with aviation kerosene as fuel

Experimental

Sl. No.	***Combustor Configuration***	***Fuel***	***Entry Mach No.***	***Equivalence Ratio***	***Observations***
1	Full Scale 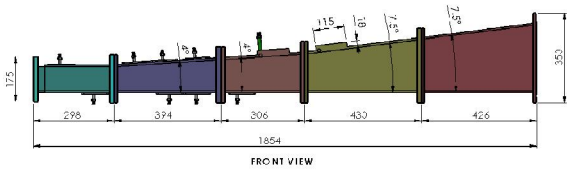	Aviation kerosene	2	1.13	3 experiments
2	Sub Scale 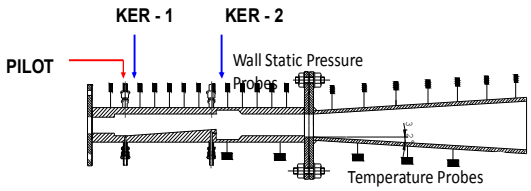	Aviation kerosene	2		3 experiments

6. Recommendations for future work

Based on the present experimental and computational studies on sustained supersonic combustion with ramps and cavities the following recommendations are proposed:

1. Extensive studies may be conducted for higher combustion entry Mach numbers.
2. Dual mode combustion ramjet studies may be conducted with ramp cavity configuration.
3. Computational studies with unsteady conditions may be pursued to evaluate the flow parameters.
4. Fuels may also be varied and studied for this configuration.

PAPERS PUBLISHED BASED ON PRESENT WORK

A) International Journals

S. No	Title of the paper	Name of the Journal	Status
1.	Scramjet Combustor Development: A review	Journal of Aerospace Engineering And Technology, Volume2, Issue 3, December,2012	Published
2.	Effect of Ramp-Cavity on Hydrogen fuelled Scramjet Combustor	Journal of Propulsion and Power Research, 2014.3(1) Elsevier	Published
3	Sustained combustion with ramp-cavity enabled scramjet combustor	ISME Journal of Thermo fluids February,2018	Accepted
3.	Experimental Evaluation of sub-scaled supersonic combustor with combined effect of Ramps and Cavities	Journal of Propulsion and Power Research , Elsevier	Under Review
4.	'Numerical studies on ethylene fueled ramp-cavity Scramjet combustor'	Journal of Aerospace Engineering and Technology, Elsevier	Under Review

B International Conferences:

1. **"**Sustained combustion with ramp-cavity enabled scramjet combustor**",** Moorthy, J.V.S. and Dr. Amba Prasad Rao, G , Proceedings of the 1st International and 18th ISME Conference, ISME 18,February 23rd – 25th, 2017, NIT Warangal, Warangal

REFERENCES

1. Abdullah Karimi, Sameera D Wijeyakulasurya, and Razi Nalim, M, "Numerical Study of Supersonic Flow over Backward-Facing Step for Scramjet Application", AIAA 2012-4001
2. Abdel Salam, T.A., Tiwari,S.N., Chaturvedi, S.K. and Mohielden, T.A., "Mixing and Combustion in Scramjet with Raised and Relieved Ramps", AIAA 2000-3709
3. Amarnatha S. Potturi , Jack R. Edwards, " Large-eddy/Reynolds-averaged Navier–Stokes simulation of cavity-stabilized ethylene combustion", Combustion and Flame 162 (2015) 1176–1192
4. Andrew Henry Zang, "Fuel injection in Scramjets, Mixing enhancement and combustion characterisation experiments", University of Maryland, 2005
5. Andrew.D.Rothstein, " A Study of the normal injection of Hydrogen into a heated supersonic flow using Planar Laser Induced Fluorescence", Massachusetts Institute of Technology, 1992
6. Aristides,M.,Bonanos,Darius,D.Sanders,Joseph,A.Schetz,Walter,F.O.Brien,Christopher,P. Goyne, Roland H.Krauss and James C. Mcdaniel, "Hot Flow Testing of an Integrated Aero-Ramp Injector/Plasma Igniter for Scramjets with Hydrogen and Hydrocarbon Fuels", AIAA 2003-6987
7. Aristides,M.,Bonanos, Joseph,A.Schetz, Walter,F. O.Brien and Christopher,P. Goyne, " Scramjet Operability Range Studies of a multifuel Integrated Aero-Ramp Injectors/Plasma Igniter, AIAA 2005-3425
8. Aristides,M.,Bonanos, Joseph,A.Schetz,Walter,F.O.Brien and Christopher,P. Goyne, "Integrated Aeroramp-Injector/Plasma-Torch Igniter for Methane and Ethylene Fueled Scramjets", AIAA 2006-813
9. Axisymmetric AFT Ramp Cavities", International Journal of Innovative Research in Science, Engineering and Technology, Vol.3, March 2014
10. Baurle,R.A., Mathur, T., Gruber, M.R. and Jackson, K.R.," A numerical and Experimental Investigation of a Scramjet combustor for Hypersonic Missile Applications", American Institute of Aeronautics and Astronautics, 1998
11. Billig, F. S., "Two-Dimensional Model for Thermal Compression," *Journal of Spacecraft and Rockets*, Vol. 9, No. 9, 1972, pp. 702, 703.
12. Billig, F. S., Dugger, G. L. andWaltrup, P. J., "Inlet-Combustor Interface Problems in Scramjet Engines," *Proceedings of the First International Symposium on Air Breathing Engines*, International Society for Airbreathing Engines, June 1972.

13. Billig, F. S., and Sullins, G. A., "Optimization of Combustor–Isolator in Dual-Mode Ram Scramjets," AIAA Paper 93-5154, Nov.–Dec. 1993

14. Bouchez, M., Hachemin, J. V., Leboucher, C., Scherrer, D., and Saucerau, D., "Scramjet Combustor Design in French PREPHA Program—Status in 1996," AIAA Paper 96-4582-CP, Nov. 1996

15. Bouchez,M., Levine,V., Davidenko, D., Avrashkov, D., and Genevieve,nP, "Airbreathing Space Launcher Interest of a Fully Variable Geometry Propulsion System and Corresponding French–Russian Partnership," AIAA Paper 2000-3340, July 2000

16. Chase, R. L., and Tang, M. H., "A History of the NASP Program from the Formation of the Joint Program Office to the Termination of the HySTP Scramjet Performance Demonstration Program," AIAA Paper 95-6051, April 1995

17. Chapuis,M., Fedina.E., Fureby, C.,Hannemann.K., Karl.S., Martinez Schramm., " A Computational studynof the Hyshot II combustor performance" , Proceedings of the Combustion Institute 34 (2013) 2101–2109

18. Eklund, D.R.,Baurle,R.A. and Gruber, M, "Numerical study of a Scramjet Combustor fuelled by an Aerodynamic Ramp Injector in a Dual Mode Combustion". AIAA 2001-0379

19. Faulkner, R. F., and Weber, J. W., "Hydrocarbon Scramjet Propulsion System Development, Demonstration and Application," AIAA Paper 99-4922, Nov. 1999

20. Ferri, A., "Review of Problems in Application of Supersonic Combustion," *Journal of the Royal Aeronautical Society*, Vol. 68, No. 645, 1964, pp.575–597

21. Falempin, F., and Serre, L., "The French PROMETHEE Program: Main Goals and Status in 1999," AIAA Paper 99-4814, Nov. 1999

22. Frank W. Barnes, Corin Segal, "Cavity-based flame holding for chemically-reacting supersonic flows", Progress in Aerospace Sciences 76(2015) 24–41

23. Gruber,M. R., Donbar, J. M., Carter C. D. and Hsu K.-Y., "Mixing and Combustion Studies Using Cavity-Based Flameholders in a Supersonic Flow", JOURNAL OF PROPULSION AND POWER,Vol. 20, No. 5, September–October 2004

24. Gruenig, C and Mayinger, F., "Supersonic Combustion of Kerosene/H2-Mixtures in a Model Scramjet Combustor", Combustion Science and Technology 1999,146: 1, 1 – 22

25. Gruber, M.R., Baurle, R.A.,Mathur,T. and Hsu,K.Y."Fundamental Studies of Cavity-Based Flameholder Concepts for Supersonic Combustors", American Institute of Aeronautics & Astronautics,1999-2248

26. Gruber, M., Donbar,J.,Jackson,T.,Mathur,T.,Eklund,D. and Billig,F., " Performance of an Aerodynamic Ramp Fuel Injector in a Scramjet Combustor", AIAA 2000-3708

27. Haiyan Wu, Meng Ding and Yi Su, "The Study of Cavity Flow and Transpiration Cooling in Supersonic Combustion", Applied Mechanics and Materials, 2013, Vol.390, pp370-374

28. Hongbo Wang, Zhenguo Wang , Mingbo Sun, Haiyan Wu, HOU Lingyuna "Combustion modes of hydrogen jet combustion in a cavity-based supersonic combustor", International journal of hydrogen energy 38 (2013) 12078-12089

29. Hongbo Wang, Zhenguo Wang , MingboSun,Ning Qin, " Combustion characteristics in a supersonic combustor with hydrogen injection upstream of cavity flameholder", Proceedings of the Combustion Institute, Volume 34, Issue 2,2013, Pages 2073-2082.

30. HOU Lingyuna, Bernhard WEIGAND, Marius BANICA, "Effects of Staged Injection on Supersonic Mixing and Combustion", Chinese Journal of Aeronautics 24 (2011) 584-589

31. Jeyakumar, s., Surjith, N., Venkateshwaran,V., Karkuvelraja, A., Samy G.S., Jagannathan, K.D., " Experimental Investigations on the Characteristics of Supersonic Flow past.

32. Kanda,T., Wakamatsu, W.,Sakuranaka,N., Izumikava, M., Ono, F and Murakami.A.,"Mach 8 Testing of a Scramjet Engine with Ramp Compression",AIAA 2000-0616.

33. Kumaran, K., and Babu, V., "Mixing and Combustion Characteristics of Kerosene in a Model Supersonic Combustor", Journal of Propulsion and Power, Vol. 25, No. 3, May–June 2009

34. Kyung Moo Kim, Seung Wook Baek, Cho Young Han, "Numerical study on supersonic combustion with cavity-based fuel injection", International Journal of Heat and Mass Transfer 47 (2004) 271–286.

35. LIU Gang , XU Xu and XIE Yongfeng, " Numerical Investigation on the Supersonic Combustion of Liquid Kerosene in a Dual-staged Strut Based Scramjet Combustor", AIAA2014-3665

36. Liu Gang, Zhu Shaohua, Tian Liang, Luo Yu and XuXu, "Numerical Investigation of the Effect of Reaction Models on the Supersonic Combustion of Liquid Kerosene" AIAA2015-4167.

37. Mark P. Wilson, Rodney D. W. Bowersox and Diana D. Glawe, "The Role of Downstream Ramps on Penetration and Mixing Enhancement for Supersonic Injection Flows", American Institute of Aeronautics and Astronautics, Inc., 1997

38. McClinton, C. R., Hunt, J. L., Ricketts, R. H., Reukauf, P., and Peddie, C. L., "Air breathing Hypersonic Technology Vision Vehicles and Dreams, "AIAA Paper 99-4978, Nov. 1999.

39. Meshcheryakov, E. A., and Sabel'nikov, V. A., "Reduced Heat Production Due to Mixing and Kinetic Factors in Supersonic Combustion of Unmixed Gases in an Expanding Channel," *FizikaGoreniyaiVzryva*, Vol.24, No. 5, 1988, pp. 23–32.

40. Mitani, T., Hiraiwa, T., Sato, S., Tomioka, S., Kanda, T., and Tani, K., "Comparison of Scramjet Engine Performance in Mach 6 Vitiated and Storage-Heated Air," *Journal of Propulsion and Power*, Vol. 13,No. 5, 1997,pp. 635–642.

41. Miller,M.F., Allen,M.G.,Rawlins, W.T. and Parker, T.E., "An Experimental Comparison of swept ramp injectors in a model scramjet flow", AIAA 96-0845

42. Ming-Bo Sun, Zhen-Guo Wang, Jian –Han Liang and Hui Geng, "Flame Characteristics in Supersonic Combustor with Hydrogen Injection upstream of a Cavity flameholder", Journal of Propulsion and Power", Vol.24, No.4, July-August 2008.

43. Mishra, D.P. and Sridhar, K.V., "Numerical Study of Effect of Fuel Injection Angle on the Performance of 2D Supersonic Cavity Combustor", J. Aerosp. Eng., 2012, 25(2): 161-167

44. Mohamed Arif,R., Sangeetha,S., " Effect of Ramp-Cavity Injector in Supersonic Combustion", International journal of Scientific and Engineering Research, Volume 4, Issue 5 , May-2013.

45. Pandey, K.M., and Sivasakthivel,T., "CFD Analysis of Mixing and Combustion of a Scramjet Combustor with a Planer Strut Injector", International Journal of Environmental Science and Development, Vol. 2, No. 2, April 2011.

46. Pandey, K.M., Kalita, P.,Barman,K.,Rajkhowa,A. And Saikia,S.N., "CFD Analysis of Wall Injection with Large Sized Cavity Based Scramjet Combustion at Mach 2", International Journal of Engineering and Technology",Vol.3, No.2, April,2011

47. Pandey, K.M. and Singh, A.P., " Recent advances in Experimental and Numerical analysis of combustor Flow fields in Supersonic Flow Regime", International Journal of Chemical Engineering and Applications, Vol. 1, No. 2, August 2010

48. Paull, A., and Stalker, R. J., "Scramjet Testing in the T4 Impulse Facility," AIAA Paper 98-1533, April 1998.

49. Peter Gerlinger , Peter Stoll, Markus Kindler, Fernando Schneider, Manfred Aigner, "Numerical investigation of mixing and combustion enhancement in supersonic combustors by strut induced stream wise vorticity", Aerospace Science and Technology 12 (2008) 159–168.

50. Prashant Dinde, Rajasekaran,A., and Babu,V., "3D numerical simulation of the supersonic Combustion of H2", The Aeronautical Journal, December,2006 pp773-782.

51. Prateek Srivastava and Pandey,K.M.,"Computational Analysis Of Supersonic Combustion using Cavity based Fuel Injection with Species Transport Model at Mach Number 4.17", International Journal of Science, Environment and Technology, Vol. 3, No 3, 2014, 923 – 930

52. Rajasekaran,A, Satishkumar,G. and Babu,V., "Numerical simulation of the supersonic combustion of kerosene in a model combustor", Progress in Computational Fluid Dynamics",2009.

53. RakeshArasu, Sasitharan Ambicapathy, Sivaraj Ponnusamy, Mohanraj Murugesan and Sanal Kumar, V.R., "Numerical Studies on Flow Field Characteristics of Cavity based Scramjet

54. Sabelnikov,V. A., Voloschenko, O. V., Ostras, V. N., Sermanov,V. N., and Walther, R., "Gas dynamics of Hydrogen-Fueled Scramjet Combustors, "AIAA Paper 93-2145, June 1993.

55. Sancho,M., Colin,Y., and Johnson, C., "Program Overview: The French Hypersonic Research Program PREPHA," AIAA 7th International Space Planes and Hypersonic Systems and Technologies Conference, Nov. 1996.

56. Shakil Ahmed, Mohammad Ali, Sadrul Islam, A.K.M., "The Effect of Injection Angle on Mixing and Flame Holding in a Supersonic Combustor", Journal of Thermal Science, Vol.II, No. I, 2001.

57. Shreenivasan,O.J., RakeshKumar, SaiKumar,T., Sujith,R.I.,and Chakravarthy,S.R., "Mixing in Confined Supersonic Flow Past Strut Based Cavity and Ramps", 40th AIAA/ ASME/ SAE/ASEE Joint Propulsion Conference and Exhibit 11-14 July 2004, Florida.

58. Sivabalan Mani, Tharikaa Ramesh kumar, Ajith.S, Hemasai.N.D, and Sanal Kumar.V.R., "3D Flow Visualization and Geometry Optimization of Cavity based Scramjet Combustors using k-ω Model", 51st AIAA/SAE/ASEE Joint Propulsion Conference, July 27-29, 2015, Orlando, FL.

59. Stouffer,S.D.,Baker, N.R.,Capriotti, D.P.,Northam,G.B., "Effect of Compression and Expansion Ramp Fuel Injector Configurations on Scramjet Combustion and Heat Transfer",AIAA 93-0609

60. Tani, K., Kanda, T., Sunami, T., Hiraiwa, T., and Tomioka, S., "GeometricalEffects to Aerodynamic Performance of Scramjet Engine," AIAA Paper 97-3018, July 1997

61. Tahsini, A.M., Tadayon Mousavi, S., "Investigating the supersonic combustion efficiency for the jet-in-cross-flow", International journal of Hydrogen energy, 40 (2015) 3091-3097

62. Taichang Zhang, Jing Wang ,and Xuejun Fan and Peng Zhang, "Combustion of Vaporized Kerosene in Supersonic Model Combustors with Dislocated Dual Cavities", Journal of Propulsion and Power, Vol. 30, No. 5, September–October 2014

63. Tarun Mathur, Mark Gruber, Kevin Jackson, Jeff Donbar, Wayne Donaldson, Thomas Jackson and Fred Billig, "Supersonic Combustion Experiments with a Cavity-Based Fuel Injector", Journal of Propulsion and Power, Vol. 17, No. 6, November–December 2001

64. Tianwen FANG, Meng DING, Jin ZHOU, "Supersonic flows over cavities", Front. Energy Power Eng. China 2008, 2(4): 528–533

65. Timothy M. Ombrello, Campbell D. Carter, Chung Jen Tam, Kuang Yu Hsu, "Cavity ignition in supersonic flow by spark discharge and pulse detonation", Proceedings of the Combustion Institute 35 (2015) 2101–2108

66. Vinogradov, V., Grachev, V., Petrov, M., and Sheechman, J., "Experimental Investigation of 2-D Dual Mode Scramjet with Hydrogen Fuel at Mach 4-6," AIAA Paper 90-5269, Oct. 1990.

67. Walther, R., Sabelnikov, V., Koronstsvit, Y., Voloschenko, O., Ostras,V., and sermanov,V., "Progress in the Joint German–Russian Scramjet Technology Programme," *Proceedings of the 12th International Symposium on Air Breathing Engines*, ISABE Paper 95-7121, Sept. 1995

68. Wei Huang , Mohamed Pourkashanian, Lin Ma, Derek B. Ingham, Shi-bin Luo, Zhen-guo Wang , "Effect of geometric parameters on the drag of the cavity flame holder based on the variance analysis method", Aerospace Science and Technology 21 (2012) 24–30

69. Wei Huang , Shi-bin Li, Li Yan, Zhen-guo Wang, “Performance evaluation and parametric analysis on cantilevered ramp injector in supersonic flows”, Acta Astronautica 84 (2013) 141–152

70. Wei Huang, Jian - guo Tan, Jun Liu, Li Yan, “Mixing augmentation induced by the interaction between the oblique shock wave and a sonic hydrogen jet in supersonic flows”, Acta Astronautica 117(2015)142–152.

71. Wei Huang, Jun Liu, Liang Jin, Li Yan, “Molecular weight and injector configuration effects on the transverse injection flow field properties in supersonic flows”, Aerospace Science and Technology 32 (2014) 94–102

72. Xuejun Fan,Gong Yu, Jianguo Li, Xinyu Zhang and Chih-Jen Sung, “Investigation of Vaporized Kerosene Injection and Combustion in a Supersonic Model Combustor”, JOURNAL OF PROPULSION AND POWER,Vol. 22, No. 1, January–February 2006.

73. Ye Tian, Baoguo Xiao, Shunping Zhang, Jianwen Xing, “ Experimental and computational study on combustion performance of a kerosene fueled dual-mode scramjet engine”, Journal of Aerospace Science and Technology, 2015

74. YouhaiZong; Wen Bao; Juntao Chang; Jichao Hu; Qingchun Yang; Jian Song; and Meng Wu**, “**Effect of Fuel Injection Allocation on the Combustion Characteristics of a Cavity-Strut Model Scramjet, J. Aerosp. Eng., 2015, 28(1)

75. Yu, G., Li, J.G., Zhao, J.R., Yue, L.J., Chang, X.Y., Sung, C.J., “An experimental study of kerosene combustion in a supersonic model combustor using effervescent atomization”, Proceedings of the Combustion Institute 30 (2005) 2859–2866

76. YU,G,. LI, J. G., ZHANG, X.Y., CHEN, L.H., HAN, B. and SUNG, C. J., “Experimental Investigation on Flameholding Mechanism and Combustion Performance in Hydrogen-fueled Supersonic Combustors”, Combust. Sci. andTech.,174: 1_27, 2002

77. Zhen Huaping, GaoZhenxun , Lee Chunhian, “Numerical investigation on jet interaction with a compression ramp”, Chinese Journal of Aeronautics, 2013,26(4): 898–908

78. Zhenxun Gao, Jingying Wang, Chongwen Jiang and Chunhian Lee, “Application and theoretical analysis of the flamelet model for supersonic turbulent combustion flows in the scramjet engine”, Combustion Theory and Modelling, 2014,Vol. 18, No. 6, 652–691

APPENDIX –1

A.1: Experimental studies on Sub-scale Combustor with aviation kerosene as a fuel:

A.1.1 Variation of wall static pressure on top wall of sub-scale combustor

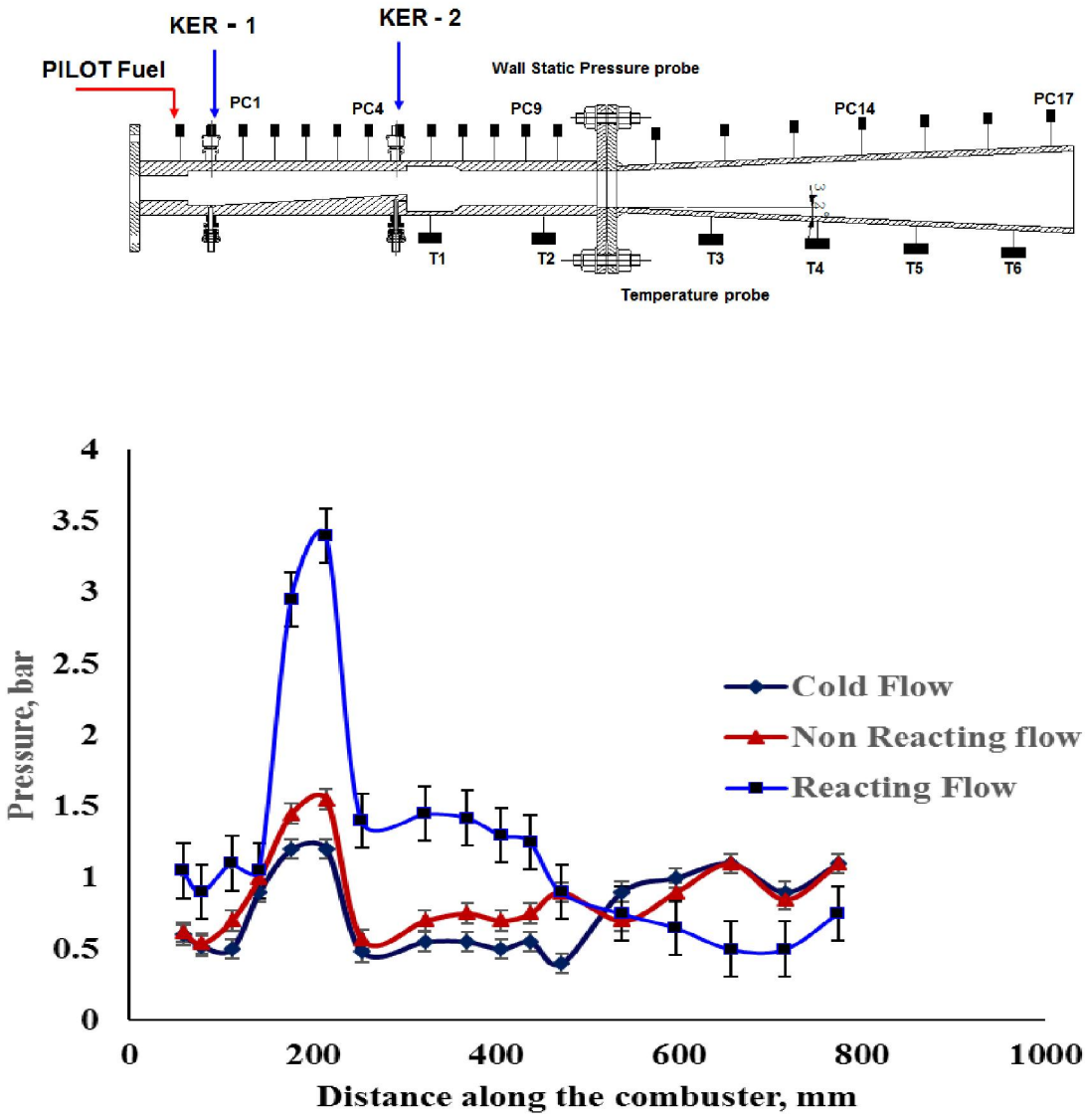

Fig A.1 (a) Top wall static pressure along the sub-scale combustor

Experiments are conducted on ramp-cavity based sub-scale combustor with aviation kerosene as fuel. The experiment is conducted with combustor entry hot air Mach number of 2. Total pressure conditions are simulated at the exit of the vitiated air

heater. Wall static pressures are measured along the top wall. Gas temperatures are measured with R-type thermocouples. The performance of the ramp-cavity combustor has been evaluated in terms of wall static pressures and temperatures along the combustor. The role of ramps in mixing is established with the static pressure rise. The rise in temperature in the combustor is indicative of the flame holding and sustained combustion.

Fig.A.1 (a) depicts variation of static pressure along the top wall of the sub-scale ramp-cavity scramjet combustor for three different cases. Wall static pressures are measured at different instances during the test. Static pressure measurements are made when supersonic airstream alone flows in the combustor, when pilot Hydrogen is injected and for a case after the injection of liquid aviation kerosene along with pilot hydrogen and combustion of supersonic airstream takes place.

Wall pressures along the combustor show the variation of static pressure in line with variation of area in the case of supersonic airstream flowing in the combustor (cold flow). Hydrogen is injected into the supersonic flow to provide conditions for ignition of liquid kerosene. During combustion of supersonic air at Mach 2 with hydrogen, it is observed that there is a pressure rise due to presence of ramps and also due to combustion in the ramp zone. Wall static pressure is observed to decrease in the cavities due to expansion and further decreases in the diverging portion of the combustor due to area increase and thus indicating supersonic combustion. Wall static pressure at the exit is found to match with the ambient pressure of 1 bar since the combustor exit is kept open to the atmosphere.

With the injection of aviation kerosene with supersonic stream of air at combustor entry Mach 2 condition, it is observed that the static pressure rise is high compared to non-reacting case and when pilot hydrogen is injected into the supersonic airstream. This is due to the mixing and combustion of aviation kerosene along with hydrogen that provides self-ignition temperature for aviation kerosene fuel. Wall static pressure in the case of aviation kerosene reaches a higher value of above 3.4 bar in the ramps. The wall pressure is observed to decrease to about 2 bar in the cavities and continues to decrease in the diverging portion of the combustor.

Variation of wall static pressure is shown in the Fig. A.1 (b) and (c) as obtained in two other experiments conducted for the same experimental conditions on the sub-scale scramjet combustor. Pilot Hydrogen is injected for self – ignition of the aviation kerosene fuel. Aviation kerosene fuel is injected in two stages, one ahead of the ramps and second stage of injection is at the ramp-base. In the second and third experiments conducted on sub-scale combustor, it is observed that the static pressure rise with injection of kerosene is about 2.2 bar at the ramps as against 3.4 bar in the first experiment. This may have been due to injection of more amount of pilot hydrogen in the first experiment. However, it is seen that there is a reduction in the wall static pressure in the cavities and in the diverging portion of the combustor. In the three experiments that have been conducted on sub-scale combustor, the trend remains in line with the literature. There is a static pressure rise of about 1 bar in the combustor due to heat release in the second and third experiments, indicating supersonic combustion.

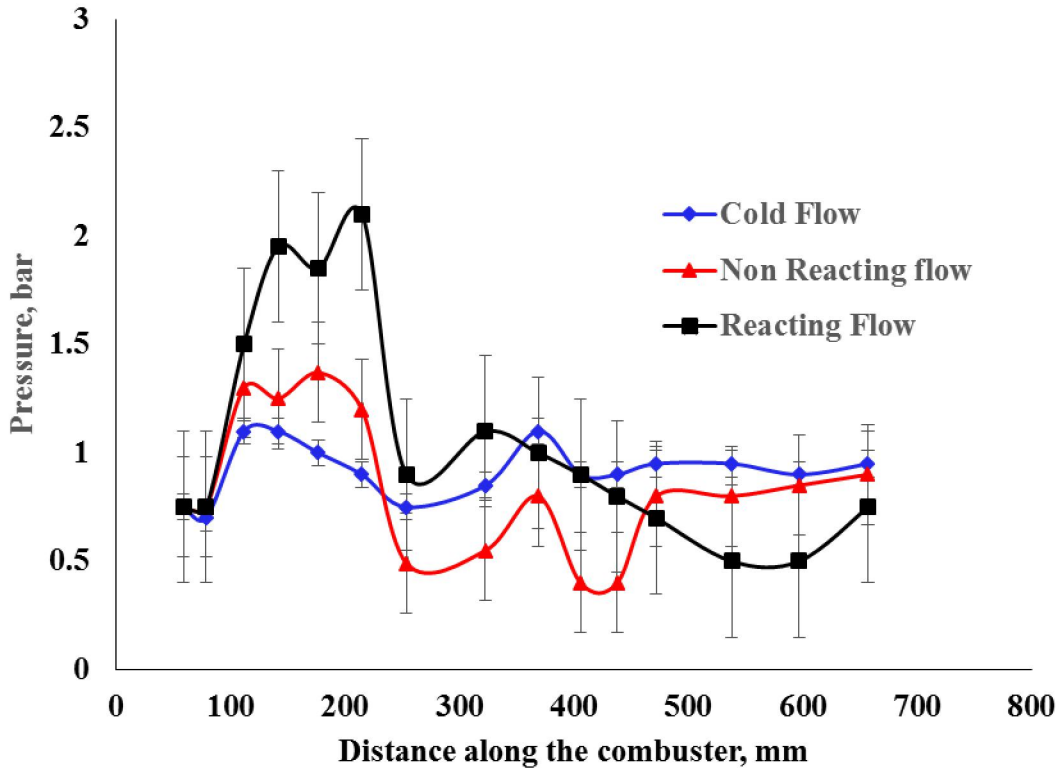

Fig A.1 (b) Top wall static pressure along the sub-scale combustor in the 2nd test

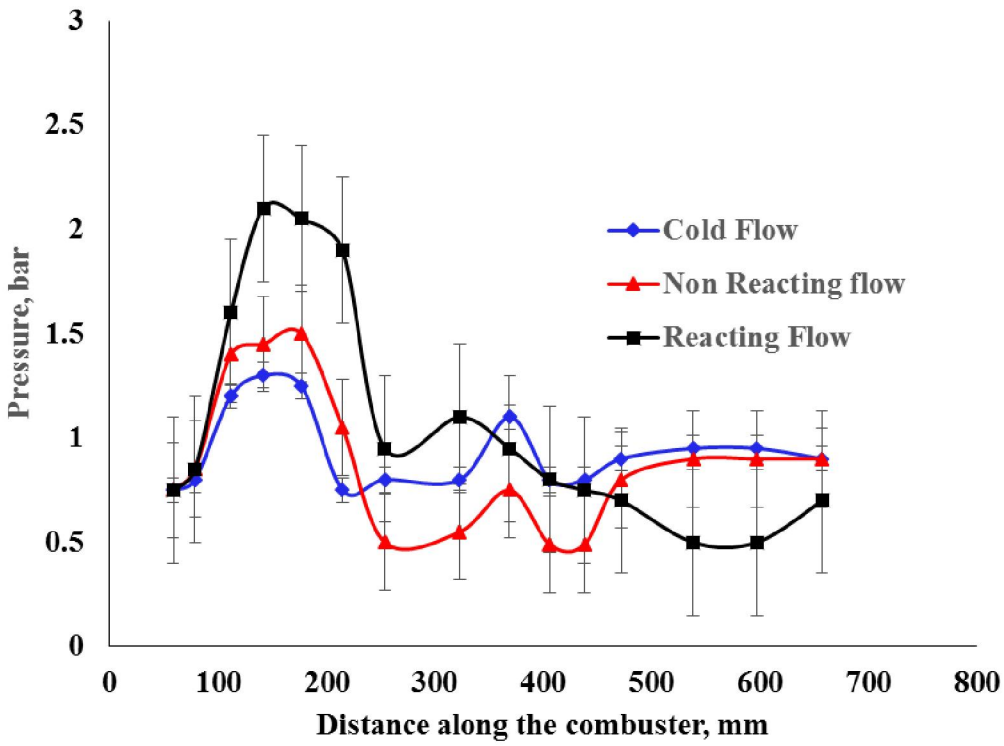

Fig A.1 (c) Top wall static pressure along the sub-scale combustor in the third test

Fig. A.1 Variation of static pressure along the top wall of sub-scale combustor

A.1.2 Variation of Temperature along the sub-scale combustor:

Temperature variation along the combustor as measured with R-type thermocouples is depicted in Fig.A.1.2 (a), (b) and (c). The variations in temperature with cold air flow, hot air flow, when the pilot Hydrogen was injected, with both hydrogen and kerosene and with kerosene fuel alone when pilot Hydrogen is withdrawn are shown in the figure A.1.2 (a). It can be observed that there is a rise in temperature with the injection of hydrogen and aviation kerosene indicating mixing with hot air and combustion. The temperature is found to be high in the constant area combustor, about 1300 K, in the vicinity of ramps and cavities. The temperatures measured in the diverging portion of the combustor indicate sustained supersonic combustion. It can be seen from Fig.A.1.2 (b) that the measured temperatures of 1200ºC – 1400ºC in the constant area and diverging portion of the combustor indicate heat release and combustion.

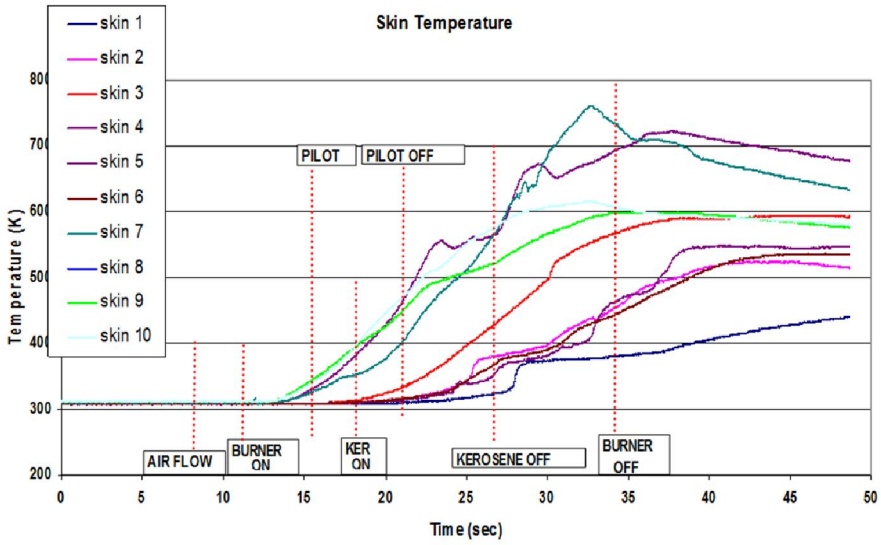

Fig. A.1.2 (a) Variation of temperature with time in the 1st test

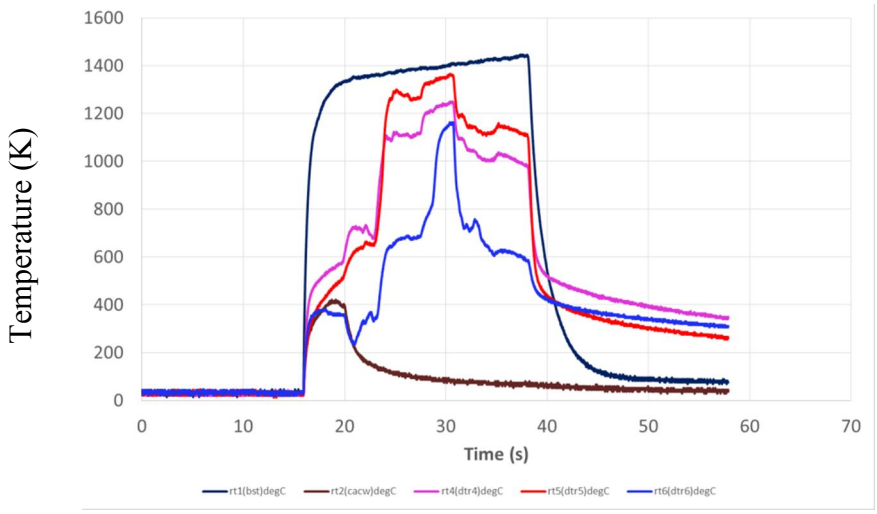

Fig. A.1.2 (b) Variation of temperature with time in the 2nd test

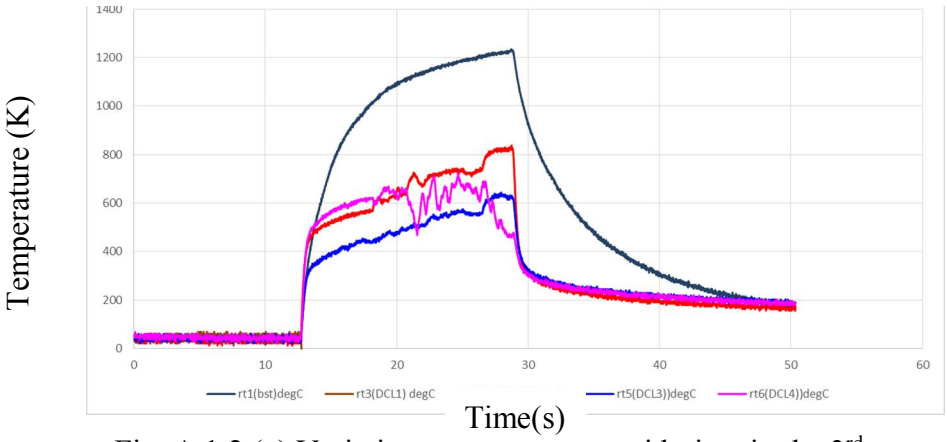

Fig. A.1.2 (c) Variation of temperature with time in the 3rd test

APPENDIX – 2

A.2 Experimental studies on full-scale combustor with aviation kerosene as a fuel:

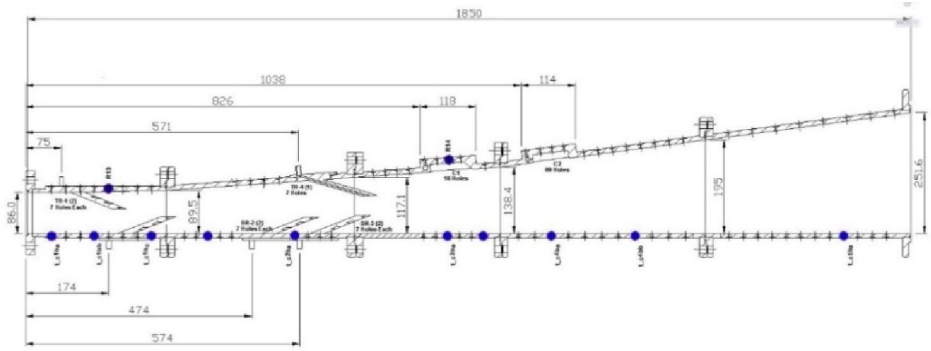

Fig.A.2. Schematic diagram of Full-scale combustor

A 2.1 Variation of static pressure along full scale combustor

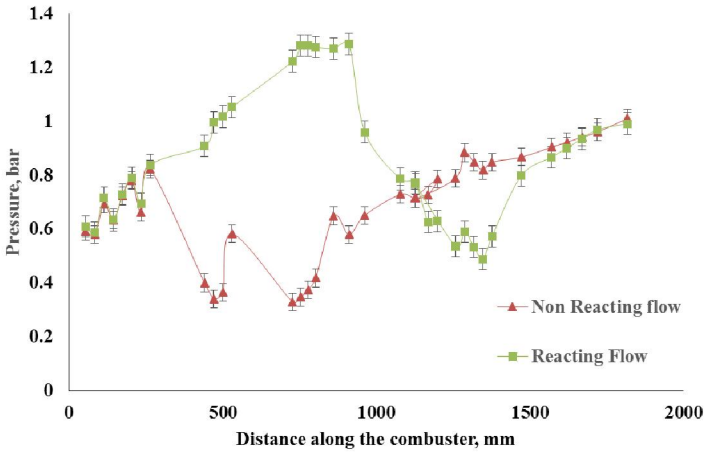

Fig: A.2 (a) Variation of static pressure during 2nd test

Fig.A.2 (a) and (b) depicts the wall static pressure variation along the full-scale combustor for non-reacting flow (without combustion) and reacting flow (with combustion) cases. Aviation kerosene in liquid state is introduced through the ramps located in the combustor. High altitude conditions are simulated in the experimental facility such that supersonic airstream flows in the combustor with the entry Mach number of 2. To achieve supersonic air at Mach 2 condition at the exit of the test-facility nozzle, the cold air flows through a burner which is heated to provide stagnation pressure and temperature corresponding to the required free stream conditions. Hot air flows through the supersonic nozzle and enters supersonic combustor with entry Mach number

2. Ramps are staggered in the combustor section for thorough mixing of fuel with air and for combustion. Aviation kerosene is injected into the combustor with an equivalence ratio of 1.13. Wall static pressures along the top wall of the combustor are shown in Fig. A.2 (a) and (b) for two experiments.

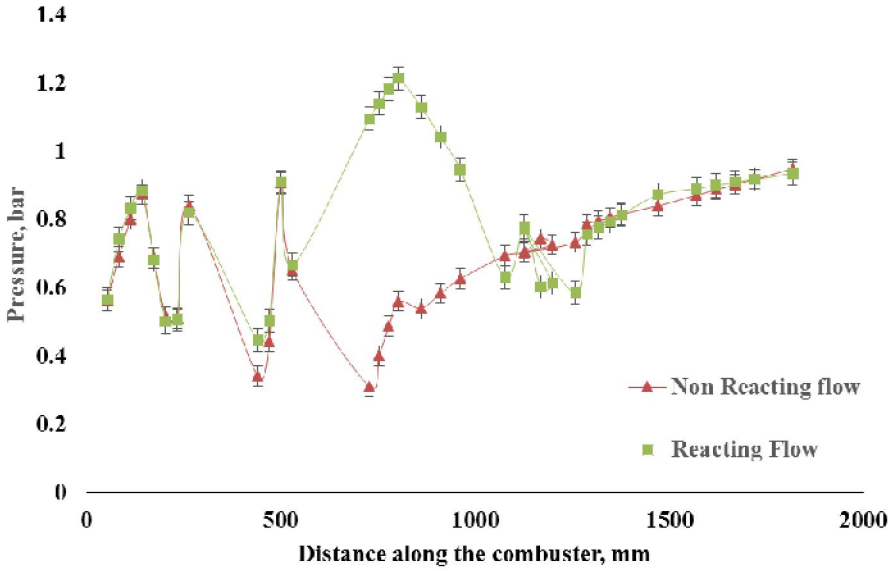

Fig.A.2 (b) Variation of static pressure during 3rd test

In the non-reacting case, the wall static pressures show the mixing pattern of kerosene with air. It can be observed that there is rise in the wall static pressure at the ramps and reduction in wall static pressure where ramps are not located in the combustor. The wall static pressure shows an increase in the cavities and will match with the atmospheric pressure at the exit of the combustor. In the case of reacting flow, the wall pressure increases continuously in the ramps to a value of about 1.3 bar indicating mixing and combustion. Wall static pressures are measured with the pressure transducers along the combustor. It can be observed that the measurements show rise in pressure in the constant area of combustor, ramps and near cavities. Static pressures measured in the diverging portion of the combustor also depict higher pressure initially and reduction with time indicating supersonic combustion. Wall static pressure rise can be observed in the ramps and first cavity in the reacting flow. It can be observed that there is a reduction in wall

static pressure after the first cavity and in the diverging portion of combustor which indicates supersonic combustion. It can be seen that the static pressure towards the exit of the combustor shows rise in pressure to equalise with the ambient conditions.

It can be observed that the pressure rise in the first cavity is high in all these experiments and the contribution of second cavity needs to be explored. Aviation kerosene being liquid fuel is required to break into fine droplets, vaporise and mix with the oxygen content in the air for combustion to take place. To overcome the issues with liquid fuels, gaseous fuels may be used to achieve mixing and supersonic combustion within the short residence time of the combustor.

A.2.2 Variation of temperature along the full scale combustor:

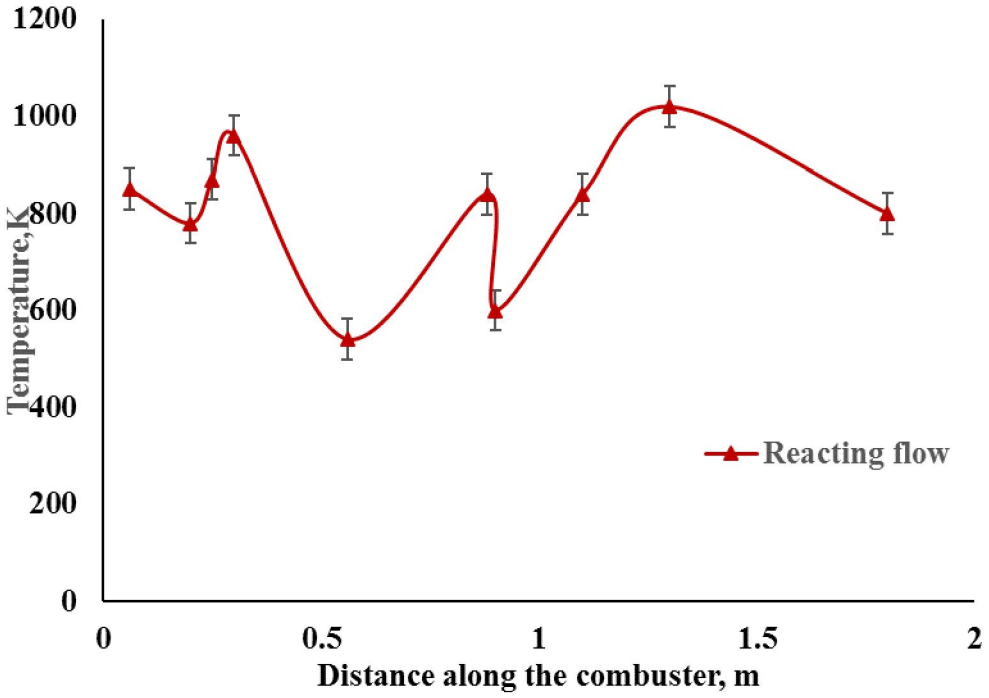

Fig.A.2. (c) Variation of Temperature along the full- scale combustor in the 2nd test

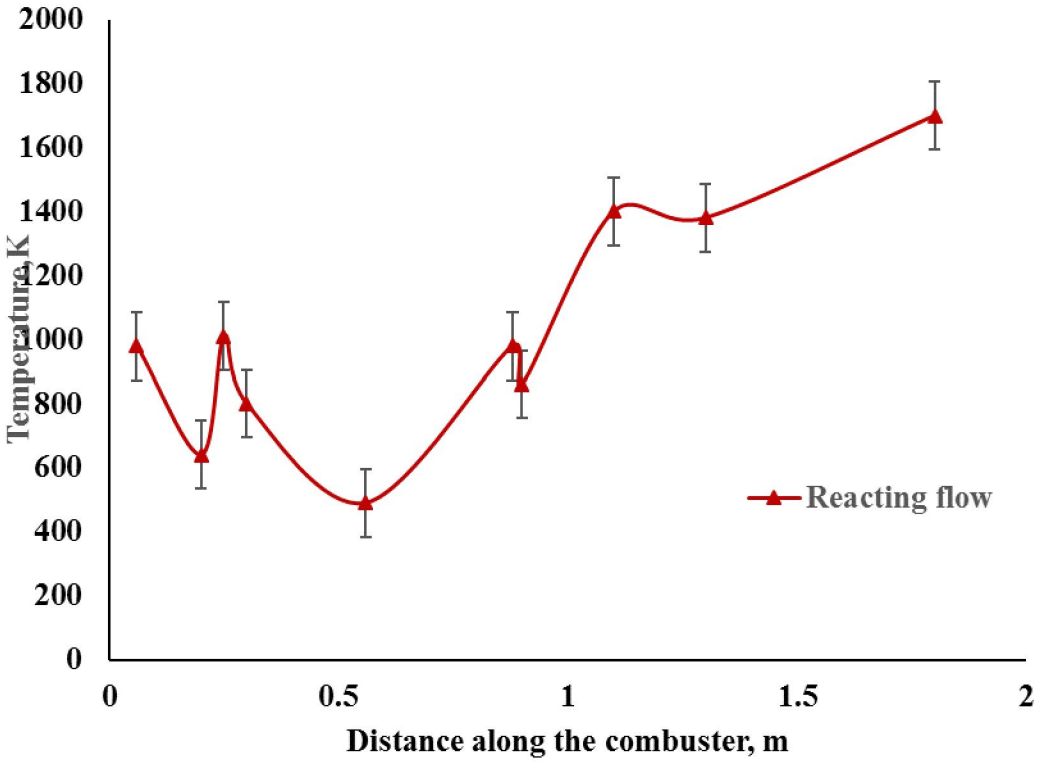

Fig.A.2. (d) Variation of Temperature along the full- scale combustor in 3rd test

The thermocouples mounted along the combustor have shown rise in temperature along the length of the combustor, in constant area as well as diverging portions of the combustor. Variation of temperature along the combustor for two additional tests on the full-scale combustor is depicted in Fig.A2. (c) and Fig.A.2 (d) respectively. It can be observed that the temperature rise in 2nd test is about 1100 K only while the temperature rise in 3rd test is about 1700 K. The lower temperature in the second test could be because of delay in mixing of liquid fuel with supersonic airstream. Similarly, it can be seen from Fig.A.2.(c) and (d), that the wall temperatures along the combustor show less rise in temperature during the test whereas the temperatures in the constant area of combustor depict higher values indicating mixing of fuel with airstream and combustion..

It can be seen from the tests conducted on sub-scale and full-scale combustors with aviation kerosene that the mixing and sustained combustion could be achieved in all the tests. However, in one test each of the sub-scale and full-scale combustors, the wall static pressures and temperatures are comparatively less than that in other tests. This could be because of issues with the break-up of liquid droplets, vaporising and mixing of the aviation kerosene fuel with the supersonic airstream. For these reasons, it is necessary to use a gaseous fuel which can easily be miscible with supersonic airstream. Gaseous ethylene is a candidate fuel for achieving supersonic combustion. Computational studies are carried out with ethylene as fuel to study the performance of the ramp-cavity supersonic combustor.

As seen from the results of sub-scale and full-scale experiments, the wall static pressure is 3.5 bar in one experiment and 2.2 bar in the remaining two experiments in the case of subscale combustor, the wall static pressure in case of full scale combustor is 1.2 bar in full-scale combustor. The temperatures in sub-scale combustor are about 1400 K - 2000 K in sub-scale combustor and 1200 K-1600 K in two tests of the full-scale combustor.

APPENDIX-3

A3 Computational studies on sub-scale combustor:

A.3.1 Computational studies on sub-scale combustor with hydrogen as PILOT fuel & KEROSENE AS MAIN FUEL at COMBUSTOR entry Mach number 2:

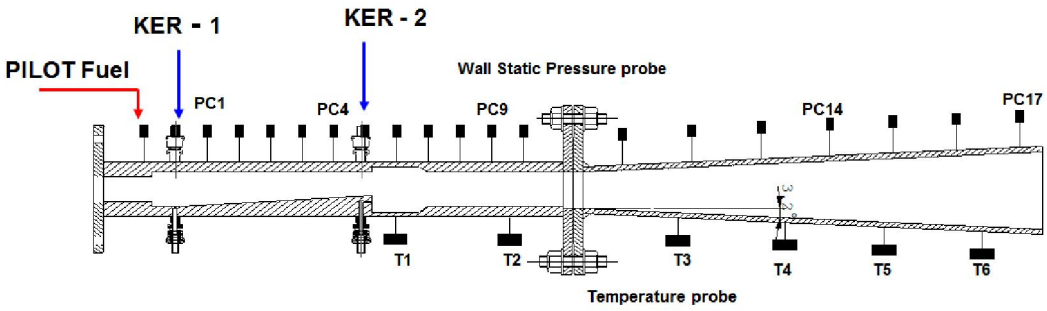

Fig.A.3.1 Sub-scale Ramp-Cavity combustor

Sub-scale ramp-cavity combustor consists of three ramps on the bottom wall and two ramps on the top wall of the combustor for mixing of fuel and two cavities along the cross section of top and bottom walls of the combustor providing flame stabilization. Supersonic airstream enters the combustor with entry Mach number 2. Hydrogen is used as pilot fuel in the simulation study. Fig.A.3.1. (a) shows variation of Mach number along the sub-scale combustor for non-reacting flow. It can be observed that there is a reduction in Mach number to Mach 1.9 due to backward facing step with corresponding area increase. Mach number reduces to 1.2 along the top and bottom walls of the combustor due to boundary layer effect and in the ramps due to compression and shock structure. The flow becomes locally subsonic at the cavity floor but remains supersonic in the core of the combustor. Mach number increases to 2 after the cavities except along the top and bottom wall where a layer of lower Mach number continues till the exit of the combustor. Due to diverging portion of the combustor, the Mach number increases to above 2 towards the exit of the combustor. In case of reacting flow, as seen in Fig.A.3.1.(b), Mach number decreases to about Mach 1.1 in the core of the combustor from the beginning of the backward facing step, continues in the ramps and a thin layer of very low Mach number can be observed at the walls. As the flow reaches cavities, at the end

of the ramps, the Mach number increases to above 1.5 and the lifting effect is also observed. The flow is locally subsonic in the cavities, recovers to supersonic flow after the cavities along the walls of the combustor and above Mach 1.5 in the diverging portion of the combustor. Mach number increases to 2.4 towards the exit of the combustor.

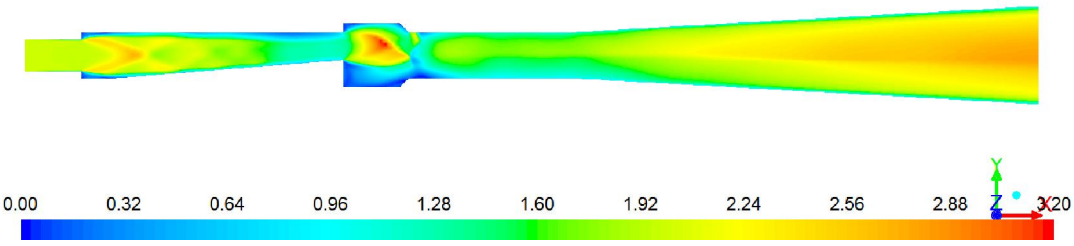

Fig.A.3.1 (a) Mach number contour along the combustor for non-reacting flow

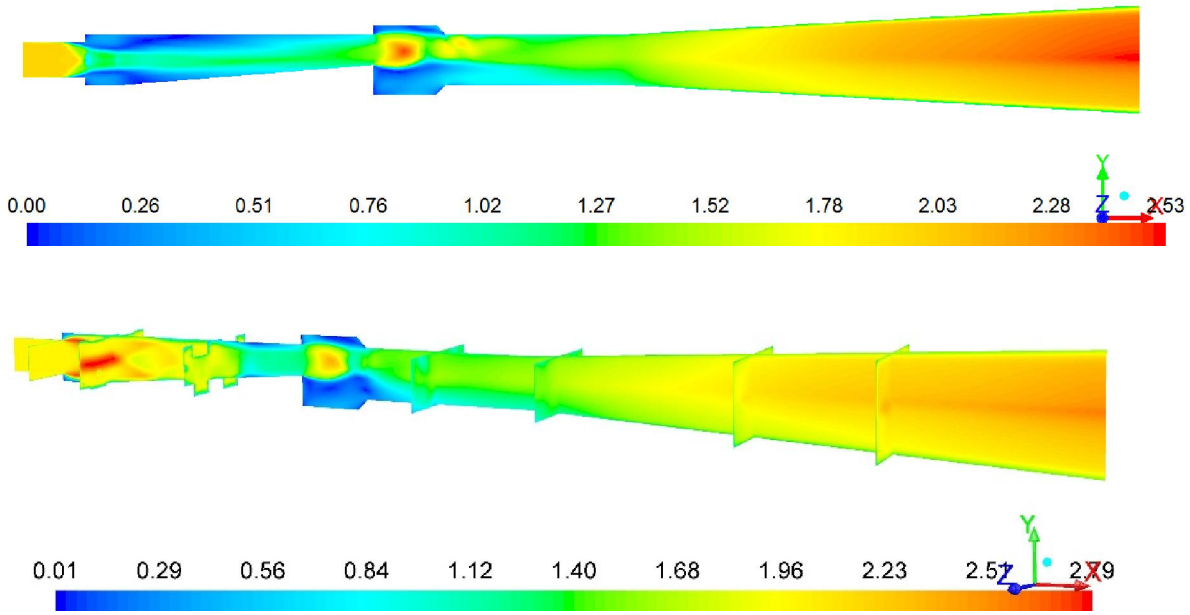

Fig.A.3.1 (b) Mach number contour along the combustor for reacting flow

Variation of static pressure along the combustor is shown in Fig.A.3.1 (c) for non – reacting flow in which reduction in pressure at the backward facing step and increase in pressure with oblique shock waves due to ramps in the combustor can be observed. It can be observed that static pressure increases to about 1.4 bar due to compressing ramps and

decreases in the cavities. Static pressure increase can be seen at the end of the cavity due to shear layer reattachment which reduces in the diverging portion of the combustor. In the case of reacting flow, the static pressure increases in the ramps due to mixing and combustion as shown in Fig. A.3.1 (d), the shocks developed due to combustion increase the static pressure in the ramps to about 1.9 bar which reduces to 1.6 bar at the end of the ramps, in the cavity plane and after the cavities in the combustor. Static pressure decreases in the diverging portion of the combustor.

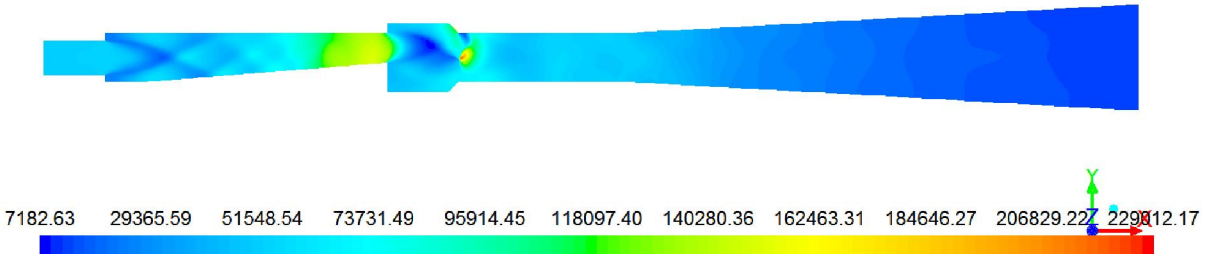

Fig.A.3.1(c) Static pressure contour along the combustor for non-reacting flow

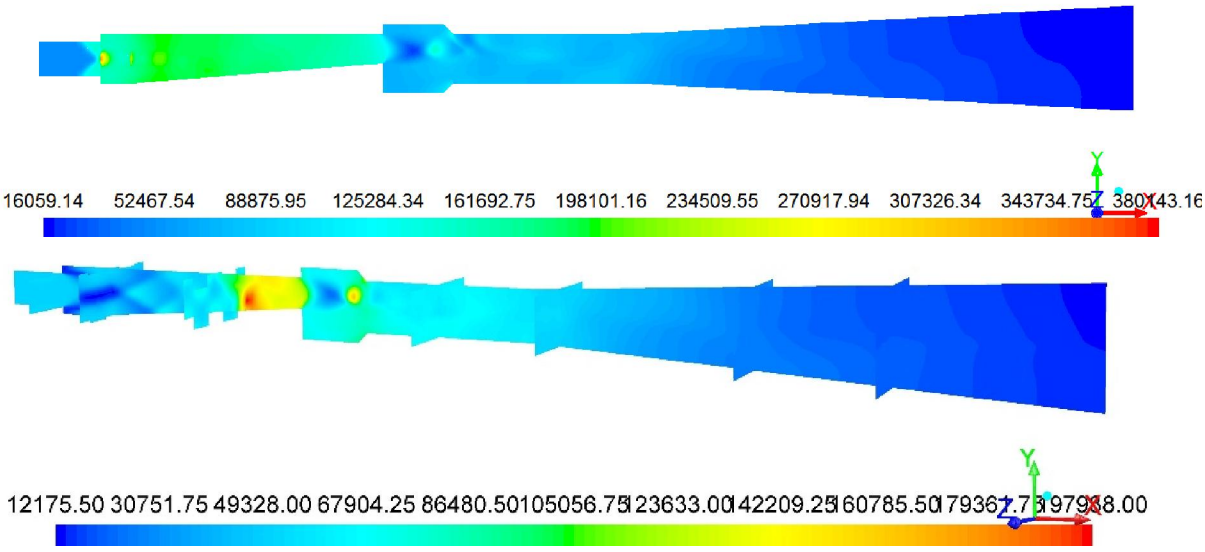

Fig.A.3.1 (d) Static pressure contour along the combustor for reacting flow

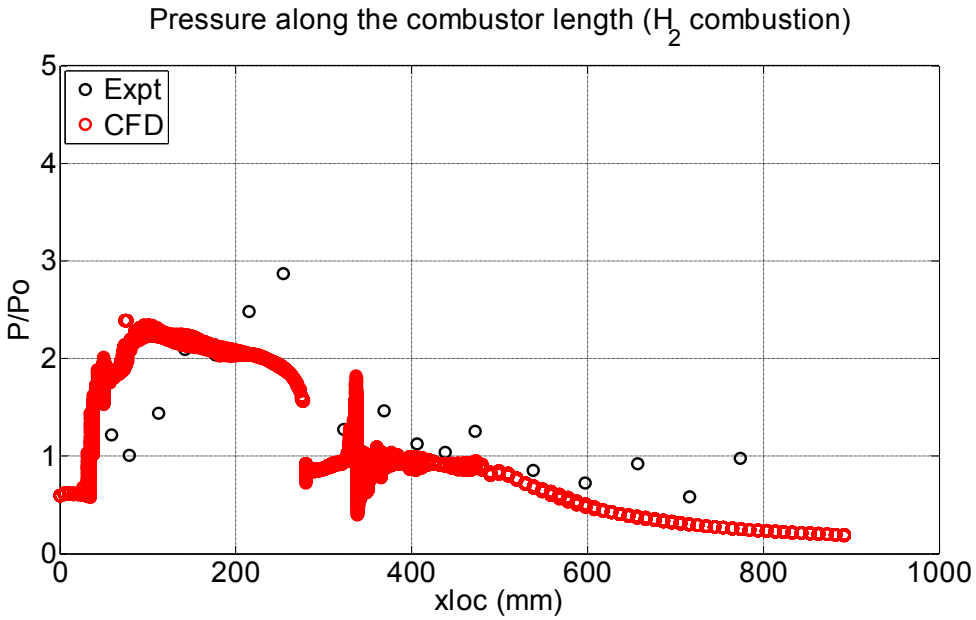

Fig.A.3.1. (e) Comparison of numerical studies with experimental work for a sub-scale combustor.

Comparison of wall static pressure with Hydrogen fuel at Mach 2 is compared with experimental results in Fig. A.3.1(e). The results match closely at the combustor entry and also in the diverging portion of the combustor. In the ramps, the experimental wall static pressures are higher than the computational values. It can be observed that experimental values of static pressure and simulation values are closely matching from 400 mm of the start of the combustor and continue in the diverging portion of the combustor. This comparison validates the computational study carried out with fluent commercial software for ramp-cavity combustor configuration.

Fig. A.3.1 (f) depicts the variation of static temperature along the combustor for non-reacting flow conditions. It can be seen that there is high temperature in the ramps due to compression and multiple shocks generated at the ramps. Higher temperature can be observed in the cavities because of recirculation zone and in the diverging portion of the combustor which decreases towards the exit of the combustor. In the case of reacting flow as shown in Fig.A.3.1 (g), the heat release due to Hydrogen combustion with supersonic air stream can be observed with fuel injection at the beginning of the ramps

and in the cavities due to recirculation zone. Static temperature continues to be high in the combustor after the cavities and in most of the diverging portion of the combustor.

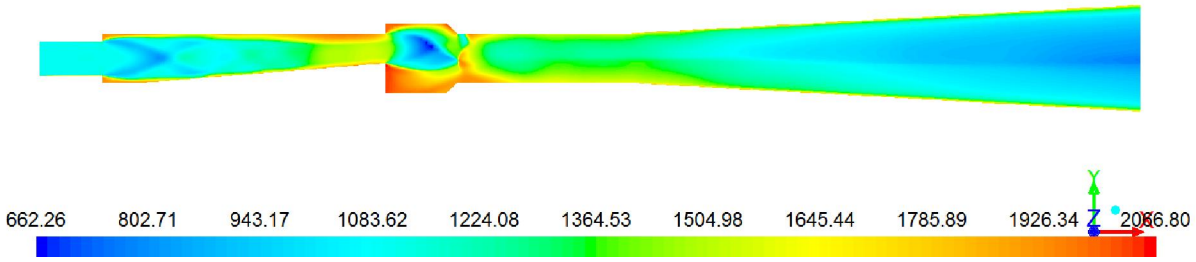

Fig.A.3.1 (f) Static temperature contour along the combustor for non-reacting flow

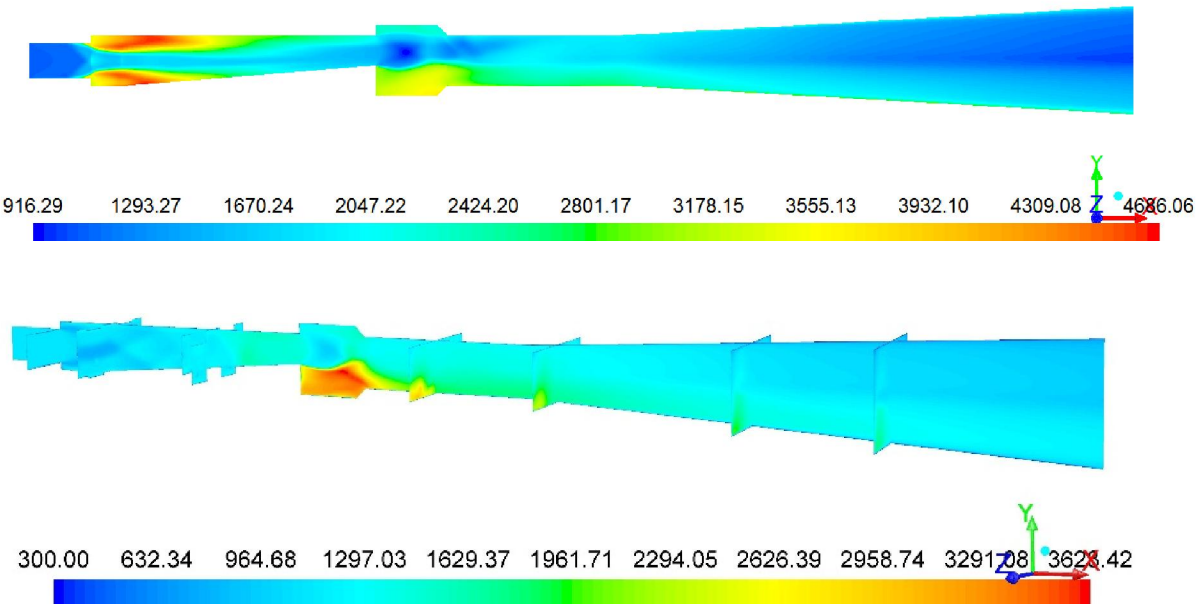

Fig. A.3.1 (g) Static temperature contour along the combustor for reacting flow

Hydrogen is considered as reference fuel as it mixes easily with supersonic airstream within the short residence time available in the combustor. Hydrogen is used as fuel in the experimental studies on sub-scale combustor for providing self-ignition condition for aviation kerosene. The static pressure variation along the combustor with pilot hydrogen as fuel is compared for both experimental and numerical conditions to validate the computational work.

A.3.2 Studies on a sub-scale combustor with Aviation kerosene as fuel at entry Mach number 2.5:

Aviation kerosene is used as fuel in the experimental studies on sub-scale combustor at entry Mach number 2. Computational studies with aviation kerosene as fuel have been carried out to simulate the combustor entry condition Mach 2.5. In addition, computational study has been carried out on sub-scale combustor with combustor entry Mach number 2.5 to evaluate the performance at higher Mach number. The studies on the effect of aviation kerosene as fuel in the sub-scale combustor are discussed.

Flow field of the combustor has been studied in terms of Mach number, static pressure, static temperature contours along the combustor for non-reacting flow (with fuel addition for mixing studies) and for reacting flow (with combustion) for sub-scale combustor with ramp-cavity configuration. The configuration consists of three ramps on the bottom wall, two ramps on the top wall followed by cavities on both top and bottom walls along the combustor cross section. In this study, supersonic airstream is considered to enter the combustor at Mach number 2.5.

Variation of Mach number along the combustor is shown in Fig. A.3.2 (a) and (b) for non-reacting and reacting flows respectively. Mach number increases as the flow enters the backward facing step due to expansion and area increase. In the ramps zone, it is observed that the Mach number reduces at the ramps zone due to compression of flow. Mach number along the top and bottom walls is further less due to boundary layer effect. In the cavities, the flow is locally subsonic at the cavity wall due to prevalence of recirculation zones and recovers as the flow passes through the diverging portion of the combustor. The flow is supersonic in the core of the combustor. Supersonic flow can be seen in most of the diverging portion of the combustor. In the case of reacting flow, as in Fig.A3.2 (b), it can be observed that the Mach number reduces to about Mach 1.4 towards the end of the ramps due to combustion of fuel with air. Flow velocity reduces and pressure increases due to mixing of fuel with the air in the ramps caused by contra-rotating vortices. Lifting of the fuel towards the core of the combustor is also observed. The flow is locally subsonic in the cavities as recirculation zone is present. The flow in

the core of the combustor in cavity zone is supersonic which can be seen in diverging portion of the combustor.

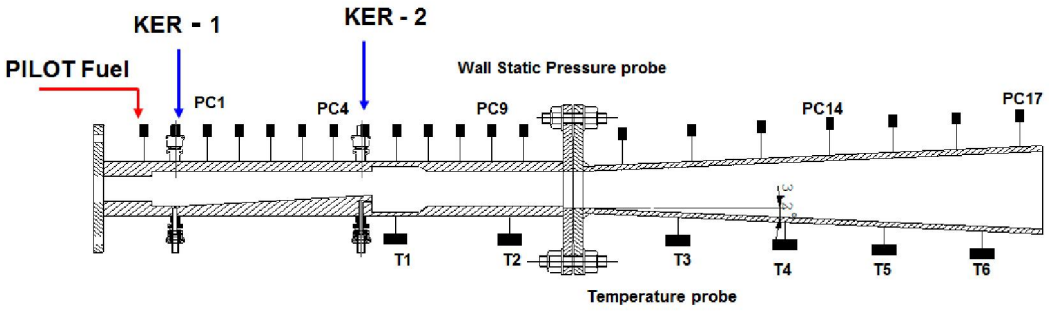

Fig.A.3.2 (a) Mach number contour along the combustor with fuel addition

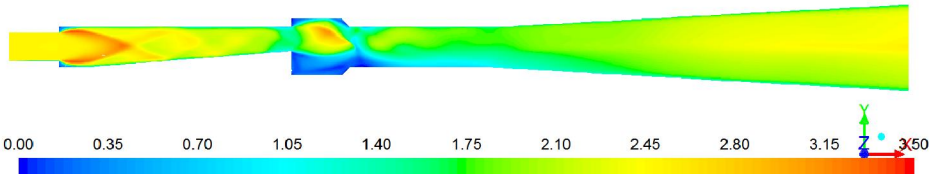

Fig.A.3.2 (b) Mach number contour along the combustor with combustion

The static pressure variation along the combustor is shown in Fig.A.3.2 (c) and (d) for non-reacting and reacting flows respectively. The static pressure reduces in the backward facing step due to expansion of area in the combustor. It can be observed that static pressure increases in the ramps due to compression and contra-rotating vortices which cause mixing. As the supersonic airstream passes through the cavities, the static pressure reduction can be observed in the core of the flow. Higher pressure can be seen at the aft wall of the top cavity as the shear layer reattaches with the supersonic airstream. Static pressure decreases in the diverging portion of the combustor. In the reacting flow, it can be seen that there is a reduction in static pressure as the flow enters the backward facing step, due to expansion of flow. Multiple oblique shocks can be seen in the ramps zone. The flow stream experiences compression in the ramps and expansion where ramps are not located. Local, high pressure zones can be seen at the end of the ramps and at the aft wall of the cavities indicating mixing of fuel and combustion of fuel with supersonic

airstream. It can be observed that there is a static pressure rise of about 1.5 bar in the combustor which decreases in the diverging portion of the combustor.

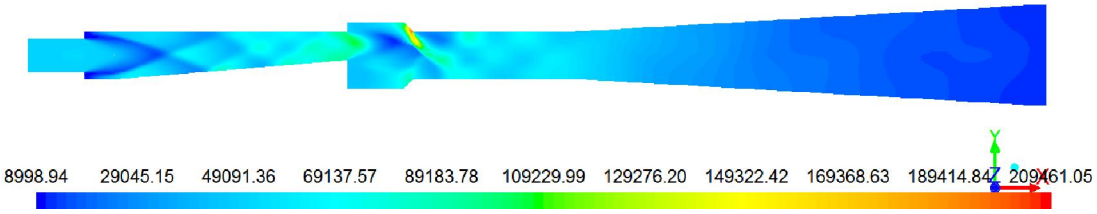

Fig.A.3.2 (c) Static pressure (Pa) contour for non-reacting flow

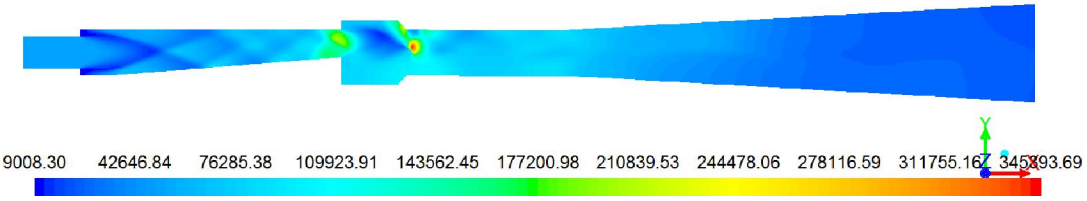

Fig.A.3.2 (d) Static pressure (Pa) contour along the combustor for reacting flow

Static temperature variation along the combustor is depicted in Fig.A.3.2 (e) and (f) for non-reacting and reacting flows respectively. Static temperature increase can be seen after the backward facing step and in the ramps due to compression, mixing of the fuel with air due to formation of vortices. Higher temperature can be seen in the cavities and in the diverging portion of the combustor. Static temperature rise can be seen in the reacting condition, from the beginning of the combustor. Higher temperature can be observed in the cavities of the combustor due to recirculation zones, and act as flame holders. The static temperature rise can be seen along the bottom wall of the combustor after cavities and continues to be high in the diverging combustor. All the characteristics indicate sustained supersonic combustion.

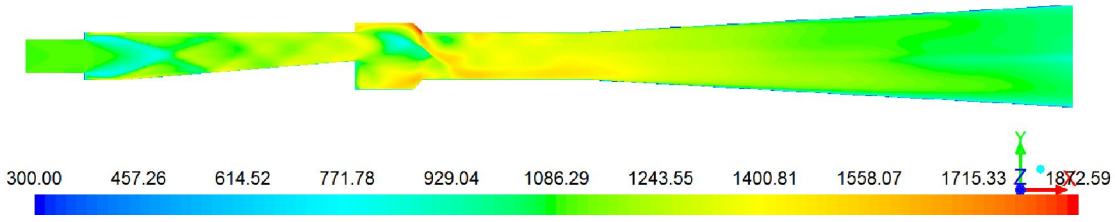

Fig.A.3.2 (e) Static temperature (K) contour along the combustor for non-reacting flow

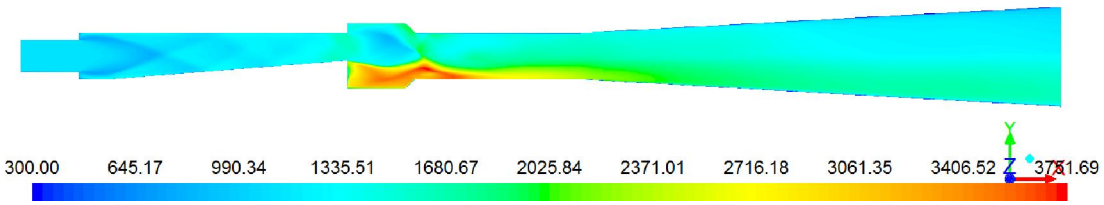

Fig.A.3. (f) Static temperature (K) contour along the combustor for reacting flow

Fig.A.3.2 (g) depicts the flow parameters in terms of variation of Mach number, static pressure and static temperature along the combustor for non-reacting flow and reacting flow respectively. It can be observed that Mach number increases in the backward facing step due to increase in area, decreases in the ramps, vary in the ramp zone due to compression of flow due to ramps and expansion where ramps are not located. The flow becomes subsonic in the cavities in the case of combustion as seen in Fig.A.3.2 (h) due to recirculation zone present, recovers to supersonic Mach number and continues to be supersonic in the diverging portion of the combustor. Variation of static pressure along the combustor depicts similar trend of decrease in the backward facing step due to expansion, rise in pressure due to compressing ramps and expansion at the end of ramps. The static pressure can be seen increasing in the cavity zone due to recirculation and decreases in the diverging portion of the combustor. In the case of reacting flow, the pressure in the ramps rises to above 1.2 bar and locally to above 2 bar in the cavity zone due to recirculation of flow. Static pressure decreases in the diverging portion of the combustor indicating supersonic combustion. It can be observed that static temperature decreases in the backward facing step, increases in the ramps due to mixing and combustion. Static temperature rise can be observed to be high in the cavities due to recirculation zone that acts as flame stabilizer for sustained supersonic combustion. Higher static temperature can be seen in the diverging portion of the combustor indicating heat release during the reacting flow.

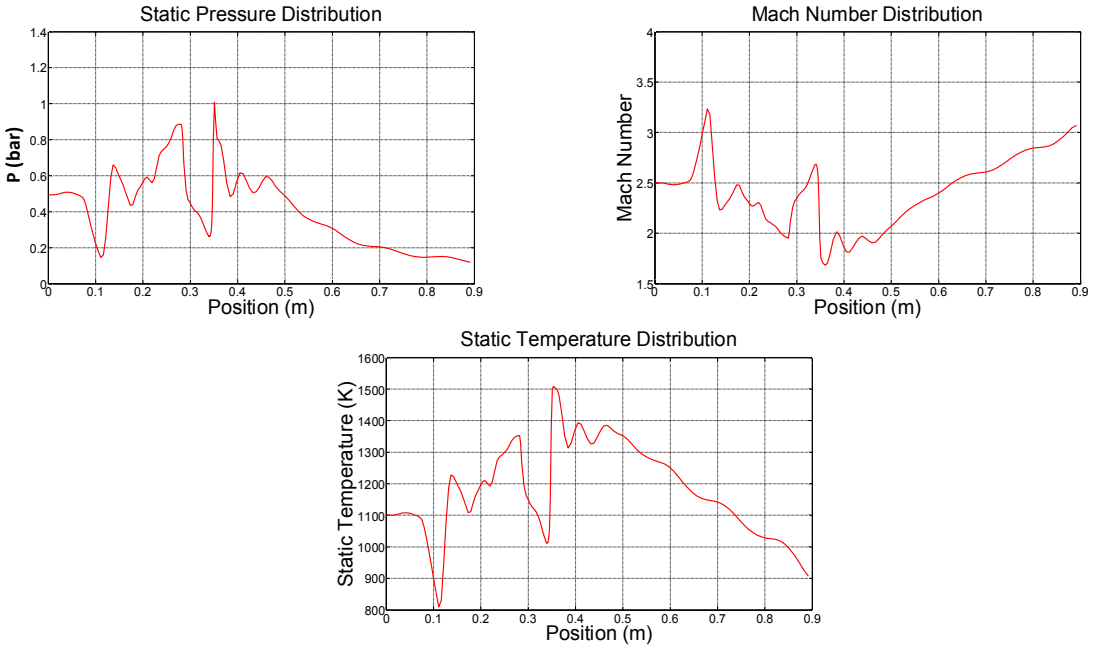

Fig.A.3.2 (g) Flow parameters along the combustor for non-reacting flow

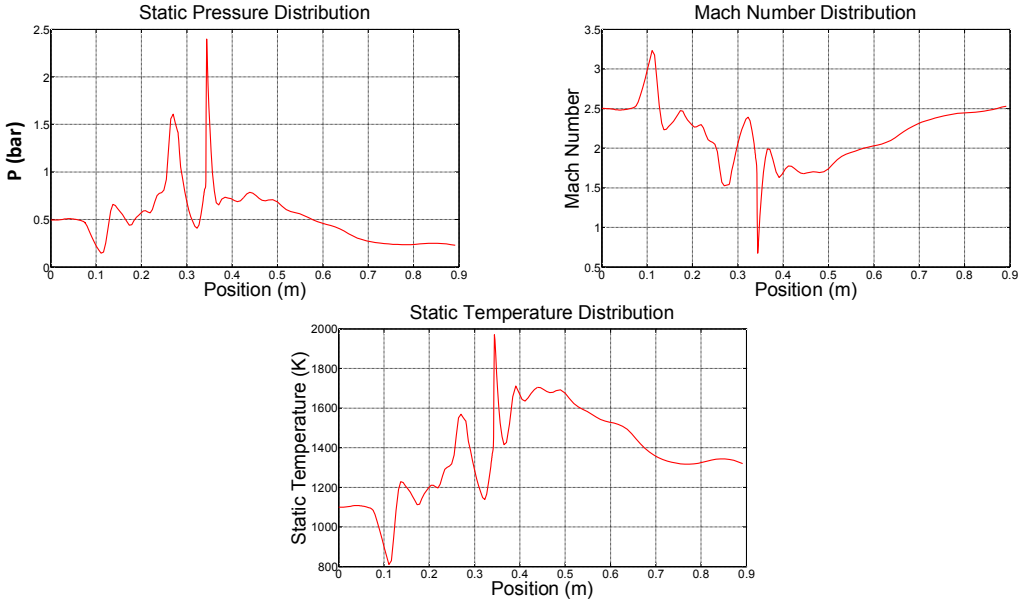

Fig.A.3.2 (h) Flow parameters along the combustor for reacting flow at entry Mach 2.5

APPENDIX-4

Computational studies on full-scale combustor:

A.4 Full scale combustor with Wall Injection and without ramps and cavities:

A computational study has also been carried out with supersonic combustor without ramps and cavities. However, the fuel is allowed to be injected through orifices from the wall. Ethylene is used as a fuel with combustor entry Mach number of supersonic stream of air at 3. This simulation is carried out to study the effect of wall injection into the combustor without ramps and cavities for the cases of with and without combustion. It can be seen there is substantial rise in static pressure and temperatures for case with combustion.

A.4.1 Combustor with cavities and Wall Injection for combustor entry Mach 3:

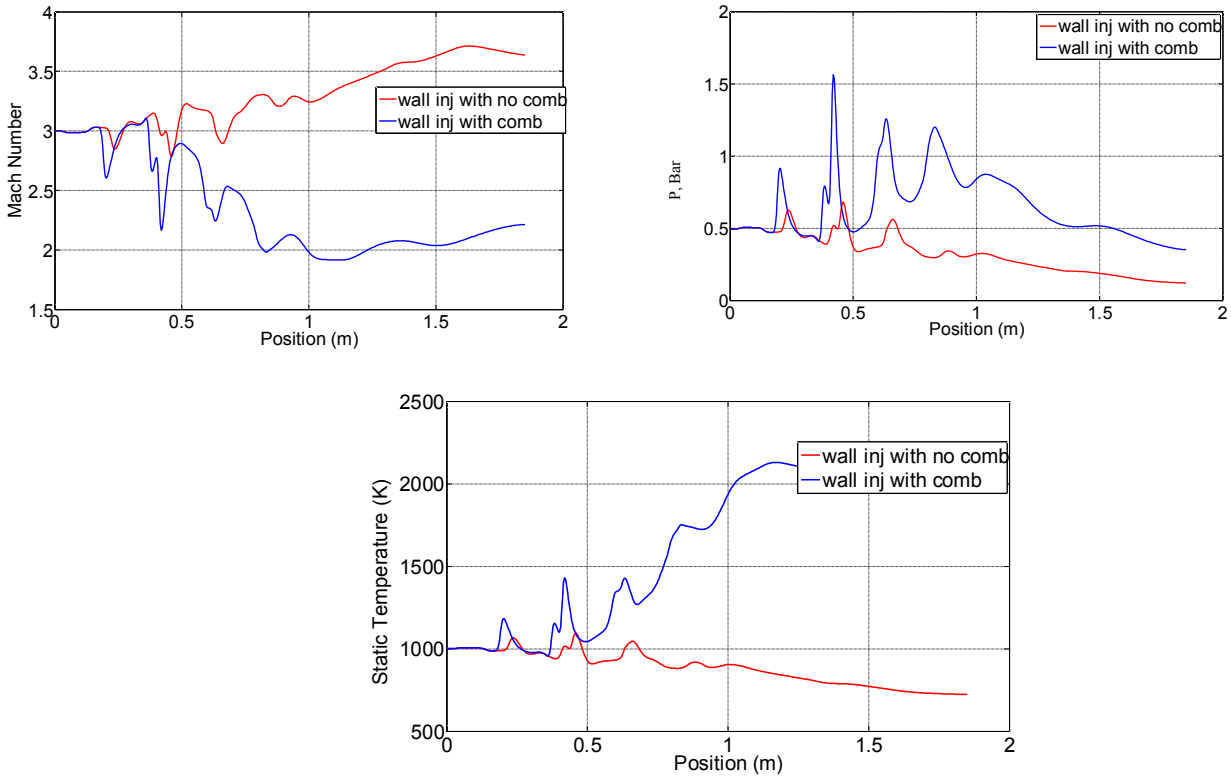

Fig.A.4.1 Comparison of flow field for wall injection with and without combustion.

It is observed from the cases that have been studied that sustained supersonic combustion has been obtained with higher values of static pressures and temperatures with wall injection. Further, the effect of flame holding with the introduction of cavities has been explored. The flow field contours are illustrated in Fig.A.4.1along the combustor with and without cavities and wall injection of fuel. The computational study has revealed that Mach number is higher than that without cavities. Static pressure plot shows that the variation in static pressure is marginally higher for wall injection of fuel without cavities. However, static temperature with combustion shows appreciable rise in temperature from 0.6 m of the combustor entry, till the end of the combustor indicating sustained supersonic combustion. Cavities have provided higher temperature and flame stabilization due to recirculation zones. The presence of cavities in the combustor improved the heat release during combustion of ethylene fuel from combustor walls.

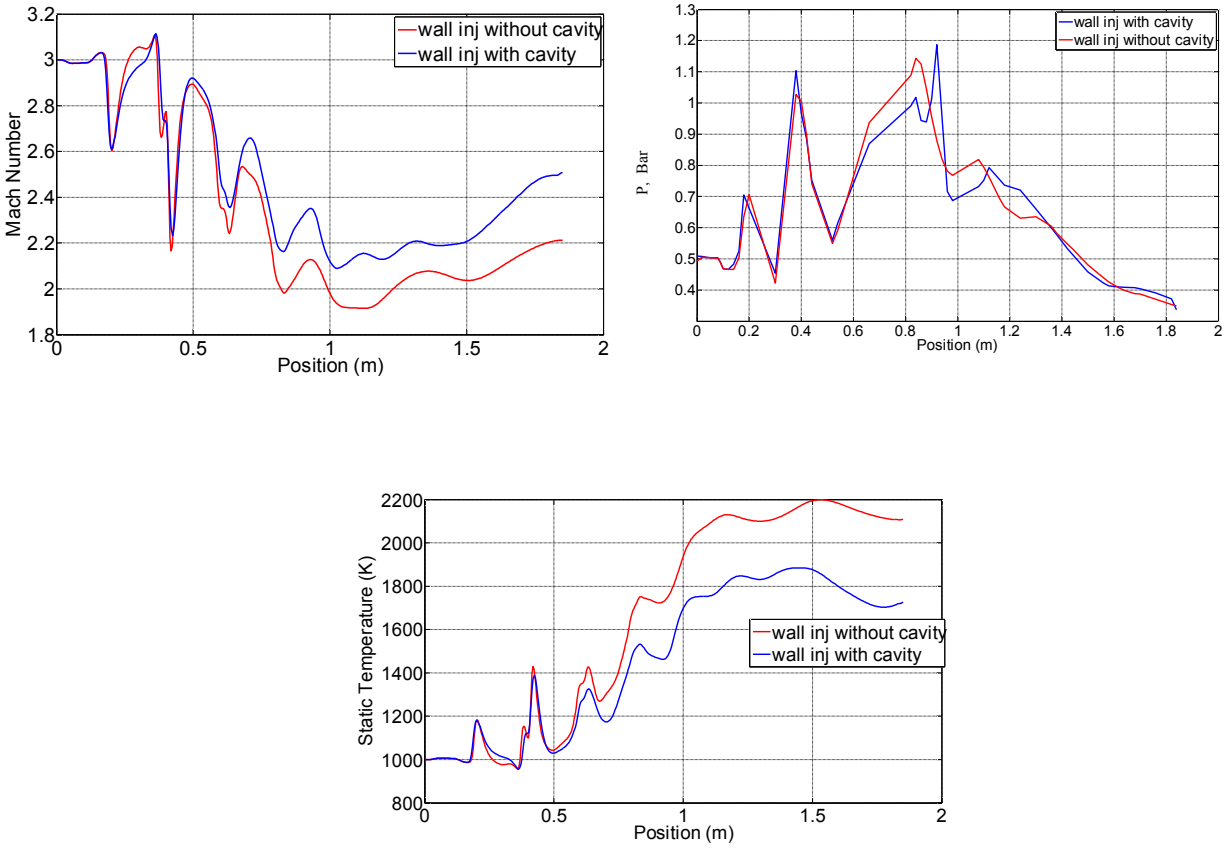

Fig. A.4.1 (a) Comparison of wall injection and fuel combustion with and without cavities

Mach number, static pressure, static temperature and mass fractions of species along the combustor are depicted in Fig.A.4.2.

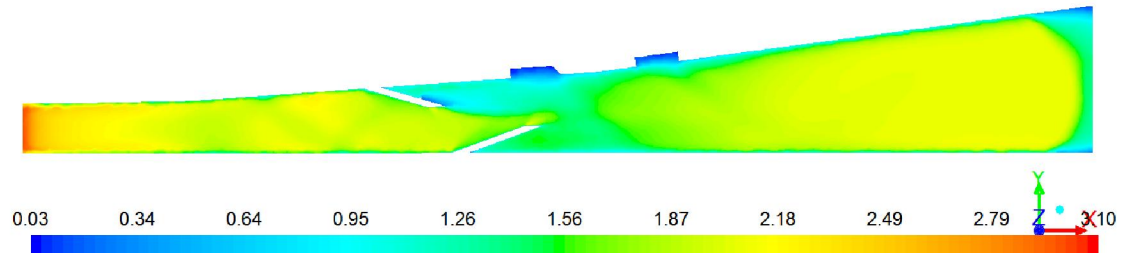

Fig.A.4.2 (a) Mach number distribution along combustor with combustor entry Mach 3

Mach number contour is shown in Fig.A.4.2 (a). Supersonic airstream enters combustor at Mach 3 and passes through the ramps and due to multiple oblique shocks, reduces to Mach 1.8. A layer of subsonic Mach number can be seen at the boundary of top and bottom walls and near the ramps. The Mach number in the diverging combustor near the cavities is about 1.2 indicating combustion of the fuel with the air. The Mach number is locally subsonic in the cavities and increases to 2.2 in the core of diverging portion of the combustor. Mach number is observed to be about 1.2 along the walls of the diverging portion and towards the exit of the combustor.

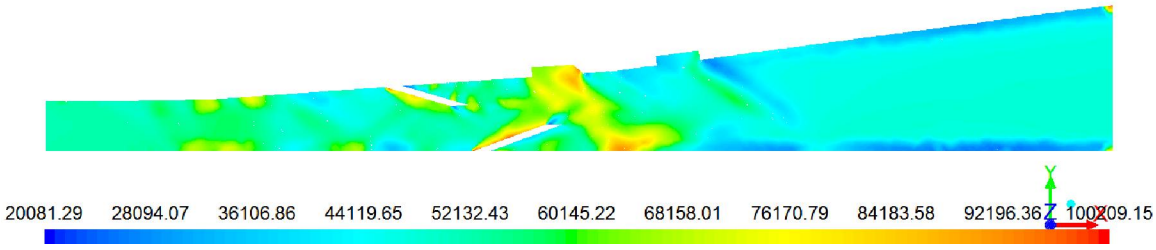

Fig.A.4.2 (b) Static pressure (Pa) distribution with combustor entry Mach 3

Static pressure contour for combustion of ethylene fuel with supersonic airstream is shown in Fig.A.4.2 (b). Static pressure increases in the ramps due to multiple shocks and compressions. Static pressure rise can also be observed near the ramps where fuel is injected, in the cavities and in the diverging portion of the combustor where cavities are located. The pressure rise near the first cavity and wall opposite to the first cavity is very high. It can be seen that there is a rise in pressure near the aft wall of the second cavity

followed by low pressure along the top wall of the combustor. Static pressure rise in the diverging portion of the combustor continues to be high though the pressure along the top and bottom walls is low.

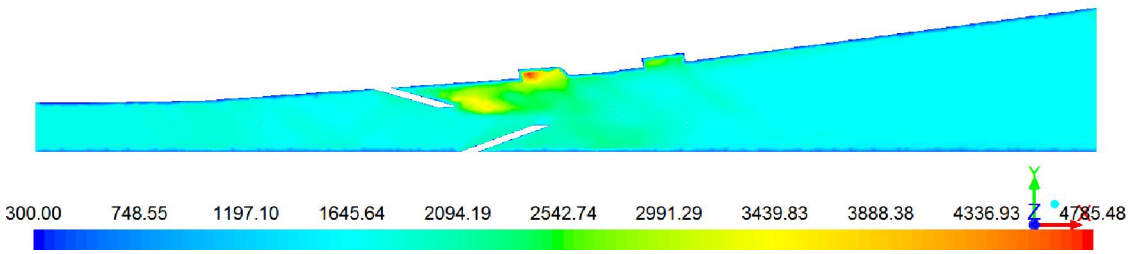

Fig.A.4.2 (c) Static temperature (K) distribution along the combustor with entry Mach 3

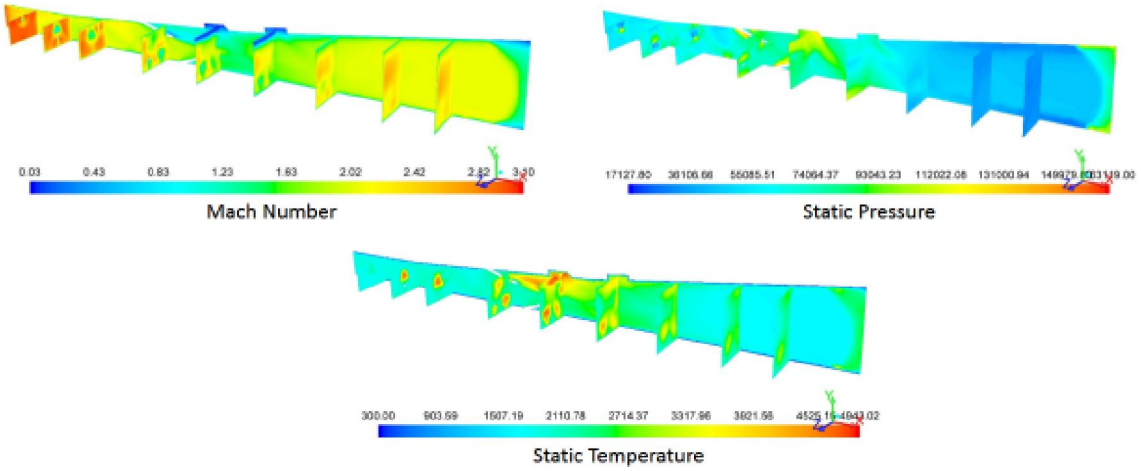

Fig.A.4.2 (d) Flow parameters across the combustor

Variation of static temperature contour along the combustor with ethylene as fuel and is shown in Fig.A.4.2 (c) considering the combustor entry Mach number 3 for reacting flow. It can be seen that static temperature rises near the ramps where fuel injection takes place. Intense temperature can be observed in the first cavity and static temperature is high in the second cavity which helps in flame stabilization and thereafter sustained supersonic combustion in the combustor. The static temperature contour shows a temperature of about 1600 K-2000K in the combustor indicating sustained supersonic combustion.

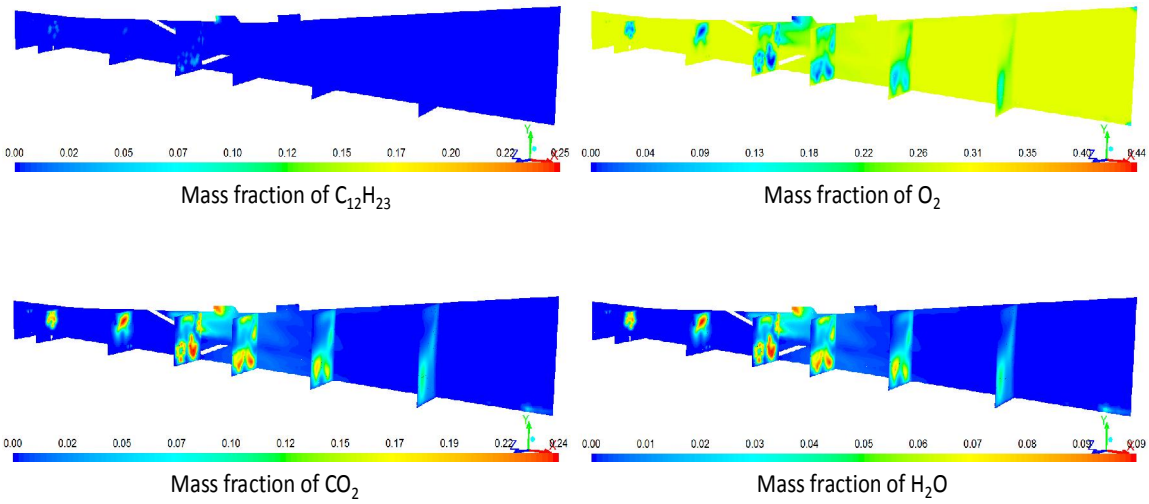

Fig.A.4.2 (e) Mass fractions of species along combustor with combustor entry Mach3

Fig.A.4.2 (d) shows the flow parameters along the combustor. It can be seen from Mach number plot that Mach number reaches a minimum value near the cavities but continues to be supersonic, above 1.7. Static pressure plot shows rise in pressure in the ramps and cavities. Maximum static pressure of about 0.8 bar is observed in the cavities. Similar trend is observed with static temperature plot along the combustor showing rise in temperature in ramps and considerable rise in the cavities. Static pressure and static temperature values reduce in the diverging portion of the combustor indicating supersonic flow in the combustor.

Fig.4.2 (e) shows the mass fractions of ethylene, oxygen and the products of combustion. It can be seen that oxygen mass fraction reduces near the ramps and cavities indicating combustion. Mass fractions of CO_2 and H_2O also indicate the combustion.

A.4.2. Studies with full scale combustor at entry Mach 3 with Aviation kerosene:

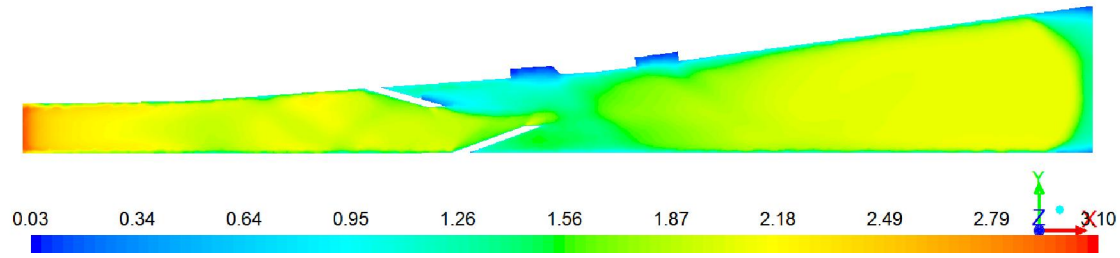

Fig.A.4.3 (a) Mach number contour along the combustor with combustor entry Mach 3

Studies are carried out on a ramp-cavity, full-scale combustor with aviation kerosene as fuel at an equivalence ratio of 0.6. Supersonic airstream with combustor entry Mach number 3 is considered. Mach number, static pressure, static temperature and mass fractions of species along the combustor are depicted in Fig.A.4.3. Mach number contour is shown in Fig.A.4.3 (a). Supersonic airstream enters combustor at Mach 3 and passes through the ramps and due to multiple oblique shocks, reduces to Mach 1.8. A layer of subsonic Mach number can be seen at the boundary of top and bottom walls and near the ramps. The Mach number in the diverging combustor near the cavities is about 1.2 indicating combustion of the fuel with the air. The Mach number is locally subsonic in the cavities and increases to 2.2 in the core of diverging portion of the combustor. Mach number is observed to be about 1.2 along the walls of the diverging portion and towards the exit of the combustor.

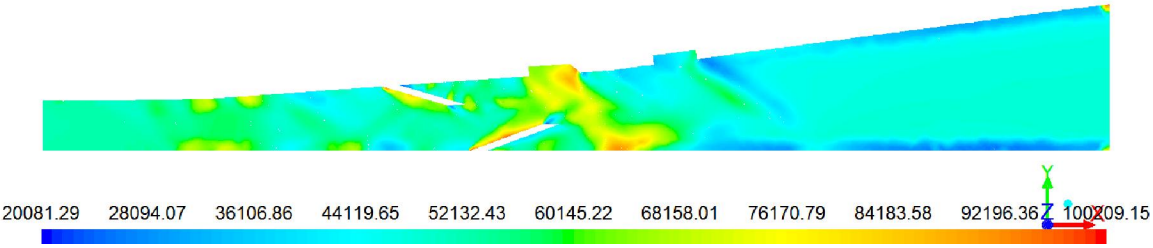

Fig.A.4.3 (b) Static pressure (Pa) distribution with combustor entry Mach 3

Static pressure contour for combustion of kerosene fuel with supersonic airstream is shown in Fig.A.4.3 (b). Static pressure increases in the ramps due to multiple shocks and compressions. Static pressure rise can also be observed near the ramps where fuel is

injected, in the cavities and in the diverging portion of the combustor where cavities are located. The pressure rise near the first cavity and wall opposite to the first cavity is very high. It can be seen that there is a rise in pressure near the aft wall of the second cavity followed by low pressure along the top wall of the combustor. Static pressure rise in the diverging portion of the combustor continues to be high though the pressure along the top and bottom walls is low.

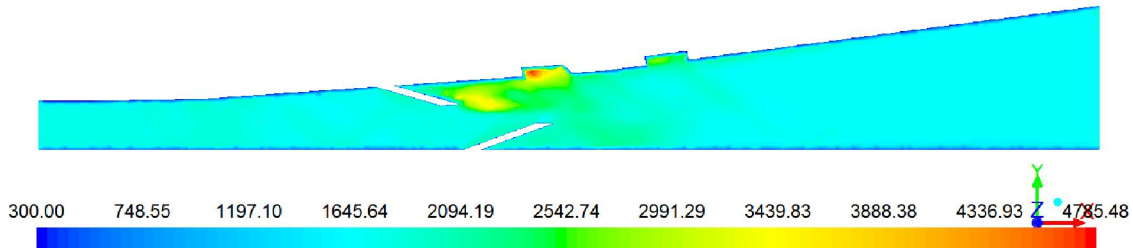

Fig.A.4.3 (c) Static temperature (K) distribution along the combustor with entry Mach 3

Variation of static temperature contour along the combustor with aviation kerosene as fuel and is shown in Fig.A.4.3 (c) considering the combustor entry Mach number 3 for reacting flow. It can be seen that static temperature rises near the ramps where fuel injection takes place. Intense temperature can be observed in the first cavity and static temperature is high in the second cavity which helps in flame stabilization and thereafter sustained supersonic combustion in the combustor. The static temperature contour shows a temperature of about 1600 K -2000K in the combustor indicating sustained supersonic combustion.

Fig.A.4.3 (d) shows the mass fractions of species along the combustor when combustion takes place with aviation kerosene as fuel. Aviation kerosene is found in the vicinity of ramps and near the cavity front wall. Oxygen mass fraction shows that there is a decrease in the concentration near the ramps and first cavity indicating combustion in that zone of the combustor. The cross section at different planes along the combustor show that oxygen mass fraction depletes along the combustor till the diverging portion of the combustor. The mass fractions of CO_2 and H_2O also show that the concentration of these species is high at the ramps, cavities and in the diverging portion of the combustor. However, the combustion is high near the ramps and cavities indicating effective combustion near the ramps and cavities

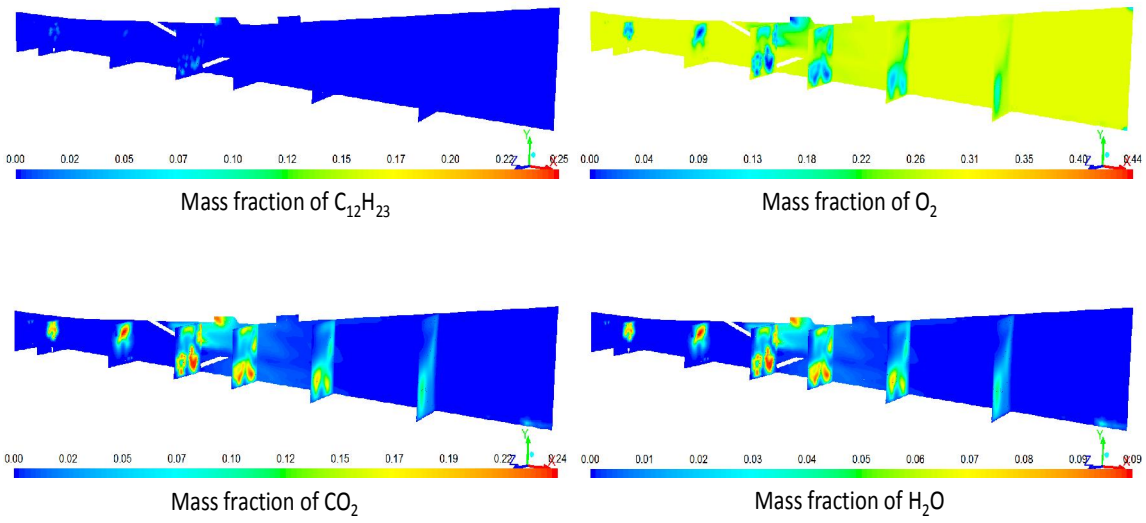

Fig.A.4.3 (d) Mass fractions of species along the combustor with combustor entry M3

APPENDIX-5

Note on Development work on scramjet combustion in various countries:

Initial work was done by Ferri and Billig on the basic, fundamental processes and issues related to shock structures and heat release due to combustion. Work included building fixed geometry engines over a wide range of Mach numbers and maximising the performance of the engines. Efforts were made to achieve supersonic combustion with Hydrogen and hydrocarbon fuels. While struts and cavities have been used for compression, fuel injection and mixing with supersonic airstream by many American researchers, Russians have conducted experiments with cavities as the fuel mixing and flame holding devices in the combustor. To realize the supersonic combustion of free stream hypersonic air, fuel injection devices such as struts, cavities and ramps are tried in addition to wall injection of fuel. Experimental studies made use of non-intrusive techniques such as schilerian photography; Planar Induced Fluorescence (PLIF) etc. have been used to capture the flow field. Computational studies have aimed at understanding the flow physics with both commercial software and software developed to meet the specific requirements. In this section, scramjet combustor supersonic combustion starting with Ferri has been studied. Various fuel injection devices development efforts in various countries are reviewed and listed. Work carried out on such as struts, ramps and cavities have been used in the combustor to achieve mixing and combustion. Very few references are available in the published literature about the application of the combined effect of ramps and cavities in a supersonic combustor wherein ramps are used for fuel mixing with supersonic airstream and cavities are used for flame holding. X-51 and X-53 flight tests by U.S.A. have been reported. Australian University has conducted flight testing of Hyshot programme. Russia, Germany and France have also carried out flight test programmes in the development of supersonic combustor.

The efforts of various researchers in the area of supersonic combustion have been studied extensively.

APPENDIX-6

THEORETICAL ROCKET PERFORMANCE ASSUMING FROZEN COMPOSITION DURING EXPANSION

0PC = 174.0 PSIA

CASE NO. 1

	WT FRACTION	ENERGY	STATE	TEMP	DENSITY
CHEMICAL FORMULA		CAL/MOL		DEG K	G/CC
FUEL H 2.00000	1.00000	.000	G	300.15	.0000
OXIDANT O 2.00000	.20810	.000	G	300.15	.0000
OXIDANT N 1.56180 O .41960 C .00030 AR .00930	79190	.000	G	300.15	.0000

O/F= 55.0800 PERCENT FUEL= 1.7832 EQUIVALENCE RATIO= .3686

	CHAMBER	THROAT	EXIT
PC/P	1.0000	1.8172	7.6723
P, ATM	11.843	6.5171	1.5436
T, DEG K	1893	1667	1212
RHO, G/CC	2.0234-3	1.2645-3	4.1207-4
H, CAL/G	.0	-79.5	-233.7
S, CAL/ (G) (K)	2.1970	2.1970	2.1970
M, MOL WT	26.544	26.544	26.544
CP, CAL/ (G) (K)	.3553	.3478	.3278
GAMMA (S)	1.2669	1.2742	1.2960
SON VEL, M/SEC	866.8	815.8	701.4
MACH NUMBER	.000	1.000	1.994
AE/AT		1.0000	1.7900
CSTAR, FT/SEC		3817	3817
CF		.701	1.202
IVAC, LB-SEC/LB		148.5	170.3
ISP, LB-SEC/LB		83.2	142.6

MOLE FRACTIONS

AR	.00663	CO2	.00021	H2	.00002	H2O	.23430
NO	.00488	NO2	.00003	N2	.55417	O	.00004
OH	.00095	O2	.19876				

ADDITIONAL PRODUCTS WHICH WERE CONSIDERED BUT WHOSE MOLE

FRACTIONS WERE LESS THAN .50000E-05 FOR ALL ASSINGED CONDITIONS

C(S) C CH CH2 CH2O CH3 CH4 CN CN2 CO
C2 C2H C2H2 C2H4 C2N C2N2 C2O C3 C3O2 C4
C5 H HCN HCO HNO HO2 H2O(S) H2O (L) H2O2 N
NH NH2 NH3 N2C N2H4 N2O N2O4
NOTE. WEIGHT FRACTION OF FUEL IN TOTAL FUELS AND OF OXIDANT IN TOTAL OXIDANTS

2. NASA CEC-71 Computation;

Ramp-Cavity Combustor Inlet Conditions

Calculated Quantities

NASA CEC-71 Computation

Total Pressure	:	3.87363 bar
Mixture Fractions (Mass Basis)		
H_2		0 .0210
O_2		0.2478
Air		0.7312
Total Temperature	:	2087 K
NOZZLE Exit Flow Parameters		
Static Pressure	:	0.51 bar
Static Temperature :	:	1382 K
Ratio of Sp. Heats	:	1.2786
Mach Number	:	1.99
Computed Mass flow	:	4.188 Kg/s (Cd=1)

Measured Quantities

- Total Mass flow Rate : 4.076 kg/s
- Total Pressure : 3.87363 bar
- Static Pressure : 0.52 bar
- Total Temperature : 1755 K
- Kerosene mass flow rate : 352 g/s
- Overall Equivalence ratio : 1.13